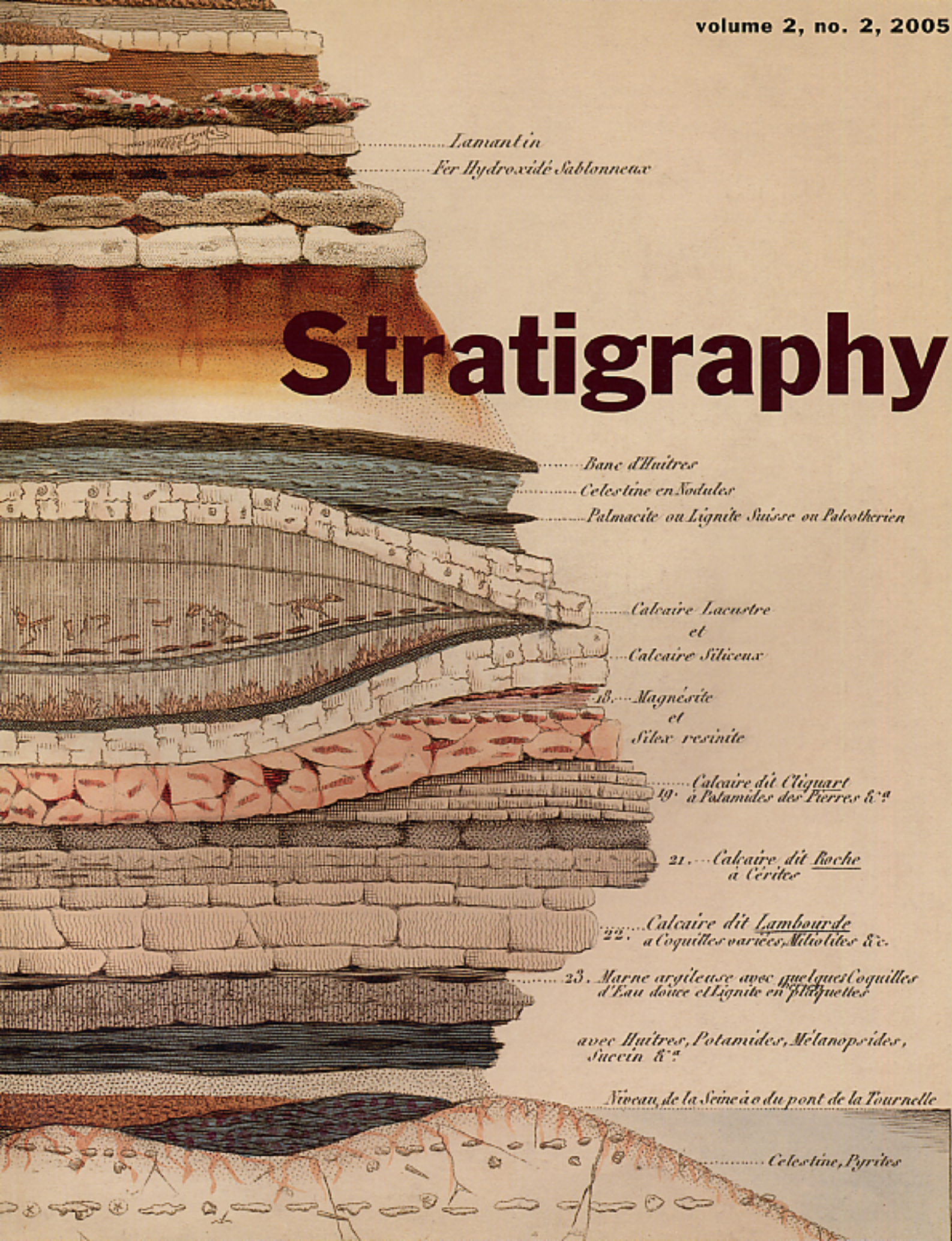


Stratigraphy



CONTENTS **Volume 2** **Number 2** **2005**

TEPHROSTRATIGRAPHY

101 Lindsay J. McHenry

Phenocryst composition as a tool for correlating fresh and altered tephra, Bed I, Olduvai Gorge, Tanzania

BIOSTRATIGRAPHY

117 T. Markham Puckett

Santonian-Maastrichtian planktonic foraminiferal and ostracode biostratigraphy of the northern Gulf Coastal Plain, USA

SEQUENCE STRATIGRAPHY

147 Kaiyu Liu

Upper Cretaceous Sequence Stratigraphy, Sea-level Fluctuations and Oceanic Anoxic Events 2 and 3, Northeastern Gulf of Mexico

CHRONOSTRATIGRAPHY

167 Markus Aretz and John Nudds

The coral fauna of the Holkerian/Asbian boundary stratotype section (Carboniferous) at Little Asby Scar (Cumbria, England) and implications for the boundary

ICS FORUM

191 Felix M. Gradstein

Definition and status of the Quaternary

Phenocryst composition as a tool for correlating fresh and altered tephra, Bed I, Olduvai Gorge, Tanzania

Lindsay J. McHenry

*Department of Biological Sciences, Rutgers University, 610 Taylor Road, Piscataway, New Jersey 08854 USA
email: lmchenry@uwm.edu

ABSTRACT: Olduvai Gorge, Tanzania, often cited as a textbook example of continental stratigraphic study (as depicted by Hay 1976 and others) is well known for its abundant Plio-Pleistocene fauna, hominin fossils, stone artifacts, and well-dated tephra layers used widely in the calibration of human evolution. However, precise stratigraphic correlation between various sites within Olduvai has been hampered by the rarity of unaltered volcanic glass suitable for geochemical characterization. Geochemical characterization of tephra for stratigraphic correlation purposes is difficult when fresh glass is absent or secondarily altered. A multi-component approach using the major and minor element compositions of phenocrysts and glass (where present) provides successful results at Olduvai and is proposed here as a viable methodology for use elsewhere. Six widespread Bed I (~2.1-1.79 myr) tephra layers of the Olduvai area are geochemically fingerprinted and used here to show the viability of the multi-component method. This method for geochemically fingerprinting tephra successfully provides a means for distinguishing similar looking tephra layers and for correlating fresh and altered tephra layers amongst a variety of depositional and diagenetic environments (freshwater wetlands, saline-alkaline lake, and fluvial plain). Application of this technique at Olduvai is providing high-resolution stratigraphic correlations and should prove applicable to other volcaniclastic sequences where tephra is poorly preserved.

INTRODUCTION

Tephrochronology provides stratigraphers a means for establishing regional correlations, time planes and chronological frameworks (e.g., Brown 1982; Feibel et al. 1989; Sarna-Wojcicki and Davis 1991; Brown et al. 1992; deMenocal and Brown 1999; and Perkins and Nash 2002). Compositional analysis of volcanic glass is the preferred method for geochemical tephrostratigraphy (Froggatt 1992, Feibel 1999), but this approach has a number of limitations. Fresh glass weathers very rapidly in many depositional environments (Hay 1960), and even slight degrees of alteration can significantly alter its composition (Cerling et al. 1985). Clean glass separates are generally difficult or impossible to make for particularly frothy or phenocryst-laden glasses, limiting potential analytical methods to high-spatial-resolution methods such as electron microprobe. Thus, high-precision trace-element analysis is difficult. Tephrochronology has rarely been applied in regions where fresh glass is absent (notable exceptions including work on Ordovician K-bentonites by Huff et al. 1992; Delano et al. 1994; and Kolata et al. 1996). Phenocryst composition is often used in New Zealand (e.g., Lowe 1988; Cronin et al. 1996a and b), but is rarely applied elsewhere (e.g., Izett et al. 1988).

Olduvai Gorge Bed I is an ideal site for testing tephrostratigraphic methods. Olduvai Gorge contains a rich paleontological and cultural record, preserved within sediments including numerous tephra layers. In attempts to provide a refined stratigraphic framework and develop wide-spread timeslices as part of the ongoing Olduvai Landscape Paleoanthropology Project (OLAPP)(Blumenshine and Peters 1998; Blumenshine et al. 2003), accurate identification of individual tephra layers preserved in a wide variety of depositional environments was needed. Fresh volcanic glass is rarely preserved,

as saline-alkaline lake and groundwater have altered most of the glass to zeolite and clay (Hay 1970). Fortunately, phenocrysts (augite, feldspar, titanomagnetite, amphibole) have been less affected by the diagenesis. The combination of geochemical information from fresh glass (where present) with the geochemistry of phenocrysts should allow unique characterization of individual pyroclastic units. Specifically, correlations could be made between exposures of fresh tephra and exposures of highly altered tephra from a saline-alkaline lacustrine depositional environment, where no geochemical correlations were previously possible.

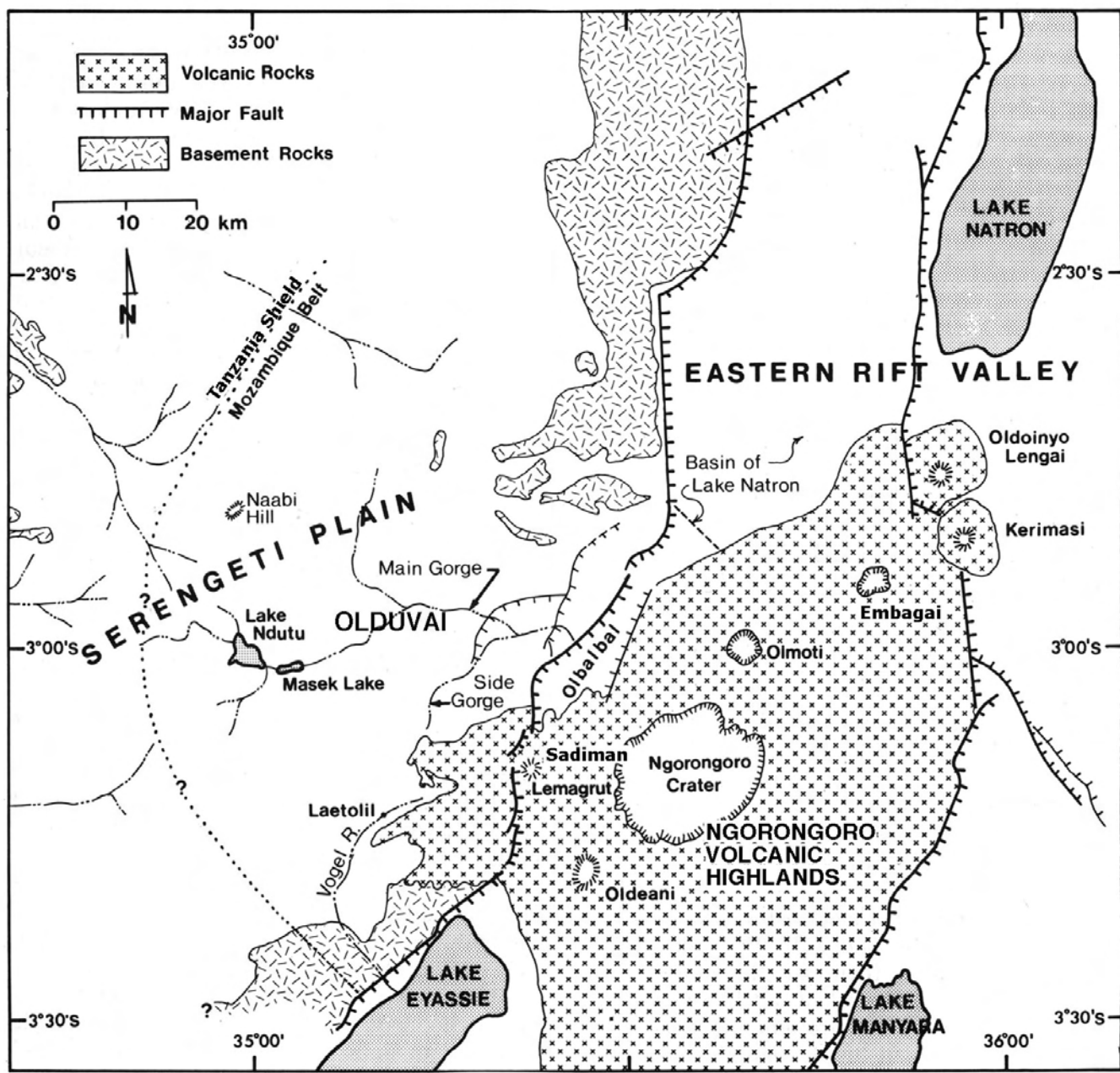
This paper examines and develops a multi-component technique for uniquely identifying and correlating altered tephra layers within the Olduvai Basin. This approach could be an important breakthrough in providing reliable correlation in the faulted and highly altered volcaniclastic sediments that are typical of continental rift settings.

GEOLOGIC SETTING AND STRATIGRAPHY

Olduvai Gorge is a 20-km long, deeply incised canyon located between the Serengeti Plains to the west and the Ngorongoro Volcanic Highlands (NVH) to the east and south (text-figure 1). Along its course, the gorge exposes a ~100m thick section of late Pliocene to Holocene sediments in addition to tephra layers, lava flows and ash flows. The gorge contains two main branches, the Main Gorge and Side Gorge, which meet in the central “Junction” area about 7km up from the mouth of the gorge (text-figure 2). A detailed introduction to the geology of Olduvai Gorge can be found in Hay (1976). Throughout this paper, tephra layers and localities will, where possible, be referred to using his nomenclature.

An extensive and compositionally varied tephra record is preserved at Olduvai, derived from the nearby Ngorongoro Volcanic Highlands (NVH). This volcanic province marks the

Present address: Department of Geosciences, University of Wisconsin - Milwaukee, 3209 N. Maryland Avenue, Milwaukee, WI 53211, USA.

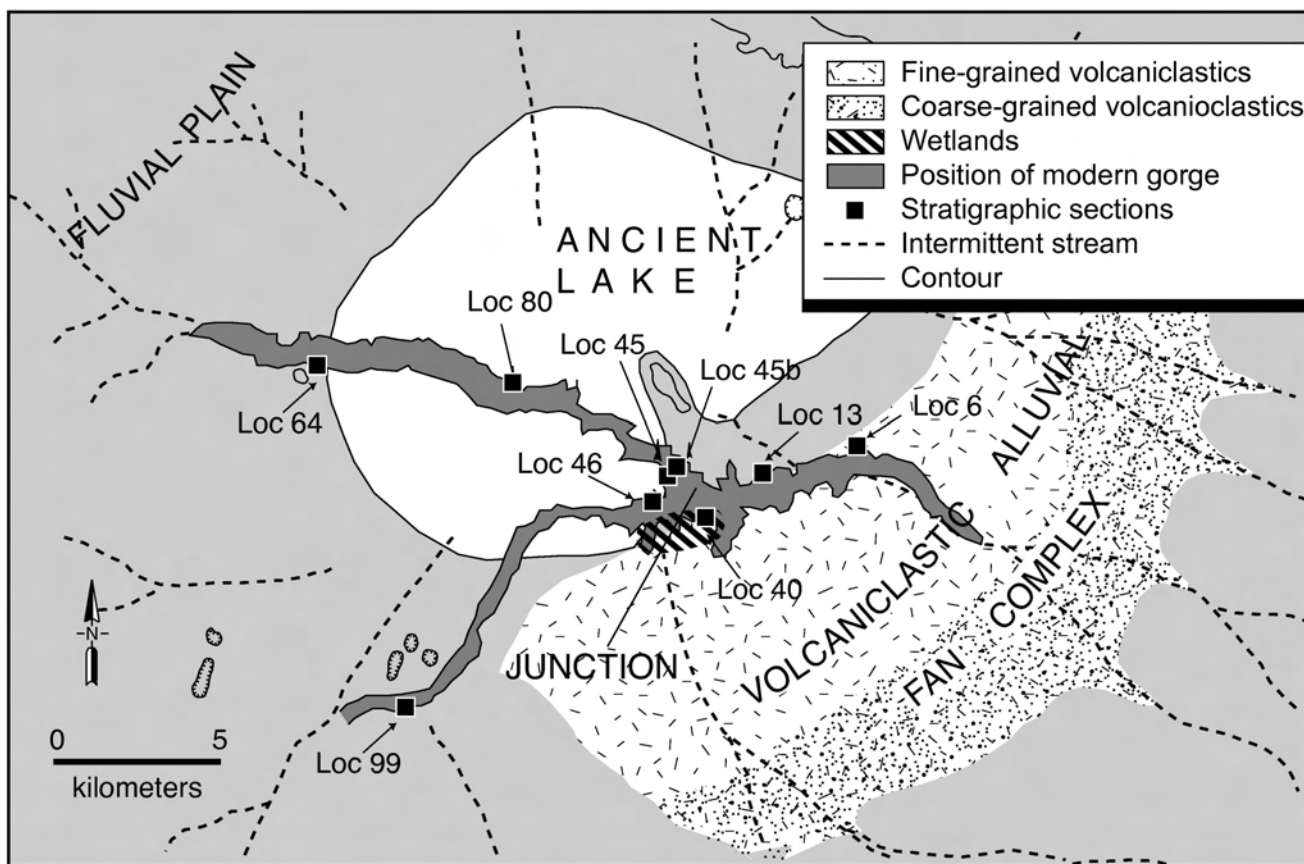


TEXT-FIGURE 1

Regional map showing the relative positions of Olduvai Gorge and the Ngorongoro Volcanic Highlands (NVH). Modified from Hay 1976.

southern end of the eastern branch of the East African Rift System, which includes the rift valleys and rift-related volcanics of Ethiopia, Kenya, and northern Tanzania (Baker et al. 1972). This paper focuses on the predominantly trachytic tephra record of upper Bed I, the oldest and thickest of the Olduvai beds (text-figure 3a). These late Pliocene- early Pleistocene tephra layers are more widely distributed and generally better preserved than the later tephra at Olduvai, are represented in a range of depositional and diagenetic environments, and cover a narrow compositional range that requires geochemical means to ensure proper identification and correlation. These tephra layers, named Tuff IB through Tuff IF from oldest (1.85 myr,

Blumenschine et al. 2003) to youngest (1.79 myr, Hay and Kyser 2001), are thought to have erupted from Olmoti or another volcano in the NVH (Hay 1976). A previously undefined tephra layer between Tuffs IE and IF, referred to as the Ng'eju Tuff after the local Maasai word for "new," is also included. These tephra layers vary from ash flows (meters thick) in the Eastern Volcaniclastic Alluvial Fan proximal to source, to airfall tuffs (centimeters thick) in the Lake and Fluvial Plain deposits (text-figure 2). Previous studies on the Olduvai tephra (Hay, 1976) focused on physical mapping, which proved to be insufficient in some areas of the gorge, particularly to the west (e.g., Blumenschine et al. 2003).



TEXT-FIGURE 2

Locality map of sample sites, showing upper Bed I/lower Bed II paleoenvironmental reconstructions based on Hay 1976, and Peters and Blumenschein 1995. The “Junction” includes Localities 45, 45b, 46, and 40 on this map, and the “saline-alkaline lake” section is at Locality 80. Tephra layers thin from east to the west across the basin. Saline-alkaline lake and groundwater caused extensive alteration to clay and zeolite throughout much of the Olduvai Basin. Modified from Ashley and Hay 2002.

METHODOLOGY

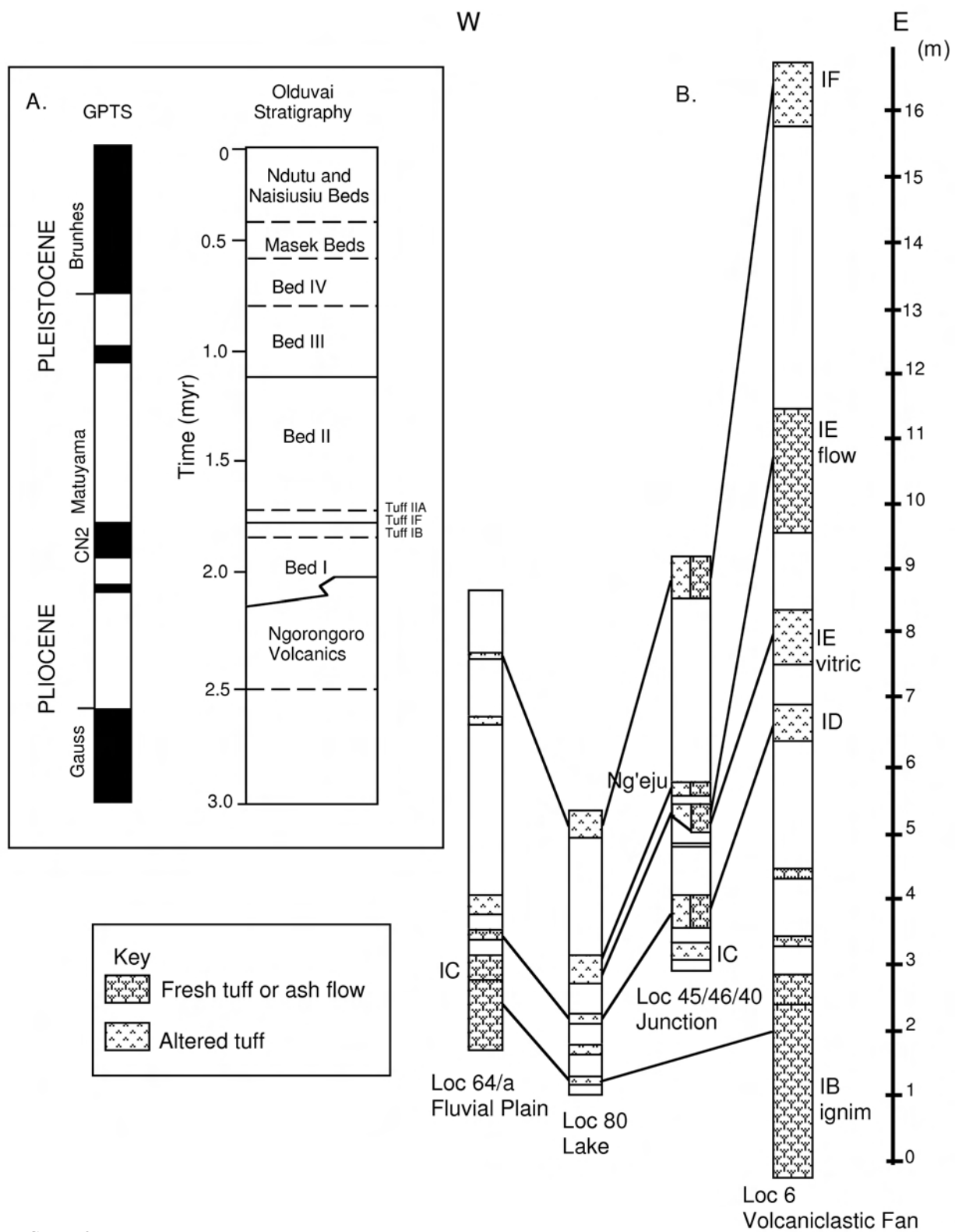
Field

Representative samples of the six tephra layers were chosen from sites in the central “Junction” area and Eastern Volcaniclastic Alluvial Fan. In this region, the tephra layers have been well constrained due to their importance in determining the stratigraphic placement of the Olduvai hominin fossil and artifact localities (Hay 1976). These localities are indicated on text-figure 2, and GPS coordinates for the sample sites are presented in Table 1. Tuffs IB and IE are best preserved in their ash flow facies at Locality 6 in the east, and these samples were analyzed along with the air fall samples from other sites. As not all tephra layers preserve fresh glass in the east, a few supplemental samples from the east and west were also chosen. For comparison between fresh and altered tephra, a series of presumably correlative tephra layers were collected at Locality 80, near the center of the saline-alkaline lake environment, where tephra preservation is poorest. Samples were collected at these and many other sites throughout the basin in collaboration with Richard Hay to assure integration into his earlier stratigraphic studies (Hay 1976). Stratigraphic sections for the chosen sites are shown in text-figure 3b.

Laboratory

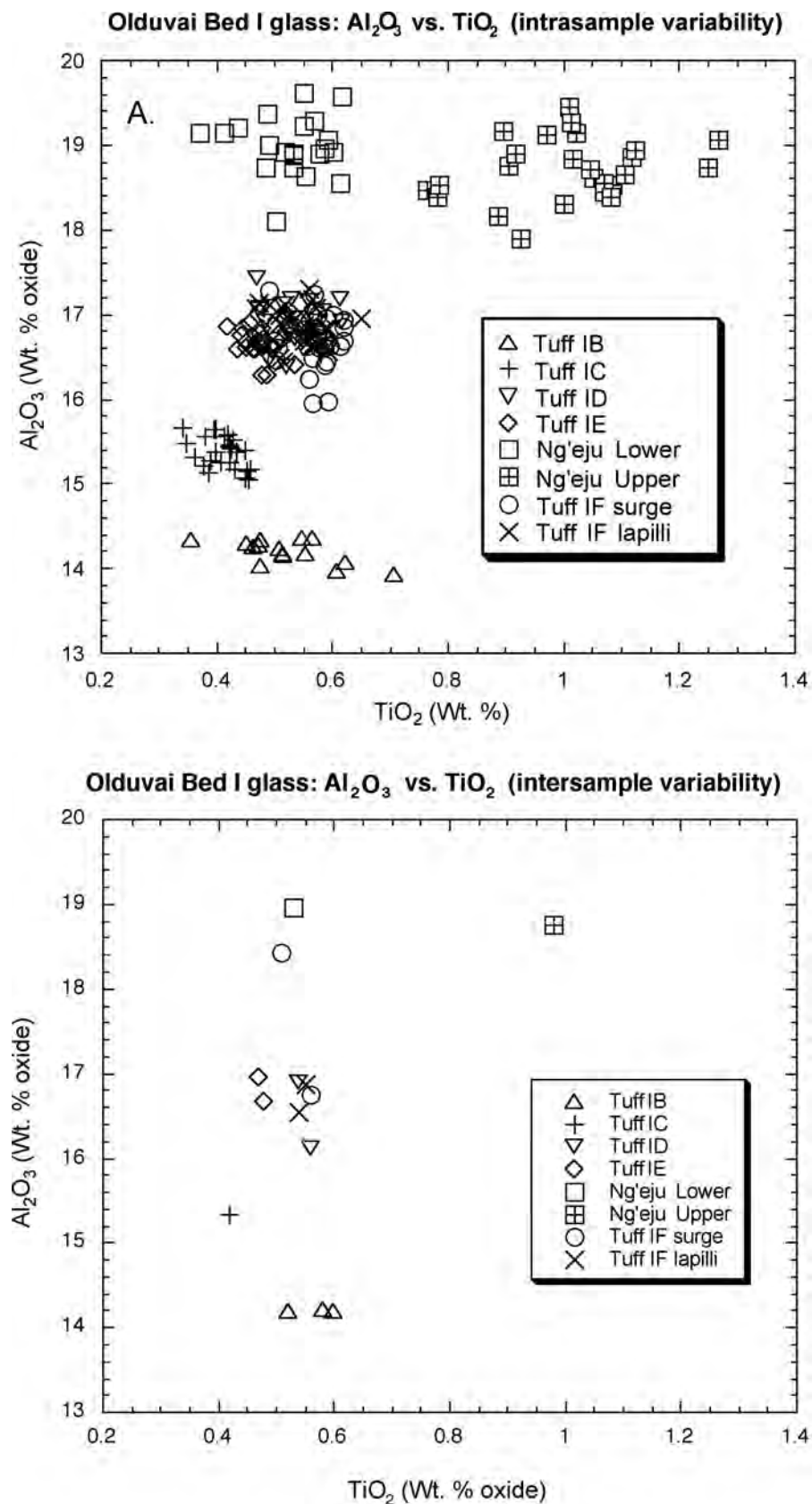
Several grams of each sample were crushed in a mortar and pestle and sieved, with the 60-mesh size fraction reserved for analysis. Each sample was washed for less than one minute in 5% HF in a sonic bath, to remove adhering clays and altered glass. Washed samples were rinsed three times in distilled water to remove the acid. The washed samples were dried and then separated into non-magnetic and magnetic splits using a Frantz isodynamic magnetic separator. Grain mounts were made by hand-picking individual grains of feldspar, oxide, and mafic phenocrysts and glass. Grains that showed evidence of rounding or discoloration were excluded, and in the least altered samples grains with adhering glass were preferentially selected. About 15–60 grains of glass and of each type of phenocryst were selected for each sample. These grains were mounted in epoxy, polished, and carbon coated for analysis by electron microprobe. At least one thin section for each tephra layer was also prepared, polished, and carbon coated.

Analysis of phenocrysts was conducted on a JEOL JXA-8600 Superprobe operating at 20 kV and 20 na with the electron beam rastering over a 4 μm square. A 20-second count time was used for each element. Glass analyses were conducted at 15 kV, 15 na with the beam rastering over a 12 μm square. A volatile cor-



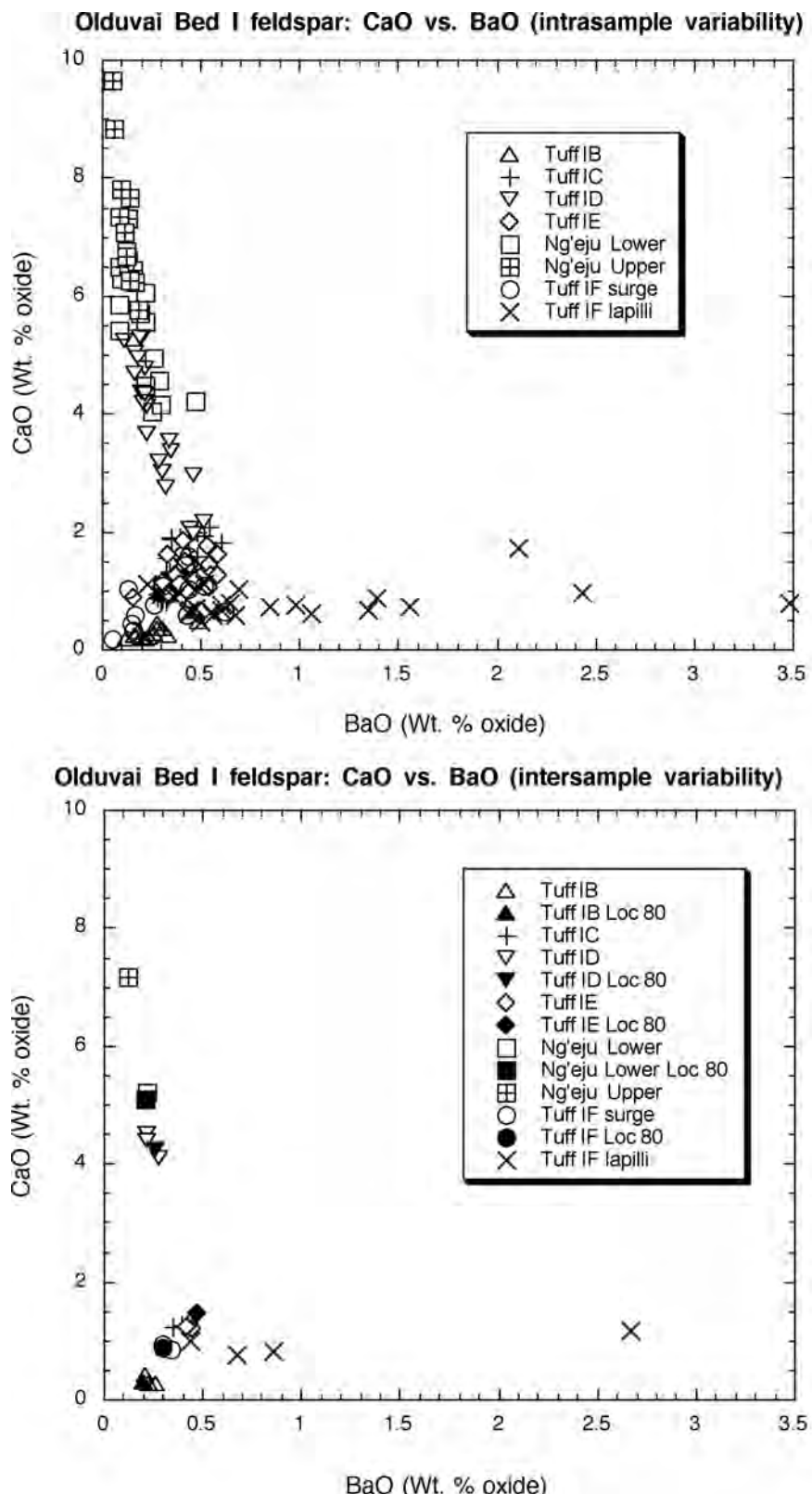
TEXT-FIGURE 3

A. Stratigraphic divisions within the Olduvai Basin. Geomagnetic polarity time scale (GPTS) after Berggren et al. 1995. Correlation to the GPTS is based on dates from Walter et al. 1992 and Hay 1976. Olduvai magnetics of Tamrat et al. 1995. Dashed lines are used either where insufficient age control is available (for Bed transitions) or for important tephra layers that do not mark Bed transitions (Tuffs IB and IIA). The focus of this paper is the tephra record from upper Bed I. Modified from Hay 1976. B. Stratigraphic sections several sites sampled for this paper, showing the relative positions and thicknesses of upper Bed I tephra layers and their reconstructed depositional environments. Nearby similar stratigraphic sections (e.g., Loc 40, 45, 45b, and 46) have been merged for simplicity. Distances between sections are not to scale, but can be determined using text-figure 2. All correlations presented were confirmed geochemically in this study.



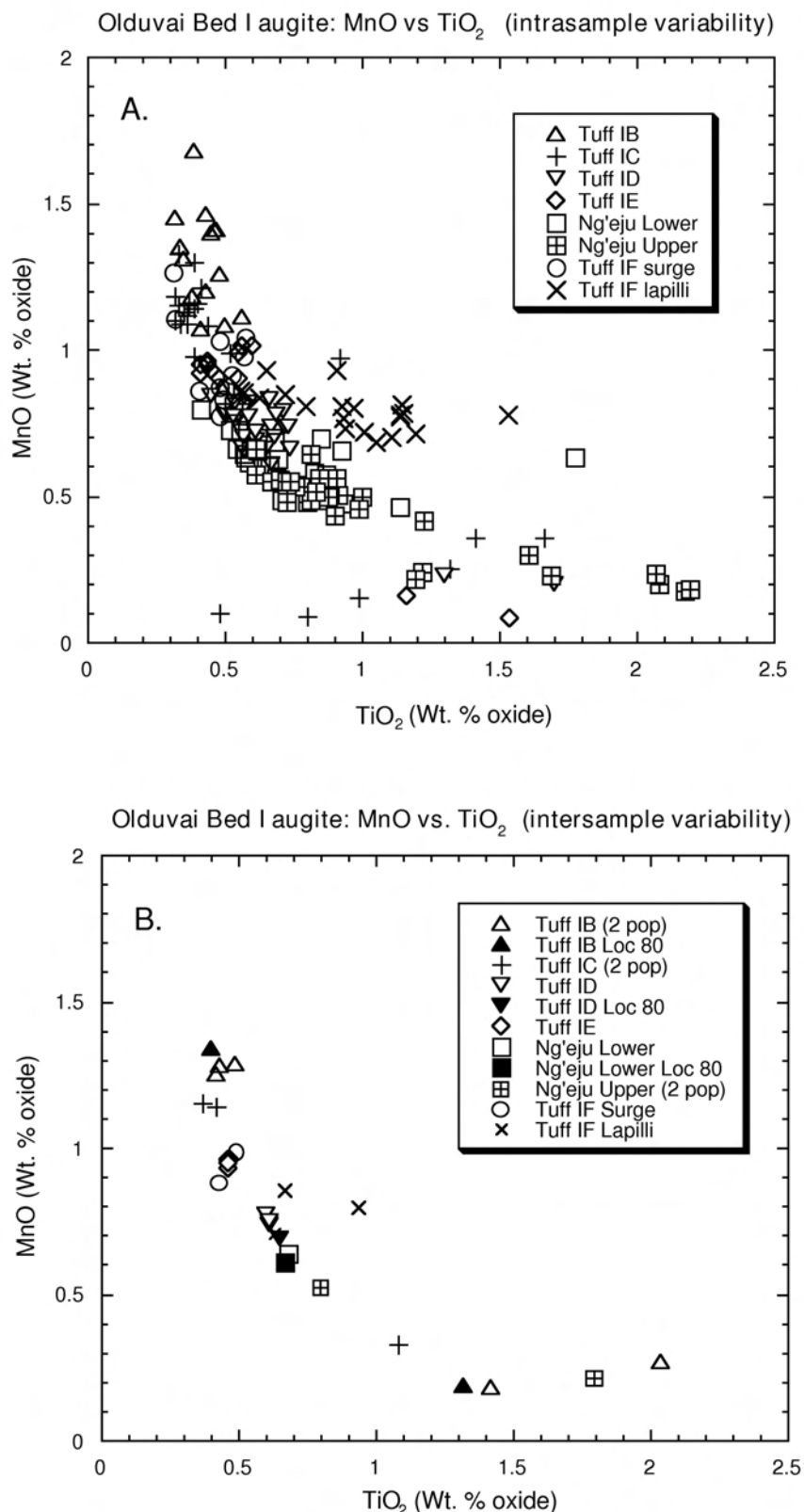
TEXT-FIGURE 4

Al_2O_3 vs. TiO_2 in Olduvai Bed I tephra glasses, as measured by electron microprobe. Note the distinctively high aluminum content of the Ng'eju Tuff, and the similarity between Tuffs ID, IE, and IF. Plot A shows the compositional range within a single sample for each tephra layer (Tuff IB: Locality 6; Tuff IC: Locality 64; Tuff ID: Locality 40; Tuff IE: Locality 6; Ng'eju Lower Tuff and Upper Tuff: Locality 46; Tuff IF: Locality 40). Plot B shows the averages for all samples of each tephra layer.



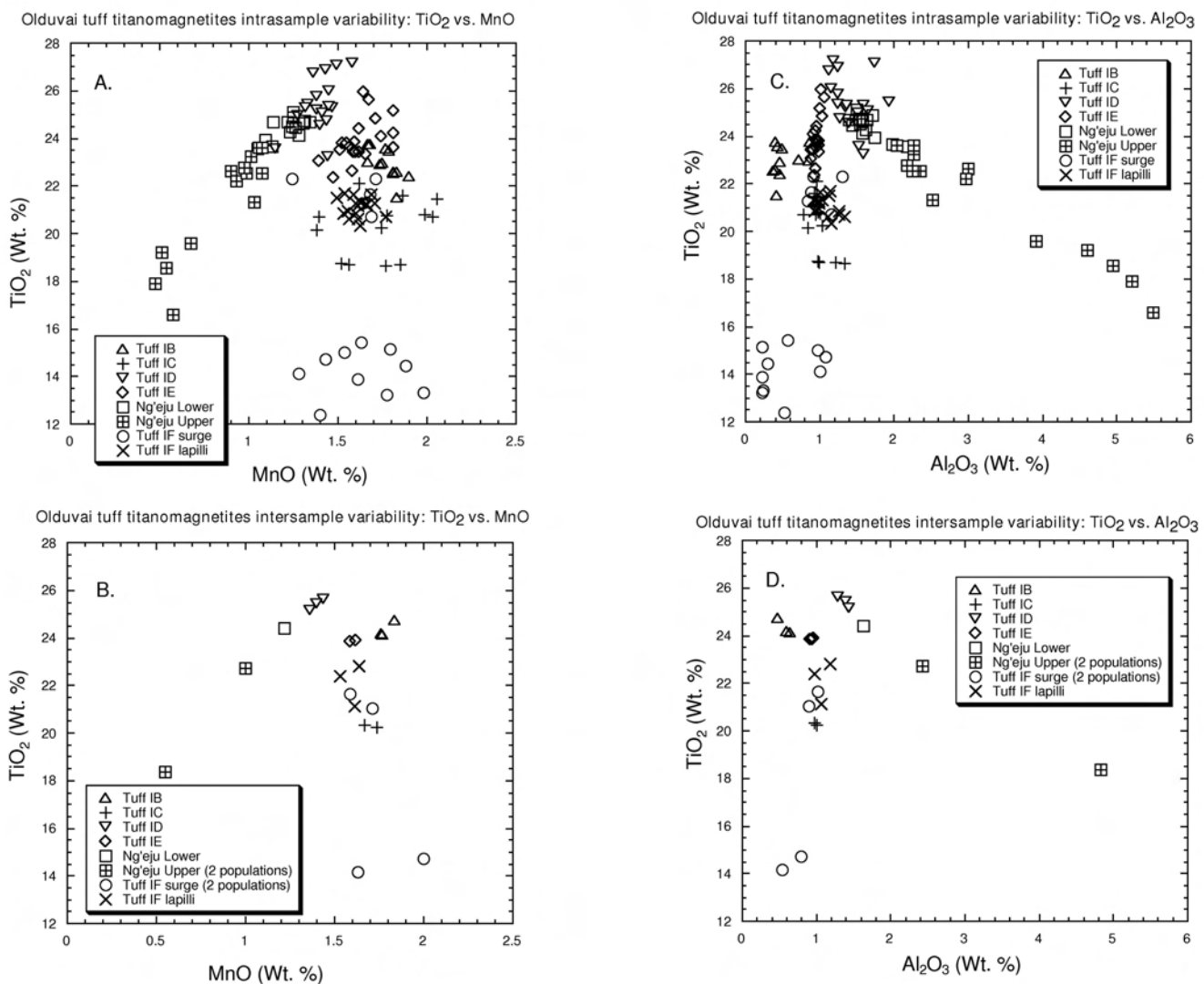
TEXT-FIGURE 5

A. CaO vs. BaO in Olduvai Bed I tephra feldspar, as measured by electron microprobe, showing the compositional range within a single sample for each tephra layer (Tuff IB: Locality 6; Tuff IC: Locality 45b; Tuff ID: Locality 45; Tuff IE: Locality 6; Ng'eju Lower Tuff and Upper Tuff: Locality 46; Tuff IF: Locality 40). Note the distinctively high barium concentration of the Tuff IF lapilli, and the distinctively low concentration of the Tuff IB feldspar. The Tuff IF grain with the highest barium concentration (3.48%) is excluded. B. Average compositions for feldspar in each tephra layer at a number of sites. Dark symbols indicate feldspar compositions for the Locality 80 (saline-alkaline lake) section tephra layers.



TEXT-FIGURE 6

MnO vs. TiO_2 in Olduvai Bed I tephra augites, as measured by electron microprobe. Tuff IB has high and the Upper Ng'eju Tuff has distinctively low MnO. A second (minor) high- TiO_2 population is present in most of the tephra layers. Plot A shows the compositional range within a single sample for each tephra layer (same samples as text-figure 5A). B shows the average composition for the major compositions for each tephra layer at a number of sites. Dark symbols indicate augite compositions for the Locality 80 (saline-alkaline lake) section tephra layers. The high TiO_2 population was not observed in Tuff IB at Locality 6, though it is present in most other Tuff IB samples.



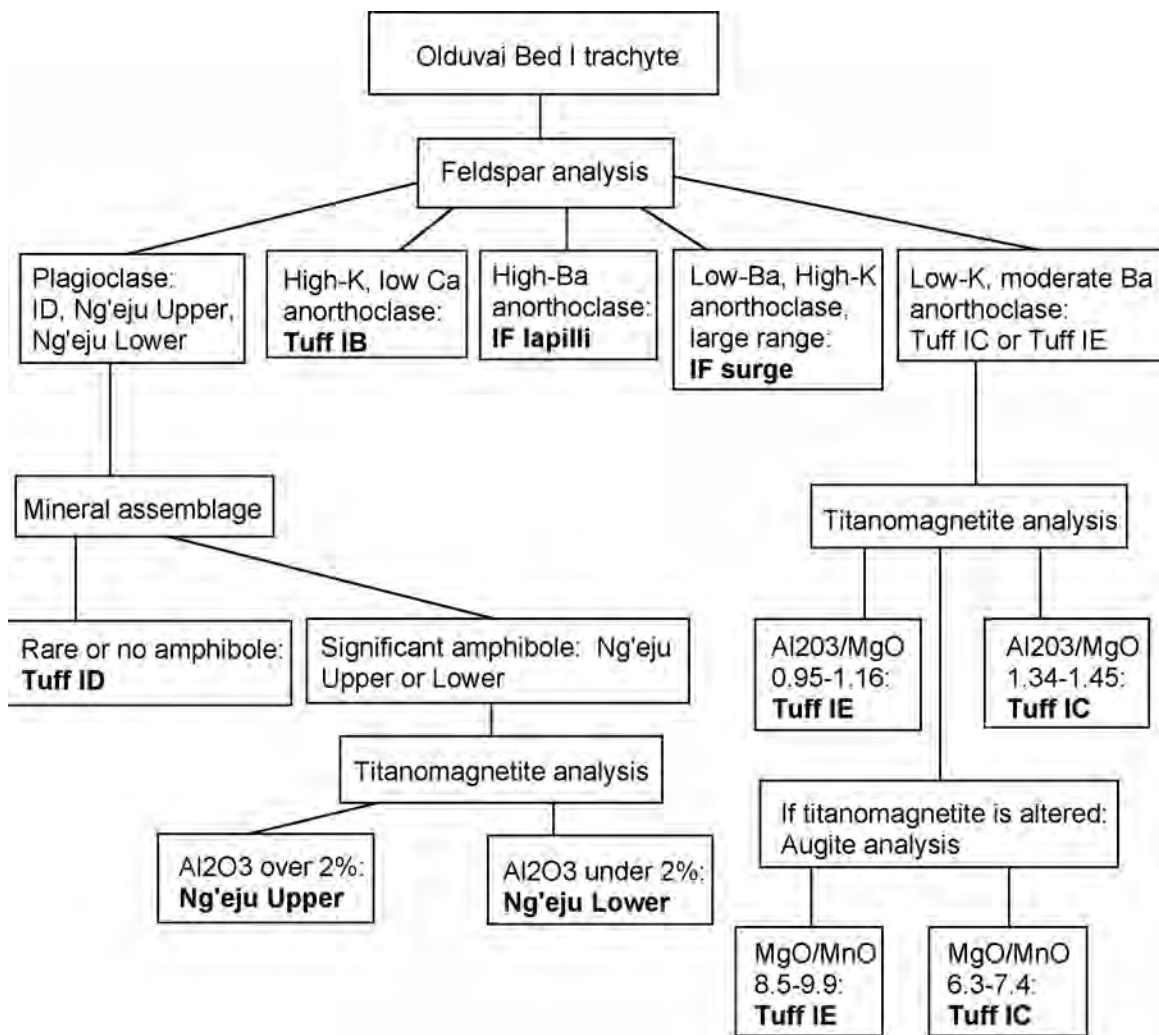
TEXT-FIGURE 7

A. TiO_2 vs. MnO in Olduvai Bed I tephra titanomagnetites, as measured by electron microprobe, showing the compositional range within a single sample for each tephra layer (same samples as Figure 5A). Plot **B** shows the average composition for the main population for each tephra layer at a number of sites. The Tuff IF surge has a distinctive bimodal composition. **C.** TiO_2 vs. Al_2O_3 in Olduvai Bed I tephra titanomagnetites, as measured by electron microprobe, showing the compositional range within a single sample for each tephra layer (same samples as A). Plot **D** shows the average composition for the major compositions for each tephra layer at a number of sites.

rection routine (Donovan 2000a), in which the 20-second count time was broken down into 10 segments of 2 seconds each, was applied to the first element measured on each spectrometer for the glass samples to minimize the effect of Na, K, and Si loss during analysis. Si, Ti, Al, Fe, Mg, Ca, Na, K, Ba, and Mn were all analyzed for most samples. A combination of feldspar, amphibole, and pyroxene standards was used for calibration for the glass, feldspar, and mafic phenocrysts, including Lake County Plagioclase, Tiburon Albite, Kakanui Anorthoclase, Microcline, Great Sitkin Anorthite, Kakanui Hornblende, Kakanui Augite, Natural Bridge Diopside, and Tatahouine Orthopyroxene. Ba was calibrated to benitoite and Mn to a synthetic tephroite. For the oxide minerals, Fe and Ti were calibrated to magnetite and ilmenite, respectively. Glass standards were not used for calibration, but were analyzed to monitor volatile loss. Accessory minerals were identified in the thin sections but not quantitatively analyzed.

For most samples, a single point was analyzed on each grain, as far as possible from the edge of the grain and any cracks or inclusions. Few grains showed compositional zoning; where zoning was present, a point was selected within the innermost zone as determined by electron backscatter imaging. Tests involving more (3-7) analyses per grain showed no significant change in the inter-grain standard deviations.

Feldspar, mafic, and oxide phenocrysts and glass in thin sections were also analyzed. In the thin sections, the textural relationships of the different minerals were more obvious than in the grain mounts, and phenocrysts within altered lapilli or associated with zeolite or clay still preserving volcanic glass textures could be selectively analyzed, excluding non-primary grains. Little difference in phenocryst composition was found between samples of the same tephra layer in grain mounts and thin sections, suggesting that detrital contamination is not a



TEXT-FIGURE 8
Flowchart for Olduvai Bed I trachyte tephra identification using phenocryst compositions.

problem in the primary airfall or only slightly reworked phases of the Olduvai Bed I tephra.

Absorption, fluorescence and backscatter corrections were conducted using the phi-rho-z routine provided by the Probe for Windows software package, optimized for silicates by John Armstrong (Donovan 2000b). All data were converted to weight percent oxide format. First, analyses with low analytical totals (<96% for feldspar and mafic, <90% for glass and oxide grains) were removed. The 90% cutoff for glasses was arbitrary, and intended to omit glass shards with significant post-depositional alkali loss. Each set of analyses was qualitatively divided into different populations based on consistent differences in composition (e.g., Fe-rich from Mg-rich augite). Means and standard deviations were calculated for each population, and any analysis more than 3 standard deviations from the mean in any detectable element was excluded and the means recalculated. Stoichiometries were calculated based on 6 oxygens (pyroxene), 8 oxygens (feldspar), and 23 oxygens (amphibole) to ensure proper identification of the different mineral phases.

RESULTS

Analytical results for glass, augite, feldspar, and titanomagnetite are reported, by mineral, in Tables 2-5. Based on glass composition, most of the tephra layers are trachytes, except for Tuff IF, a phonolite, and the Ng'eju Tuff, a trachyandesite (after LeBas et al. 1986). Results for the individual tephra layers at selected localities are outlined below, in chronological order. All concentrations are presented in weight percent oxide format. Data plots (text-figures 4-7) show both the variability within an individual representative sample, and a comparison of the average compositions for multiple samples of each tephra layer.

Tuff IB, which forms an ash flow deposit in the east (Localities 6, 13) and an airfall deposit to the west, has a distinct glass composition. The concentrations of SiO₂ (60.5%), Al₂O₃ (14.2%), and TiO₂ (0.57%) in the glass help to distinguish Tuff IB from the others (text-figure 4). Its K-rich, Ca-poor and Ba-poor anorthoclase phenocrysts (Ab₇₃Or₂₄An₁) differ from those of any other Bed I tephra layer (text-figure 5). At Locality 6, its augite phenocrysts (Ca₄₃Mg₂₄Fe₃₃) are comparatively higher in

TABLE 1
GPS coordinates for the sample sites.

Locality	Latitude	Longitude	Environment
6	S 02°58'38.1"	E 35°23'38.1"	Eastern Volcaniclastic Alluvial Fan
13	S 02°59'02.3"	E 35°22'29.4"	Eastern Volcaniclastic Alluvial Fan
40	S 02°59'32.1"	E 35°21'25.0"	Eastern Volcaniclastic Alluvial Fan
45	S 02°59'14.1"	E 35°20'52.7"	Junction
45b	S 02°59'08.0"	E 35°20'50.7"	Junction
46	S 02°59'25.6"	E 35°20'56.1"	Junction
80	S 02°57'40.9"	E 35°18'29.4"	Saline-alkaline lake
99	S 03°02'41.0"	E 35°16'20.3"	Side Gorge
64	S 02°57'06.8"	E 35°14'28.8"	West

MnO than those of the other major tephra layers (text-figure 6). A second, minor augite population is represented at many sites, with a MgO-rich composition of $\text{Ca}_{43}\text{Mg}_{42}\text{Fe}_{15}$. Rare phenocrysts of amphibole are also present, and the Tuff IB titanomagnetite composition (usp₆₂mgt₃₈) differs slightly from the other tephra layers in Al_2O_3 (0.60%) (text-figure 7).

Tuff IC, which had not previously been identified outside of the Junction, is trachytic in composition and is highly altered throughout its exposures. At Locality 45b, this tephra layer contains high-Ca, low-K, moderate-Ba anorthoclase phenocrysts ($\text{Ab}_{77}\text{Or}_{16}\text{An}_6$), similar in composition to Tuff IE anorthoclase (text-figure 5). Its augites ($\text{Ca}_{44}\text{Mg}_{25}\text{Fe}_{31}$) and titanomagnetites (usp₅₄mgt₄₆) are distinct from the other tephra layers, especially in their TiO_2 concentrations (text-figures 6 and 7). Fresh glass from a potentially correlative tephra layer at Locality 64 in the west is subtly different from the other tephra layers based on its TiO_2 (0.42%), CaO (1.09%), and Al_2O_3 (15.34%) concentrations (text-figure 4).

Tuff ID is a trachytic tephra layer found extensively throughout the Junction and in the Eastern Volcaniclastic Alluvial Fan. At Locality 45, it contains plagioclase phenocrysts (range: $\text{Ab}_{77}\text{Or}_{10}\text{An}_{12}$ to $\text{Ab}_{63}\text{Or}_3\text{An}_{33}$, average: $\text{Ab}_{72}\text{Or}_6\text{An}_{22}$) that are on average slightly less Ca-rich than those of the Ng'etu Tuff (text-figure 5). Tuff ID differs significantly in its augite ($\text{Ca}_{46}\text{Mg}_{31}\text{Fe}_{23}$) composition (MnO: 0.74%; TiO_2 : 0.62%) and its titanomagnetite (usp₇₁mgt₂₉) composition (TiO_2 : 25.39%, MnO: 1.40%) (text-figures 6 and 7). It also lacks significant amphibole. Its glass is unique, distinguishable from the other tephra layers by its CaO (1.52%) and FeO (4.95%) concentrations.

Tuff IE is another trachytic volcanic unit that prior to this study had only been recognized in its ash flow facies in the Eastern Volcaniclastic Alluvial Fan. At Locality 6, it contains a high-Ca, low-K anorthoclase ($\text{Ab}_{76}\text{Or}_{17}\text{An}_6$), indistinguishable from Tuff IC anorthoclase (text-figure 5). Its augite ($\text{Ca}_{47}\text{Mg}_{28}\text{Fe}_{25}$) differs in TiO_2 (0.46%) and MnO (0.95%), and its titanomagnetite (usp₇₁mgt₂₉) differs in TiO_2 (23.87%) and Al_2O_3 (0.94%) (text-figures 6 and 7). Its glass is very similar to the other Olduvai trachytic tephra layers. This tephra layer is now identified in the Junction and to the west.

The Ng'etu Tuff, which was not mentioned by Hay (1976) in his stratigraphic mapping, is present in the Junction. Situated between Tuffs IE and IF, it is often topped by a darker layer, which at some sites is useful for easy field identification. At Locality 46, the lower layer is trachytic/trachyandesitic and contains plagioclase similar to that in Tuff ID (range: $\text{Ab}_{79}\text{Or}_{13}\text{An}_{12}$ to $\text{Ab}_{52}\text{Or}_2\text{An}_{45}$, average: $\text{Ab}_{66}\text{Or}_6\text{An}_{27}$) (text-figure 5). However, its augite ($\text{Ca}_{47}\text{Mg}_{31}\text{Fe}_{22}$) and titanomagnetite compositions (usp₆₅mgt₃₅) are unique (text-figures 6 and 7), and it is easily distinguished from Tuff ID by the presence of abundant amphibole. The upper layer is trachyandesitic. Its feldspars are on average more Ca-rich ($\text{Ab}_{61}\text{Or}_3\text{An}_{35}$) than those of the lower layer (text-figure 5). It has two titanomagnetite compositions, both of which are richer in Al_2O_3 (2.43 and 4.83%) and MgO (2.67 and 4.99%) and poorer in MnO (1.00 and 0.55%) than the other Upper Bed I tephra layers, including the Lower Ng'etu Tuff. Its augite ($\text{Ca}_{47}\text{Mg}_{36}\text{Fe}_{19}$) differs substantially in Al_2O_3 (1.85%), TiO_2 (0.79%), SiO_2 (52.81%), FeO (11.52%), MgO (11.99%), and MnO (0.53%) (text-figures 6 and 7). A second augite population ($\text{Ca}_{45}\text{Mg}_{40}\text{Fe}_{14}$) is also present. Its glass is richer in FeO (6.84%), MgO (1.19%), TiO_2 (0.98%), and CaO (2.48%) (text-figure 4).

Tuff IF is the most distinctive and thickest volcanic deposit in the Junction, and is also recognized in the Eastern Volcaniclastic Alluvial Fan. Originally interpreted as water-lain based on its plane laminated and cross bedded upper and lower units (Hay 1976), it has more recently been interpreted as pyroclastic surge deposits, with an airfall lapilli layer between distinct surge layers (OLAPP, ongoing study). At Locality 40, the surge units are rich in trachytic lava fragments with little glass. The lava fragments are distinct from anything seen in the Olduvai tephra: they contain sodic augite, aenigmatite, sodic amphibole, low-K sanidine, occasional sodalite, analcite, and titanomagnetite. This assemblage is occasionally represented in the loose phenocryst population outside of the lava fragments, but is not found within the lapilli. Anorthoclase from the loose phenocryst population has variable composition (range: $\text{Ab}_{74}\text{Or}_{21}\text{An}_5$ to $\text{Ab}_{64}\text{Or}_{34}\text{An}_2$, average: $\text{Ab}_{66}\text{Or}_{30}\text{An}_3$), generally more K-rich than the other tephra layers. The augite and titanomagnetite phenocrysts in Tuff IF are variable, probably due to the contribution of the lava fragments. The dominant augite population in the lower surge unit ($\text{Ca}_{46}\text{Mg}_{27}\text{Fe}_{28}$) has higher Na_2O (1.05%) than any of the other tephra layers. There are two distinct and limited compositions represented by the titanomagnetite phenocrysts (usp₅₆mgt₄₄ and usp₃₅mgt₆₅). The upper surge layer contains a mixture of the compositions found in the lower surge and the lapilli layers.

Lapilli are found in small concentrations within the Tuff IF surge deposits, but also form a widespread air-fall deposit almost devoid of lava fragments. The air-fall lapilli are vitric with few small phenocrysts. Their anorthoclase phenocrysts form a single, tight population distinct from that of the surge feldspars, with higher Na_2O and BaO and lower K_2O ($\text{Ab}_{74}\text{Or}_{21}\text{An}_4\text{Cn}_1$). The BaO concentration of these grains is extremely variable, some are close to the values of the other Olduvai tephra layers (as low as 0.2 wt. %), whereas others have BaO rich cores (up to 3.5 wt. %) (text-figure 5). The average augite in the lapilli ($\text{Ca}_{44}\text{Mg}_{34}\text{Fe}_{23}$) is high in TiO_2 (0.78%) and Al_2O_3 (1.33%) and is distinct from that in the surge layers (text-figure 6).

The glasses of the surge and lapilli layers are very similar in most elements measured. They differ slightly from the other tephra in

TABLE 2
Olduvai Bed I tephra glass compositions, as measured by electron microprobe.

Tuff Locality	IB 6	IB 13	IB 64	IC 64	ID 40	ID 46	IE 6	IE 40	Ngeju 46 lower	Ngeju 46 upper	IF 40 lapilli	IF 99 lapilli	IF 40 surge	IF 99 surge
unit/pop									lower	upper	lapilli	lapilli	surge	surge
n	15	26	19	28	25	16	25	23	27	27	27	10	15	18
SiO ₂	60.00	61.57	59.91	60.05	59.37	58.16	60.25	58.80	59.52	56.47	58.27	57.13	58.15	57.74
St dev	1.14	1.17	0.98	1.06	1.11	0.81	0.86	2.48	1.50	1.58	0.47	0.51	1.88	0.78
TiO ₂	0.52	0.58	0.60	0.42	0.54	0.56	0.48	0.47	0.53	0.98	0.55	0.54	0.51	0.56
St dev	0.08	0.08	0.17	0.04	0.04	0.11	0.03	0.08	0.06	0.16	0.04	0.14	0.04	0.24
Al ₂ O ₃	14.19	14.20	14.18	15.34	16.90	16.12	16.66	16.96	18.96	18.76	16.88	16.54	18.43	16.74
St dev	0.14	0.39	0.55	0.23	0.23	0.26	0.17	1.11	0.32	0.39	0.21	0.15	0.32	0.18
FeO	5.41	5.83	5.71	5.36	4.72	5.18	4.65	5.31	4.92	6.84	5.19	5.70	5.51	5.47
St dev	0.18	0.25	0.36	0.22	0.19	0.41	0.21	0.47	0.24	0.59	0.17	0.43	0.11	0.39
MnO	0.27	0.28	0.25	0.23	0.17	0.20	0.18	0.20	0.18	0.22	0.24	0.20	0.27	0.22
St dev	0.14	0.10	0.10	0.10	0.08	0.04	0.05	0.06	0.11	0.08	0.10	0.05	0.09	0.03
MgO	0.34	0.31	0.34	0.30	0.40	0.45	0.34	0.35	0.49	1.19	0.47	0.54	0.48	0.50
St dev	0.07	0.10	0.14	0.06	0.06	0.10	0.03	0.13	0.07	0.24	0.03	0.01	0.02	0.03
CaO	0.90	1.07	1.00	1.09	1.44	1.59	1.02	0.93	1.20	2.48	0.89	0.86	0.69	0.75
St dev	0.04	0.15	0.21	0.06	0.08	0.25	0.04	0.24	0.18	0.51	0.04	0.24	0.09	0.23
Na ₂ O	7.48	7.48	7.64	7.31	7.08	6.27	7.63	6.94	6.02	6.36	8.19	7.09	7.12	7.62
St dev	0.39	1.13	0.76	0.45	0.89	0.67	0.42	0.67	1.33	0.57	0.97	0.99	1.42	1.76
K ₂ O	4.29	4.24	4.08	4.04	3.87	3.76	4.35	4.31	4.01	3.52	4.27	4.46	4.36	4.65
St dev	0.23	0.32	0.45	0.21	0.20	0.20	0.13	0.26	0.28	0.46	0.28	0.22	0.41	0.29
BaO	0.15	0.16	0.16	0.09	0.16	0.15	0.10	0.11	0.18	0.21	0.11	0.00	0.09	0.01
St dev	0.05	0.09	0.12	0.05	0.06	0.05	0.07	0.07	0.06	0.06	0.06	0.00	0.07	0.04
SUM	93.54	95.71	93.87	94.23	94.64	92.44	95.66	94.37	96.02	97.02	95.07	93.06	95.60	94.26
St dev	1.40	1.57	1.39	1.38	1.68	1.00	1.04	2.52	1.91	1.74	1.19	0.82	2.01	1.51

All concentrations in wt.% oxide.

All analyses conducted by electron microprobe operating at 15 kV, 15 na, 12-micron raster area.

n= number of glass shards analyzed.

Locality numbers after Hay (1976).

SiO₂, Na₂O and K₂O, resulting in a phonolite compositional range for Tuff IF. In other elements, Tuff IF glass is indistinguishable from other Bed I trachytic tephra layers (text-figure 4).

The tephra layers preserved in the saline-alkaline lake deposits at Locality 80 were also analyzed. There is no fresh glass preserved and even the titanomagnetite phenocrysts are altered or absent, limiting the number of minerals that can be used for characterization and identification. Fortunately, feldspar, augite, and amphibole phenocrysts remain intact. Many feldspar phenocrysts at Locality 80 had overgrowths of K-feldspar, which were avoided by analyzing the pristine cores.

DISCUSSION

Significant differences between the tephra layers are found using a combination of feldspar, augite, and titanomagnetite compositions, and the presence and absence of amphibole. A summary of some of the major distinguishing features of each of these Olduvai Bed I tephra layers is presented in text-figure 8. Two of the trachytes (Tuffs IB and IF) are distinguished using feldspar major element composition alone, with a more rigorous identification possible when augite and titanomagnetite compositions are also used. Tuffs IC and IE contain very similar feldspar, thus requiring the use of other minerals to distin-

guish between them. The plagioclase-bearing tephra layers (Tuff ID and the Ng'eju Tuff) have very similar plagioclase compositions but differ in augite and titanomagnetite compositions. The presence of significant amphibole also helps distinguish Tuff IF and the Ng'eju Tuff from the others.

In general, the oxide phenocrysts provided the greatest compositional contrasts for distinguishing among the Olduvai Bed I trachytes. The variation in oxide composition between different samples of the same tephra layer was very low, with minimal overlap with the compositional ranges of the other tephra layers. The bimodal oxide composition of Tuff IF is particularly distinctive.

The Locality 80 lacustrine samples contained no fresh glass, which prevented the application of traditional glass-based geochemical correlation techniques, and contained no pristine oxide minerals. However, the cores of the feldspar and augite phenocrysts remained intact, and combined with stratigraphic position and the presence or absence of amphibole, can be used to uniquely identify Tuffs IB, ID, IE, Ng'eju, and IF. The black symbols in text-figures 5 and 6 represent phenocrysts from the Locality 80 samples, for comparison to the fresher tephra com-

TABLE 3
Olduvai Bed I tephra augite compositions, as measured by electron microprobe.

Tuff Locality	IB * 6	IB 13	IB 13	IB * 80	IB * 80	IB 64	IB 64	IC 45b	IC 64	ID 40	ID 45	ID 80	ID 64	IE 6 flow	IE 6 vitric	IE 40	IE 45	Ngeju 46 lower	Ngeju 80 lower	Ngeju 46 upper	Ngeju 46 upper 1	Ngeju 40 upper 2	IF 99 surge	IF 40 lapilli	IF 99 lapilli	IF 64
n	15	15	4	12	4	15	2	17	17	30	33	17	16	25	21	22	14	20	12	23	8	8	4	21	16	
SiO ₂	49.06	50.62	50.85	52.44	47.28	49.45	49.31	50.85	50.10	50.83	50.67	48.22	52.62	51.50	50.29	50.52	50.08	52.85	49.09	52.81	51.00	52.12	52.13	50.93	51.55	51.69
St dev	0.79	0.86	0.56	1.18	1.07	2.14		0.67	0.58	0.60	1.29	1.28	0.53	0.94	0.59	0.56	0.94	0.81	0.65	0.72	1.18	0.96	1.58	0.58	1.34	1.14
TiO ₂	0.43	0.49	1.42	0.40	1.32	0.42	2.04	0.37	0.42	0.60	0.61	0.65	0.61	0.47	0.46	0.46	0.46	0.68	0.67	0.79	1.78	0.48	0.44	0.93	0.63	0.66
St dev	0.07	0.12	0.08	0.05	0.20	0.03		0.03	0.09	0.13	0.07	0.12	0.09	0.08	0.05	0.06	0.05	0.15	0.10	0.11	0.41	0.09	0.05	0.26	0.16	0.42
Al ₂ O ₃	0.48	0.67	2.75	0.51	2.46	0.44	3.78	0.70	0.75	1.07	1.07	1.26	1.21	0.78	0.79	0.76	0.80	1.47	1.36	1.85	4.78	1.23	0.97	1.45	1.21	1.38
St dev	0.08	0.32	0.23	0.09	0.39	0.12		0.08	0.21	0.24	0.19	0.29	0.26	0.14	0.12	0.08	0.10	0.39	0.23	0.35	1.48	0.27	0.18	0.39	0.39	1.27
FeO	18.83	18.68	8.74	19.27	10.29	20.48	9.40	17.75	18.26	14.20	14.35	14.67	14.61	14.95	17.55	16.51	16.65	12.88	12.93	11.52	8.51	15.77	14.10	13.48	12.43	13.94
St dev	1.78	2.38	0.78	1.82	1.05	0.83		1.38	2.79	1.11	1.07	0.94	1.00	0.78	0.54	0.59	1.02	1.26	0.87	0.38	0.30	2.01	1.27	0.45	0.92	1.87
MnO	1.28	1.29	0.18	1.34	0.19	1.25	0.27	1.15	1.14	0.77	0.74	0.69	0.75	0.96	0.93	0.96	0.95	0.64	0.61	0.53	0.22	0.98	0.89	0.80	0.71	0.86
St dev	0.20	0.19	0.06	0.10	0.02	0.16		0.08	0.08	0.08	0.06	0.06	0.07	0.05	0.06	0.04	0.07	0.09	0.05	0.05	0.04	0.14	0.10	0.07	0.10	0.25
MgO	7.60	7.53	13.98	7.79	13.57	6.08	13.77	7.95	6.97	9.51	10.32	10.26	9.94	9.29	8.15	9.03	8.97	10.93	11.15	11.99	13.20	8.52	10.48	11.20	11.92	9.93
St dev	1.22	1.69	0.61	1.42	0.49	0.54		1.07	2.02	0.79	0.75	0.64	0.85	0.43	0.33	0.39	0.72	0.96	0.60	0.31	0.66	1.57	0.83	0.39	0.67	1.17
CaO	19.68	19.07	20.18	18.50	20.07	20.12	20.75	19.47	19.57	20.54	21.39	20.73	20.58	21.66	20.73	20.56	20.49	20.81	20.99	20.69	20.71	20.51	20.11	20.27	19.61	20.46
St dev	0.21	0.59	0.56	0.44	0.59	0.53		0.39	0.43	0.29	0.35	0.21	0.56	0.37	0.19	0.28	0.21	0.18	0.19	0.23	0.55	0.82	0.61	0.31	0.51	0.26
Na ₂ O	0.82	0.74	0.39	0.69	0.43	0.72	0.30	0.72	0.75	0.52	0.41	0.48	0.45	0.53	0.66	0.59	0.63	0.46	0.50	0.45	0.45	1.29	0.81	0.82	0.66	0.63
St dev	0.20	0.14	0.08	0.08	0.09	0.17		0.08	0.15	0.13	0.13	0.12	0.03	0.09	0.13	0.13	0.14	0.04	0.13	0.06	0.06	0.46	0.07	0.10	0.09	0.13
K ₂ O	n.d	n.d	n.d	n.d	n.d	n.d	n.d	n.d	n.d	n.d	n.d	n.d	n.d	n.d	n.d	n.d	n.d	n.d	n.d	n.d	n.d	n.d	n.d	n.d	n.d	
BaO	n.d	n.d	n.d	n.d	n.d	n.d	n.d	n.d	n.d	n.d	n.d	n.d	n.d	n.d	n.d	n.d	n.d	n.d	n.d	n.d	n.d	n.d	n.d	n.d	n.d	
SUM	98.22	99.13	98.61	100.95	95.69	99.01	99.67	98.99	97.99	98.08	99.60	97.01	100.80	100.17	99.58	99.42	99.06	100.74	97.33	100.67	100.74	100.97	99.92	99.93	98.77	99.59
St dev	0.93	0.77	0.90	1.15	1.03	2.04		0.76	0.54	0.63	1.24	1.09	0.53	1.33	0.72	0.68	1.02	0.78	0.51	0.82	0.78	0.77	0.89	0.49	1.32	0.80

All concentrations in wt.% oxide.

All analyses conducted by electron microprobe operating at 20 kV, 20 na with a 4-micron raster area,

except * samples which were run at 15 kV, 15 na, with a 12-micron raster area.

n= number of grains analyzed.

pop= population.

Locality numbers after Hay (1976).

positions designated by open symbols. As Tuffs IE and IC are very similar in feldspar and augite composition, Tuff IE is positively identified at this site only by its stratigraphic position above Tuff ID. The absence of Tuff IC is puzzling, as it is present on either side of the lake. Perhaps Tuff IC is not identifiable in the lake sediments because it is too fine grained and was therefore more affected by alteration processes. Tuff IC to the west of the lake is finer grained than the other tephra layers (silt sized). Another possibility is that Locality 80 does not represent the center of the saline-alkaline lake deposits, and that an excavation to the south of the gorge (in an area not currently exposed) could reveal deeper lake sediments containing all of the tephra layers (Hay 1976). Also, if the tephra was light enough it may have floated and been preferentially deposited at the shores and not in the center of the lake.

These new compositional “fingerprints” can now form a quantitative test for tephra identification within Upper Bed I at Olduvai. Using these compositional differences between the major tephra layers, correlations can now be made between the well-mapped Junction and the less well known saline-alkaline lake and alluvial plain deposits to the west, and to the massive ignimbrites and ash flows proximal to Olmoti to the east. These correlations can be used to form a new framework for Olduvai stratigraphy that will tie together the various regions of the gorge, and with potential volcanic sources (McHenry 2004).

Similarities in glass composition and phenocryst assemblage can also provide insight into potential sources for these tephra layers. The very consistent glass compositions found in Tuffs IB, IC, ID, and IE imply a constant volcanic source for these eruptions. Even the Lower Ng’eju Tuff and Tuff IF show a similar pattern in major elements, while only the Upper Ng’eju Tuff is truly distinct. Olmoti is considered to be the main volcanic source because of stream-channel orientations and eastward coarsening in alluvial fan deposits, and dates of Ngorongoro eruptive rocks older than Tuffs IB through IF (Hay 1976). This correlation is strengthened by the recent discovery of Ba-rich feldspar and trachytic lavas similar to the lava fragments in Tuff IF in the Olmoti crater walls (Mollel and McHenry 2004).

In this study, the glass compositions were not very useful, showing less variation in major elements between different tephra layers than any of the phenocrysts. This was unexpected, as glass composition is the preferred method for distinguishing tephra layers elsewhere. These findings imply that multiple eruptions from the same magma source, with recurrence intervals of on the order of 10,000 years, result in glass compositions that are relatively constant in major element concentrations, while phenocryst compositions are more variable. As few sites (e.g., Locality 40) preserve fresh glass at Olduvai, it is not of general use for tephra correlation throughout the basin. Phenocryst composition is of much more widespread applica-

TABLE 4
Olduvai Bed I tephra feldspar compositions, as measured by electron microprobe.

Tuff Locality unit/pop	IB * 6	IB 13	IB* 80	IB 64	IC 45b	IC 64	ID 40	ID 45	ID 80	ID 64	IE 6 flow	IE 6 vitric	IE 40	IE 45	IE 80	Ngeju 46 lower	Ngeju 80 lower	Ngeju 46 upper	IF 40 lapilli 1	IF 40 lapilli 2	IF 99 lapilli surge	IF 99 surge	IF 80	IF 64	
n	14	23	19	9	53	24	31	72	24	30	25	25	43	19	18	14	21	14	22	3	31	21	31	27	13
SiO ₂	65.30	67.29	67.19	66.04	64.20	66.29	62.28	60.02	62.52	64.27	65.34	65.19	66.29	66.06	66.11	59.39	61.78	60.50	66.51	64.65	66.48	68.35	66.92	66.81	67.51
St dev	0.67	0.32	0.68	0.83	1.12	0.53	1.33	1.53	1.51	1.75	0.75	0.45	0.51	0.55	0.77	2.03	1.66	1.29	0.65	0.28	0.88	0.88	0.72	0.45	1.24
TiO ₂	n.d.	n.d.	n.d.	n.d.	n.d.	n.d.	n.d.	n.d.	n.d.	n.d.	n.d.	n.d.	n.d.	n.d.	n.d.	n.d.	n.d.	n.d.	n.d.	n.d.	n.d.	n.d.	n.d.	n.d.	n.d.
Al ₂ O ₃	19.31	20.19	19.81	19.33	20.74	20.89	23.45	23.67	23.35	23.00	20.86	19.55	20.14	21.03	20.71	24.52	24.07	23.02	19.09	20.10	20.11	19.58	19.94	20.01	20.20
St dev	0.21	0.30	0.36	0.37	0.40	0.33	0.81	0.95	0.99	1.07	0.38	0.27	0.40	0.28	0.63	1.72	1.14	1.04	0.47	0.58	0.39	0.74	0.51	0.49	0.50
FeO	0.32	0.31	0.30	0.34	0.23	0.24	0.23	0.21	0.22	0.21	0.20	0.19	0.20	0.19	0.20	0.25	0.23	0.27	0.41	0.41	0.22	0.27	0.21	0.20	0.21
St dev	0.09	0.05	0.05	0.11	0.03	0.03	0.06	0.04	0.05	0.07	0.09	0.03	0.02	0.02	0.03	0.04	0.05	0.03	0.11	0.04	0.04	0.11	0.04	0.03	0.02
MnO	n.d.	n.d.	n.d.	n.d.	n.d.	n.d.	n.d.	n.d.	n.d.	n.d.	n.d.	n.d.	n.d.	n.d.	n.d.	n.d.	n.d.	n.d.	n.d.	n.d.	n.d.	n.d.	n.d.	n.d.	n.d.
MgO	n.d.	n.d.	n.d.	n.d.	n.d.	n.d.	n.d.	n.d.	n.d.	n.d.	n.d.	n.d.	n.d.	n.d.	n.d.	n.d.	n.d.	n.d.	n.d.	n.d.	n.d.	n.d.	n.d.	n.d.	n.d.
CaO	0.30	0.27	0.29	0.40	1.26	1.22	4.11	4.51	4.24	4.40	1.30	1.20	1.19	1.24	1.46	5.20	5.08	7.18	0.75	1.16	0.82	0.86	0.93	0.89	0.99
St dev	0.13	0.08	0.12	0.19	0.33	0.30	1.01	1.07	1.23	1.18	0.25	0.18	0.19	0.29	0.55	1.59	1.39	1.06	0.18	0.51	0.10	0.49	0.50	0.31	0.29
Na ₂ O	8.94	8.70	7.52	8.22	8.90	9.31	8.39	8.23	7.88	7.61	8.72	9.12	8.31	7.81	8.89	7.45	8.03	6.94	8.15	7.46	7.98	7.33	7.38	7.56	7.75
St dev	0.43	0.15	0.27	0.57	0.11	0.21	0.36	0.44	0.36	0.51	0.23	0.22	0.16	0.19	0.22	0.65	0.57	0.52	0.27	0.36	0.22	0.60	0.42	0.27	0.13
K ₂ O	4.36	4.41	4.27	4.42	2.76	2.87	1.16	0.98	1.18	0.88	3.05	3.18	3.15	3.06	2.79	0.61	0.98	0.58	3.59	3.26	3.27	3.79	4.28	4.24	3.31
St dev	0.75	0.27	0.53	0.64	0.28	0.32	0.33	0.31	0.43	0.44	0.23	0.25	0.23	0.29	0.57	0.36	0.35	0.11	0.39	0.52	0.16	1.16	1.08	0.65	0.39
BaO	0.27	0.26	0.20	0.21	0.39	0.35	0.28	0.22	0.26	0.22	0.44	0.39	0.45	0.42	0.47	0.22	0.21	0.12	0.67	2.67	0.86	0.34	0.30	0.30	0.44
St dev	0.10	0.08	0.08	0.09	0.08	0.08	0.09	0.09	0.11	0.14	0.10	0.05	0.08	0.09	0.13	0.18	0.11	0.04	0.39	0.71	0.22	0.22	0.17	0.15	0.12
SUM	98.88	101.50	99.64	99.06	98.56	101.28	100.00	97.94	99.74	100.67	100.02	98.91	99.83	99.89	100.71	97.69	100.47	98.71	99.30	100.10	99.90	100.60	100.02	100.08	100.51
St dev	1.07	0.22	0.75	0.93	1.28	0.46	0.67	1.07	0.75	0.62	0.70	0.60	0.73	0.48	0.68	2.13	0.39	0.41	0.59	0.47	0.99	0.94	0.66	0.59	0.95

All concentrations in wt.% oxide.

All analyses conducted by electron microprobe operating at 20 kV, 20 na with a 4-micron raster area, except * samples which were run at 15 kV, 15 na, with a 12-micron raster area.

n= number of grains analyzed.

pop= population.

Locality numbers after Hay (1976).

bility, as it can be applied at all Olduvai sites, and has a better ability to distinguish the individual upper Bed I tephra layers.

One possible concern with this method is the possibility of contamination by grains from other sources. Careful selection of fresh-looking, non-rounded crystals, and the analysis of multiple samples of the same tephra layer from nearby exposures, can help to limit this possibility. Where fresh and altered glasses are present, crystals within lapilli or with adhering glass can be chosen for analysis. The use of thin sections which show which phenocrysts are directly associated with fresh or altered glass can also limit the accidental analysis of contaminant grains. Careful sample collection and preparation methods can minimize or eliminate the effects of contaminant grains in analysis and tephra identification and correlation.

More extensive regional correlation projects in East Africa have relied almost exclusively on glass compositions (e.g., Feibel et al. 1989). In order to integrate the Olduvai tephra into this regional database, major and trace element analysis of fresh glass is required; or, alternatively, selected more widespread units can be analyzed for phenocryst composition. Fortunately, a few sites at Olduvai do preserve fresh glass, and these sites could be used to form a framework for regional correlation based on traditional glass chemistry techniques. Thus, tephra layers can be identified locally regardless of diagenetic history using phenocryst compositions, and if these tephra layers can be correlated to any local site preserving fresh glass, they can

then be correlated regionally using the more conventional fresh glass techniques.

CONCLUSIONS

Tephra correlations between fresh and highly altered pyroclastic rocks are possible with a multi-component approach that uses major-element glass and phenocryst composition, in addition to stratigraphic information. Many phenocrysts survived the harsh weathering environment of saline-alkaline groundwater and lake water at Olduvai (an arid interior basin) making geochemical correlation of tephra possible. Distinctive geochemical fingerprints were determined for the six widespread tephra layers in upper Bed I and these allowed reliable correlation of beds throughout the basin. The correlations produce a high-resolution stratigraphic framework that can be applied to the late Pliocene and early Pleistocene archaeological and paleoecological record at Olduvai. Interpretation of the analytical data suggests that phenocryst compositions varied more between individual tephra layers than did the overall glass composition, and that phenocrysts were more likely to be preserved. Thus, this multi-component method is applicable regardless of the quality of glass preservation, and should prove successful elsewhere where tephra is highly altered.

ACKNOWLEDGMENTS

I would like to acknowledge Carl Swisher, Richard Hay, and the other OLAPP (Olduvai Landscape Paleoanthropology Project) scientists for their invaluable assistance and insights in the field.

TABLE 5

Olduvai Bed I tephra titanomagnetite compositions, as measured by electron microprobe.

Tuff Locality	IB*	IB	IB	IC*	IC*	ID*	ID*	ID	IE*	IE*	IE*	Ngeju	Ngeju	Ngeju	IF	IF	IF	IF	IF	IF	
unit/pop	6	13	64	45b	64	40	45	64	6	6	40	46	46	46	40	40	99	99	40	99	64
n	20	19	16	13	15	20	18	15	20	19	20	14	9	5	5	10	6	1	18	9	15
SiO ₂	0.24	0.13	0.11	0.17	0.15	0.08	0.11	0.08	0.10	0.13	0.08	0.06	0.09	0.08	0.05	0.24	0.07	0.26	0.39	0.11	0.07
St dev	0.10	0.12	0.07	0.08	0.08	0.03	0.05	0.03	0.04	0.14	0.04	0.02	0.03	0.01	0.02	0.15	0.03		0.44	0.11	0.03
TiO ₂	24.16	24.10	24.74	20.25	20.34	25.60	25.41	25.17	23.90	23.85	23.85	24.42	22.71	18.37	21.63	14.16	21.05	14.74	21.12	22.39	22.79
St dev	0.52	0.87	0.95	1.20	1.69	0.39	1.09	0.67	0.92	0.32	0.47	0.46	0.72	1.19	0.69	0.98	1.43		0.40	0.99	1.28
Al ₂ O ₃	0.60	0.65	0.48	1.00	0.98	1.29	1.40	1.44	0.96	0.95	0.91	1.64	2.43	4.83	1.02	0.54	0.90	0.80	1.06	0.97	1.19
St dev	0.20	0.18	0.10	0.14	0.20	0.14	0.24	0.17	0.05	0.04	0.05	0.21	0.34	0.60	0.21	0.36	0.20		0.13	0.22	0.73
FeO	67.68	65.96	65.99	67.23	67.24	65.93	64.30	64.27	65.80	68.49	68.92	67.10	66.32	66.13	69.22	73.83	70.79	72.30	65.32	68.55	66.65
St dev	2.14	1.45	1.41	1.66	2.04	0.81	1.52	1.57	1.97	2.08	1.15	0.38	0.48	0.38	1.14	1.49	1.94		1.59	1.87	1.22
MnO	1.76	1.77	1.84	1.74	1.67	1.44	1.40	1.36	1.62	1.59	1.59	1.22	1.00	0.55	1.59	1.63	1.71	2.00	1.61	1.53	1.64
St dev	0.10	0.14	0.11	0.23	0.18	0.09	0.09	0.06	0.11	0.06	0.08	0.09	0.06	0.08	0.20	0.22	0.12		0.07	0.12	0.31
MgO	0.71	0.73	0.52	0.74	0.70	1.25	1.32	1.19	1.00	0.78	0.86	1.59	2.67	4.99	1.18	0.04	1.15	0.16	1.33	1.41	1.41
St dev	0.19	0.25	0.05	0.11	0.15	0.15	0.30	0.37	0.06	0.07	0.05	0.28	0.31	0.38	0.31	0.08	0.10		0.13	0.20	0.96
CaO	0.04	0.03	0.02	0.01	0.01	0.03	0.08	0.15	0.07	0.06	0.03	0.02	0.09	0.03	0.01	0.10	0.00	0.12	0.07	0.02	0.11
St dev	0.05	0.06	0.05	0.01	0.03	0.04	0.09	0.13	0.18	0.09	0.07	0.02	0.06	0.01	0.01	0.11	0.01		0.04	0.03	0.07
SUM	95.39	93.79	93.86	92.26	92.19	95.79	94.23	94.92	93.59	96.04	96.44	97.26	96.48	95.91	95.88	91.41	95.99	90.40	92.16	95.55	95.01
St dev	1.98	1.48	1.11	1.47	1.10	0.71	1.70	1.41	1.81	2.10	1.25	0.35	0.62	0.52	0.77	0.77	1.42		1.34	0.68	0.53

All concentrations in wt.% oxide.

All analyses conducted by electron microprobe operating at 20 kV, 20 na with a 4-micron raster area, except * samples which were run at 15 kV, 15 na, with a 12-micron raster area.

n= number of grains analyzed, pop= population.

Locality numbers after Hay (1976).

I would also like to thank the Tanzania Commission for Science and Technology and the Tanzania Antiquities Department for granting me permission to pursue my research goals at Olduvai Gorge. I would also like to thank Godwin Mollel, Gail Ashley, and Carl Swisher for their insightful discussions on Olduvai stratigraphy and geochemistry, and Jeremy Delaney for his extensive help with the electron microprobe analyses. Funding was provided in part by the L. S. B. Leakey Foundation, the Geological Society of America, Sigma Xi, and NSF (EAR 9903258, BCS-0109027).

REFERENCES

- ASHLEY, G.M. and HAY, R.L., 2002. Sedimentation patterns in a Plio-Pleistocene volcaniclastic rift-margin basin, Olduvai Gorge, Tanzania. In: Ashley, G. M. and Renaut, R.W., Eds., *Sedimentation in Continental Rifts*. SEPM Special Publication 73: 107-122.
- BAKER, B.H., MOHR, P.A. and WILLIAMS, L.A.J., 1972. *Geology of the Eastern Rift System of Africa*. Geological Society of America Special Paper, 136. 67 pp.
- BERGGREN, W.A., HILGEN, H.J., LANGEREIS, C.G., KENT, D.V., OBRADOVICH, J.D., RAFFI, I., RAYMO, M.E., SHACKLETON, N.J., 1995. Late Neogene chronology: New perspectives in high-resolution stratigraphy. *Geological Society of America Bulletin* 107(11): 1272-1287.
- BLUMENSCHINE, R.J., PETERS, C.R., MASAO, F.T., CLARKE, R.J., DEINO, A.L., HAY, R.L., SWISHER, C.C., STANISTREET, I.G., ASHLEY, G.M., MCHENRY, L.J., SIKES, N.E., VAN DER MERWE, N.J., TACTIKOS, J.C., CUSHING, A.E., DEOCAMPO, D.M., NJAU, J.K., EBERT, J.I., 2003. Late Pliocene *Homo* and hominid land use from western Olduvai Gorge, Tanzania. *Science* 299: 1217-1221.
- BLUMENSCHINE, R.J. and PETERS, C.R., 1998. Archaeological predictions for hominid land use in the paleo-Olduvai Basin, Tanzania, during lowermost Bed II times. *Journal of Human Evolution*, 34: 565-607.
- BROWN, F.H., SARNA-WOJCICKI, A.M., MEYER, C.E., and HAILEAB, B. 1992. Correlation of Pliocene and Pleistocene tephra layers between the Turkana basin of East Africa and the Gulf of Aden. *Quaternary International* 13-14: 55-67.
- BROWN, F.H., 1982. Tulu Bor tuff at Koobi Fora correlated with the Sidi Hakoma tuff at Hadar. *Nature* 300: 631-635.
- CERLING, T.E., BROWN, F.H. and BOWMAN, J.R., 1985. Low-temperature alteration of volcanic glass: hydration, Na, K, ¹⁸O and Ar mobility. *Chemical Geology* 52: 281-293.
- CRONIN, S.J., NEALL, V.E., STEWART, R.B. and PALMER, A.S., 1996a. A multi-parameter approach to andesitic tephra correlation, Ruapehu volcano, New Zealand. *Journal of Volcanology and Geothermal Research* 72: 199-215.
- CRONIN, S.J., WALLACE, R.C. and NEALL, V.E., 1996b. Sourcing and identifying tephras using major oxide titanomagnetite and hornblende chemistry, Egmont volcano and Tongariro Volcanic Centre, New Zealand. *Bulletin of Volcanology* 58: 33-40.
- DELANO, J.W., TICE, S., MITCHELL, C.E. and GOLDMAN, D., 1994. Rhyolitic glass in Ordovician K-bentonites: A new stratigraphic tool. *Geology* 22: 115-118.
- DEMENOCAL, P.B. and BROWN, F.H., 1999. Pliocene tephra correlations between East African hominid localities, the Gulf of Aden, and the Arabian Sea. In: Augusti, L., Rook, L., and Andrews, P., Eds.

- Hominid Evolution and Climatic Change in Europe*, vol. 1, pp. 23-52. Cambridge University Press.
- DONOVAN, J., 2000a. *Probe for Windows: Analysis and Automation for EPMA, version 5.11*. Software package distributed by Advanced Microbeam, Vienna, OH.
- , 2000b. *User's guide and reference*. Probe for Windows: Analysis and Automation for EPMA, version 5.11. Advanced Microbeam, Vienna, OH.
- FEIBEL, C. S., 1999. Tephrostratigraphy and geological context in paleoanthropology. *Evolutionary Anthropology* 8(3): 87-100.
- FEIBEL, C.S., BROWN, F.H. and MCDOUGALL, I., 1989. Stratigraphic context of fossil hominids from the Omo group deposits, Northern Turkana Basin, Kenya and Ethiopia. *American Journal of Physical Anthropology* 76: 595-622.
- FROGGATT, P.C., 1992. Standardization of the chemical analysis of tephra deposits. Report of the ICCT working group. *Quaternary International* 13-14: 93-96.
- HAY, R.L., 1960. Rate of clay formation and mineral alteration in a 4000-year-old volcanic ash soil on St. Vincent, B.W.I. *American Journal of Science* 258: 354-368.
- , 1970. Silicate reactions in three lithofacies of a semi-arid basin, Olduvai Gorge, Tanzania. *Mineralogical Society of America Papers* 3: 237-255.
- , 1976. *Geology of the Olduvai Gorge: A Study of Sedimentation in a Semi-arid Basin*. University of California Press, Berkeley, 203 pp.
- HAY, R.L. and KYSER, T.K., 2001. Chemical sedimentology and paleoenvironmental history of Lake Olduvai, a Pliocene lake in northern Tanzania. *Geological Society of America Bulletin* 113(12): 1505-1521.
- HUFF, W.D., BERGSTRÖM, S.M. and KOLATA, D.R., 1992. Gigantic Ordovician volcanic ash fall in North America and Europe: Biological, tectonomagmatic, and event-stratigraphic significance. *Geology* 20: 875-878.
- IZETT, G.A., OBRADOVICH, J.D. and MEHNERT, H.H. The Bishop ash bed (middle Pleistocene) and some older (Pliocene and Pleistocene) chemically and mineralogically similar ash beds in California, Nevada, and Utah. *U.S. Geological Survey Bulletin* B 1675, 37p.
- KOLATA, D.R., HUFF, W.D. and BERGSTRÖM, S.M., 1996. *Ordovician K-bentonites of eastern North America*. Geological Society of America Special Paper, 313.
- LEBAS, M.J., LEMAITRE, R.W., STRECKEISEN, A., and ZANET-TIN, B., 1986. A chemical classification of volcanic rocks based on the total alkali silica diagram. *Journal of Petrology* 27: 745-750.
- LOWE, D.J., 1988. Stratigraphy, age, composition, and correlation of late Quaternary tephras interbedded with organic sediments in Waikato lakes, North Island, New Zealand. *New Zealand Journal of Geology and Geophysics* 31: 125-165.
- MCHENRY, L.J., 2004. "Characterization and Correlation of Altered Plio-Pleistocene Tephra Using a "Multiple Technique" Approach: Case Study at Olduvai Gorge, Tanzania." Ph.D. Thesis, Rutgers University, New Brunswick, NJ, 382 pp.
- MOLLEL, G.F., and MCHENRY, L.J., 2004. *Temporal evolution of the Ngorongoro Volcanic Highland (NVH) in relation to Bed I of Olduvai Gorge, Tanzania: A progress report*. Abstract: 2004 Paleoanthropology Society Annual Meeting (Montreal, April, 2004).
- PERKINS, M.E. and NASH, B.P., 2002. Explosive silicic volcanism of the Yellowstone hotspot: The ash fall tuff record. *Geological Society of America Bulletin* 114: 367-381.
- PETERS, C.R. and BLUMENSCHINE, R.J., 1995. Landscape perspectives on possible land use patterns for Early Pleistocene hominids in the Olduvai Basin, Tanzania. *Journal of Human Evolution* 29: 321-362.
- SARNA-WOJCICKI, A.M. and DAVIS, J.O., 1991. *Quaternary tephrochronology, Quaternary Nonglacial Geology: Conterminous U.S., The Geology of North America*, pp. 93-116. Geological Society of America.
- TAMRAT, E., THOUVENY, N., TAÏEB, M. and OPDYKE, N.D., 1995. Revised magnetostratigraphy of the Plio-Pleistocene sedimentary sequence of the Olduvai Formation (Tanzania). *Palaeogeography, Palaeoclimatology, Palaeoecology* 114: 273-283.
- WALTER, R.C., MANEGA, P.C. and HAY, R.L., 1992. Tephrochronology of Bed I, Olduvai Gorge: An application of the laser-fusion 40Ar/39Ar dating to calibrating biological and climatic change. *Quaternary International* 13-14: 37-46.

Santonian-Maastrichtian planktonic foraminiferal and ostracode biostratigraphy of the northern Gulf Coastal Plain, USA

T. Markham Puckett

Department of Physics and Earth Science, P.O. Box 5130, University of North Alabama, Florence, AL 35632
e-mail: tmpuckett@una.edu

ABSTRACT: The Santonian-Maastrichtian deposits of the northern Gulf Coastal Plain of the United States (Mississippi-Alabama) are richly fossiliferous and structurally uncomplicated, offering an excellent setting in which to study calcareous microfossil biostratigraphy. Eight planktonic foraminiferal zones and seven ostracode zones are recognized in these strata, based on the stratigraphic occurrence of 45 species of planktonic foraminifera and 112 taxa of ostracodes. The planktonic foraminiferal zonation is based on standard global biozones. These include the *Dicarinella asymetrica* Taxon Range Zone, the *Globotruncanita elevata* Interval Zone, the *Globotruncana ventricosa* Interval Zone, the *Globotruncanita calcarata* Taxon Range Zone, the *Globotruncanella havanensis* Interval Zone, the *Globotruncana aegyptiaca* Interval Zone, the *Gansserina gansseri* Interval Zone, and the *Contusotruncana contusa-Racemiguembelina fructicosa* Interval Zone. Three new ostracode zones are defined, and the upper boundary of two previously defined zones are amended. These zones are the *Veenia quadrialira* Interval Zone (amended), the *Acuminobrachycythere acuminata* Interval Zone (new), the *Brachycythere pyriforma* Interval Zone (new), the *Asctoleberis plummeri* Taxon Range Zone (amended), the *Curfsina communis* Interval Zone (new), the *Escharacytheridea pinochii* Interval Zone, and the *Platycosta lixula* Interval Zone. The planktonic foraminiferal biostratigraphy indicates that the age of these deposits range from early Santonian to early Maastrichtian. The Santonian-Campanian boundary is recognized on the basis of the highest occurrence surface of *Dicarinella asymetrica*, and demonstrates that the contact between the Tombigbee Sand Member of the Eutaw Formation and the Mooreville Chalk is diachronous. The Campanian-Maastrichtian boundary cannot be defined by calcareous microfossils due to the lack of a proxy for the newly established definition. The high-resolution biostratigraphy of the ostracodes, which are indigenous to the North American Coastal Plain, will enable subsequent studies of Late Cretaceous paleobiogeography and Gulf of Mexico-Caribbean tectonic development to be conducted.

INTRODUCTION

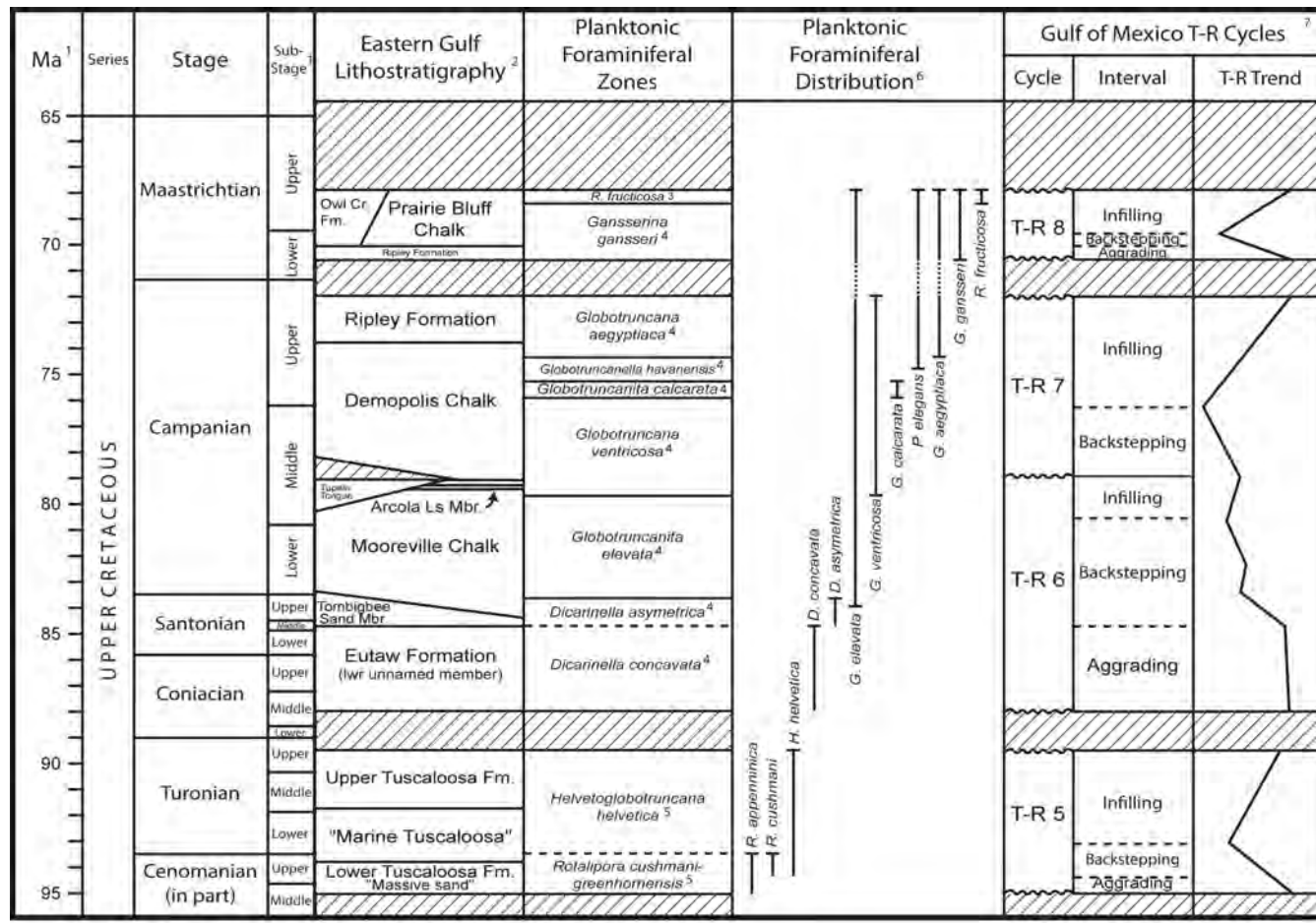
The Late Cretaceous (Santonian-Maastrichtian) marine strata of the northeastern Gulf Coastal Plain (primarily Mississippi and Alabama, USA) are among the most complete and richly fossiliferous in the world. The strata are, with geographically restricted exceptions, uncomplicated by post-depositional tectonic displacement. These Late Cretaceous deposits represent an excellent geologic setting in which to calibrate the chronostratigraphic ranges of marine fossils.

High-resolution biostratigraphy of the ostracodes and planktonic foraminifera are the subject of the present study. Ostracodes are unsurpassed in their utility for deciphering evolving paleogeographies, and have great potential as tools in understanding the plate tectonic evolution of complex terranes. For example, Babinot and Bourdillon-de-Grissac (1989) demonstrated that the mid- to Late Cretaceous ostracode faunas of North Africa differ fundamentally from coeval faunas in southern Europe, even though the two regions were not separated by a great geographic distance; deepwater barriers, even though geographically narrow, provide effective genetic barriers for most benthic ostracodes. Puckett (2002) showed that one of the most common ostracode taxa of the Late Cretaceous, the brachycytherine ostracodes, is distinct between North America, South America, Africa and India. Babinot and Colin (1988; 1992) delineated five Tethyan ostracode faunal provinces for the Late Cretaceous: a South European bioprovince, a North-Central American bioprovince, an African-Arabian bioprovince, and Austral bioprovince (including Australia, India, Madagascar and South Africa), and a Dinaro-Hellenic sub-

province (located between the South European and African-Arabian provinces). At the generic level, these bioprovinces include very few taxa in common.

Recently (2001), the author had the opportunity to collect samples for ostracodes and planktonic foraminifera in Cuba. Although a previous reconnaissance work of Mesozoic and Cenozoic ostracodes (Lubimova and Sánchez Arango 1974) had referred to some Cuban ostracode species by names of North American species, the Late Cretaceous ostracodes collected by the author are almost completely different than coeval faunas of North America. Another reconnaissance work, from the Maastrichtian of Jamaica by Hazel and Kamiya (1993), indicates some similarities with coeval faunas of North America. Late Cretaceous ostracodes of northeastern Brazil described by Viviers et al. (2000), however, are distinct from those in North America and in Cuba. These observations indicate that complex faunal barriers between these regions had been established by the Late Cretaceous. Future work on ostracode paleobiogeography, particularly in the Greater Antilles region, may help unravel some of the complexities of plate tectonic evolution of the Caribbean and Gulf of Mexico region. To do this, however, it is essential that the chronostratigraphic distributions of ostracodes in neighboring regions are known as a means of comparison. It is primarily for this reason that the present work has been undertaken.

Despite the utility of the ostracodes for paleogeographic reconstruction due to their provincialism, the same attribute also makes it difficult or impossible to correlate faunas across



1 = Modified from Gradstein et al. (1994).

2 = Modified from Mancini et al. (1987) and Mancini et al. (1996).

3 = Zonation from Smith and Pessagno (1973).

4 = Zonation from Caron (1985).

5 = Zonation from Pessagno (1969).

6 = Planktonic foraminiferal distribution based on the work of Pessagno (1969), Mancini (1979), Mancini et al. (1980), Puckett (1995a), Mancini et al. (1996), and the present work.

7 = Transgressive-regressive cycles based on Mancini and Puckett (in press).

TEXT-FIGURE 1

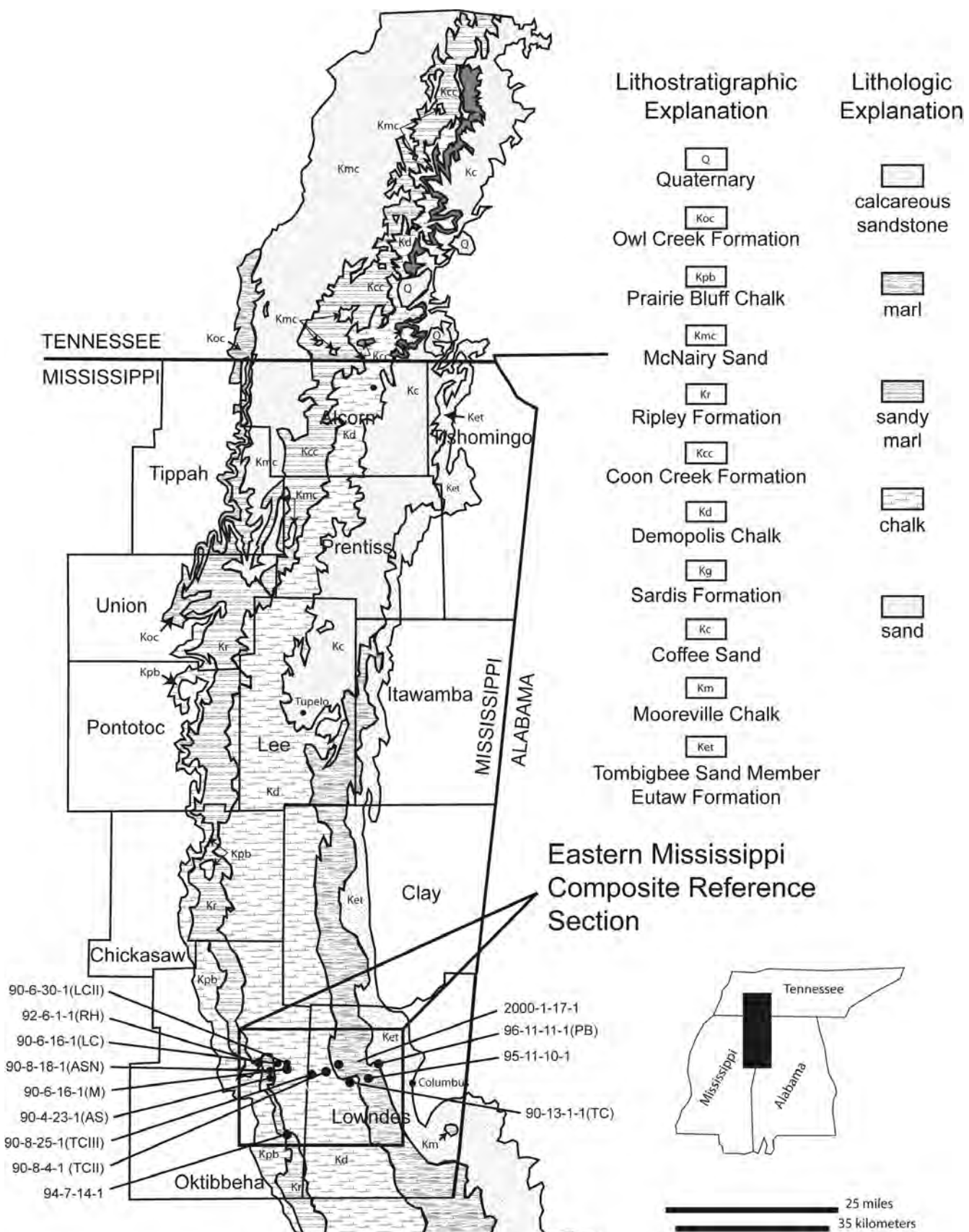
Chronostratigraphy, lithostratigraphy, planktonic foraminiferal zonation, and transgressive-regressive cycles in the Upper Cretaceous deposits of the northern Gulf Coastal Plain, USA.

paleogeographic provinces. Thus, planktonic foraminifera, which occur along with the ostracodes in the samples collected in this research, are used for chronostratigraphic control. The taxonomy and chronostratigraphy of the Late Cretaceous planktonic foraminifera are well established, and thus they constitute an excellent means of correlation.

STRATIGRAPHY

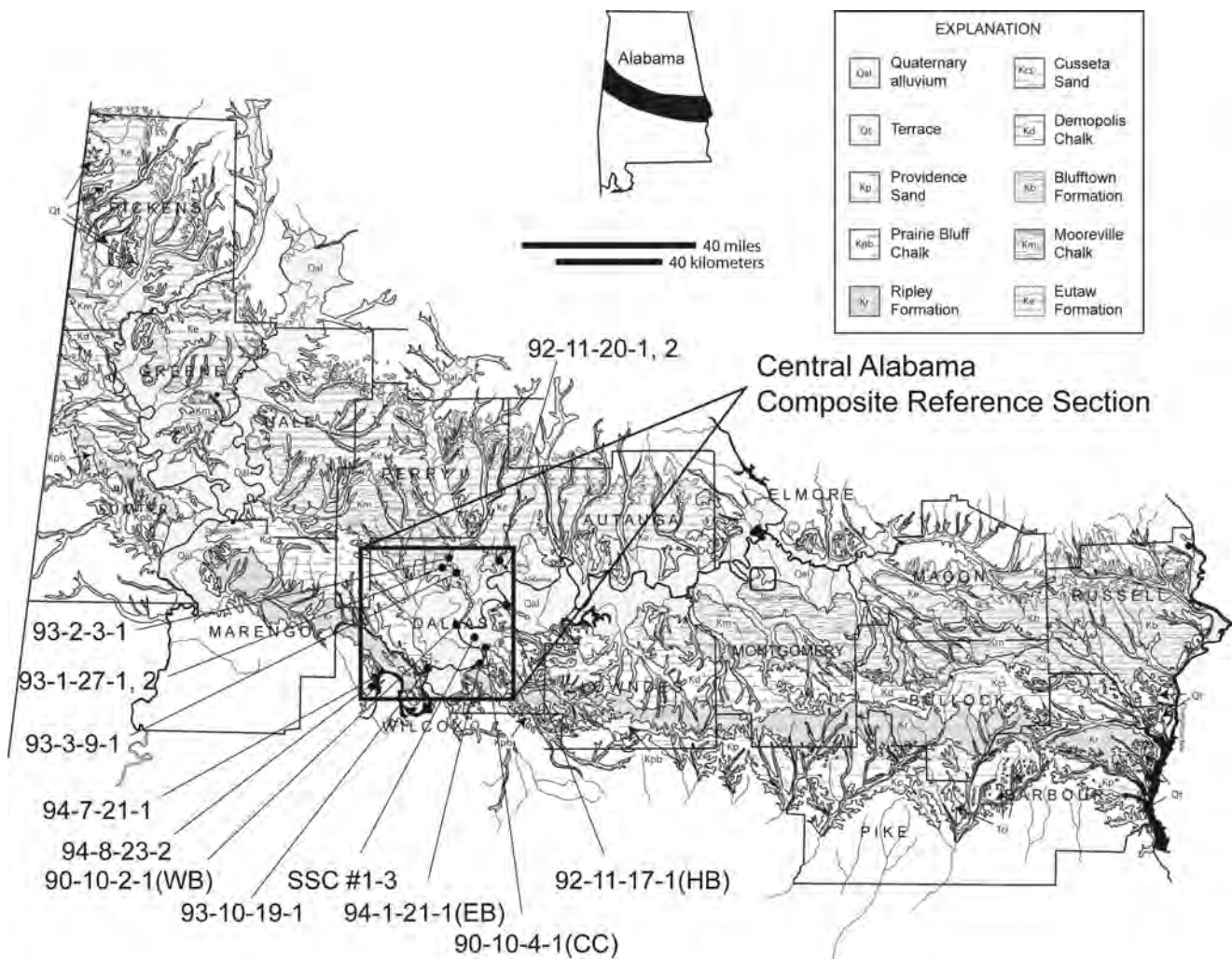
The Santonian-Maastrichtian strata of the northern Gulf Coastal Plain, USA, consist primarily of three chalk and marl transgressive-regressive (T-R) cycles that are defined by sedimentological and paleontological evidence (text-fig.1). The base of the oldest cycle (T-R 6; Mancini and Puckett 2005) is at the unconformity between the nonmarine beds of the Tuscaloosa Group and the glauconitic sands and clays of the lower, unnamed member of the Eutaw Formation. The upper part of the lower member of the Eutaw consists of intertidal and marginal marine sands and clays. These lower nonmarine and

marginal marine strata define the aggrading interval of the T-R cycle, which are strata deposited between a lower bounding unconformity and a marine transgressive surface. The initial marine incursion in the area, which is the base of the Tombigbee Sand, varies considerably along strike. The Tombigbee loses its distinction near Montgomery, Alabama, and eastward is referred to as the undifferentiated Eutaw Formation. The Eutaw Formation in eastern Alabama consists mainly of alternating oyster beds, sand and clay. Puckett (1994) described a low-diversity, high-dominance ostracode assemblage consisting mainly of the genera *Haplocytheridea*, *Fossocytheridea* (see Tibert and others 2003), *Brachycythere*, *Fissocarinocythere*, and *Cytherella*. Near Montgomery, the transgressive surface is observed as a well-cemented sandstone rich in the echinoid *Hardouinia bassleri* with occasional oysters, but near Selma, a few miles to the west of Montgomery, oyster beds of *Flemingostrea cretacea* occur at the base of the Tombigbee. The Tombigbee is considerably thicker in Mississippi, where it is more than 180 ft (58m) thick (Russell and Keady 1983).



TEXT-FIGURE 2

Geologic map of the marine Upper Cretaceous stratigraphic units in northeastern Mississippi showing sample localities. Map based on Russell and Keady (1983).



TEXT-FIGURE 3

Geologic map of the marine Upper Cretaceous stratigraphic units of central Alabama showing sample localities. Map based on Osborne et al. (1989).

These shallow marine, biohermal deposits are overlain by hemipelagic marls of the Mooreville Chalk. High-order, Milankovich-type cyclicity is manifest in the upper part of the Mooreville Chalk at Hatcher's Bluff (see central Alabama composite reference section), with which the stratigraphic arrangement of the four marl/limestone rhythmites of the Arcola Limestone Member of the Mooreville are consistent. The origin of the thin (2-4 in (0.8cm-1.6cm)) individual limestone beds remains unclear, although it is known that they are comprised almost exclusively of the calcisphere *Pithonella spherica* Kaufmann (Russell and Keady 1983). The top of the Arcola Limestone Member marks the base of the Demopolis Chalk.

The Demopolis Chalk is divided into three members, which are, from bottom to top, the Tibbee Creek Member, the herein-named Muldrow Member, and the Bluffport Marl Member. The Demopolis Chalk includes the deepest part of the T-R K7 transgressive-regressive cycle (Mancini and Puckett 2005) grading, from bottom to top, gray, fossiliferous marl of the Tibbee Creek Member to light gray and white chalk of the Muldrow Member to gray, fossiliferous marl of the Bluffport Marl Member. High-resolution planktonic foraminiferal biostratigraphy of Puckett (1995a) and Puckett and Mancini (1998)

indicate that the influx of marl of the Bluffport Marl Member occurred over a significant amount of time, as demonstrated by the diachroneity of the contact between the Muldrow Member and the Bluffport Marl Member relative to the *Globotruncana calcarata* Range Zone, with the Bluffport Marl Member being considerably younger toward the south (eastern Mississippi and Alabama) than in the north (northern Mississippi). The marl of the Bluffport Marl Member grades up-section into sandy marl of the lower Ripley Formation in the shallowing-upward part of the cycle, which is capped by an unconformity (Mancini et al. 1996; Mancini and Puckett 1998). Overlying the unconformity are non-marine sands of the aggrading phase of the T-R K8 cycle (Mancini and Puckett 2005), which are, in turn, overlain by marginal marine oyster beds of the basal Prairie Bluff Chalk, relatively pure chalk of the Prairie Bluff, and the K-T boundary that caps the T-R K8 cycle.

METHODS

The results of this research are based on samples collected along two composite reference sections (CRS): the eastern Mississippi CRS and the central Alabama CRS (see Appendix 1 for details). Each CRS is comprised of several measured sections

that were correlated on the basis of structure contour maps of two stratigraphic horizons: the lower part of the section (Mooreville Chalk) was correlated based on the top of the sands of the Eutaw Formation (Tombigbee Sand Member-Mooreville contact) and the upper part of the section (Demopolis Chalk, Ripley Formation and Prairie Bluff Chalk) were correlated based on the top of the Arcola Limestone Member at the Mooreville-Demopolis contact. Elevations of these two stratigraphic horizons in the areas of the CRSs were determined by examination of surface exposures and well-defined deflections on electric logs. Details of these two stratigraphic horizons in the central Alabama CRS are presented in Puckett (1995a). Locations of the measured sections are presented on text-figure 2 for the eastern Mississippi CRS and on text-figure 3 for the central Alabama CRS. Data on the measured sections are presented in the appendix. The stratigraphic position of each measured section was calibrated based on two elevations: the altitude of the section and the altitude of the stratigraphic horizon used for correlation. The lithostratigraphy, biostratigraphy, chronostratigraphy, measured sections and ranges of ostracode and planktonic foraminiferal taxa for the eastern Mississippi CRS are presented on text-figure 4 and for the central Alabama CRS on text-figure 5.

Approximately 2-3 kg of sample was collected at five-ft (1.6 m) intervals. Samples were broken into small (1-3cm) pieces, oven dried at approximately 60°C, placed overnight in a dilute (3%) hydrogen peroxide solution, then sieved through a 200µm screen. Random samples of 300 specimens of ostracodes were picked for a previous study (Puckett 1996), and additional specimens of ostracodes and planktonic foraminifera were picked for biostratigraphic calibration. The samples were randomized by splitting the samples until fewer than 300 specimens remained, picking all of the specimens, then repeating the process until approximately 300 specimens were picked.

The ranges of the ostracodes and planktonic foraminifera in the two CRSs were correlated into a composite standard section by graphic correlation (text-fig. 6) using methodologies developed by Shaw (1964) (also see Carney and Pierce 1995; Edwards 1995; Macleod and Sadler 1995). Correlation was computed using the software package GraphCor (Hood 1986-1998). Seven stratigraphic horizons were selected to define the line of correlation: (1) the highest occurrence surface (HOS) of the planktonic foraminifer *Dicarinella asymetrica*, which marks the Santonian-Campanian Stage boundary; (2) the top of the Arcola Limestone Member of the Mooreville Chalk, which is an essentially synchronous surface (Smith 1995); (3) a bed of the oyster *Pycnodonte convexa*, which occurs in the middle portion of the Demopolis Chalk; (4) the lowest occurrence surface (LOS) and (5) HOS of the planktonic foraminifer *Globotruncanita calcarata*; (6) the LOS of the planktonic foraminifer *Globotruncana aegyptiaca*; and (7) the top of the Cretaceous. The consistent stratigraphic occurrence of *P. convexa* was pointed out to the author in 1989 by Don Keady, then at Mississippi State University. The oyster bed occurs in relatively pure chalk facies and contains specimens of the hemispherical species in apparently the same ontogenetic stage, but its origin is unknown. Its occurrence is, however, apparently related to a single event, thus accounting for its synchroneity. The chronostratigraphic age of four of the seven stratigraphic markers is established on a global standard: the HOS of *D. asymetrica*, the LOS and HOS of *G. calcarata*, and the LOS of *G. aegyptiaca*. The composite ranges of the ostracodes are presented in text-figure 7 and the

composite ranges of the planktonic foraminifera are presented in text-figure 8.

BIOSTRATIGRAPHY

The common sampling of ostracodes and planktonic foraminifera allows direct correlation of the two groups of microfossils for the northern Gulf Coastal Plain. The planktonic foraminiferal biostratigraphic zonation used herein follows well-established global standards of Robaszynski et al. (1984), Caron (1985), and Premoli Silva and Sliter (1999). The chronostratigraphic calibration of absolute age dates follows that of Gradstein et al. (1994). The planktonic foraminifera zones recognized in this study are defined below.

Planktonic Foraminifera

Dicarinella asymetrica Taxon Range Zone

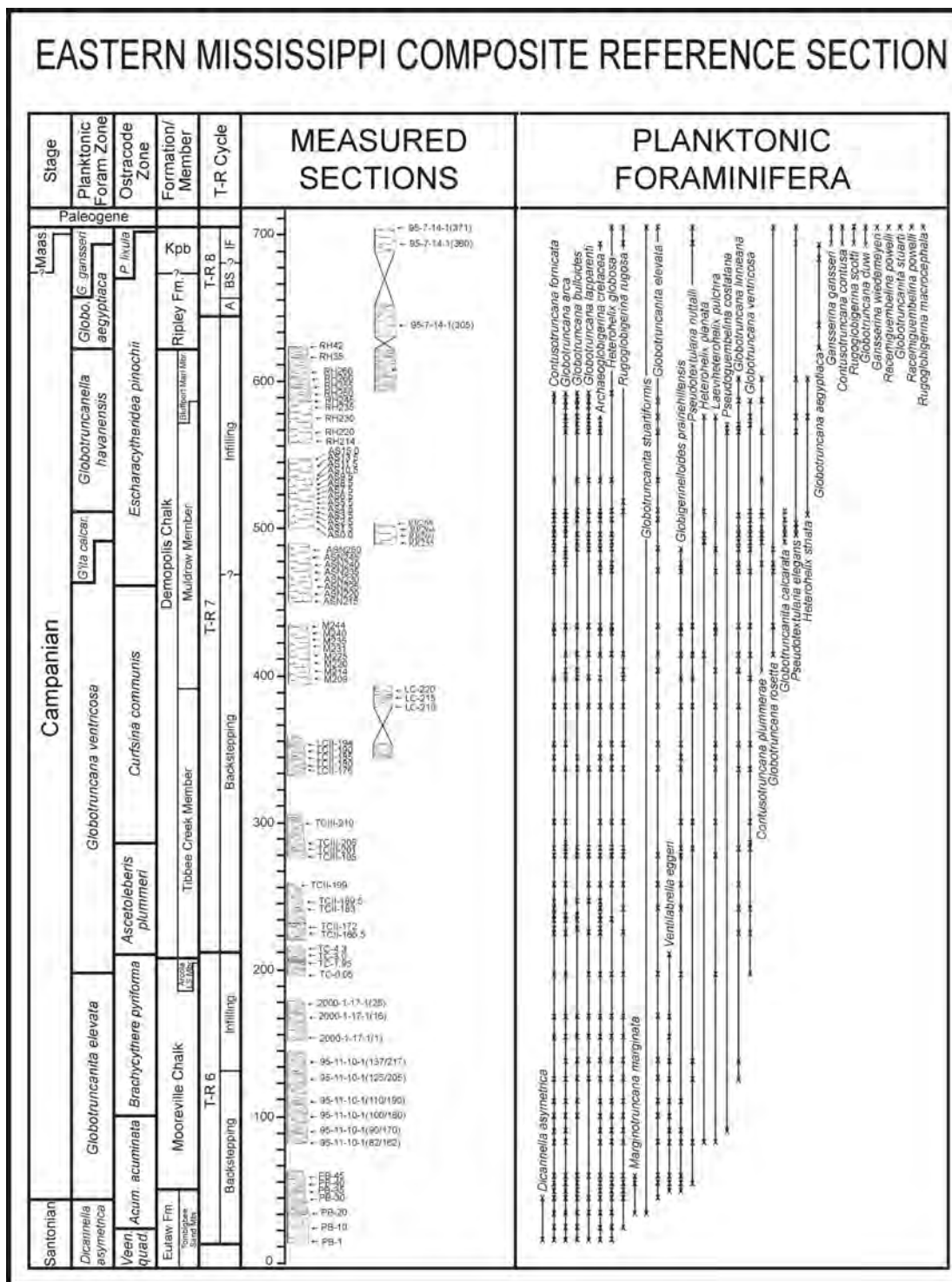
Boundary definitions: The base and top of this zone are defined by the LOS and HOS, respectively, of the nominal taxon (Postuma 1971). The LOS of *D. asymetrica* occurs in the early part of the Santonian (Caron 1985; Premoli Silva and Sliter 1999); in fact, Premoli Silva and Sliter (1999) considered this zone to include almost all of the Santonian. The HOS of *D. asymetrica* is essentially coincidental with the Santonian-Campanian Stage boundary, which is officially marked by the HOS of *Marsupites testudinarius* (Hancock and Gale 1996). The age of the Santonian-Campanian boundary is 85.8 Ma (Gradstein et al. 1994; Premoli Silva and Sliter 1999).

The position of the LOS of *D. asymetrica* in the northern Gulf Coastal Plain is not known precisely. In the central Alabama CRS, which includes the chronostratigraphically oldest marine Late Cretaceous strata in the region, *D. asymetrica* occurs among the earliest planktonic foraminifera (text-fig. 5) and thus its LOS cannot be determined reliably. Circumstantial evidence suggests, however, that the LOS of *D. asymetrica* in central Alabama is near its global LOS. In central Alabama, the LOS is approximately 104 ft (33.1m) below its HOS in marl facies. The chronostratigraphic framework of Primoli Silva and Sliter (1999) indicates that the *D. asymetrica* Zone ranges from approximately 85.7 Ma to 83.4 Ma, a time interval of 2.3 Ma. By comparison, the *Globotruncanita calcarata* Zone ranges from approximately 75.0 Ma to 75.8 Ma, a time interval of 0.8 Ma. The *G. calcarata* Zone is approximately 30 ft (9.6 m) thick throughout the northern Gulf Coastal Plain. Assuming that the net rate of sediment accumulation during the *D. asymetrica* Zone was of the same magnitude as during the *G. calcarata* Zone, the thickness of the sediments that accumulated during the *D. asymetrica* Zone would be calculated to be 86 ft (27.4 m) thick. [Note: This ratio calculation is as follows:

$$\frac{30 \text{ feet}}{0.8 \text{ MA}} = \frac{x}{2.3 \text{ MA}}, x = 86.2 \text{ ft (27.4 m)}$$

The *D. asymetrica* Zone in central Alabama is, in fact, even greater than this predicted value, supporting the conclusion that the LOS of *D. asymetrica* in central Alabama is close to its earliest global chronostratigraphic position, which is of early Santonian age.

The HOS of *D. asymetrica* is well defined in the northern Gulf Coastal Plain and is an excellent biostratigraphic marker horizon. The *D. asymetrica* Zone ranges paleoenvironmentally throughout marl facies in central Alabama to sandy marl facies in western Alabama and eastern Mississippi. These strata occur in the T-R K6 cycle of Mancini and Puckett (2005). As noted

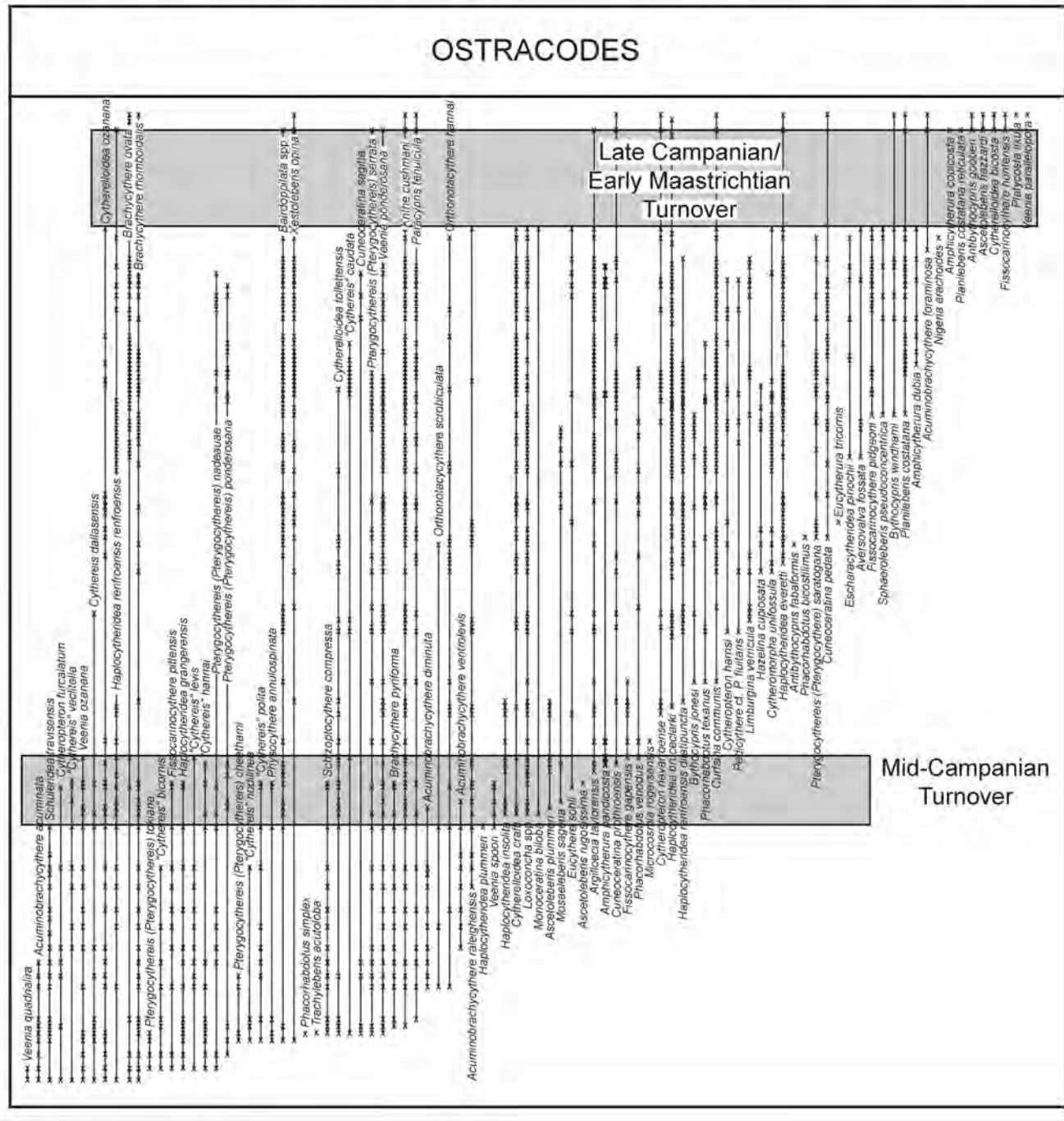


TEXT-FIGURE 4

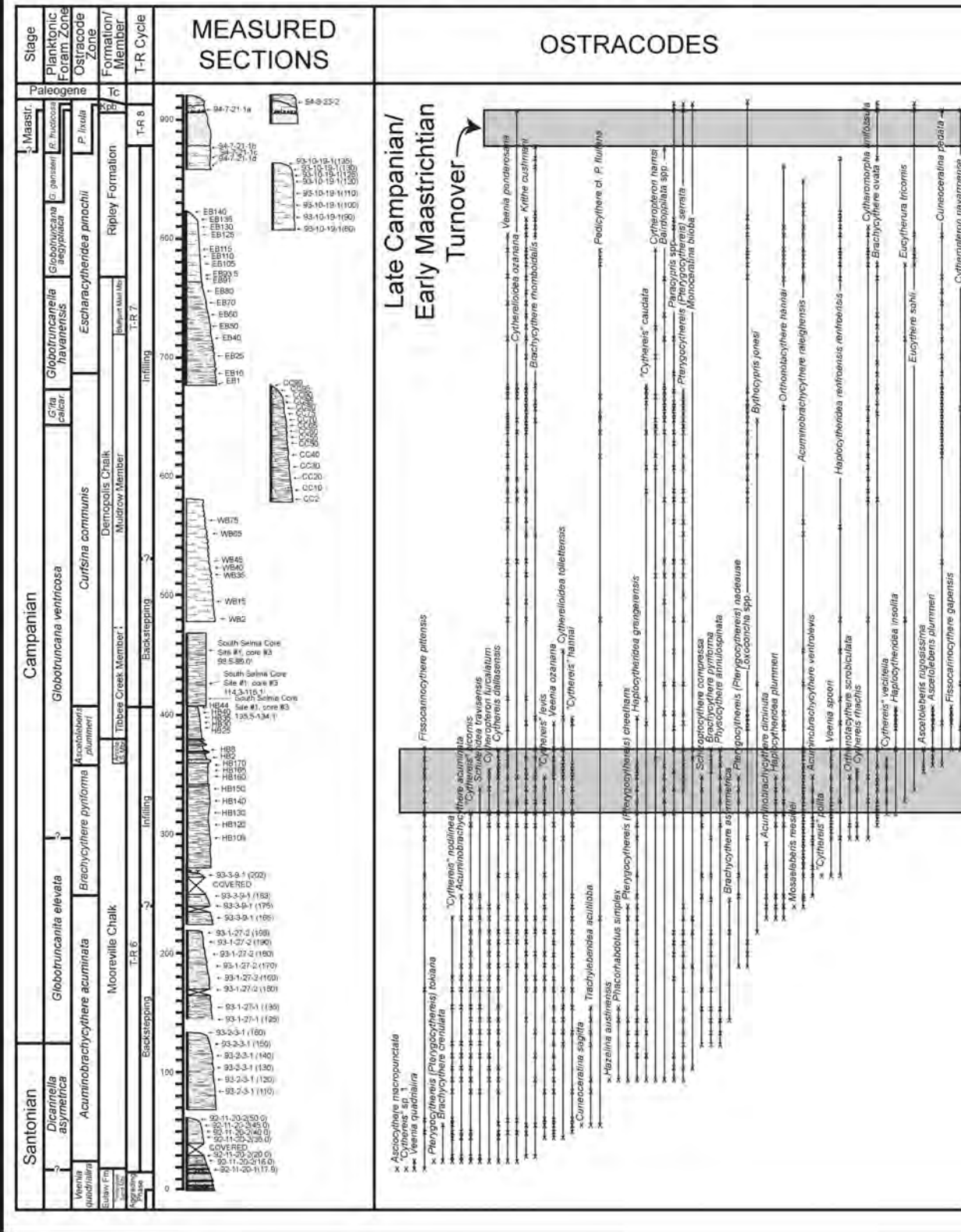
TEXT-FIGURE 4
Chronostratigraphy, biostratigraphy, lithostratigraphy, transgressive-regressive cycles, measured sections, and ranges of ostracodes and planktonic foraminifera in the eastern Mississippi composite reference section.

EASTERN MISSISSIPPI COMPOSITE REFERENCE SECTION

OSTRACODES

TEXT-FIGURE 4
continued

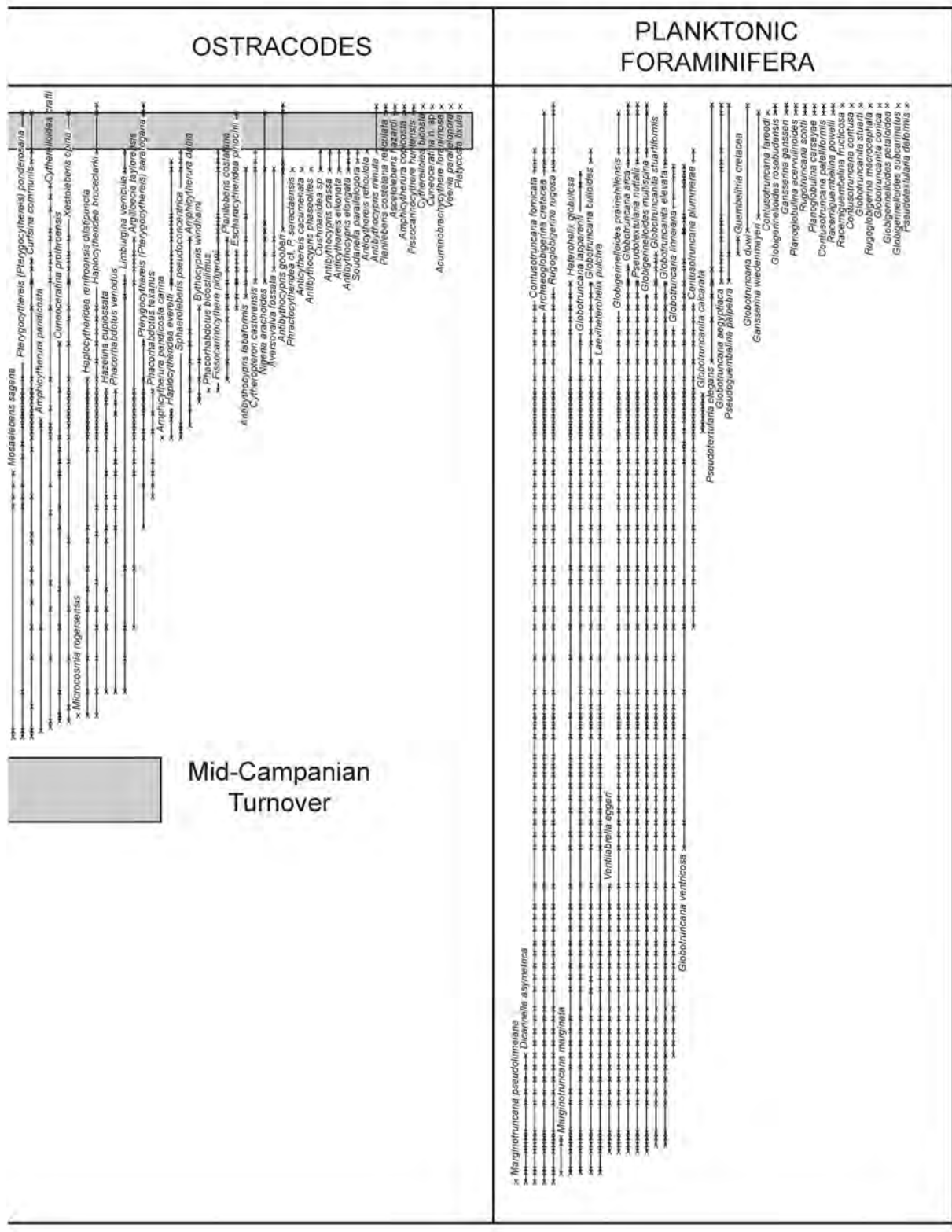
ALABAMA RIVER COMPOSITE SECTION



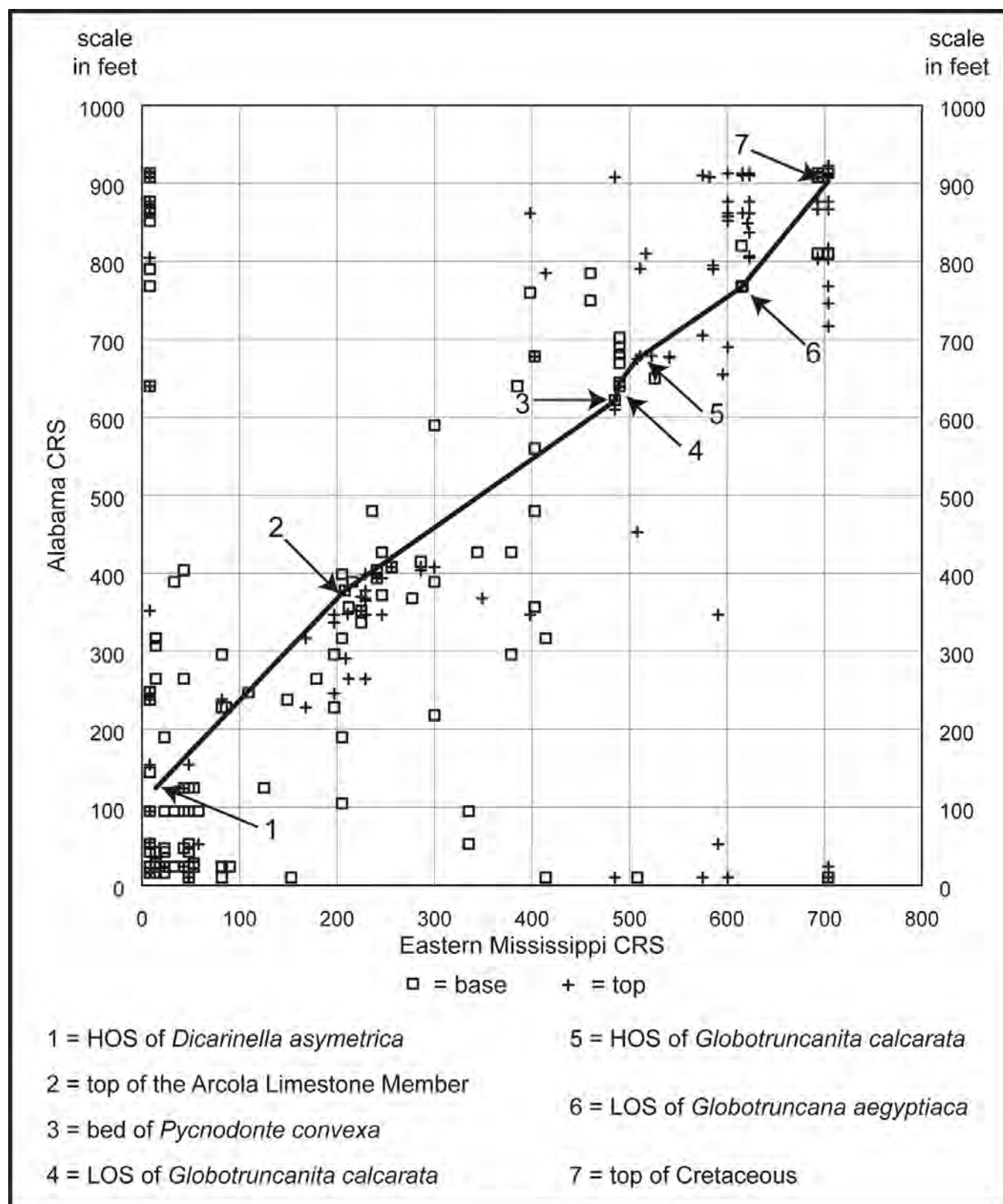
TEXT-FIGURE 5

Chronostratigraphy, biostratigraphy, lithostratigraphy, transgressive-regressive cycles, measured sections, and ranges of ostracodes and planktonic foraminifera in the central Alabama composite reference section.

ALABAMA RIVER COMPOSITE SECTION

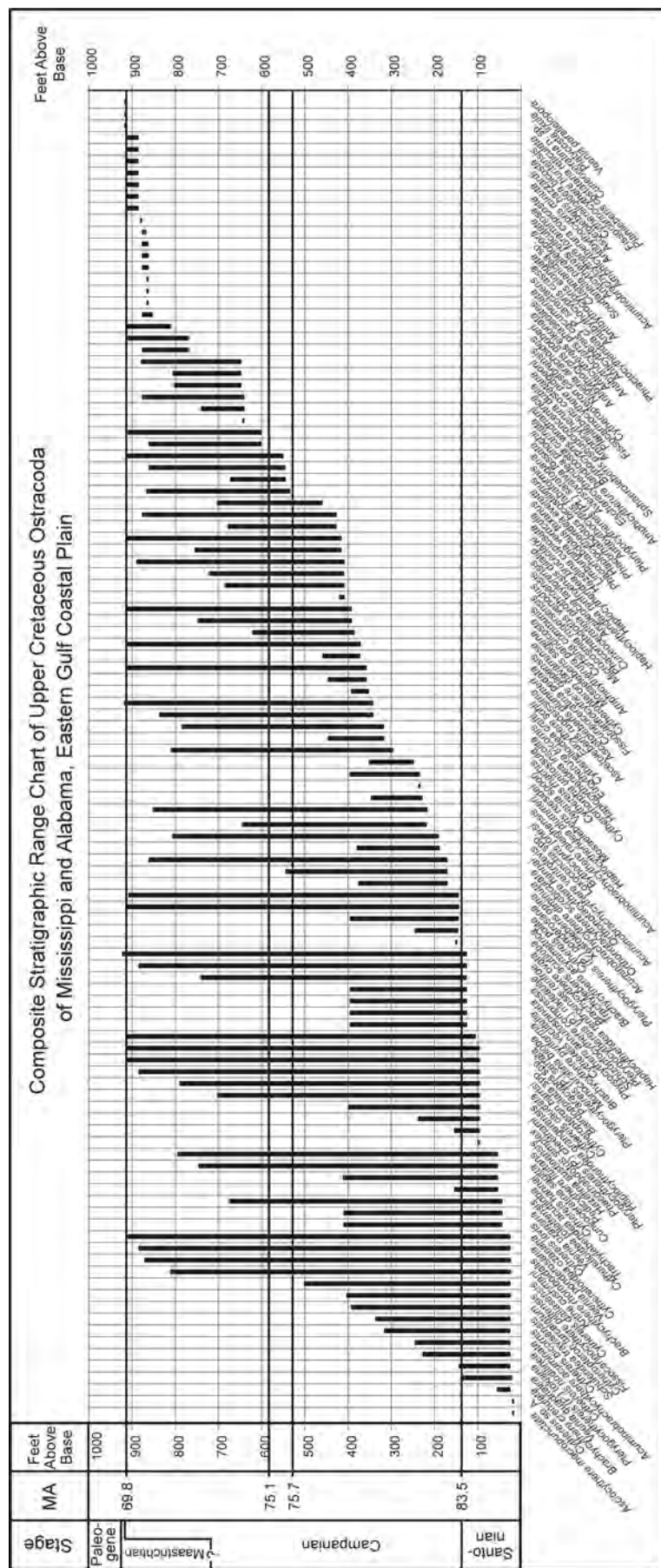


TEXT-FIGURE 5
continued.



TEXT-FIGURE 6

Graphic correlation of central Alabama and eastern Mississippi composite reference sections. See text for discussion.



TEXT-FIGURE 7 Composite stratigraphic ranges of ostracodes in the eastern Mississippi and central Alabama composite reference sections based on graphic correlation.

previously, the top of this zone occurs 104 ft (33.1 m) above the Tombigbee Sand Member-Mooreville Chalk lithostratigraphic boundary in central Alabama, but occurs at this boundary in eastern Mississippi. The eastern Mississippi area apparently continued to receive an influx of relatively coarse-grained sediment much later than in central Alabama, as indicated by an inverse thickness relationship between the Tombigbee Sand and Mooreville Chalk in eastern Mississippi as observed in well log signatures. If the base of the global chronostratigraphic zone of *D. asymmetrica* is at the base of the Mooreville Chalk in central Alabama, and the HOS is known to be at the base of the Mooreville Chalk in eastern Mississippi, then the Tombigbee Sand Member-Mooreville Chalk boundary is approximately 2.3 Ma younger in eastern Mississippi than in central Alabama. The source of the sediment influx in eastern Mississippi is interpreted to be the ancestral Tombigbee River, which was in the same general location as the modern Tombigbee River (text-fig. 2).

The *Globotruncanita elevata* Interval Zone

Boundary definitions: HOS of *Dicarinella asymmetrica* to the LOS of *Globotruncana ventricosa*, with the presence of the nominal taxon (Postuma 1971). The base of the *G. elevata* Zone corresponds closely to the base of the Campanian Stage, and the top of the zone occurs near the top of the lower third of the Campanian (Premoli Silva and Sliter 1999). The *G. elevata* Zone occurs in the middle of the Mooreville Chalk in the central Alabama CRS and throughout the Mooreville Chalk in the eastern Mississippi CRS. The discrepancy in the upper boundary of the zone is probably due to the rarity of *Globotruncana ventricosa*, whose LOS is poorly defined. These strata occur in the upper part of the T-R K6 cycle of Mancini and Puckett (2005). The LOS of *G. elevata* occurs well below the HOS of *D. asymmetrica* (Robaszynski et al. 1984; Caron 1985; Premoli Silva and Sliter 1999). The zone of overlap has, in fact, proven to be a very useful biostratigraphic interval (Wagreich 1992). In the central Alabama CRS, the LOS of *G. elevata* occurs only 40 ft (12.7 m) above the LOS and 64 ft (20.4 m) below the HOS of *D. asymmetrica*. In eastern Mississippi, the LOS of *G. elevata* occurs only slightly above the LOS of *D. asymmetrica* due to the relatively younger age of the marine strata in that area. Unfortunately, the LOS of *G. ventricosa* is poorly defined due to its rare occurrence. *Globotruncana ventricosa* is, in fact, rare throughout its stratigraphic extent, except in the chalky facies of the middle portion of the Demopolis Chalk (Muldrow Member). The lowest occurrence of *G. ventricosa* in the northern Gulf region is just below the base of the Arcola Limestone Member of the Mooreville Chalk. The top of the *G. elevata* Zone is at the approximate top of the lower 1/3 of the Campanian Stage (Premoli Silva and Sliter 1999). Thus, the lower unnamed member of the Mooreville Chalk ranges in age from early Santonian to early Campanian.

The *Globotruncana ventricosa* Interval Zone

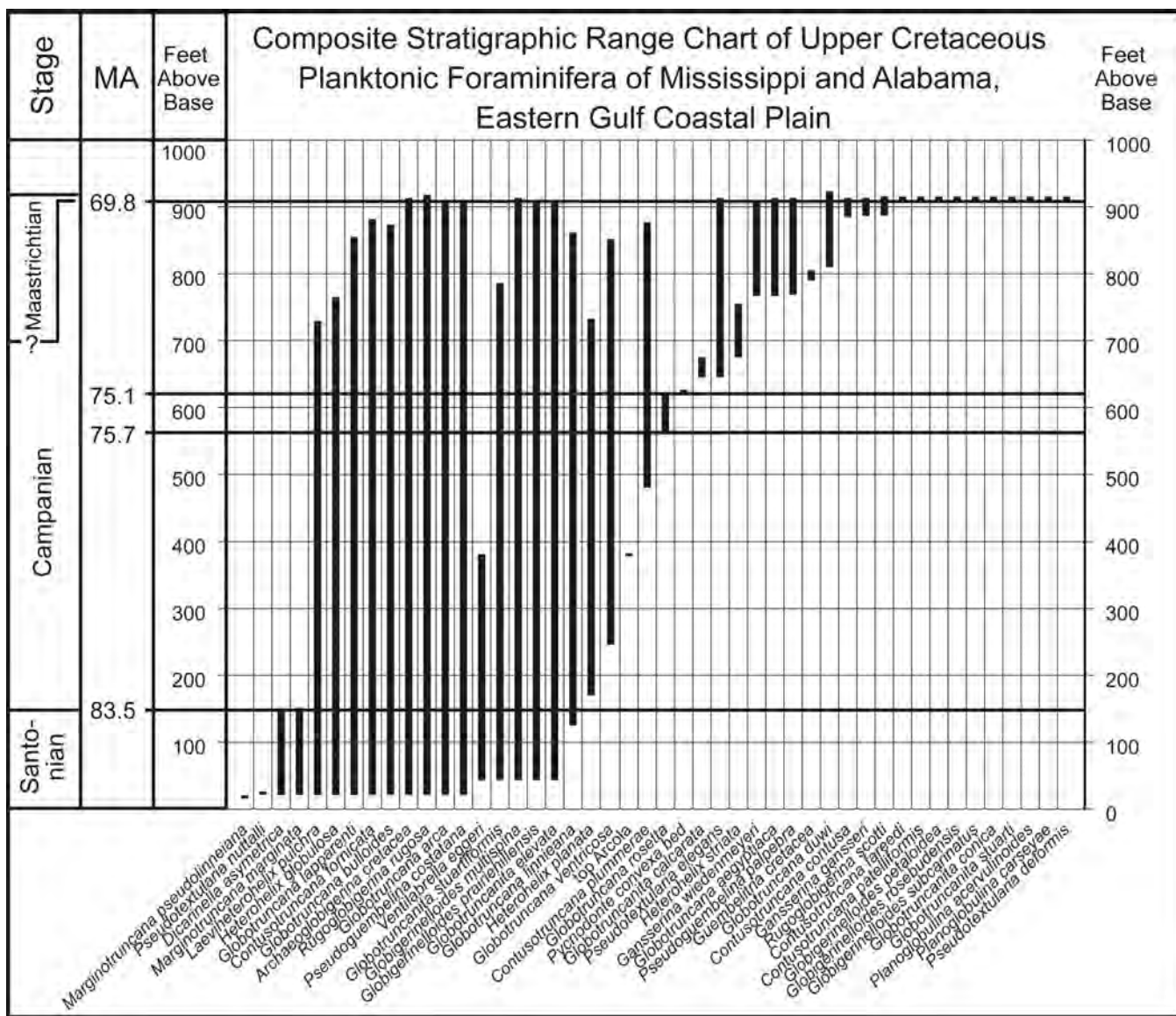
Boundary Definitions: The base of the *G. ventricosa* Interval Zone is defined on the basis of the LOS of the nominal taxon and the top of the zone is based on the LOS of *Globotruncanita calcarata* (Dalbiez 1955). As noted previously, the LOS of *G. ventricosa* is poorly defined in the Mississippi-Alabama area, but the LOS of *G. calcarata* is well defined. Lithostratigraphically, the LOS of *G. ventricosa* occurs near the top of the lower unnamed member of the Mooreville Chalk, and the zone

extends up through the Arcola Limestone Member of the Mooreville and the Tibbee Creek Member of the Demopolis Chalk and into the Muldrow Member of the Demopolis. These strata occur in the T-R K7 cycle of Mancini and Puckett (2005). Within the *G. ventricosa* Zone, the strata vertically change from marl to chalk facies; this change occurs at the approximate top of the lower 1/3 of the Demopolis Chalk. The LOS of *G. calcarata* occurs near the middle of the Muldrow Member of the Demopolis, but occurs just above the chalky member (within the Bluffport Marl Member of the Demopolis) in northern Mississippi.

The *Globotruncanita calcarata* Taxon Range Zone

Boundary Definitions: The upper and lower boundaries of the *Globotruncanita calcarata* Taxon Range Zone are defined on the basis of the LOS and HOS, respectively, of the nominal taxon (Herm 1962). An in-depth discussion of the zone, including its global occurrences, was presented in Puckett and Mancini (1998) and further details of the zone in Mississippi and Alabama were presented by Puckett (1995b). The HOS of this zone was used for many years to define the Campanian-Maastrichtian stage boundary; for example, Puckett and Mancini (1998) listed more than 30 publications on planktonic foraminiferal biostratigraphy that used the HOS of *G. calcarata* to mark the Campanian-Maastrichtian boundary. Unfortunately, the Maastrichtian Working Group elected to use the LOS of the ammonite *Pachydiscus neubergicus* to mark the boundary (Odin 1996), which is well above the HOS of *G. calcarata*. This selection was unfortunate because *P. neubergicus* does not occur in the Americas and there is no reliable calcareous macro- or microfossil proxy (it occurs somewhere in the *Gansserina gansseri* Zone). Further, when the recommendation of the ammonite definition was published (Hancock and Gale 1996; Odin 1996), the precise position of its LOS was not known, being described as "...somewhere in the range of levels 112-127..." Nonetheless, the ammonite definition of the base of the Maastrichtian places the HOS of *G. calcarata* near the base of the upper third of the Campanian and ranging in age from approximately 75.8 to 75.1 Ma (Premoli Silva and Sliter 1999).

The *G. calcarata* Zone is one of the most useful planktonic foraminiferal zones in the northern Gulf Coastal Plain. The boundaries of the zone are well defined, the zone is chronostratigraphically narrow, and ranges geographically almost from one end of the marine basin to the other. The zone in the Mississippi-Alabama area was initially difficult to find, due both to the lithostratigraphically thin distribution and to the general rarity of the taxon. Once the zone was found, however, its consistent stratigraphic position made it easy to project across the basin. In addition, a distinctive bed of the oyster *Pycnodonte convexa* occurs 23 ft (7.3 m) below the LOS of *G. calcarata* and is an excellent field marker for the zone. In the regions of the eastern Mississippi and central Alabama CRSs, the *G. calcarata* Zone occurs in the Muldrow Member of the Demopolis Chalk. In northern Mississippi, however, the *G. calcarata* Zone occupies beds of the Bluffport Marl Member and farther north, in central Tennessee, the zone occurs in the transitional clays between the Demopolis Chalk and Coon Creek Formation, which is near the northern terminus of the Upper Cretaceous marine deposits. In far eastern Alabama, the *G. calcarata* Zone occurs in sandy marl of the Cusseta Sand. These strata occur in the lower part of the T-R K7 cycle of Mancini and Puckett (2005).



TEXT-FIGURE 8
Composite stratigraphic ranges of planktonic foraminifera in the eastern Mississippi and central Alabama composite reference sections based on graphic correlation.

The *Globotruncanella havanensis* Interval Zone

Boundary Definitions: The upper and lower boundaries of the *Globotruncanella havanensis* Interval Zone are defined on the basis of the HOS of *G. calcarata* and LOS of *Globotruncana aegyptiaca*, respectively, with the occurrence of *G. havanensis* (Caron 1978). This zone is in the upper Campanian Stage. In the northern Gulf Coastal Plain, *G. havenensis* is very rare, and its upper and lower boundaries have not been defined. The zone occurs in the Muldrow Member of the Demopolis Chalk and in the Ripley Formation; the top of the zone is nearly coincidental with the Bluffport Marl Member-Ripley Formation contact in both eastern Mississippi and central Alabama. These strata occur in the middle portion of the T-R K7 cycle of Mancini and Puckett (2005).

The *Globotruncana aegyptiaca* Interval Zone

Boundary Definitions: The LOS and HOS of the *Globotruncana aegyptiaca* Interval Zone are defined by the LOS of the nominal taxon and the LOS of *Gansserina gansseri*, respectively (Caron 1985). In Alabama and Mississippi, this zone occurs in the lower part of the Ripley Formation. This interval corresponds to the upper part of T-R K7 of Mancini and Puckett (2005). The nominal taxon occurs rarely, particularly in the lower part of its range.

The upper part of T-R K7 is comprised of the backstepping phase of the cycle, and is observed as a shallowing-upward interval. The sediments grade upward from marl to sandy marl and are capped by an unconformity, marking the top of the T-R

K7 cycle. As noted by Puckett (1996), planktonic foraminifera and ostracodes generally display an inverse abundance and diversity relationship, which is observed in the backstepping phase of the lower and middle parts of the Ripley Formation. The aggrading phase of the T-R K8 cycle overlies the unconformity separating the T-R K7 and T-R K8 cycles, which is overlain by a transgressive ravinement surface containing abundant oysters near the top of the Ripley Formation. Calcareous microfossil biostratigraphy of the overlying Prairie Bluff Chalk indicates a significant time gap between the shallow marine deposits of the T-R K7 cycle and the Prairie Bluff that probably includes the global LOS of *Gansserina gansseri*. Thus, the global occurrence of the top of the *G. aegyptiaca* Zone is not believed to be observed in the northern Gulf Coastal Plain.

The *Gansserina gansseri* Interval Zone

Boundary Definitions: The LOS of the nominal taxon marks the base of this zone (Brönnimann 1952) and the top is marked by the lowest co-occurrence surface of *Contusotruncana contusa* and *Racemiguembelina fructicosa*. The top of the *G. gansseri* Zone was originally defined (Brönnimann 1952) as the LOS of *Abathomphalus mayaroensis*, and many workers have subsequently used that definition as the top of the zone (Caron 1985). Premoli Silva and Sliter (1994; 1999), however, used the LOS of *Contusotruncana contusa* and *R. fructicosa* to mark the upper boundary of the *G. gansseri* Zone, a practice followed herein. There are two reasons for adopting this system. First, *A. mayaroensis* has not been observed in the northern Gulf Coastal Plain; thus, based on *A. mayaroensis* the top of the *G. gansseri* Zone can not be identified in this area. Second, the LOS of *C. contusa* and *R. fructicosa* occurs at an interval of the appearance of a significant number of planktonic foraminifera, such as several species of *Rugoglobigerina*, *Contusotruncana patelliformis*, and *Racemiguembelina powelli*, that show highly evolved morphologies that are characteristic of the Maastrichtian, and thus marks a distinctive biostratigraphic horizon.

The *G. gansseri* Zone occurs throughout the Prairie Bluff Chalk. As noted previously, the first global appearance of *G. gansseri* probably does not occur in the northern Gulf Coastal Plain because, during that chronostratigraphic interval, nonmarine paleoenvironmental conditions were prevalent. The nonmarine interval is the aggrading phase of the T-R K8 cycle, which is overlain by backstepping deposits, including a ravinement surface and a marginal marine oyster bed, all of which are in the upper Ripley Formation. *G. gansseri* appears above this nonmarine interval. *Gansserina wiedenmeyeri*, which is very similar morphologically to *G. gansseri*, appears below this nonmarine interval. Globally, *Gansserina wiedenmeyeri* occurs only slightly below the LOS of *G. gansseri* (Robaszynski et al. 1984; Premoli Silva and Sliter 1999), indicating that the relatively high stratigraphic position of *G. gansseri* relative to *G. wiedenmeyeri* is due to unfavorable paleoenvironmental conditions.

According to Odin (1996), the Campanian-Maastrichtian boundary occurs at the LOS of the ammonite *Pachydiscus neubergicus*. This stratigraphic position occurs somewhere in the *G. gansseri* Zone. Unfortunately, there is no microfossil proxy for the Campanian-Maastrichtian boundary and, with the absence of *P. neubergicus* in the Americas, the position of this boundary cannot be determined.

The *Contusotruncana contusa-Racemiguembelina fructicosa* Interval Zone

Boundary Definitions: The LOS of the nominal taxa marks the lower boundary of this zone and the LOS of *Abathomphalus mayaroensis* marks the upper boundary (Premoli Silva and Sliter 1994, 1999). Smith and Pessagno (1973) described the *Racemiguembelina fructicosa* Zonule as the upper part of the *G. gansseri* Subzone of the *Globotruncana contusa-stuartiformis* Assemblage Zone. Although the nomenclature of Smith and Pessagno (1973) is different than that used herein, the *Racemiguembelina fructicosa* Zonule of Smith and Pessagno (1973) has the same boundary definitions as the *C. contusa-R. fructicosa* Zone as defined by Premoli Silva and Sliter (1994; 1999).

The upper boundary of the *C. contusa-R. fructicosa* Zone has not been observed in the northern Gulf Coastal Plain because of the absence of *A. mayaroensis*. Only the uppermost parts of the Prairie Bluff Chalk along the Alabama River occur within the *C. contusa-R. fructicosa* Zone. At the type locality of the Prairie Bluff Chalk in Wilcox County, Alabama, along the Alabama River (the uppermost Cretaceous section included in this study), the unconformity between the Cretaceous Prairie Bluff and the Paleogene Clayton Formation is observable as an undulating surface, and only the uppermost Prairie Bluff contains *R. fructicosa*. In the eastern Mississippi CRS, the uppermost part of the Prairie Bluff includes *C. contusa* but not *R. fructicosa*. With the revised definition of the Maastrichtian Stage (Odin 1996), *G. gansseri* occurs in the lower third of the stage, the *C. contusa-R. fructicosa* Zone occupies a narrow interval just below the middle of the stage, and the *A. mayaroensis* Zone occupies the upper half of the stage. Thus, in reference to planktonic foraminiferal biozonation, the approximate upper two-thirds of the Maastrichtian Stage are missing.

Some authors have maintained that the K/P boundary section in Alabama is among the most complete in the world, with very little time missing (Habib et al. 1992; Olsson and Liu 1993). This interpretation is due to the presence of the latest Maastrichtian calcareous nannofossil species *Micula prinsii*, the basal Danian *Guembelitria cretacea* P0 planktonic foraminiferal zone, and the dinoflagellate species *Damassadinium californicum*, also of earliest Danian age (Habib et al. 1996; Olsson et al., 1996). The absence of *A. mayaroensis* was interpreted to be due to unfavorable paleoenvironmental conditions. Smith (1997) disagreed with the interpretation that the K/P boundary hiatus in Alabama is of minimal duration, citing evidence from calcareous microfossils. A distinctive bed of abundant, phosphatized macrofossils (oysters, ammonites and gastropods) occurs within the Prairie Bluff Chalk at several localities, mostly clearly at Moscow Landing in western Alabama. Mancini et al. (1989), Mancini et al. (1996), Smith (1997) and Mancini and Puckett (2003b) interpreted this bed to be the surface of maximum transgression in the latest Cretaceous depositional sequence (T-R K8 cycle of Mancini and Puckett 2005). The interval in the Prairie Bluff below this phosphatic zone was assigned to the lower portion of the *G. gansseri* Zone (Mancini et al. 1989; Smith 1997), whereas the interval above this phosphatic zone was assigned to the *Racemiguembelina fructicosa* Zone. In addition, Mancini et al. (1989) and Smith (1997) assigned the lowermost Clayton Formation to the *Morozovella pseudobulloides* planktonic foraminiferal zone of middle early Paleocene age, indicating a hiatus between the Cretaceous and Paleogene that includes most of the Maastrichtian Stage and the early portion



TEXT-FIGURE 9

Type locality of the Muldrow Chalk Member of the Demopolis Chalk, Oktibbeha County, Mississippi. The contact between the Muldrow Member and the Bluffport Marl Member of the Demopolis Chalk is well exposed at the "Rock Hill" section, in the NE $\frac{1}{4}$ sec. 14, T. 19 N, R14 E, Cedar Bluff 7.5 minute topographic quadrangle, Oktibbeha County, Mississippi, lat. 33°30'58", long. 88°47'13". This locality is approximately 5 miles (8 km) from the Muldrow Member type locality. The lower contact of the Muldrow Member is poorly exposed at the small creek at the base of the section at the type locality. The lower and upper contacts are distinct. The Muldrow Member is approximately 35 ft (11.1m) thick at the type locality and approximately 180 ft (57m) thick in the region of the type locality.

of the early Paleocene. The results of the present study are in agreement with those of Mancini et al. (1989) and Smith (1997).

For the present study, it is clear that the uppermost Maastrichtian is missing. Along the troughs of the undulating unconformity between the Prairie Bluff and the overlying fluvial deposits at section 94-8-23-2, highly evolved planktonic foraminifera such as *Contusotruncana patelliformis* and *Racemiguembelina powelli* are present, but *R. fructicosa* and *C. contusa* are absent. These latter two taxa are found, however, in the crests of the undulating surface. These observations indicate that the unconformity at this locality straddles the base of the *C. contusa-R. fructicosa* Interval Zone, indicating a middle Maastrichtian age.

Ostracoda

Ostracodes are more than twice as diverse as planktonic foraminifera in the northern Gulf Coastal Plain and are thus useful for biostratigraphy. The key to the great paleobiogeographic utility of the ostracodes lies in their endemism; that is, nearly all ostracode species are restricted to North America (from New Jersey in the Atlantic Coastal Plain to Texas in the Gulf Coastal Plain) and are therefore biostratigraphically useful only for local or regional correlation. The combination of the

global chronostratigraphic utility of the planktonic foraminifera and the diverse ostracode fauna offers a means of high-resolution biostratigraphic subdivision of the marine Upper Cretaceous strata in the Gulf Coast.

In contrast to the global biostratigraphic work that has been accomplished for planktonic foraminifera, the published work on ostracode biostratigraphy is relatively limited. Hazel and Brouwers (1982) published the first and most comprehensive biostratigraphic zonation of ostracodes for the North American Gulf Coastal Plain, which was subsequently modified by Pitakpaivan and Hazel (1994). Puckett (1995a), Mancini et al. (1996) and Mancini and Puckett (1998) applied the biostratigraphic zonation of Hazel and Brouwers (1982) to subdivide the Santonian-early Maastrichtian portion of the Upper Cretaceous of the northern Gulf Coastal Plain. The biostratigraphic zonation of Hazel and Brouwers (1982) and Pitakpaivan and Hazel (1994) is therefore a valuable tool followed herein, with rare and noted exceptions.

The *Veenia quadrialira* Taxon Range Zone (Amended)

Boundary Definitions: The lower boundary and upper boundaries of the *Veenia quadrialira* Taxon Range Zone are defined on the basis of the LOS and HOS, respectively, of the nominal

taxon. Hazel and Brouwers (1982) originally defined this zone as the interval between the LOS of the nominal taxon and the LOS of *Pterygocythereis (Pterygocythereis) cheethami*. Previous studies (Puckett 1995a) and the results of the present study indicate that the LOS of *P. (P.) cheethami* occurs well above the HOS of the nominal taxon; thus, there is a significant gap in the *V. quadrialira* Zone where the nominal taxon is not present. Further, there are other limitations with using *P. (P.) cheethami* as a biostratigraphic taxon in the sense of Hazel and Brouwers (1982). For example, the upper boundary of *P. (P.) cheethami* occurs well below the LOS of *Ascetoleberis plummeri*, which defined the upper boundary of the *P. (P.) cheethami* Zone. It is for these reasons that the zonal boundaries have been amended from their original definitions.

The *Veenia quadrialira* Zone is relatively thin in the northern Gulf Coastal Plain. The nominal taxon occurs at the base of the Upper Cretaceous marine deposits, but its HOS occurs only about 10 feet (3.1 m) above that surface in the central Alabama CRS, and it occurs only on the lowest sample in the eastern Mississippi CRS, and in the Tombigbee Sand Member of the Eutaw Formation in both localities. As has been noted previously, the Tombigbee Sand Member and the lower Mooreville Chalk are considerably older in central Alabama than in eastern Mississippi. The restriction of *V. quadrialira* to the lower part of the Tombigbee Sand Member suggests that the taxon was restricted to shallow marine paleoenvironments, and therefore its HOS is probably time-transgressive, being older in central Alabama. The Tombigbee Sand Member occurs in the initial backstepping phase of the T-R K6 cycle of Mancini and Puckett (2003a; 2005). The *V. quadrialira* Zone occurs in the *Dicarinella asymetrica* planktonic foraminiferal zone of late Santonian age.

The *Acuminobrachycythere acuminata* Interval Zone

Boundary Definitions: The HOS of *Veenia quadrialira* defines the base of this zone and the HOS of the nominal taxon defines the top of the zone. In terms of planktonic foraminifera, the base of the zone occurs in the *Dicarinella asymetrica* Zone of late Santonian age and top of the zone occurs in the lower part of the *Globotruncanita elevata* Zone of early Campanian age.

The *A. acuminata* Zone subdivides *P. (P.) cheethami* Zone of Hazel and Brouwers (1982) into two parts, with the upper part comprising the *Brachycythere pyriforma* Interval Zone, defined below. Both *A. acuminata* and *B. pyriforma* are much more reliable biostratigraphic indicators due to more consistent stratigraphic occurrences.

The *A. acuminata* Zone occurs in the uppermost part of the Tombigbee Sand Member and in the lower part of the Mooreville Chalk. These strata occur in the backstepping phase of the T-R K6 cycle of Mancini and Puckett (2005).

The *Brachycythere pyriforma* Interval Zone

Boundary Definitions: The lower boundary of the *Brachycythere pyriforma* Interval Zone is defined on the basis of the HOS of *Acuminobrachycythere acuminata* and the upper boundary is defined on the basis of the LOS of *Ascetoleberis plummeri*, with the occurrence of the nominal taxon. In the northern Gulf Coastal Plain, the stratigraphic occurrence of *Ascetoleberis plummeri* is a distinctive and reliable marker zone. This zone occupies the upper part of *P. (P.) cheethami* Zone (Hazel and Brouwers 1982). Lithostratigraphically, the *B.*

pyriforma Zone occurs in the upper part of the Mooreville Chalk. In eastern Mississippi, the top of this zone occurs just above the Arcola Limestone Member and, in central Alabama, the top of this zone occurs near the base of the Arcola Limestone Member. The stratigraphic occurrences are in the infilling phase of Mancini and Puckett's (2003a, 2005) T-R K6. The top of the *B. pyriforma* Zone occurs near the top of the *G. elevata* planktonic foraminiferal zone of early Campanian age.

The *Ascetoleberis plummeri* Taxon Range Zone

Boundary Definitions: The LOS and HOS of the nominal taxon marks the lower and upper boundary surfaces, respectively (Hazel and Brouwers 1982). With one exception, the *A. plummeri* Zone could be amended on the basis of all species of the genus, because all but one species, *A. hazzardi*, occur in a narrow stratigraphic zone. The species that group together closely include *A. plummeri* and *A. rugosissima*; in addition, Hazel and Brouwers (1982) calibrated *A. crassicarinata* to occur in this same stratigraphic interval, although the species has been observed in the Mississippi-Alabama area too rarely for its range to be defined (Puckett 1996). The stratigraphic range of the other species in this genus, *A. hazzardi*, occurs significantly higher in the section than the other species, occurring in the *G. gansseri* and the *C. contusa-R. fructicosa* planktonic foraminiferal zones. This stratigraphic relationship is anomalous because, although the morphologic similarity of *A. hazzardi* to the other species is remarkable, no species has been observed that connects the earlier species with *A. hazzardi*. Nonetheless, *A. plummeri* and *A. rugosissima* are very distinctive stratigraphic markers, resulting in the *A. plummeri* Zone as one of the most useful biostratigraphic markers in the marine Upper Cretaceous section in the northern Gulf Coastal Plain.

The *A. plummeri* Zone occurs from the base of the Arcola Limestone Member of the Mooreville Chalk to the lower portion of the Tibbee Creek Member of the Demopolis Chalk. This stratigraphic interval includes the uppermost part of the infilling phase of the T-R K6 cycle and the lowermost part of the backstepping phase of the T-R K7 cycle of Mancini and Puckett (2005), which include relatively shallow water deposits. These strata occur in the basal portion of the *G. ventricosa* planktonic foraminiferal zone of early middle Campanian age.

The *Curfsina communis* Interval Zone

Boundary Definitions: The lower and upper boundaries of the *Curfsina communis* Interval Zone are defined by the HOS of *A. plummeri* and the LOS of *Escharacytheridea pinochii*, respectively, with *C. communis*. *Curfsina communis* is one of the most persistent ostracode species in the northern Gulf Coastal Plain, and is present in virtually every sample within its stratigraphic range, making it a reliable stratigraphic marker species. Hazel and Brouwers (1982) defined a different zone for this stratigraphic interval, the *Limburgina verricula* Interval Zone, which was defined on the basis of the LOS of *L. verricula* and the LOS of *E. pinochii*. In this study, *L. verricula* occurred only sporadically, making it an unreliable stratigraphic marker species.

The *C. communis* Zone occurs in the upper portion of the Tibbee Creek Member and most of the Muldrow Member of the Demopolis Chalk. This stratigraphic interval occurs in the backstepping phase of the T-R K7 cycle of Mancini and Puckett (2005), and in the upper portion of the *G. ventricosa* to lower *G. havanensis* planktonic foraminiferal zones of middle Campanian age.

The *Escharacytheridea pinochii* Interval Zone

Boundary Definitions: The lower and upper boundaries of the *Escharacytheridea pinochii* Interval Zone are defined by the LOS of the nominal taxon and the LOS of *Platycosta lixula*, respectively (Hazel and Brouwers 1982). The nominal species of this zone occurs fairly persistently, and thus defines a good stratigraphic marker.

The *E. pinochii* Zone occurs in the upper part of the Muldrow Member and the Bluffport Member of the Demopolis Chalk, in the Ripley Formation, and in the lower part of the Prairie Bluff Chalk. These strata are in the upper, infilling phase of the T-R K7 and in the lower, backstepping phase of the T-R K8 cycles of Mancini and Puckett (2005). This stratigraphic interval occurs in the upper part of the *G. ventricosa* to lower part of the *G. gansseri* planktonic foraminiferal zones, ranging in age chronostratigraphically from the middle to upper Campanian Stage. As with *G. gansseri*, it is not likely that the LOS of *P. lixula* in the northern Gulf Coastal Plain represents its global LOS, as it appears coincidentally with the initial marine transgressive deposits of the T-R K8 cycle; its global LOS probably occurred during deposition of the nonmarine sediments of the infilling phase of the T-R K8 cycle.

The *Platycosta lixula* Interval Zone

Boundary Definitions: The lower and upper boundaries of the *Platycosta lixula* Interval Zone are defined by the LOS of the nominal taxon and the LOS of *Brachycythere plena* (Hazel and Brouwers 1982; Pitakpaivan and Hazel 1994). Originally, Hazel and Brouwers (1982) defined the *P. lixula* Interval Zone as the biostratigraphic interval between the LOS of the nominal taxon and the LOS of *Brachycythere plena* of early Paleocene age. This zone was subdivided by Pitakpaivan and Hazel (1994) to include a lower *P. lixula* Zone and an upper *V. parallelopora* Zone. In their emendation, the *P. lixula* Zone was described to occur in the Ripley Formation, and the *V. parallelopora* Zone occurred in the Prairie Bluff Chalk. In both the eastern Mississippi and central Alabama CRSs, *P. lixula* and *V. parallelopora* occur simultaneously in the uppermost sampled interval of the Prairie Bluff Chalk; thus, the *P. lixula* Zone of Pitakpaivan and Hazel (1994) was not observed. It is for this reason that the more inclusive, older definition of Hazel and Brouwers (1982) is used herein.

As stated previously, the *P. lixula* Zone occurs only in the uppermost Prairie Bluff Chalk collected in both eastern Mississippi and central Alabama. This horizon occurs immediately below the K-P boundary in both areas. These strata probably occur in the upper portion of the backstepping phase of the T-R K8 cycle of Mancini and Puckett (2005). The surface of maximum transgression (phosphatic zone) in both eastern Mississippi and central Alabama was not observed, and it is interpreted that this surface was eroded prior to the deposition of the overlying Clayton Formation. This interpretation is consistent with the planktonic foraminiferal biozonation, in which this interval is in the basal portion of the *C. contusa*-*R. fructicosa* Interval Zone of the lower third of the Maastrichtian Stage (Premoli Silva and Sliter 1999).

Biostratigraphic Summary

Based on planktonic foraminiferal biostratigraphy, the marine Late Cretaceous sediments of eastern Mississippi and central Alabama range from early Santonian to early Maastrichtian in age. The planktonic foraminiferal zones range from the *Dicari-*

nella asymmetrica Taxon Range Zone to the *Contusotruncana contusa*-*Racemiguembelina fructicosa* Interval Zone. The HOS of *D. asymmetrica*, which is essentially coincidental with the Santonian-Campanian Stage boundary, is an excellent biostratigraphic marker horizon, and occurs consistently across a wide range of paleodepositional facies. This surface clearly demonstrates that the boundary between the Tombigbee Sand Member of the Eutaw Formation and the Mooreville Chalk is diachronous, being considerably older in central Alabama (early Santonian) than in eastern Mississippi (earliest Campanian). The upper boundary of the *G. elevata* Zone of early Campanian age is poorly defined due to the rare occurrence of *G. ventricosa* in the lower part of its range. In contrast, the *G. calcarata* Zone is well defined throughout the northern Gulf Coastal Plain, where it forms a very useful stratigraphic marker interval. The stratigraphic position of the *G. calcarata* Zone demonstrates that the boundary between the Muldrow Member and Bluffport Marl Member of the Demopolis Chalk is diachronous, being older in northern Mississippi than in eastern Mississippi or central Alabama.

DISCUSSION

The record of ostracodes and planktonic foraminifera in the central Alabama and eastern Mississippi CRSs is almost complete from the early Santonian to the early Maastrichtian, with the most significant hiatus occurring in the late Campanian-earliest Maastrichtian. Both of these localities provide almost complete coverage of the stratigraphic interval. In addition, the lack of structural complications permits accurate placement of outcrop sections in their proper stratigraphic positions. These factors contribute to making the northern Gulf Coastal Plain an excellent setting in which to study Late Cretaceous biostratigraphy.

One of the major shortcomings of the paleontological record in the area is the rarity of several species of planktonic foraminifera in specific stratigraphic intervals, most notably the lower ranges of the globotruncanids *G. ventricosa* and *G. aegyptiaca*, *Gansserina gansseri*, and *Globotruncanella havanensis*. The rarity of these taxa is possibly related to the depositional environment, which was probably no more than 100 ft (31 m) deep (Puckett 1991). The boundaries of several planktonic foraminiferal zones are, however, well defined, including the HOS of *D. asymmetrica*, the LOS and HOS of *G. calcarata*, and the LOS of *R. fructicosa*.

It is apparent that there are many more taxa of ostracodes than there are planktonic foraminifera; there are, in fact, almost 2.5 times as many (112 ostracode taxa recognized herein versus 45 species of planktonic foraminifera). The high diversity of ostracodes makes them very useful for regional biostratigraphy, although almost all of the species are, in contrast to planktonic foraminifera, restricted to North America. The presence of abundant ostracodes and the global utility of the foraminifera together form a powerful high-resolution tool for biostratigraphy.

Faunal Turnovers

Analysis of the ranges of both groups of microfossils studied herein indicates that there are two intervals of significant faunal turnover. The first turnover occurred in the mid-Campanian, and affected mainly the ostracodes. This mid-Campanian turnover (MCT) occurs between the extinction of several species of ostracode (*Cytheropteron furcalatum*, several species of an undescribed genus including the species "Cythereis" *veclitella*,

"C." *levis* and "C." *polita*, *Veenia ozanana*, *V. spoori*, *Fissocarinocythere pittensis*, *Haplocytheridea grangerensis*, "Cythereis" *hannai*, *Schizoptocythere compressa*, *Brachycythere pyriforma*, *Acuminobrachycythere diminuta*, and *A. ventrolevis*), all of which occur in a narrow stratigraphic interval, and the evolutionary appearance of several taxa including *Haplocytheridea insolita*, *H. renfroensis dilatipuncta*, *Cytherelloidea crafti*, *Loxoconcha* spp., *Monoceratina biloba*, *Mosae-leberis sagena*, *Eucythere sohli*, *Argilleoecia taylorensis*, *Amphicytherura pandicosta*, *Cuneoceratina prothroensis*, *Fissocarinocythere gapensis*, *Phacorhabdotus venodus*, and *Cytheropteron navarroense*.

The upper faunal turnover occurs in late Campanian-early Maastrichtian strata (termed LCEMT). The lower boundary of this turnover is characterized by the extinction of several species of ostracode, including *Acuminobrachycythere raleighensis*, *Cytherelloidea crafti*, *Monoceratina biloba*, *Eucythere sohli*, *Cytheromorpha unifossula*, *Fissocarinocythere pidgeoni*, *Sphaeroberis pseudoconcentrica*, and *Amphicytherura dubia*. The upper boundary is a profound event that ushers in many new species of both planktonic foraminifera and ostracodes. Among the distinctive Maastrichtian species of planktonic foraminifera to appear at or near this surface are *Gansserina gansseri*, *Contusotruncana contusa*, *C. fareedi*, *C. patelliformis*, *Globotruncanita conica*, *Rugotruncana scotti*, *Globotruncana duwi*, *Planoglobulina acervulinoides*, *P. carseyae*, *Racemiguembelina powelli*, *R. fructicosa*, and *Pseudotextularia deformis*. Species of ostracode that appear at or near this upper surface include *Amphicytherura copicosta*, *Planileberis costata*, *reticulata*, *Antibithocypris crassa*, *A. elongata*, *A. minuta*, *Cushmanidea* sp., "Soudanella" *parallelopora*, several species of *Anticythereis*, *Acuminobrachycythere foraminosa*, *Ascetoleberis hazzardi*, *Fissocarinocythere huntensis*, *Platycosta lixula*, and *Veenia parallelopora*.

It is evident that these faunal turnovers are related to the record of transgressive and regressive stratigraphic cycles. The MCT occurs in the uppermost part of the lower unnamed member of the Mooreville Chalk, in the Arcola Limestone Member, and in the lower part of the Tibbee Creek Member of the Demopolis Chalk. These strata are at the transition between the T-R K6 and T-R K7 cycles of Mancini and Puckett (2005). This interval represents a relatively shallow-water zone separating hemipelagic sedimentation in the Mooreville Chalk to more open conditions characterized by pelagic sedimentation. A significant shift from decreasing to increasing planktonic/benthic foraminiferal ratios is also observed in this interval (Mancini et al. 1996). Clearly, increased rates of speciation and extinction are associated with the T-R cycle boundary.

The LCEMT occurs in a more pronounced T-R cycle boundary with associated unconformity and nonmarine, aggradational sedimentation. The lower boundary of the LCEMT occurs at the top of the marine strata in the Ripley Formation, and upper boundary occurs just above the ravinement surface associated with the marine transgression of cycle T-R K8 of Mancini and Puckett (2005). A significant marine hiatus occurs between the two bounding surfaces. In terms of planktonic foraminifera, this hiatus includes most of the *Gansserina gansseri* Zone, and also includes all of the CC24 nannoplankton zone of Sissingh (1977) and Perch-Nielsen (1985) (Mancini et al. 1996). Clearly, this time interval was characterized by significant speciation and extinction.

SUMMARY AND CONCLUSIONS

The Upper Cretaceous (Santonian-Maastrichtian) deposits in eastern Mississippi and Alabama occur in an excellent setting in which to study planktonic foraminiferal and ostracode biostratigraphy. The strata are unaffected by post-depositional deformation and were deposited in marine water that was sufficiently deep to sustain rich planktonic and benthic faunas but shallow enough to record sea level changes. Further, the two composite reference sections (one in eastern Mississippi and one in central Alabama) are in close enough proximity to allow high-precision correlation of event horizons that define a line of correlation.

The marine Upper Cretaceous strata in Mississippi and Alabama range in age from the early Santonian (early part of the *Dicarinella asymetrica* planktonic foraminiferal zone) to the early Maastrichtian (earliest part of the *Contusotruncana contusa*-*Racemiguembelina fructicosa* Interval Zone). The planktonic foraminiferal zones recognized in this area include the *D. asymetrica* Taxon Range Zone, the *Globotruncanita elevata* Interval Zone, the *Globotruncana ventricosa* Interval Zone, the *Globotruncanita calcarata* Taxon Range Zone, the *Globotruncanella havanensis* Interval Zone, the *Globotruncana aegyptiaca* Interval Zone, the *Gansserina gansseri* Interval Zone, and the *Contusotruncana contusa*-*Racemiguembelina fructicosa* Interval Zone. Seven ostracode zones are recognized in the area, including the *Veenia quadrialira* Taxon Range Zone, the *Acuminobrachycythere acuminata* Interval Zone (new), *Brachycythere pyriforma* Interval Zone (new), the *Ascetoleberis plummeri* Taxon Range Zone, the *Curfsina communis* Interval Zone (new), the *Escharacytheridea pinochii* Interval Zone, and the *Platycosta lixula* Interval Zone. The Santonian-Campanian boundary is well defined in Mississippi and Alabama, and is recognized by the highest occurrence surface of *Dicarinella asymetrica*. The Campanian-Maastrichtian boundary cannot be recognized precisely due to the lack of a calcareous microfossil proxy for the boundary in its stratotype section. The combination of the planktonic foraminiferal and ostracode zonation, correlated between the two composite reference sections using graphic correlation, enable not only high-resolution biostratigraphic subdivision of the northern Gulf Coastal Plain strata, but also help define the ages and diachroneity of the transgressive-regressive cyclicity.

Two faunal turnovers are recognized in these strata, which are referred to as the mid-Campanian turnover (MCT) and the late Campanian-early Maastrichtian turnover (LCEMT). Both of these faunal turnovers are clearly related to the transgressive-regressive (T-R) cyclicity. The MCT occurs at the transition interval between the T-R K6 and T-R K7 cycles of Mancini and Puckett (2005), and is recognized by a high turnover rate of ostracodes; planktonic foraminifera are unaffected. The LCEMT occurs between the latest marine strata of the T-R K7 and the earliest marine strata of the T-R K8 cycle; both planktonic foraminifera and ostracodes are dramatically affected by this turnover, with the sudden appearance of complex morphologies in both groups of microfossils.

Premoli Silva and Sliter (1999) observed that the interval of greatest diversification of planktonic foraminifera in the Cretaceous was during the Santonian *Dicarinella asymetrica* Zone and affected all trophic groups. New forms appearing during this interval include the heterohelicids *Laeviheterohelix*, *Sigilia*, and *Ventilarella*, and the inflated globigerinelloidids; in addition, the globotruncanids and globotruncanitids became

dominant. Most of this diversification occurred just prior to the deposition of the Santonian strata in the Mississippi-Alabama area or during the initial phase of marine sedimentation in the area. This time interval (represented by the *D. asymetrica* Zone) was a time of transition between the older “greenhouse” ocean and a more modern type ocean displaying significant latitudinal temperature gradients and well-defined bioprovinces.

Barrera and Savin (1999) presented carbon and oxygen isotope data suggesting that global cooling and increased latitudinal temperature gradients were initiated approximately 71 Ma (earliest Maastrichtian), punctuated by two episodes of substantial increases in $\delta^{18}\text{O}$ values, one between 71 and 69.5 Ma and the other between 68 and 67.5 Ma, events that indicate an influx of cooler intermediate waters penetrated into the tropics. The initiation of the cooling of the world ocean increased latitudinal gradients and the temporary episode of high-latitude intermediate waters introduced into tropical regions coincides with the boundary between the T-R K7 and T-R K8 cycles in the Mississippi-Alabama area and the marine hiatus associated with it. By the time of deposition of subsequent marine sediments of the uppermost Ripley Formation and the Prairie Bluff Chalk, the planktonic foraminiferal faunas had changed significantly, possibly as a result of evolutionary changes associated with the change in the world ocean.

The ostracode faunas of the North American Gulf Coastal Plain were clearly isolated reproductively from coeval faunas of both South America and from Europe. Results of a reconnaissance-collecting trip in Cuba by the author in the spring of 2002 indicate that the Late Cretaceous ostracode faunas of Cuba are quite different than those of North America. Paleobiogeographically, then, the Gulf and Atlantic Coastal Plains of North America represent an island in which evolution proceeded among the indigenous species. The two intervals of faunal turnover, closely associated with the boundaries between transgressive-regressive cycles, are possibly related to the relative drop in sea level at these times and changes in the shallow-water circulation and loss of area of the shallow marine habitats in which they thrived. The more significant turnover during the late Campanian-early Maastrichtian, although related to the marine depositional hiatus, was probably affected by the changes in temperature and circulation of the world ocean.

The biostratigraphic calibration of the microfossil faunas documented herein, particularly of the ostracodes, enables coeval faunal comparisons on a regional scale that will, hopefully, aid in unraveling some of the complexities of the separation of North and South America, the opening of the Gulf of Mexico and Caribbean Sea, and of the relationship between lithospheric processes (plate tectonic movements) and biological evolution.

REFERENCES

- BABINOT, J.-F., and BOURDILLON-DE-GRISSAC, C., 1989. Associations d’Ostracodes de l’Albien-Maastrichtien du Dhofar (Oman). Affinités paléobiogéographiques et implications géodynamiques. *Bulletin de la Société géologique de France*, 8(2): p. 287-294.
- BABINOT, J.-F., and COLIN, J.-P., 1988. Paleobiogeography of Tethyan Cretaceous marine ostracods. In: Hanai, T., Ikeya, N., and Ishikazi, K., Eds., *Evolutionary Biology of Ostracoda, Its Fundamental and Applications: Proceedings of the Ninth International Symposium on Ostracoda*. Amsterdam and Tokyo: Elsevier Scientific Publishing Co., and Kodansha, 823-839.
- _____, 1992. Marine ostracode provincialism in the Late Cretaceous of the Tethyan realm and the Austral Province. *Palaeogeography, Palaeoclimatology, Palaeoecology*, 92:283-293.
- BARRERA, E., and SAVIN, S. M., 1999. Evolution of late Campanian-Maastrichtian marine climates and oceans. In: Barrera, E., and Johnson, C., Eds., *Evolution of the Cretaceous Ocean-Climate System*. Denver, Geological Society of America: 245-282.
- BRÖNNIMANN, P., 1952. Globigerinidae from the Upper Cretaceous (Cenomanian-Maastrichtian) of Trinidad, B. W. I. *Bulletins of American Paleontology*, 34(140):1-71.
- CARNEY, J. L., and PIERCE, R. W., 1995. Graphic correlation and composite standard databases as tools for the exploration biostratigrapher. In: Mann, K. O., and Lane, H. R., Eds. *Graphic Correlation*. Tulsa Society of Economic Paleontologists and Mineralogists Special Publication 53: 23-43.
- CARON, M., 1978, 14. Cretaceous planktonic foraminifers from DSDP Leg 40, southeastern Atlantic Ocean. In: Bolli, H., Ryan, W. B. F., and others, Eds., *Initial Reports of the Deep Sea Drilling Project*, volume 40:651-661. Washington, DC: US Government Printing Office.
- _____, 1985. Cretaceous planktic foraminifera. In: Bolli, H. M., Saunders, J. B., and Perch-Nielsen, K., Eds., *Plankton stratigraphy*, 17-86. Cambridge: Cambridge University Press.
- DALBIEZ, F., 1955. The genus *Globotruncana* in Tunisia. *Micro-paleontology*, 1(2):161-171.
- EDWARDS, L. E., 1995. Graphic correlation: some guidelines on theory and practice and how they relate to reality. In: Mann, K. O., and Lane, H. R., Eds., *Graphic Correlation*. Tulsa, Society of Economic Paleontologists and Mineralogists Special Publication 53:45-50.
- GRADSTEIN, F. M., AGTERBERG, F. P., OGG, J. G., HARDELBOL, J., VAN VEEN, P., THIERRY, J., and HUANG, Z., 1994. A Mesozoic time scale. *Journal of Geophysical Research*, 99(B12): 24,051-24,074.
- HABIB, D., MOSHKOVITZ, S., and KRAMER, C., 1992. Dinoflagellate and calcareous nannofossil response to sea-level change in the Cretaceous-Tertiary boundary sections. *Geology*, 20:165-168.
- HABIB, D., OLSSON, R. K., LIU, C., and MOSHKOVITZ, S., 1996. High-resolution biostratigraphy of sea-level low, biotic extinction, and chaotic sedimentation at the Cretaceous-Tertiary boundary in Alabama, north of the Chicxulub crater. In: Ryder, G., Fastovsky, D., and Gartner, S., Eds., Geological Society of America Special Paper 307:243-252.
- HANCOCK, J. M., and GALE, A. S., 1996. The Campanian Stage. *Bulletin de l’Institut Royal des Sciences Naturelles de Belgique, Sciences de la Terre* 66 – supplement: 103-109.
- HAZEL, J. E., and BROUWERS, E. M., 1982. Biostratigraphic and chronostratigraphic distribution of ostracodes in the Coniacian-Maastrichtian (Austinian-Navarroan) in the Atlantic and Gulf Coastal Provinces. In: Maddocks, R. F., Ed., *Texas Ostracoda, Guidebook of excursions and related papers for the 8th International Symposium on Ostracoda*, 166-198. Houston, University of Houston: .
- HAZEL, J. E., and KAMIYA, T., 1993. Ostracode biostratigraphy of the *Titanosarcolites*-bearing limestones and related sequences of Jamaica. In: Wright, R. M., and Robinson, E., Eds., *Biostratigraphy of Jamaica*. Boulder, Geological Society of America Memoir 182: 65-76.
- HERM, D., 1962. Stratigraphische und mikropaläontologische Untersuchungen der Oberkreide im Lattengebirge und im Nierental.

- Bayerische Akademie der Wissenschaften, München, Mathematisch-Naturwissenschaftliche Klasse, Abhandlungen, Neue Folge 104:1-119.
- HOOD, K. C., 1986-1998. *GraphCor*. Houston, Kenneth C. Hood.
- LUBIMOVA, P. S., and SÁNCHEZ ARANGO, J. R., 1974. Los Ostrácodos del Cretácico Superior y del Terciario de Cuba. *Organismos, Instituto Cubano del Libro*, 17(903):1-171.
- MACLEOD, N., and SADLER, P., 1995. Estimating the line of correlation. In: MANN, K. O., and LANE, H. R., Eds., *Graphic Correlation*. Society of Economic Paleontologists and Mineralogists Special Publication 53: 51-64.
- MANCINI, E.A., 1979. Late Albian and early Cenomanian Grayson ammonite biostratigraphy in north-central Texas. *Journal of Paleontology*, 53:1013-1022.
- MANCINI, E.A., MINK, R.M., PAYTON, J.W., and BEARDEN, B.L., 1987. Environments of deposition and petroleum geology of Tuscaloosa Group (Upper Cretaceous), South Carlton and Pollard Fields, southwestern Alabama. *American Association Petroleum Geologists Bulletin*, 71:1128-1142.
- MANCINI, E. A., and PUCKETT, T. M., 1998. *Sequence stratigraphy and biostratigraphy of Upper Cretaceous strata of the Alabama Coastal Plain, Guidebook for the 35th Annual Field Trip of the Alabama Geological Society*, 1-41. Tuscaloosa, Geological Society of Alabama.
- _____, 2003a. Integrated biostratigraphic and sequence stratigraphic approach for correlation and basin interpretation. *Transaction of the Gulf Coast Association of Geological Societies* 53 (CD-ROM).
- _____, 2003b. Integrated biostratigraphic and sequence stratigraphic approach for correlation and basin interpretation. *Transaction of the Gulf Coast Association of Geological Societies* 53 (CD-ROM).
- _____, 2005. Jurassic and Cretaceous transgressive-regressive (T-R) cycles, northern Gulf of Mexico, USA. *Stratigraphy*, 2(1):31-48.
- MANCINI, E. A., PUCKETT, T. M., and TEW, B. H., 1996. Integrated biostratigraphic and sequence stratigraphic framework for Upper Cretaceous strata of the eastern Gulf Coastal Plain. *Cretaceous Research*, 17:645-669.
- MANCINI, E.A., SMITH, C.C., and PAYTON, J.M., 1980. *Geologic age and environment of deposition of the Pilot Sand and Marine Shale, Tuscaloosa Group, South Carlton Field, south Alabama*. First Annual Gulf Coast Section SEPM Foundation, Research Conference. Houston, Gulf Coast Section SEPM, 24-25.
- MANCINI, E. A., TEW, B. H., and SMITH, C. C., 1989. Cretaceous-Tertiary contact, Mississippi and Alabama. *Journal of Foraminiferal Research*, 19(2):93-104.
- ODIN, G. S., 1996. Definition of a global boundary stratotype section and point for the Campanian/Maastrichtian boundary. *Bulletin de l'Institut Royal des Sciences Naturelles de Belgique, Sciences de la Terre*, 66 (supplement):111-117.
- OLSSON, R. K., and LIU, C., 1993. Controversies on the placement of Cretaceous-Paleogene boundary and the K/P extinction of planktonic foraminifera. *Palaios*, 8:127-139.
- OLSSON, R. K., LIU, C., and VAN FOSSEN, M., 1996. The Cretaceous-Tertiary catastrophic event at Millers Ferry, Alabama. In Ryder, G., Fastovsky, D., and Gartner, S., Eds., *Geological Society of America Special Paper* 307:263-277.
- OSBORNE, W. E., SZABO, M. W., COPELAND, C. W., and NEATHERLY, T. L., 1989. *Geologic map of Alabama*. Geological Survey of Alabama, scale 1:500,000.
- PERCH-NIELSEN, K., 1985. Mesozoic calcareous nannofossils. In: Bolli, H., Saunders, J. B., and Perch-Nielsen, K., Eds., *Plankton stratigraphy*. Cambridge: Cambridge University Press, 329-426.
- PESSAGNO, E.A., Jr., 1969. *Upper Cretaceous stratigraphy of the western Gulf Coastal area, Mexico, Texas, and Arkansas*. Boulder, Geological Society of America Memoir 111: 1-130.
- PITAKPAIVAN, K., and HAZEL, J. E., 1994. Ostracodes and chronostratigraphic position of the Upper Cretaceous Arkadelphia Formation of Arkansas. *Journal of Paleontology*, 68(1):111-122.
- POSTUMA, J., 1971. *Manual of Planktonic Foraminifera*. Amsterdam: Elsevier Publishing Company, 1-420.
- PREMOLI SILVA, I., and SLITER, W. V., 1994. Cretaceous planktonic foraminiferal biostratigraphy and evolutionary trends from the Bottaccione section, Gubbio, Italy. *Palaeontographica Italiana*, 82:1-89.
- _____, 1999. Cretaceous paleoceanography: evidence from planktonic foraminiferal evolution. In: Barrera, E., and Johnson, C., Eds., *Evolution of the Cretaceous Ocean-Climate System*, 301-328.. Boulder, Geological Society of America
- PUCKETT, T. M., 1991. Absolute paleobathymetry of Upper Cretaceous chalks based on ostracodes—evidence from the Demopolis Chalk (Campanian and Maastrichtian) of the northern Gulf Coastal Plain. *Geology*, 19:449-452.
- _____, 1994. New Ostracoda species from an Upper Cretaceous oyster reef, northern Gulf Coastal Plain, U.S.A. *Journal of Paleontology*, 68(6):1321-1335.
- _____, 1995a. Planktonic foraminiferal and ostracode biostratigraphy of the late Santonian through early Maastrichtian strata in Dallas County, Alabama. *Geological Survey of Alabama Bulletin* 164: 1-59.
- _____, 1995b. Upper Cretaceous ostracode paleoecology, SE USA. In: Ríha, J., Ed., *Ostracoda and biostratigraphy*, 141-15. Rotterdam: A.A. Balkema1.
- _____, 1996. *Ecologic atlas of Upper Cretaceous ostracodes of Alabama*. Geological Survey of Alabama Monograph 14: 1-176.
- _____, 2002. Systematics and paleobiogeography of brachycytherine Ostracoda. *Micropaleontology* 48(S2): 1-87.
- PUCKETT, T. M., and MANCINI, E. A., 1998. Planktonic foraminiferal Globotruncanita calcarata total range zone: its global significance and importance to chronostratigraphic correlation in the Gulf Coastal Plain, USA. *Journal of Foraminiferal Research*, 28(2): 124-134.
- ROBASZYNSKI, F., CARON, M., GONZALEZ DONOSA, J. M., and WONDERS, A. A. H., 1984. Atlas of Late Cretaceous globotruncanids. *Revue de Micropaléontologie*, 26(3-4):145-305.
- RUSSELL, E. A., and KEADY, D. M., 1983. Notes on Upper Cretaceous lithostratigraphy of the eastern Mississippi embayment. In: Russell, E. A., Keady, D. M., Mancini, E. A., and Smith, C. C., Eds., *Upper Cretaceous lithostratigraphy and biostratigraphy in northeast Mississippi, southwest Tennessee and northwest Alabama, shelf chalks and coastal clastics*. Tuscaloosa, Society of Economic Paleontologists and Mineralogist, Gulf Coast Section, 1-15.
- SHAW, A. B., 1964. *Time in Stratigraphy*. New York: McGraw-Hill, 1-365.

- SISSINGH, W., 1977. Biostratigraphy of Cretaceous calcareous nannoplankton. *Geologie et Mijnbouw*, 56:37-65.
- , 1995. Regional lithostratigraphy and calcareous nannofossil biostratigraphy of the Arcola Limestone Member, Mooreville Chalk, of eastern Mississippi and Alabama. *Transactions of the Gulf Coast Association of Geological Societies*, 45:529-535.
- , 1997. The Cretaceous-Tertiary boundary at Moscow Landing, west-central Alabama. *Transaction of the Gulf Coast Association of Geological Societies*, 47:533-539.
- SMITH, C.C. and PESSAGNO, E.A., Jr., 1973. *Planktonic foraminifera and stratigraphy of the Corsicana Formation (Maastrichtian) north-central Texas*. Cushman Foundation for Foraminiferal Research Special Publication No. 12, 1-68.
- TIBERT, N. E., COLIN, J.-P., LECKIE, R. M., and BBINOT, J.-F., 2003. Revision of the ostracode genus *Fossocytheridea* Swain and Brown 1964: Mesozoic ancestral root for the modern eurytopic *Cyprideis*. *Micropaleontology*, 49(3):205-230.
- VIVIERS, M. C., KOUTSOUKOS, E. A. M., SILVA-TELLES, A. C. d., and BENGTSON, P., 2000. Stratigraphy and biogeographic affinities of the late Aptian-Campanian ostracods of the Potiguar and Sergipe basins of northeastern Brazil. *Cretaceous Research*, 21:407-455.
- WAGREICH, M., 1992. Correlation of Late Cretaceous calcareous nannofossil zones with ammonite zones and planktonic foraminifera: the Austrian Gosau sections. *Cretaceous Research*, 13:505-516.

APPENDIX 1

Sample localities. Following 9 pages.

APPENDIX 2

Definition of the Muldrow Member of the Demopolis Chalk.

The Muldrow Member of the Demopolis Chalk is defined herein as the middle, chalky interval that occurs between the lower, marly Tibbee Creek Member and the upper marly Bluffport Marl Member. The type locality is near the community of Muldrow, in Oktibbeha County, Mississippi (text-fig. 9). The exact location of the type locality is: NE $\frac{1}{4}$ sec. 3, T. 19 N., R. 15 E., West Point 7.5 minute topographic quadrangle, Oktibbeha County, Mississippi, lat. 33°42'35", long. 88°41'57". The Muldrow Member at this locality occurs in a gullied area on the south side of the dirt road, and consists of white, brittle, sparsely fossiliferous chalk interbedded with light gray, slightly more marly interbeds that are approximately 2 feet (0.6 m) thick. The Muldrow Member consists of the most pure chalk in the Upper Cretaceous of the Mississippi-Alabama area, consisting of about 90% pure calcium carbonate (Russell and Keady 1983).

Station Number	Sample ID	Formation	Section	Member	Township	Range	Quadrangle	County	State Latitude	Longitude
Comments										
2000-1-17-1	2000-1-17-1(1)	Mooreville Chalk	E 1/2 sec. 31	Sample collected on south-facing cut bank on Tibbee Creek, about 1 foot above water level (sample elevation = 164 ft. a.m.s.l.).	17S	07E	Waverly	Clay	MS	33° 33' 42"
2000-1-17-1	2000-1-17-1(16)	Mooreville Chalk	E 1/2 sec. 31	Sample collected on south-facing cut bank on Tibbee Creek, about 16 foot above water level (sample elevation = 180 ft. a.m.s.l.).	17S	07E	Waverly	Clay	MS	33° 33' 42"
2000-1-17-1	2000-1-17-1(25)	Mooreville Chalk	E 1/2 sec. 31	Sample collected on south-facing cut bank on Tibbee Creek, about 25 foot above water level (sample elevation = 189 ft. a.m.s.l.).	17S	07E	Waverly	Clay	MS	33° 33' 42"
90-10-2-1(WB)	90-10-2-1(WB15)	Demopolis Chalk	SW 1/4 sec. 15	Sample collected from relatively pure chalk, 15 feet above water level on 2-10-90 (water level = 79.72 feet a.m.s.l.; sample elevation = -82 feet a.m.s.l.).	Muldrow	09E	Orville	Dallas	AL	32° 08' 18"
90-10-2-1(WB)	90-10-2-1(WB2)	Demopolis Chalk	SW 1/4 sec. 15	Sample collected from relatively pure chalk, 2 feet above water level on 2-10-90 (water level = 79.72 feet a.m.s.l.; sample elevation = -82 feet a.m.s.l.).	Muldrow	09E	Orville	Dallas	AL	32° 08' 18"
90-10-2-1(WB)	90-10-2-1(WB35)	Demopolis Chalk	SW 1/4 sec. 15	Sample collected from relatively pure chalk, 35 feet above water level on 2-10-90 (water level = 79.72 feet a.m.s.l.); sample elevation = -115 feet a.m.s.l.	Muldrow	09E	Orville	Dallas	AL	32° 08' 18"
90-10-2-1(WB)	90-10-2-1(WB40)	Demopolis Chalk	SW 1/4 sec. 15	Sample collected from relatively pure chalk, 40 feet above water level on 2-10-90 (water level = 79.72 feet a.m.s.l.); sample elevation = -120 feet a.m.s.l.	Muldrow	09E	Orville	Dallas	AL	32° 08' 18"
90-10-2-1(WB)	90-10-2-1(WB45)	Demopolis Chalk	SW 1/4 sec. 15	Sample collected from relatively pure chalk, 45 feet above water level on 2-10-90 (water level = 79.72 feet a.m.s.l.); sample elevation = -125 feet a.m.s.l.	Muldrow	09E	Orville	Dallas	AL	32° 08' 18"
90-10-2-1(WB)	90-10-2-1(WB65)	Demopolis Chalk	SW 1/4 sec. 15	Sample collected from relatively pure chalk, 65 feet above water level on 2-10-90 (water level = 79.72 feet a.m.s.l.); sample elevation = -145 feet a.m.s.l.	Muldrow	09E	Orville	Dallas	AL	32° 08' 18"
90-10-2-1(WB)	90-10-2-1(WB75)	Demopolis Chalk	SW 1/4 sec. 15	Sample collected from relatively pure chalk, 75 feet above water level on 2-10-90 (water level = 79.72 feet a.m.s.l.); sample elevation = -155 feet a.m.s.l.	Muldrow	09E	Orville	Dallas	AL	32° 08' 18"
90-10-4-1(CC)	90-10-4-1(CC10)	Demopolis Chalk	SW 1/4 sec. 4	"Cedar Creek" section, on north-west facing cutbank of Cedar Creek, a tributary to the Alabama River; sample collected approximately 10 feet above water level (water elevation = 79.80 feet a.m.s.l.; sample elevation = -90 feet a.m.s.l.).	Muldrow	10E	Elm Bluff	Dallas	AL	32° 12' 17"
90-10-4-1(CC)	90-10-4-1(CC2)	Demopolis Chalk	SW 1/4 sec. 4	"Cedar Creek" section, on north-west facing cutbank of Cedar Creek, a tributary to the Alabama River; sample collected approximately 2 feet above water level (water elevation = 79.80 feet a.m.s.l.); sample elevation = -82 feet a.m.s.l.	Muldrow	10E	Elm Bluff	Dallas	AL	32° 12' 17"
90-10-4-1(CC)	90-10-4-1(CC20)	Demopolis Chalk	SW 1/4 sec. 4	"Cedar Creek" section, on north-west facing cutbank of Cedar Creek, a tributary to the Alabama River; sample collected approximately 10 feet above water level (water elevation = 79.80 feet a.m.s.l.; sample elevation = -90 feet a.m.s.l.).	Muldrow	10E	Elm Bluff	Dallas	AL	32° 12' 17"
90-10-4-1(CC)	90-10-4-1(CC30)	Demopolis Chalk	SW 1/4 sec. 4	"Cedar Creek" section, on north-west facing cutbank of Cedar Creek, a tributary to the Alabama River; sample collected approximately 20 feet above water level (water elevation = 79.80 feet a.m.s.l.); sample elevation = -100 feet a.m.s.l.	Muldrow	10E	Elm Bluff	Dallas	AL	32° 12' 17"
90-10-4-1(CC)	90-10-4-1(CC40)	Demopolis Chalk	SW 1/4 sec. 4	"Cedar Creek" section, on north-west facing cutbank of Cedar Creek, a tributary to the Alabama River; sample collected approximately 55 feet above water level (water elevation = 79.80 feet a.m.s.l.); sample elevation = -130 feet a.m.s.l.	Muldrow	10E	Elm Bluff	Dallas	AL	32° 12' 17"
90-10-4-1(CC)	90-10-4-1(CC50)	Demopolis Chalk	SW 1/4 sec. 4	"Cedar Creek" section, on north-west facing cutbank of Cedar Creek, a tributary to the Alabama River; sample collected approximately 60 feet above water level (water elevation = 79.80 feet a.m.s.l.); sample elevation = -135 feet a.m.s.l.	Muldrow	10E	Elm Bluff	Dallas	AL	32° 12' 17"
90-10-4-1(CC)	90-10-4-1(CC55)	Demopolis Chalk	SW 1/4 sec. 4	"Cedar Creek" section, on north-west facing cutbank of Cedar Creek, a tributary to the Alabama River; sample collected approximately 65 feet above water level (water elevation = 79.80 feet a.m.s.l.); sample elevation = -145 feet a.m.s.l.	Muldrow	10E	Elm Bluff	Dallas	AL	32° 12' 17"
90-10-4-1(CC)	90-10-4-1(CC60)	Demopolis Chalk	SW 1/4 sec. 4	"Cedar Creek" section, on north-west facing cutbank of Cedar Creek, a tributary to the Alabama River; sample collected approximately 70 feet above water level (water elevation = 79.80 feet a.m.s.l.); sample elevation = -150 feet a.m.s.l.	Muldrow	10E	Elm Bluff	Dallas	AL	32° 12' 17"
90-10-4-1(CC)	90-10-4-1(CC65)	Demopolis Chalk	SW 1/4 sec. 4	"Cedar Creek" section, on north-west facing cutbank of Cedar Creek, a tributary to the Alabama River; sample collected approximately 75 feet above water level (water elevation = 79.80 feet a.m.s.l.); sample elevation = -155 feet a.m.s.l.	Muldrow	10E	Elm Bluff	Dallas	AL	32° 12' 17"
90-10-4-1(CC)	90-10-4-1(CC70)	Demopolis Chalk	SW 1/4 sec. 4	"Cedar Creek" section, on north-west facing cutbank of Cedar Creek, a tributary to the Alabama River; sample collected approximately 80 feet above water level (water elevation = 79.80 feet a.m.s.l.); sample elevation = -160 feet a.m.s.l.	Muldrow	10E	Elm Bluff	Dallas	AL	32° 12' 17"
90-10-4-1(CC)	90-10-4-1(CC75)	Demopolis Chalk	SW 1/4 sec. 4	"Cedar Creek" section, on north-west facing cutbank of Cedar Creek, a tributary to the Alabama River; sample collected approximately 85 feet above water level (water elevation = 79.80 feet a.m.s.l.); sample elevation = -165 feet a.m.s.l.	Muldrow	10E	Elm Bluff	Dallas	AL	32° 12' 17"

Comments	Station Number	Sample ID	Formation	Section	Township	Range	Quadrangle	County	State Latitude	Longitude
	Member				Member					
90-10-4-(CC) "Cedar Creek" section, on north-west facing cutbank of Cedar Creek, a tributary to the Alabama River; sample collected approximately 90 feet above water level (water elevation = 79.80 feet a.m.s.l.; sample elevation = -170 feet a.m.s.l.)	90-10-4-(CC390)	90-10-4-(CC390)	Denopolis Chlk	SW 1/4 sec. 4	Muldrow	14N	10E	Elm Bluff	Dallas	35° 12' 17"
90-10-4-(CC) "Cedar Creek" section, on north-west facing cutbank of Cedar Creek, a tributary to the Alabama River; sample collected approximately 95 feet above water level (water elevation = 79.80 feet a.m.s.l.; sample elevation = -175 feet a.m.s.l.)	90-10-4-(CC95)	90-10-4-(CC95)	Denopolis Chalk	SW 1/4 sec. 4	Muldrow	14N	10E	Elm Bluff	Dallas	35° 12' 17"
90-10-4-(CC) "Cedar Creek" section, on north-west facing cutbank of Cedar Creek, a tributary to the Alabama River; sample collected approximately 99 feet above water level (water elevation = 79.80 feet a.m.s.l.; sample elevation = -179 feet a.m.s.l.)	90-10-4-(CC99)	90-10-4-(CC99)	Denopolis Chalk	SW 1/4 sec. 4	Muldrow	14N	10E	Elm Bluff	Dallas	35° 12' 17"
"Cedar Creek" section, on north-west facing cutbank of Cedar Creek, a tributary to the Alabama River; sample collected just above water level and 5.8 ft. below bottom of Arcola Limestone Member of Mooreville Chalk.	90-1-13-1(TC) 90-1-13-1(TC0.05)	90-1-13-1(TC) 90-1-13-1(TC0.05)	Mooreville Chalk	NW 1/4 sec. 9	Arcola Limestone	19N	16E	West Point	Clay	35° 32' 15"
"Tibbee Creek" section, at north-facing cutbank of Tibbee Creek, immediately west of railroad bridge; sample collected just above water level and 5.8 ft. below bottom of Arcola Limestone Member of Mooreville Chalk.	90-1-13-1(TC) 90-1-13-1(TC1.95)	90-1-13-1(TC) 90-1-13-1(TC1.95)	Mooreville Chalk	NW 1/4 sec. 9	Arcola Limestone	19N	16E	West Point	Clay	35° 32' 15"
"Tibbee Creek" section, at north-facing cutbank of Tibbee Creek, immediately west of railroad bridge; sample collected immediately above lower limestone unit of Arcola Limestone Member of Mooreville Chalk.	90-1-13-1(TC) 90-1-13-1(TC2.2)	90-1-13-1(TC) 90-1-13-1(TC2.2)	Mooreville Chalk	NW 1/4 sec. 9	Arcola Limestone	19N	16E	West Point	Clay	35° 32' 15"
"Tibbee Creek" section, at north-facing cutbank of Tibbee Creek, immediately west of railroad bridge; sample collected immediately below upper limestone unit of Arcola Limestone Member of Mooreville Chalk.	90-1-13-1(TC) 90-1-13-1(TC3.0)	90-1-13-1(TC) 90-1-13-1(TC3.0)	Denopolis Chalk	NW 1/4 sec. 9	Tibbee Creek	19N	16E	West Point	Clay	35° 32' 15"
"Tibbee Creek" section, at north-facing cutbank of Tibbee Creek, immediately west of railroad bridge; sample collected immediately above upper limestone unit of Arcola Limestone Member of Mooreville Chalk. This is the type locality for the Tibbee Creek Member of the Denopolis Chalk.	90-1-13-1(TC) 90-1-13-1(TC4.5)	90-1-13-1(TC) 90-1-13-1(TC4.5)	Denopolis Chalk	NW 1/4 sec. 9	Tibbee Creek	19N	16E	West Point	Clay	35° 32' 15"
"Tibbee Creek" section, at north-facing cutbank of Tibbee Creek, immediately west of railroad bridge; sample collected approximately 6 ft. above Arcola Limestone Member of Mooreville Chalk. This is the type locality of the Tibbee Creek Member of the Tibbee Creek Member of the Denopolis Chalk.	90-1-13-1(TC) 90-1-13-1(TC5.0)	90-1-13-1(TC) 90-1-13-1(TC5.0)	Denopolis Chalk	NW 1/4 sec. 9	Tibbee Creek	19N	16E	West Point	Clay	35° 32' 15"
90-4-23-(AS) "Alexander Schoolhouse" section, up hillside on east side of Okribbeha County road, beginning approximately 12.5 feet above base of section, and 500 feet above top of Tombigbee Sand Member of Etowah Formation.	90-4-23-(AS0.0)	90-4-23-(AS0.0)	Denopolis Chalk	NE 1/4 sec. 8	Muldrow	19N	15E	West Point	Oktibbeha	MS 35° 32' 10"
90-4-23-(AS) "Alexander Schoolhouse" section, up hillside on east side of Okribbeha County road, beginning approximately 12.5 feet above base of section, and 500 feet above top of Tombigbee Sand Member of Etowah Formation.	90-4-23-(AS1.5)	90-4-23-(AS1.5)	Denopolis Chalk	NE 1/4 sec. 8	Muldrow	19N	15E	West Point	Oktibbeha	MS 35° 32' 10"
90-4-23-(AS) "Alexander Schoolhouse" section, up hillside on east side of Okribbeha County road, beginning approximately 2000 feet south of T-intersection with east-west Okribbeha County road, extending to top of hill approximately 3500 feet south of intersection; sample collected from relatively pure Denopolis Chalk, approximately 8 feet above base of section, and 505 feet above top of Tombigbee Sand Member of Etowah Formation.	90-4-23-(AS) 90-4-23-1(AS0.5)	90-4-23-(AS) 90-4-23-1(AS0.5)	Denopolis Chalk	NE 1/4 sec. 8	Muldrow	19N	15E	West Point	Oktibbeha	MS 35° 32' 10"
90-4-23-(AS) "Alexander Schoolhouse" section, up hillside on east side of Okribbeha County road, beginning approximately 2000 feet south of T-intersection with east-west Okribbeha County road, extending to top of hill approximately 3500 feet south of intersection; sample collected from relatively pure Denopolis Chalk, approximately 35 feet above base of section, and 534 feet above top of Tombigbee Sand Member of Etowah Formation.	90-4-23-(AS) 90-4-23-1(AS1.5)	90-4-23-(AS) 90-4-23-1(AS1.5)	Denopolis Chalk	NE 1/4 sec. 8	Muldrow	19N	15E	West Point	Oktibbeha	MS 35° 32' 10"
90-4-23-(AS) "Alexander Schoolhouse" section, up hillside on east side of Okribbeha County road, beginning approximately 2000 feet south of T-intersection with east-west Okribbeha County road, extending to top of hill approximately 3500 feet south of intersection; sample collected from relatively pure Denopolis Chalk, approximately 35 feet above base of section, and 537 feet above top of Tombigbee Sand Member of Etowah Formation.	90-4-23-(AS) 90-4-23-1(AS3.5)	90-4-23-(AS) 90-4-23-1(AS3.5)	Denopolis Chalk	NE 1/4 sec. 8	Muldrow	19N	15E	West Point	Oktibbeha	MS 35° 32' 10"
90-4-23-(AS) "Alexander Schoolhouse" section, up hillside on east side of Okribbeha County road, beginning approximately 2000 feet south of T-intersection with east-west Okribbeha County road, extending to top of hill approximately 3500 feet south of intersection; sample collected from relatively pure Denopolis Chalk, approximately 45 feet above base of section, and 544 feet above top of Tombigbee Sand Member of Etowah Formation.	90-4-23-(AS) 90-4-23-1(AS5.0)	90-4-23-(AS) 90-4-23-1(AS5.0)	Denopolis Chalk	NE 1/4 sec. 8	Muldrow	19N	15E	West Point	Oktibbeha	MS 35° 32' 10"
90-4-23-(AS) "Alexander Schoolhouse" section, up hillside on east side of Okribbeha County road, beginning approximately 2000 feet south of T-intersection with east-west Okribbeha County road, extending to top of hill approximately 3500 feet south of intersection; sample collected from relatively pure Denopolis Chalk, approximately 50 feet above base of section, and 549 feet above top of Tombigbee Sand Member of Etowah Formation.	90-4-23-(AS) 90-4-23-1(AS2.5)	90-4-23-(AS) 90-4-23-1(AS2.5)	Denopolis Chalk	NE 1/4 sec. 8	Muldrow	19N	15E	West Point	Oktibbeha	MS 35° 32' 10"
90-4-23-(AS) "Alexander Schoolhouse" section, up hillside on east side of Okribbeha County road, beginning approximately 2000 feet south of T-intersection with east-west Okribbeha County road, extending to top of hill approximately 3500 feet south of intersection; sample collected from relatively pure Denopolis Chalk, approximately 11 feet above base of section, and 508 feet above top of Tombigbee Sand Member of Etowah Formation.	90-4-23-(AS) 90-4-23-1(AS3.5)	90-4-23-(AS) 90-4-23-1(AS3.5)	Denopolis Chalk	NE 1/4 sec. 8	Muldrow	19N	15E	West Point	Oktibbeha	MS 35° 32' 10"
90-4-23-(AS) "Alexander Schoolhouse" section, up hillside on east side of Okribbeha County road, beginning approximately 2000 feet south of T-intersection with east-west Okribbeha County road, extending to top of hill approximately 3500 feet south of intersection; sample collected from relatively pure Denopolis Chalk, approximately 14 feet above base of section, and 511 feet above top of Tombigbee Sand Member of Etowah Formation.	90-4-23-(AS) 90-4-23-1(AS4.5)	90-4-23-(AS) 90-4-23-1(AS4.5)	Denopolis Chalk	NE 1/4 sec. 8	Muldrow	19N	15E	West Point	Oktibbeha	MS 35° 32' 10"
90-4-23-(AS) "Alexander Schoolhouse" section, up hillside on east side of Okribbeha County road, beginning approximately 2000 feet south of T-intersection with east-west Okribbeha County road, extending to top of hill approximately 3500 feet south of intersection; sample collected from relatively pure Denopolis Chalk, approximately 20 feet above base of section, and 517 feet above top of Tombigbee Sand Member of Etowah Formation.	90-4-23-(AS) 90-4-23-1(AS5.5)	90-4-23-(AS) 90-4-23-1(AS5.5)	Denopolis Chalk	NE 1/4 sec. 8	Muldrow	19N	15E	West Point	Oktibbeha	MS 35° 32' 10"
90-4-23-(AS) "Alexander Schoolhouse" section, up hillside on east side of Okribbeha County road, beginning approximately 2000 feet south of T-intersection with east-west Okribbeha County road, extending to top of hill approximately 3500 feet south of intersection; sample collected from relatively pure Denopolis Chalk, approximately 23 feet above base of section, and 520 feet above top of Tombigbee Sand Member of Etowah Formation.	90-4-23-(AS) 90-4-23-1(AS6.5)	90-4-23-(AS) 90-4-23-1(AS6.5)	Denopolis Chalk	NE 1/4 sec. 8	Muldrow	19N	15E	West Point	Oktibbeha	MS 35° 32' 10"
90-4-23-(AS) "Alexander Schoolhouse" section, up hillside on east side of Okribbeha County road, beginning approximately 2000 feet south of T-intersection with east-west Okribbeha County road, extending to top of hill approximately 3500 feet south of intersection; sample collected from relatively pure Denopolis Chalk, approximately 26 feet above base of section, and 523 feet above top of Tombigbee Sand Member of Etowah Formation.	90-4-23-(AS) 90-4-23-1(AS7.5)	90-4-23-(AS) 90-4-23-1(AS7.5)	Denopolis Chalk	NE 1/4 sec. 8	Muldrow	19N	15E	West Point	Oktibbeha	MS 35° 32' 10"

Station Number	Sample ID	Formation	Section	Member	Township	Range	Quadrangle	County	State	Latitude	Longitude
Comments											
90-4-23-1(AS)	90-4-23-1(A\$7.5)	Demopolis Chalk	NE 1/4 sec. 8 "Alexander Schoolhouse" section, up hillside on east side of Okibeha County road, beginning approximately 2000 feet south of T-intersection with east-west Okibeha County road, extending to top of hill; sample collected from relatively pure Demopolis Chalk, approximately 26 feet above base of section, and 523 feet above top of Tombigbee Sand Member of Eutaw Formation.	Muldrow	19N	15E	West Point	Okitibeha	MS	33° 32' 10"	88° 44' 30"
90-4-23-1(AS)	90-4-23-1(A\$8.5)	Demopolis Chalk	NE 1/4 sec. 8 "Alexander Schoolhouse" section, up hillside on east side of Okibeha County road, beginning approximately 2000 feet south of T-intersection with east-west Okibeha County road, extending to top of hill; sample collected from relatively pure Demopolis Chalk, approximately 29 feet above base of section, and 526 feet above top of Tombigbee Sand Member of Eutaw Formation.	Muldrow	19N	15E	West Point	Okitibeha	MS	33° 32' 10"	88° 44' 30"
90-4-23-1(AS)	90-4-23-1(A\$9.5)	Demopolis Chalk	NE 1/4 sec. 8 "Alexander Schoolhouse" section, up hillside on east side of Okibeha County road, beginning approximately 32 feet above base of section, and 529 feet above top of Tombigbee Sand Member of Eutaw Formation.	Muldrow	19N	15E	West Point	Okitibeha	MS	33° 32' 10"	88° 44' 30"
90-6-16-1(LC)	90-6-16-1(LC210)	Demopolis Chalk	NW corner sec. 35 (irreg. sec.) Tibbee Creek Line Creek section; water level approximately 175 feet a.m.s.l.; sample collected 35 feet above water level at elevation 210 a.m.s.l., in uppermost part of Tibbee Creek Member of Demopolis Chalk.	Muldrow	20N	15E	West Point	Okitibeha	MS	33° 32' 35"	88° 41' 57"
90-6-16-1(LC)	90-6-16-1(LC215)	Demopolis Chalk	NW corner sec. 35 (irreg. sec.) Tibbee Creek Line Creek section; water level approximately 175 feet a.m.s.l.; sample collected 40 feet above water level at elevation 215 a.m.s.l., in uppermost part of Tibbee Creek Member of Demopolis Chalk.	Muldrow	20N	15E	West Point	Okitibeha	MS	33° 32' 35"	88° 41' 57"
90-6-16-1(LC)	90-6-16-1(LC220)	Demopolis Chalk	NW corner sec. 35 (irreg. sec.) Tibbee Creek Line Creek section; water level approximately 175 feet a.m.s.l.; sample collected 44 feet above water level at elevation 220 a.m.s.l., in uppermost part of Tibbee Creek Member of Demopolis Chalk.	Muldrow	20N	15E	West Point	Okitibeha	MS	33° 32' 35"	88° 41' 57"
90-6-16-1(M)	90-6-16-1(M231)	Demopolis Chalk	NE 1/4 sec. 3 "Muldrow" section, along north-facing gully; sample collected at elevation approximately 231 ft. a.m.s.l. and 421 ft. above Arcola Limestone Member of Mooreville Chalk. This is the type locality of the Muldray Member of the Demopolis Chalk.	Muldrow	19N	15E	West Point	Okitibeha	MS	33° 42' 25"	87° 32' 20"
90-6-16-1(M)	90-6-16-1(M235)	Demopolis Chalk	NE 1/4 sec. 3 "Muldrow" section, along north-facing gully; sample collected at elevation approximately 235 ft. a.m.s.l. and 425 ft. above Arcola Limestone Member of Mooreville Chalk. This is the type locality of the Muldray Member of the Demopolis Chalk.	Muldrow	19N	15E	West Point	Okitibeha	MS	33° 42' 25"	87° 32' 20"
90-6-16-1(M)	90-6-16-1(M240)	Demopolis Chalk	NE 1/4 sec. 3 "Muldrow" section, along north-facing gully; sample collected at elevation approximately 240 ft. a.m.s.l. and 430 ft. above Arcola Limestone Member of Mooreville Chalk. This is the type locality of the Muldray Member of the Demopolis Chalk.	Muldrow	19N	15E	West Point	Okitibeha	MS	33° 42' 25"	87° 32' 20"
90-6-16-1(M)	90-6-16-1(M244)	Demopolis Chalk	NE 1/4 sec. 3 "Muldrow" section, along north-facing gully; sample collected at elevation approximately 244 ft. a.m.s.l. and 434 ft. above Arcola Limestone Member of Mooreville Chalk. This is the type locality of the Muldray Member of the Demopolis Chalk.	Muldrow	19N	15E	West Point	Okitibeha	MS	33° 42' 25"	87° 32' 20"
90-6-16-1(M)	M209	Demopolis Chalk	NE 1/4 sec. 3 "Muldrow" section, along north-facing gully; sample collected at elevation approximately 209 ft. a.m.s.l. and 399 ft. above Arcola Limestone Member of Mooreville Chalk. This is the type locality of the Muldray Member of the Demopolis Chalk.	Muldrow	19N	15E	West Point	Okitibeha	MS	33° 42' 25"	87° 32' 20"
90-6-16-1(M)	M214	Demopolis Chalk	NE 1/4 sec. 3 "Muldrow" section, along north-facing gully; sample collected at elevation approximately 214 ft. a.m.s.l. and 404 ft. above Arcola Limestone Member of Mooreville Chalk. This is the type locality of the Muldray Member of the Demopolis Chalk.	Muldrow	19N	15E	West Point	Okitibeha	MS	33° 42' 25"	87° 32' 20"
90-6-16-1(M)	M220	Demopolis Chalk	NE 1/4 sec. 3 "Muldrow" section, along north-facing gully; sample collected at elevation approximately 220 ft. a.m.s.l. and 410 ft. above Arcola Limestone Member of Mooreville Chalk. This is the type locality of the Muldray Member of the Demopolis Chalk.	Muldrow	19N	15E	West Point	Okitibeha	MS	33° 42' 25"	87° 32' 20"
90-6-16-1(M)	M225	Demopolis Chalk	NE 1/4 sec. 3 "Muldrow" section, along north-facing gully; sample collected at elevation approximately 225 ft. a.m.s.l. and 415 ft. above Arcola Limestone Member of Mooreville Chalk. This is the type locality of the Muldray Member of the Demopolis Chalk.	Muldrow	19N	15E	West Point	Okitibeha	MS	33° 42' 25"	87° 32' 20"
90-6-30-1(LCII)	90-6-30-1(LCII194)	Demopolis Chalk	NW 1/4 sec. 35 "Line Creek II" section, at north-northwest-facing cutbank along Line Creek; sample collected 19 ft. above water level (water level approximately 279 ft. a.m.s.l.) and 358 feet above Arcola Limestone Member of Mooreville Chalk.	Tibbee Creek	20N	15E	West Point	Okitibeha	MS	33° 41' 59"	87° 33' 42"
90-6-30-1(LCII)	LCII176	Demopolis Chalk	NW 1/4 sec. 35 "Line Creek II" section, at north-northwest-facing cutbank along Line Creek; sample collected 1 ft. above water level (water level approximately 275 ft. a.m.s.l.) and 344 feet above Arcola Limestone Member of Mooreville Chalk.	Tibbee Creek	20N	15E	West Point	Okitibeha	MS	33° 41' 59"	87° 33' 42"
90-6-30-1(LCII)	LCII180	Demopolis Chalk	NW 1/4 sec. 35 "Line Creek II" section, at north-northwest-facing cutbank along Line Creek; sample collected 5 ft. above water level (water level approximately 275 ft. a.m.s.l.) and 349 feet above Arcola Limestone Member of Mooreville Chalk; sample collected at base of section at elevation approximately 215 feet a.m.s.l.	Tibbee Creek	20N	15E	West Point	Okitibeha	MS	33° 41' 59"	87° 33' 42"
90-6-30-1(LCII)	LCII185	Demopolis Chalk	NW 1/4 sec. 35 "Line Creek II" section, at north-northwest-facing cutbank along Line Creek; sample collected 10 ft. above water level (water level approximately 275 ft. a.m.s.l.) and 349 feet above Arcola Limestone Member of Mooreville Chalk.	Tibbee Creek	20N	15E	West Point	Okitibeha	MS	33° 41' 59"	87° 33' 42"
90-8-18-1(ASN)	90-8-18-1(ASN220)	Demopolis Chalk	SW 1/4 sec. 33 Alexander Schoolhouse North section, located in gulfed area approximately 1/2 mile north of terminus of Alexander Schoolhouse Road at county road; sample collected at base of section at elevation approximately 220 feet a.m.s.l.	Muldrow	20N	15E	West Point	Okitibeha	MS	33° 33' 10"	88° 44' 28"
90-8-18-1(ASN)	90-8-18-1(ASN2230)	Demopolis Chalk	SW 1/4 sec. 33 Alexander Schoolhouse North section, located in gulfed area approximately 1/2 mile north of terminus of Alexander Schoolhouse Road at county road; sample collected at base of section at elevation approximately 230 feet a.m.s.l.	Muldrow	20N	15E	West Point	Okitibeha	MS	33° 33' 10"	88° 44' 28"

Station Number	Sample ID	Formation	Section	Member	Township	Range	Quadrangle	County	State	Latitude	Longitude
Comments											
90-8-18-(ASN)	90-8-18-(ASN235)	Demopolis Chalk	SW 1/4 sec. 33	Muldrow	20N	15E	West Point	Oktibbeha	MS	33° 33' 10"	88° 44' 28"
Alexander Schoolhouse North section, located in gullied area approximately 1/2 mile north of terminus of Alexander Schoolhouse Road at county road; sample collected at base of section at elevation approximately 235 feet a.m.s.l.											
90-8-18-(ASN)	90-8-18-(ASN240)	Demopolis Chalk	SW 1/4 sec. 33	Muldrow	20N	15E	West Point	Oktibbeha	MS	33° 33' 10"	88° 44' 28"
Alexander Schoolhouse North section, located in gullied area approximately 1/2 mile north of terminus of Alexander Schoolhouse Road at county road; sample collected at base of section at elevation approximately 240 feet a.m.s.l.											
90-8-18-(ASN)	90-8-18-(ASN245)	Demopolis Chalk	SW 1/4 sec. 33	Muldrow	20N	15E	West Point	Oktibbeha	MS	33° 33' 10"	88° 44' 28"
Alexander Schoolhouse North section, located in gullied area approximately 1/2 mile north of terminus of Alexander Schoolhouse Road at county road; sample collected at base of section at elevation approximately 245 feet a.m.s.l.											
90-8-18-(ASN)	90-8-18-(ASN250)	Demopolis Chalk	SW 1/4 sec. 33	Muldrow	20N	15E	West Point	Oktibbeha	MS	33° 33' 10"	88° 44' 28"
Alexander Schoolhouse North section, located in gullied area approximately 1/2 mile north of terminus of Alexander Schoolhouse Road at county road; sample collected at base of section at elevation approximately 250 feet a.m.s.l.											
90-8-18-(ASN)	90-8-18-(ASN225)	Demopolis Chalk	SW 1/4 sec. 33	Muldrow	20N	15E	West Point	Oktibbeha	MS	33° 33' 10"	88° 44' 28"
Alexander Schoolhouse North section, located in gullied area approximately 1/2 mile north of terminus of Alexander Schoolhouse Road at county road; sample collected at base of section at elevation approximately 225 feet a.m.s.l.											
90-8-25-(TCII)	90-8-25-(TCII201)	Demopolis Chalk	E 1/2 sec. 6	Tibbee Creek	19N	16E	West Point	Clay	MS	33° 32' 30"	88° 39' 19"
Section on north-facing slope of Tibbee Creek; sample collected from marl in lower Demopolis Chalk (Tibbee Creek Member), approximately 5 feet above base of section and 74 feet above base of Demopolis Chalk.											
90-8-25-(TCII)	90-8-25-(TCII205)	Demopolis Chalk	E 1/2 sec. 6	Tibbee Creek	19N	16E	West Point	Clay	MS	33° 32' 30"	88° 39' 19"
Section on north-facing slope of Tibbee Creek; sample collected from marl in lower Demopolis Chalk (Tibbee Creek Member), approximately 9 feet above base of section and 78 feet above base of Demopolis Chalk.											
90-8-25-(TCII)	90-8-25-(TCII19)	Demopolis Chalk	E 1/2 sec. 6	Tibbee Creek	19N	16E	West Point	Clay	MS	33° 32' 30"	88° 39' 19"
Section on north-facing slope of Tibbee Creek; sample collected from marl in lower Demopolis Chalk (Tibbee Creek Member), approximately 23 feet above base of section and 92 feet above base of Demopolis Chalk.											
90-8-25-(TCII)	TCII195	Demopolis Chalk	E 1/2 sec. 6	Tibbee Creek	19N	16E	West Point	Clay	MS	33° 32' 30"	88° 39' 19"
Section on north-facing slope of Tibbee Creek; sample collected from marl in lower Demopolis Chalk (Tibbee Creek Member), at water level and 70 feet above base of Demopolis Chalk.											
90-8-4-1 (TCII)	90-8-4-1 (TCII172)	Demopolis Chalk	NE 1/4 sec. 5	Tibbee Creek	19N	16E	West Point	Clay	MS	33° 32' 12"	88° 38' 28"
Section on north-facing slope of Tibbee Creek; sample collected from marl in lower Demopolis Chalk (Tibbee Creek Member), approximately 27 feet above base of section and 21.5 feet above base of Demopolis Chalk.											
90-8-4-1 (TCII)	90-8-4-1 (TCII189.5)	Demopolis Chalk	NE 1/4 sec. 5	Tibbee Creek	19N	16E	West Point	Clay	MS	33° 32' 12"	88° 38' 28"
Section on north-facing slope of Tibbee Creek; sample collected from marl in lower Demopolis Chalk (Tibbee Creek Member), approximately 26.5 feet above base of section and 39 feet above base of Demopolis Chalk.											
90-8-4-1 (TCII)	90-8-4-1 (TCII199)	Demopolis Chalk	NE 1/4 sec. 5	Tibbee Creek	19N	16E	West Point	Clay	MS	33° 32' 12"	88° 38' 28"
Section on north-facing slope of Tibbee Creek; sample collected from marl in lower Demopolis Chalk (Tibbee Creek Member), approximately 27 feet above base of section and 31 feet above base of Demopolis Chalk.											
90-8-4-1 (TCII)	TCII165.5	Demopolis Chalk	NE 1/4 sec. 5	Tibbee Creek	19N	16E	West Point	Clay	MS	33° 32' 12"	88° 38' 28"
Section on north-facing slope of Tibbee Creek; sample collected from marl in lower Demopolis Chalk (Tibbee Creek Member), approximately 1.5 feet above base of section and 17 feet above base of Demopolis Chalk.											
90-8-4-1 (TCII)	90-8-4-1 (TCII178)	Demopolis Chalk	NE 1/4 sec. 5	Tibbee Creek	19N	16E	West Point	Clay	MS	33° 32' 12"	88° 38' 28"
Section on north-facing slope of Tibbee Creek; sample collected from marl in lower Demopolis Chalk (Tibbee Creek Member), approximately 15 feet above base of section and 29 feet above base of Demopolis Chalk.											
90-8-4-1 (TCII)	TCII183	Demopolis Chalk	NE 1/4 sec. 5	Tibbee Creek	19N	16E	West Point	Clay	MS	33° 32' 12"	88° 38' 28"
Section on north-facing slope of Tibbee Creek; sample collected from marl in lower Demopolis Chalk (Tibbee Creek Member), approximately 34 feet above base of section and 34 feet above base of Demopolis Chalk.											
91-4-13-(IRR)	91-4-13-(IRR255)	Demopolis Chalk	NW 1/4 sec. 4	Muldrow	19N	15E	West Point	Oktibbeha	MS	33° 32' 14"	88° 44' 16"
Section measured along gully approximately 1/4 mile NE of terminus of Alexander Schoolhouse Road and county road. Base of section at elevation -255 feet a.m.s.l. This sample was collected at the base of the section.											
91-4-13-(IRR)	91-4-13-(IRR260)	Demopolis Chalk	NW 1/4 sec. 4	Muldrow	19N	15E	West Point	Oktibbeha	MS	33° 32' 14"	88° 44' 16"
Section measured along gully approximately 1/4 mile NE of terminus of Alexander Schoolhouse Road and county road. Base of section at elevation -264 feet a.m.s.l. This sample was collected approximately 9 feet above the base of the section.											
91-4-13-(IRR)	91-4-13-(IRR264)	Demopolis Chalk	NW 1/4 sec. 4	Muldrow	19N	15E	West Point	Oktibbeha	MS	33° 32' 14"	88° 44' 16"
Section measured along gully approximately 1/4 mile NE of terminus of Alexander Schoolhouse Road and county road. Base of section at elevation -268 feet a.m.s.l. This sample was collected approximately 13 feet above the base of the section.											
91-4-13-(IRR)	91-4-13-(IRR268)	Demopolis Chalk	NW 1/4 sec. 4	Muldrow	19N	15E	West Point	Oktibbeha	MS	33° 32' 14"	88° 44' 16"
Section measured along gully approximately 1/4 mile NE of terminus of Alexander Schoolhouse Road and county road. Base of section at elevation -268 feet a.m.s.l. This sample was collected approximately 85 feet a.m.s.l., and 71.5 feet below base of Arcola Limestone, in lower, unnamed member of Mooreville Chalk.											
92-11-17-(HB)	92-11-17-(HB105)	Mooreville Chalk	SE 1/4 sec. 36	Blackwell Bend	Dallas	AL	10E	Blackwell Bend	Dallas	32° 19' 09"	87° 01' 06"
"Hatcher's Buff" section, on northwest-facing cutbank on Alabama River; sample collected approximately 20 feet above water surface (water surface elevation approximately 85 feet a.m.s.l.), and 66.5 feet below base of Arcola Limestone, in lower, unnamed member of Mooreville Chalk.											
92-11-17-(HB)	92-11-17-(HB109)	Mooreville Chalk	SE 1/4 sec. 36	Blackwell Bend	Dallas	AL	10E	Blackwell Bend	Dallas	32° 19' 09"	87° 01' 06"
"Hatcher's Buff" section, on northwest-facing cutbank on Alabama River; sample collected approximately 24 feet above water surface (water surface elevation approximately 85 feet a.m.s.l.), and 62.5 feet below base of Arcola Limestone, in lower, unnamed member of Mooreville Chalk.											

Station Number	Sample ID	Formation	Section	Township	Range	Quadrangle	County	State	Latitude	Longitude	
Comments				Member							
92-11-20-2	92-11-20-2(45)	Mooreville Chalk	SW 1/4 sec. 23	Moorville Chalk, approximately 35 feet above bottom of creek; (very shallow), approximately .36 feet above top of Tonibigbee Sand Member of Eutaw Formation, in Lower Mooreville Chalk.	17N	10E	Selma	Dallas	AL	33° 25' 48"	
92-11-20-2	92-11-20-2(50)	Mooreville Chalk	SW 1/4 sec. 23	Sample collected from bald area just west of Valley Creek, approximately .35 feet above bottom of creek (very shallow), approximately .41 feet above top of Tonibigbee Sand Member of Eutaw Formation, in Lower Mooreville Chalk.	17N	10E	Selma	Dallas	AL	33° 25' 48"	
92-6-1-(RH)	92-6-1-(RH214)	Demopolis Chalk	NE 1/4 sec. 14	"Rock Hill" section; sample collected from basal Ripley Formation, approximately .49 feet above base of section. This section is a composite of two sections; the lower section is in the Muldrow Formation, elevation ~214 a.m.s.l., approximately 1 foot above the base of the section.	19N	14E	Muldrow	Cedar Bluff	Oktibbeha	MS	33° 30' 53"
92-6-1-(RH)	92-6-1-(RH220)	Demopolis Chalk	NE 1/4 sec. 14	"Rock Hill" section; sample collected from basal Ripley Formation, approximately .49 feet above base of section. This section is a composite of two sections; the lower section is in the Muldrow Formation, elevation ~214 a.m.s.l., approximately 1 foot above the base of the section.	19N	14E	Muldrow	Cedar Bluff	Oktibbeha	MS	33° 30' 53"
92-6-1-(RH)	92-6-1-(RH230)	Demopolis Chalk	NE 1/4 sec. 14	"Rock Hill" section; sample collected from basal Ripley Formation, This sample was collected at elevation ~230 a.m.s.l., approximately 17 feet above the base of the section.	19N	14E	Muldrow	Cedar Bluff	Oktibbeha	MS	33° 30' 53"
92-6-1-(RH)	92-6-1-(RH235)	Demopolis Chalk	NE 1/4 sec. 14	"Rock Hill" section; sample collected from basal Ripley Formation, approximately .49 feet above base of section. This section is a composite of two sections; the lower section is in the Muldrow Formation, elevation ~235 a.m.s.l., approximately 22 feet above the base of the section.	19N	14E	Muldrow	Cedar Bluff	Oktibbeha	MS	33° 30' 53"
92-6-1-(RH)	92-6-1-(RH245)	Demopolis Chalk	NE 1/4 sec. 14	"Rock Hill" section; sample collected from basal Ripley Formation, This sample was collected at elevation ~245 a.m.s.l., approximately 32 feet above the base of the section.	19N	14E	Muldrow	Cedar Bluff	Oktibbeha	MS	33° 30' 58"
92-6-1-(RH)	92-6-1-(RH255)	Demopolis Chalk	NE 1/4 sec. 14	"Rock Hill" section; sample collected from basal Ripley Formation, and the lower Ripley Formation. This sample was collected at elevation ~255 a.m.s.l., approximately 42 feet above the base of the section.	19N	14E	Muldrow	Cedar Bluff	Oktibbeha	MS	33° 30' 58"
92-6-1-(RH)	92-6-1-(RH260)	Demopolis Chalk	NE 1/4 sec. 14	"Rock Hill" section; sample collected from basal Ripley Formation, approximately .49 feet above base of section. This section is a composite of two sections; the lower section is in the Muldrow Formation, elevation ~260 a.m.s.l., approximately 37 feet above the base of the section.	19N	14E	Muldrow	Cedar Bluff	Oktibbeha	MS	33° 30' 58"
92-6-1-(RH)	92-6-1-(RH266)	Demopolis Chalk	NE 1/4 sec. 14	"Rock Hill" section; sample collected from basal Ripley Formation, and the lower Ripley Formation. This sample was collected at elevation ~266 a.m.s.l., approximately 47 feet above the base of the section.	19N	14E	Muldrow	Cedar Bluff	Oktibbeha	MS	33° 30' 58"
92-6-1-(RH)	92-6-1-(RH270)	Demopolis Chalk	NE 1/4 sec. 14	"Rock Hill" section; sample collected from basal Ripley Formation, approximately .49 feet above base of section. This section is a composite of two sections; the lower section is in the Muldrow Formation, elevation ~270 a.m.s.l., approximately 52 feet above the base of the section.	19N	14E	Muldrow	Cedar Bluff	Oktibbeha	MS	33° 30' 58"
92-6-1-(RH)	92-6-1-(RH275)	Demopolis Chalk	NE 1/4 sec. 14	"Rock Hill" section; sample collected from basal Ripley Formation, and the lower Ripley Formation. This sample was collected at elevation ~275 a.m.s.l., approximately 42 feet above the base of the section.	19N	14E	Muldrow	Cedar Bluff	Oktibbeha	MS	33° 30' 58"
92-6-1-(RH)	92-6-1-(RH280)	Demopolis Chalk	NE 1/4 sec. 14	"Rock Hill" section; sample collected from basal Ripley Formation, approximately .49 feet above base of section. This section is a composite of two sections; the lower section is in the Muldrow Formation, elevation ~280 a.m.s.l., approximately 47 feet above the base of the section.	19N	14E	Muldrow	Cedar Bluff	Oktibbeha	MS	33° 30' 58"
92-6-1-(RH)	92-6-1-(RH286)	Demopolis Chalk	NE 1/4 sec. 14	"Rock Hill" section; sample collected from basal Ripley Formation, approximately .49 feet above base of section. This section is a composite of two sections; the lower section is in the Muldrow Formation, elevation ~286 a.m.s.l., approximately 52 feet above the base of the section.	19N	14E	Muldrow	Cedar Bluff	Oktibbeha	MS	33° 30' 58"
92-6-1-(RH)	92-6-1-(RH42)	Ripley Formation	NW 1/4 sec. 13 and NE 1/4 sec. 14	"Rock Hill" section; sample collected from basal Ripley Formation, approximately .52 feet above base of section. This section is a composite of two sections; the lower section is in the Muldrow Formation, elevation ~266 a.m.s.l., approximately 47 feet above the base of the section.	19N	05E	Bluffport Marl	Cedar Bluff	Oktibbeha	MS	33° 30' 58"
92-6-1-(RH)	RH35	Demopolis Chalk	NW 1/4 sec. 13 and NE 1/4 sec. 14	"Rock Hill" section, at northwest-facing slope; sample collected from upper part Bluffport Marl Member of Demopolis Formation, elevation approximately 269 ft. a.m.s.l. This section is a composite of two sections; the lower section is in the Muldrow Member of the Demopolis Chalk and the upper section is in the Bluffport Marl Member of the Demopolis and the lower Ripley Formation.	19N	05E	Bluffport Marl	Cedar Bluff	Oktibbeha	MS	33° 30' 58"
93-10-19-1	93-10-19-1(100)	Ripley Formation	NW 1/4 sec. 26	"Red Bluff" section, on southeast-facing cutbank on Alabama River; sample collected approximately 20 feet above water surface (water surface on 10-19-93 = 79.5 feet a.m.s.l.), and 304 feet above top of Arcola Limestone Member of Mooreville Formation, in lower Ripley Formation.	14N	08E	Tuscaloosa	Dallas	AL	32° 09' 41"	
93-10-19-1	93-10-19-1(100)	Ripley Formation	NW 1/4 sec. 26	"Red Bluff" section, on southeast-facing cutbank on Alabama River; sample collected approximately 30 feet above water level (water surface on 10-19-93 = 79.5 feet a.m.s.l.), and 404 feet above top of Arcola Limestone Member of Mooreville Formation, in lower Ripley Formation.	14N	08E	Tuscaloosa	Dallas	AL	32° 09' 41"	
93-10-19-1	93-10-19-1(120)	Ripley Formation	NW 1/4 sec. 26	"Red Bluff" section, on southeast-facing cutbank on Alabama River; sample collected approximately 40 feet above water surface (water surface on 10-19-93 = 79.5 feet a.m.s.l.), and 414 feet above top of Arcola Limestone Member of Mooreville Formation, in lower Ripley Formation.	14N	08E	Tuscaloosa	Dallas	AL	32° 09' 41"	
93-10-19-1	93-10-19-1(125)	Ripley Formation	NW 1/4 sec. 26	"Red Bluff" section, on southeast-facing cutbank on Alabama River; sample collected approximately 45 feet above water level (water surface on 10-19-93 = 79.5 feet a.m.s.l.), and 419 feet above top of Arcola Limestone Member of Mooreville Formation, in lower Ripley Formation.	14N	08E	Tuscaloosa	Dallas	AL	32° 09' 41"	

Station Number	Sample ID	Formation	Section	Member	Township	Range	Quadrangle	County	State	Latitude	Longitude
Comments											

Ripley Formation.											
93-10-19-1 "Red Bluff" section, on southeast-facing cutbank on Alabama River; sample collected approximately 55 feet above water level (water surface on 10-19-93 = 79.5 feet a.m.s.l.), and +29 feet above top of Arcola Limestone Member of Mooreville Formation, in lower Ripley Formation.	93-10-19-1(135)	Ripley Formation	NW 1/4 sec. 26	14N 08E	Tasso	Dallas	AL	32° 09' 41"	87° 14' 56"		
93-10-19-1 "Red Bluff" section, on southeast-facing cutbank on Alabama River; sample collected at water level (water surface on 10-19-93 = 79.5 feet a.m.s.l.), and 374 feet above top of Arcola Limestone Member of Mooreville Formation, in lower Ripley Formation.	93-10-19-1(80)	Ripley Formation	NW 1/4 sec. 26	14N 08E	Tasso	Dallas	AL	32° 09' 41"	87° 14' 56"		
93-10-19-1 "Red Bluff" section, on southeast-facing cutbank on Alabama River; sample collected approximately 10 feet above water level (water surface on 10-19-93 = 79.5 feet a.m.s.l.), and 384 feet above top of Arcola Limestone Member of Mooreville Formation, in lower Ripley Formation.	93-10-19-1(90)	Ripley Formation	NW 1/4 sec. 26	14N 08E	Tasso	Dallas	AL	32° 09' 41"	87° 14' 56"		
"Harrell Station" section, on north-facing cutbank of tributary to Cahaba River, at water elevation (very shallow), and approximately 125 feet above top of Tombigbee Sand Member of the Eutaw Formation, in Mooreville Chalk.	93-1-27-1 "Harrell Station" section, on north-facing cutbank of tributary to Cahaba River, at water elevation (very shallow), and approximately 135 feet above top of Tombigbee Sand Member of the Eutaw Formation, in Mooreville Chalk.	Mooreville Chalk	sec. 29	19N 09E	Marion Junction	Dallas	AL	32° 25' 17"	87° 11' 48"		
"Harrell Station" section (upper part), along east-west gully of bald area, and approximately 150 feet above top of Tombigbee Sand Member of the Eutaw Formation, in Mooreville Chalk.	93-1-27-1(135)	Mooreville Chalk	C. sec. 29	19N 09E	Marion Junction	Dallas	AL	32° 25' 17"	87° 11' 48"		
"Harrell Station" section (upper part), along east-west gully of bald area, and approximately 160 feet above top of Tombigbee Sand Member of the Eutaw Formation, in Mooreville Chalk.	93-1-27-2 "Harrell Station" section (upper part), along east-west gully of bald area, and approximately 160 feet above top of Tombigbee Sand Member of the Eutaw Formation, in Mooreville Chalk.	Mooreville Chalk	C. sec. 29	19N 09E	Marion Junction	Dallas	AL	32° 25' 16"	87° 12° 04"		
"Harrell Station" section (upper part), along east-west gully of bald area, and approximately 160 feet above top of Tombigbee Sand Member of the Eutaw Formation, in Mooreville Chalk.	93-1-27-2(150)	Mooreville Chalk	C. sec. 29	19N 09E	Marion Junction	Dallas	AL	32° 25' 16"	87° 12° 04"		
"Harrell Station" section (upper part), along east-west gully of bald area, and approximately 160 feet above top of Tombigbee Sand Member of the Eutaw Formation, in Mooreville Chalk.	93-1-27-2(135)	Mooreville Chalk	C. sec. 29	19N 09E	Marion Junction	Dallas	AL	32° 25' 16"	87° 12° 04"		
"Harrell Station" section (upper part), along east-west gully of bald area, and approximately 160 feet above top of Tombigbee Sand Member of the Eutaw Formation, in Mooreville Chalk.	93-1-27-2(160)	Mooreville Chalk	C. sec. 29	19N 09E	Marion Junction	Dallas	AL	32° 25' 16"	87° 12° 04"		
"Harrell Station" section (upper part), along east-west gully of bald area, and approximately 160 feet above top of Tombigbee Sand Member of the Eutaw Formation, in Mooreville Chalk.	93-1-27-2(170)	Mooreville Chalk	C. sec. 29	19N 09E	Marion Junction	Dallas	AL	32° 25' 16"	87° 12° 04"		
"Harrell Station" section (upper part), along east-west gully of bald area, and approximately 170 feet above top of Tombigbee Sand Member of the Eutaw Formation, in Mooreville Chalk.	93-1-27-2(180)	Mooreville Chalk	C. sec. 29	19N 09E	Marion Junction	Dallas	AL	32° 25' 16"	87° 12° 04"		
"Harrell Station" section (upper part), along east-west gully of bald area, and approximately 180 feet above top of Tombigbee Sand Member of the Eutaw Formation, in Mooreville Chalk.	93-1-27-2(190)	Mooreville Chalk	C. sec. 29	19N 09E	Marion Junction	Dallas	AL	32° 25' 16"	87° 12° 04"		
"Harrell Station" section (upper part), along east-west gully of bald area, and approximately 190 feet above top of Tombigbee Sand Member of the Eutaw Formation, in Mooreville Chalk.	93-1-27-2(198)	Mooreville Chalk	C. sec. 29	19N 09E	Marion Junction	Dallas	AL	32° 25' 16"	87° 12° 04"		
"Harrell Station" section (upper part), along east-west gully of bald area, and approximately 198 feet above top of Tombigbee Sand Member of the Eutaw Formation, in Mooreville Chalk.	93-2-3-1 93-2-3-1(10)	Mooreville Chalk	W 1/2 sec. 20	17N 09E	Marion Junction	Dallas	AL	32° 26' 08"	87° 11' 27"		
Sample collected on east-facing cutbank of Cahaba River, approximately 15 feet above water surface (water elevation = approximately 102 feet a.m.s.l. on 2-3-93), and 65 feet above top of Tombigbee Sand Member of Eutaw Formation, in lower Mooreville Chalk.	93-2-3-1 93-2-3-1(120)	Mooreville Chalk	W 1/2 sec. 20	17N 09E	Marion Junction	Dallas	AL	32° 26' 08"	87° 11' 27"		
Sample collected on east-facing cutbank of Cahaba River, approximately 25 feet above water surface (water elevation = approximately 102 feet a.m.s.l. on 2-3-93), and 75 feet above top of Tombigbee Sand Member of Eutaw Formation, in lower Mooreville Chalk.	93-2-3-1 93-2-3-1(130)	Mooreville Chalk	W 1/2 sec. 20	17N 09E	Marion Junction	Dallas	AL	32° 26' 08"	87° 11' 27"		
Sample collected on east-facing cutbank of Cahaba River, approximately 55 feet above water surface (water elevation = approximately 102 feet a.m.s.l. on 2-3-93), and 119 feet above top of Tombigbee Sand Member of Eutaw Formation, in lower Mooreville Chalk.	93-2-3-1 93-2-3-1(150)	Mooreville Chalk	W 1/2 sec. 20	17N 09E	Marion Junction	Dallas	AL	32° 26' 08"	87° 11' 27"		
Sample collected on east-facing cutbank of Cahaba River, approximately 65 feet above water surface (water elevation = approximately 102 feet a.m.s.l. on 2-3-93), and 115 feet above top of Tombigbee Sand Member of Eutaw Formation, in lower Mooreville Chalk.	93-2-3-1 93-2-3-1(160)	Mooreville Chalk	W 1/2 sec. 20	17N 09E	Marion Junction	Dallas	AL	32° 26' 08"	87° 11' 27"		
Sample collected in north-facing gully just south of Cahaba River, approximately 210 feet above top of Tombigbee Sand Member of Eutaw Formation, in middle of Mooreville Chalk.	93-3-9-1 93-3-9-1(165)	Mooreville Chalk	SE 1/4 sec. 33	17N 09E	Marion Junction	Dallas	AL	32° 09' 04"	87° 10' 15"		
Sample collected in north-facing gully just south of Cahaba River, approximately 220 feet above top of Tombigbee Sand Member of Eutaw Formation, in middle of Mooreville Chalk.	93-3-9-1 93-3-9-1(175)	Mooreville Chalk	SE 1/4 sec. 33	17N 09E	Marion Junction	Dallas	AL	32° 09' 04"	87° 10' 15"		
Sample collected in north-facing gully just south of Cahaba River, approximately 228 feet above top of Tombigbee Sand Member of Eutaw Formation, in middle of Mooreville Chalk.	93-3-9-1 93-3-9-1(183)	Mooreville Chalk	SE 1/4 sec. 33	17N 09E	Marion Junction	Dallas	AL	32° 09' 04"	87° 10' 15"		
Sample collected in north-facing gully just south of Cahaba River, approximately 246 feet above top of Tombigbee Sand Member of Eutaw Formation, in middle of Mooreville Chalk.	93-3-9-1 93-3-9-1(202)	Mooreville Chalk	SE 1/4 sec. 33	17N 09E	Marion Junction	Dallas	AL	32° 09' 04"	87° 10' 15"		
"Elm Bluff" section, on north-west facing cutbank of Alabama River; sample collected approximately 1 foot above water level (water elevation = 79.78 feet a.m.s.l.; sample elevation = -81 feet a.m.s.l.)	94-1-21-1(EB1)	Demopolis Chalk	NW 1/4 sec. 20	14N 10E	Elm Bluff	Dallas	AL	32° 10' 20"	87° 05' 54"		

Station Number	Sample ID	Formation	Section	Member	Township	Range	Quadrangle	County	State Latitude	Longitude	
Comments											
95-11-10-1	95-11-10-1(162)	Mooreville Chalk	W edge sec. 7		17E	19N	Waverly	Lowndes	MS	35° 31' 23"	
		Sample collected on west-facing embankment on Tibbee Creek, approximately 2 feet above water level (normal surface elevation = 163 feet a.m.s.l.), and approximately 165 feet a.m.s.l., behind last camp house on road.			17E	19N	Waverly	Lowndes	MS	35° 31' 23"	
95-11-10-1	95-11-10-1(170)	Mooreville Chalk	W edge sec. 7		17E	19N	Waverly	Lowndes	MS	35° 31' 23"	
		Sample collected on west-facing embankment on Tibbee Creek, approximately 10 feet above water level (normal surface elevation = 163 feet a.m.s.l.), and approximately 173 feet a.m.s.l., behind last camp house on road.			17E	19N	Waverly	Lowndes	MS	35° 31' 23"	
95-11-10-1	95-11-10-1(180)	Mooreville Chalk	W edge sec. 7		17E	19N	Waverly	Lowndes	MS	35° 31' 23"	
		Sample collected on west-facing embankment on Tibbee Creek, approximately 20 feet above water level (normal surface elevation = 163 feet a.m.s.l.), and approximately 180 feet a.m.s.l., behind last camp house on road.			17E	19N	Waverly	Lowndes	MS	35° 31' 23"	
95-11-10-1	95-11-10-1(190)	Mooreville Chalk	W edge sec. 7		17E	19N	Waverly	Lowndes	MS	35° 31' 23"	
		Sample collected on west-facing embankment on Tibbee Creek, approximately 30 feet above water level (normal surface elevation = 163 feet a.m.s.l.), and approximately 190 feet a.m.s.l., behind last camp house on road.			17E	19N	Waverly	Lowndes	MS	35° 31' 23"	
95-11-10-1	95-11-10-1(205)	Mooreville Chalk	W edge sec. 7		17E	19N	Waverly	Lowndes	MS	35° 31' 23"	
		Sample collected on west-facing embankment on Tibbee Creek, approximately 45 feet above water level (normal surface elevation = 163 feet a.m.s.l.), and approximately 208 feet a.m.s.l., behind last camp house on road.			17E	19N	Waverly	Lowndes	MS	35° 31' 23"	
95-11-10-1	95-11-10-1(217)	Mooreville Chalk	W edge sec. 7		17E	19N	Waverly	Lowndes	MS	35° 31' 23"	
		Sample collected on west-facing embankment on Tibbee Creek, approximately 57 feet above water level (normal surface elevation = 163 feet a.m.s.l.), and approximately 220 feet a.m.s.l., behind last camp house on road.			17E	19N	Waverly	Lowndes	MS	35° 31' 23"	
95-7-14-1	95-7-14-1(275)	Demopolis Chalk	SW 1/4 sec. 28	Bluffport Marl	18N	15E	Artesia	Oktibbeha	MS	35° 23' 15"	
		"Salem Church" section, along east-facing roadcut on unpaved road, just south of bridge over Catalpa Creek, base of section, approximately 420 above Arcola Limestone Member of Mooreville Chalk; sample collected approximately 275 ft a.m.s.l., and 695 ft above Arcola.			18N	15E	Artesia	Oktibbeha	MS	35° 23' 15"	
95-7-14-1	95-7-14-1(305)	Prairie Bluff Chalk	SW 1/4 sec. 28			18N	15E	Artesia	Oktibbeha	MS	35° 23' 15"
		"Salem Church" section, along east-facing roadcut on unpaved road, just south of bridge over Catalpa Creek; base of section approximately 420 above Arcola Limestone Member of Mooreville Chalk; sample collected approximately 220 ft a.m.s.l., and 725 ft above Arcola.			18N	15E	Artesia	Oktibbeha	MS	35° 23' 15"	
95-7-14-1	95-7-14-1(360)	Prairie Bluff Chalk	SW 1/4 sec. 28			18N	15E	Artesia	Oktibbeha	MS	35° 23' 15"
		"Salem Church" section, along east-facing roadcut on unpaved road, just south of bridge over Catalpa Creek; base of section approximately 420 above Arcola Limestone Member of Mooreville Chalk; sample collected approximately 275 ft a.m.s.l., and 780 ft above Arcola.			18N	15E	Artesia	Oktibbeha	MS	35° 23' 15"	
95-7-14-1	95-7-14-1(371)	Prairie Bluff Chalk	SW 1/4 sec. 28			18N	15E	Artesia	Oktibbeha	MS	35° 23' 15"
		"Salem Church" section, along east-facing roadcut on unpaved road, just south of bridge over Catalpa Creek; base of section approximately 420 above Arcola Limestone Member of Mooreville Chalk; sample collected approximately 220 ft a.m.s.l., and 725 ft above Arcola.			18N	15E	Artesia	Oktibbeha	MS	35° 23' 15"	
96-11-11-1	96-11-11-1(PB1)	Eutaw Formation	S 1/2 sec. 14	Tombigbee Sand	19N	17E	Columbus North	Lowndes	MS	35° 30' 32"	
		"Plymouth Bluff" section, at east-facing former cutbank of Tombigbee River, sample collected approximately 1 foot above water level, elevation -164 ft. a.m.s.l. and 33 ft. below top Tombigbee Sand Member of Eutaw Formation.			19N	17E	Columbus North	Lowndes	MS	35° 30' 32"	
96-11-11-1	96-11-11-1(PB10)	Eutaw Formation	S 1/2 sec. 14	Tombigbee Sand	19N	17E	Columbus North	Lowndes	MS	35° 30' 32"	
		"Plymouth Bluff" section, at east-facing former cutbank of Tombigbee River; sample collected approximately 1 foot above water level, elevation -173 ft. a.m.s.l. and 24 ft. below top Tombigbee Sand Member of Eutaw Formation.			19N	17E	Columbus North	Lowndes	MS	35° 30' 32"	
96-11-11-1	96-11-11-1(PB20)	Eutaw Formation	S 1/2 sec. 14	Tombigbee Sand	19N	17E	Columbus North	Lowndes	MS	35° 30' 32"	
		"Plymouth Bluff" section, at east-facing former cutbank of Tombigbee River; sample collected approximately 1 foot above water level, elevation -183 ft. a.m.s.l. and 14 ft. below top Tombigbee Sand Member of Eutaw Formation.			19N	17E	Columbus North	Lowndes	MS	35° 30' 32"	
96-11-11-1	96-11-11-1(PB30)	Eutaw Formation	S 1/2 sec. 14	Tombigbee Sand	19N	17E	Columbus North	Lowndes	MS	35° 30' 32"	
		"Plymouth Bluff" section, at east-facing former cutbank of Tombigbee River; sample collected approximately 1 foot above water level, elevation -193 ft. a.m.s.l. and 4 ft. below top Tombigbee Sand Member of Eutaw Formation.			19N	17E	Columbus North	Lowndes	MS	35° 30' 32"	
96-11-11-1	96-11-11-1(PB35)	Eutaw Formation	S 1/2 sec. 14	Tombigbee Sand	19N	17E	Columbus North	Lowndes	MS	35° 30' 32"	
		"Plymouth Bluff" section, at east-facing former cutbank of Tombigbee River; sample collected approximately 1 foot above water level, elevation -198 ft. a.m.s.l. and 1 ft. above top Tombigbee Sand Member of Eutaw Formation.			19N	17E	Columbus North	Lowndes	MS	35° 30' 32"	
96-11-11-1	96-11-11-1(PB40)	Eutaw Formation	S 1/2 sec. 14	Tombigbee Sand	19N	10E	Elm Bluff	Dallas	AL	32° 14' 07"	
		"Plymouth Bluff" section, at east-facing former cutbank of Tombigbee River; sample collected approximately 1 foot above water level, elevation -203 ft. a.m.s.l. and 6 ft. above top Tombigbee Sand Member of Eutaw Formation.			19N	10E	Elm Bluff	Dallas	AL	32° 14' 07"	
96-11-11-1	96-11-11-1(PB45)	Eutaw Formation	S 1/2 sec. 14	Tombigbee Sand	19N	17E	Columbus North	Lowndes	MS	35° 30' 32"	
		"Plymouth Bluff" section, at east-facing former cutbank of Tombigbee River; sample collected approximately 1 foot above water level, elevation -208 ft. a.m.s.l. and 11 ft. above top Tombigbee Sand Member of Eutaw Formation.			19N	17E	Columbus North	Lowndes	MS	35° 30' 32"	
S. Selma core #1-3	S. Selma core #1-3 (114)	Demopolis Chalk	NW 1/4 sec. 31							88° 29' 34"	
		Sample collected from core, elevation approximately 98 ft. a.m.s.l. and 189 ft. above Arcola Limestone Member of Demopolis Chalk.								88° 29' 34"	
S. Selma core #1-3	S. Selma core #1-3 (98)	Demopolis Chalk	NW 1/4 sec. 31							88° 29' 34"	
S. Selma core #1-3	S. Selma core #1-3 (133.5)	Demopolis Chalk	NW 1/4 sec. 31							87° 06' 43"	
		Sample collected from core, elevation approximately 133 ft. a.m.s.l. and 208 ft. above Arcola Limestone Member of Demopolis Chalk.								87° 06' 43"	

Upper Cretaceous Sequence Stratigraphy, Sea-level Fluctuations and Oceanic Anoxic Events 2 and 3, Northeastern Gulf of Mexico

Kaiyu Liu

Department of Geological Sciences, University of Alabama, Tuscaloosa, Alabama, 35487, U.S.A.
email: lky36@yahoo.com

ABSTRACT: The relationship between Oceanic Anoxic Events (OAEs) and sea-level fluctuations can be determined by placing OAE sediments into an integrated sequence stratigraphic framework based on biostratigraphic age control, and regional seismic and well-log data. Two Upper Cretaceous black shale units in the northeastern Gulf of Mexico area, the Marine Tuscaloosa shale and the downdip Eutaw shale, are interpreted to be deposited in association with Late Cretaceous OAE 2 (Cenomanian – Turonian boundary event) and OAE 3 (late Coniacian – early Santonian). The Marine Tuscaloosa shale accumulated during the maximum flooding event of the UK I sequence (middle Cenomanian to upper Turonian); and the downdip Eutaw shale accumulated as the early transgressive systems tract of the UK II sequence (upper Coniacian to upper Campanian). These OAEs can be classified into two categories according to their sequence stratigraphic positions. Type I OAE (e.g., OAE 2) occurred during a maximum flooding event, and the black shale associated with this type of event was deposited in an open shelf environment. Type II OAE (e.g., OAE 3) occurred during the early phase of a marine transgression that resulted in the inundation of large coastal areas and the formation of lagoons and estuaries, which acted to trap large quantities of terrestrial organic carbon.

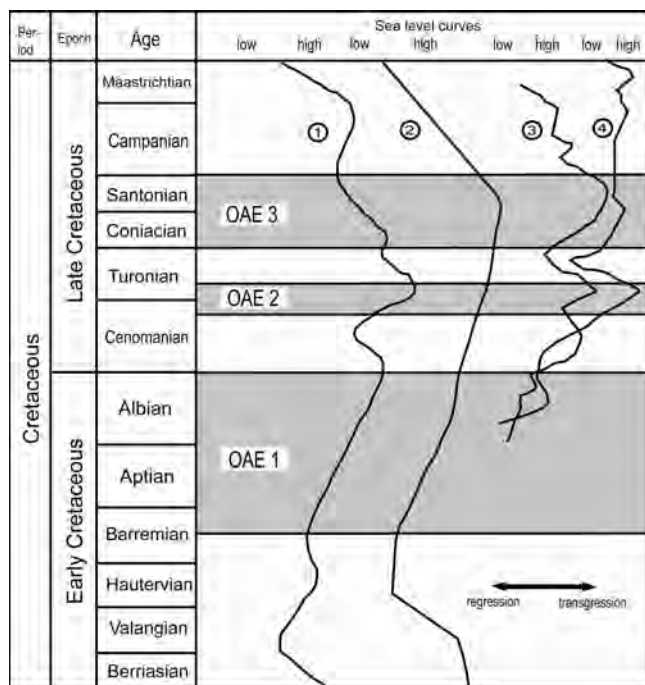
INTRODUCTION

Cretaceous Oceanic Anoxic Events (OAEs) were geological periods characterized by widespread deposition of organic carbon-rich sediments (black shales) in marine environments and by the enrichment of heavy carbon isotopes in pelagic carbonate facies (Jenkyns 1980). Although carbonaceous black shale deposition was widespread during the Cretaceous, concentrations existed in particular intervals when/where oceanographic and climatic conditions were appropriate (Arthur et al. 1990; Bralower et al. 1994; Leckie et al. 2002). Schlanger and Jenkyns (1976) first proposed the term “Oceanic Anoxic Event” to describe such conditions. Jenkyns (1980) reviewed the stratigraphic distribution of Cretaceous black shales found in outcrops and concluded that black shale deposition was widespread during three major periods: Aptian-Albian, Cenomanian-Turonian boundary, and Coniacian-Santonian. These age designations agree with previous observations from DSDP cores (Berger and von Rad 1972; Moberly and Larson 1975; Jackson and Schlanger 1976). Jenkyns (1980) suggested that global marine waters were relatively depleted in oxygen during these periods, resulting in widespread organic matter deposition or preservation in the world’s oceans. These events were defined as Oceanic Anoxic Events and numbered 1, 2 and 3, respectively (text-fig. 1). OAE 1 was later recognized as being composed of at least four discrete, short-lived black shale events (less than a million years in duration), OAE 1a, 1b 1c and 1d (Arthur et al. 1990; Bralower et al. 1993; Erbacher et al. 1996; Erbacher and Thurow 1997). Leckie et al. (2002) further recognized OAE 1b (Aptian-Albian boundary event) as an interval with three discrete events.

Although short-lived, OAEs had significant impact on the global carbon cycle, climate and biota (Erbacher and Thurow 1997; Premoli Silva et al. 1999; Erbacher et al. 2001; Leckie et al. 2002). They occurred during one of the warmest periods in

Earth’s history and their development may have contributed to the long-term cooling trend from the Cretaceous hothouse to the Cenozoic icehouse (Wagner 2002; Hofmann et al. 2003). OAEs are also associated with the deposition of oil-prone marine black shales, which are important petroleum source rocks (Arthur and Schlanger 1979; Arthur et al. 1987; Hallam 1987; Schlanger et al. 1987).

Two major issues remain in debate regarding OAE origins: the mechanism producing OAEs and the relationship between sea-level fluctuations and OAEs. Knowledge in one topic may contribute to the understanding of the other. Different mechanisms have been suggested to explain the genesis of water column or bottom water anoxia/dysoxia, although there is a general agreement that deep waters of the world’s ocean were oxygen deficient or in a state of anoxia/dysoxia during some relatively short periods in the Cretaceous. Two major contrasting theories are the productivity model and the ocean stratification model (Pedersen and Calvert 1990; Hochuli et al. 1999; Wilson and Norris 2001). The productivity model indicates that the presence of excessive organic carbon associated with OAEs was the result of increased ocean surface productivity that might have resulted from a variety of factors, such as an increase in nutrient input from the continent, an accelerated hydrological cycle associated with a warmer climate, an increase in submarine volcanism and hydrothermal activity, or an increase in the area covered by shallow seas during marine transgressions (Pedersen and Calvert 1990; Erbacher and Thurow 1997; Hochuli et al. 1999; Jones and Jenkyns 2001; Wilson and Norris 2001; Leckie et al. 2002). Increased ocean surface productivity produced excessive organic matter that reached the ocean bottom; a high consumption of dissolved oxygen in the water column by organic decomposition, probably together with the flooding of shelf areas, significantly intensified and expanded the oxygen minimum zone (OMZ) horizontally and vertically, therefore, resulted in widespread carbonaceous black shale deposition (Schlanger and Jenkyns 1976; Arthur and Schlanger 1979;



TEXT-FIGURE 1

Cretaceous Oceanic Anoxic Events (OAEs) plotted against various relative sea-level curves, from Jenkyns (1980): (1) global transgression curve of Sliter (1976); (2) transgression curve for the USSR after Hallman (1977); (3) sea-level curve from the Western Interior Seaway of North America after Hancock and Kauffman (1979); and (4) northern Europe after Hancock and Kauffman (1979).

Arthur et al. 1987; Pedersen and Calvert 1990). On the contrary, the ocean stratification model suggests that the presence of excessive organic carbon was the result of enhanced preservation: that is, during OAEs, the world's ocean waters were stratified as a result of: (1) fresh water input from the continent resulting in a low salinity layer at the ocean surface, and/or (2) dense salty water input from shallow epicontinental seas resulting in a high salinity layer at the ocean bottom. Ocean stratification resulted in decreased bottom water formation, therefore, significantly reduced the oxygen content near the ocean bottom, and led to elevated carbon burial. This process was particularly important for isolated or restricted ocean basins (Thierstein and Berger 1978; Pratt 1984; Erbacher et al. 2001; Schröder-Adams et al. 2001).

OAEs and sea-level fluctuations

The relationship between OAEs and sea-level fluctuations is the second issue. It seems likely that a relationship existed between OAEs and Cretaceous marine transgressions (Schlanger and Jenkyns 1976; Arthur and Schlanger 1979; Jenkyns 1980; Hallam 1987; Arthur et al. 1990; Whatley et al. 2003), although it is unclear whether OAEs are correlated with high sea-level stands or with transgressive pulses (Jenkyns 1980). Schlanger and Jenkyns (1976) suggested that the Aptian-Albian OAE 1 and the Cenomanian-Turonian OAE 2 were coincident with two major transgressions on the Hays and Pitman (1973) sea-level curve. Jenkyns (1980) compared the timing of three Cretaceous OAEs with the global sea-level curve of Sliter (1976) and found that OAE 1 appears to correlate with a long-term transgressive pulse and OAE 2 is associated with a peak transgression (text-fig. 1). OAE 3 is actually in the falling

limb of the global sea-level curve of Sliter (1976), but it corresponds to a peak on the sea-level curves for the U.S. Western Interior Seaway and northern Europe published by Hancock and Kauffman (1979). Since its publication, the global coastal onlap chart of Haq et al. (1987) has been widely used to determine the relationship between OAEs and sea-level changes. Erbacher et al. (1996) concluded that OAE 1a, 1b, 1d and OAE 2 were related to transgression, while OAE 1c was related to regression (text-fig. 2). Erbacher et al. (1996) referred to these as P-OAEs (P for productivity) and D-OAEs (D for detritic), respectively. The idea that OAEs might be related to regressions is not consistent with most interpretations concluding that OAEs were related to marine transgressions.

In previous studies, the major method used to interpret the relationship between OAEs and sea-level changes was comparing the timing of OAEs with established sea-level curves. To date, no detailed sequence stratigraphic studies on OAE sediments have been published. Sequence stratigraphic methods can be used to interpret the relationship between OAEs and sea-level fluctuations, because relative changes in sea level can be interpreted by recognizing depositional sequences from regional seismic data and well-log cross sections using the sequence stratigraphic model (Vail et al. 1977a; Haq et al. 1987; Posamentier et al. 1988; Posamentier and Vail 1988). The objectives of this study are, 1) to identify sediments that were deposited during the Late Cretaceous Oceanic Anoxic Events (OAE 2 and OAE 3) in the northeastern Gulf of Mexico area; 2) to document the distribution and facies patterns of these deposits; and 3) to determine the relationship between OAEs and sea-level fluctuations using an integrated sequence stratigraphic approach based on seismic data, well-log data, and well cores.

Late Cretaceous OAE 2 and OAE 3

OAE 2

OAE 2, or the Bonarelli Event, has been recognized worldwide in outcrops and in DSDP/ODP cores (Schlanger et al. 1987; Arthur et al. 1987; Arthur et al. 1988). Sediments associated with OAE 2, such as black shales, have been reported in North Africa (Lüning et al. 2004; Tsikos et al. 2004), Western Interior Seaway (Arthur et al. 1987; Schlanger et al. 1987; Kauffman and Caldwell 1993; Pratt et al. 1993; Schröder-Adams et al. 2001; Tsikos et al. 2004), Italy (Arthur and Premoli Silva 1982; Premoli Silva et al. 1999; Tsikos et al. 2004; Scopelliti et al. 2004), Southern Tibet, China (Wang et al. 2001; Wan et al. 2003), the Pacific Ocean (Moberly and Larson 1975; Vallier et al. 1979), and the Atlantic Ocean (Berger and von Rad 1972; Summerhayes 1981; Erbacher et al. 1996; Sissinghe Damsté and Köster 1998; Huber et al. 1999; Norris et al. 2002; Nzoussi-Mbassani et al. 2003).

The age of OAE 2 has been dated as latest Cenomanian to earliest Turonian (C/T event). This event extended from the upper part of the *Rotalipora cushmani* foraminiferal zone to the *Whiteinella archaeocretacea* foraminiferal zone (Leckie 1985; Schlanger et al. 1987; Hart 1993; Coccioni and Galeotti 2003; Tsikos et al. 2004; Keller and Pardo 2004). With respect to the Cretaceous calcareous nannofossil zonation, this event occurred near the boundary of the CC10 Zone (*Microrhabdulus decoratus* Zone) and CC11 Zone (*Quadrum gartneri* Zone) of Sissingh (1977) as modified by Perch-Nielsen (1985) (Bralower 1988; Coccioni and Galeotti 2003) (text-fig. 3). OAE 2 is associated with a positive carbon isotope excursion near the Ceno-

manian-Turonian boundary (Scholle and Arthur 1980; Arthur et al. 1988; Jenkyns et al. 1994; Voigt 2000; Tsikos et al. 2004).

OAE 3

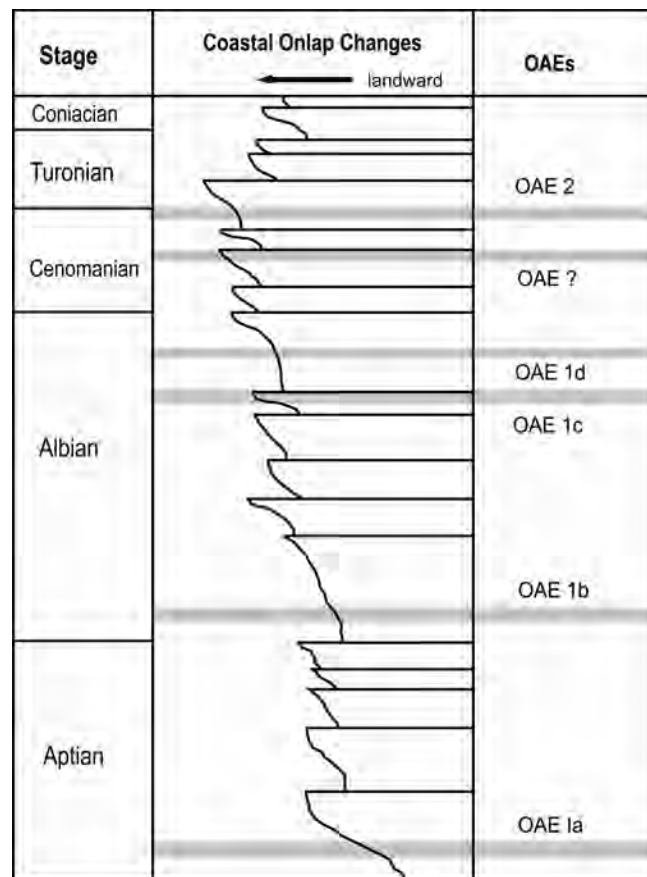
OAE 3 is the last reported Cretaceous Oceanic Anoxic Event. However, OAE 3 is not nearly as well studied as OAE 2 (Wagner 2002; Hofmann et al. 2003). Black shale sediments associated with OAE 3 were more restricted to areas associated with the Atlantic Ocean, such as the east tropical Atlantic Ocean, offshore Ghana and the Ivory Coast (Holbourn and Kuhnt 1998; Wagner 2002; Hofmann et al. 2003), Venezuela (Erlich et al. 1999; Rey et al. 2004), the Brazilian shelf and continental marginal basins (Mello et al. 1989), the Western Interior Seaway of the North America (Sterzinar and Leckie 2004) and the Tethyan regions (Jenkyns 1980). In addition, black shales associated with OAE 3 tended to be more restricted to shallow water settings and epicontinental seas (Arthur et al. 1990).

The age of OAE 3 sediments has been dated as late Coniacian to early Santonian (text-fig. 3). Nannofossil analysis by Hofmann et al. (2003) assigned OAE 3 black shales at ODP Site 959 (Leg 159B) to nannofossil zone CC15 (*Reinhardtites anthophorus* Zone). This event is associated with a moderate positive carbon isotope excursion of late Coniacian to early Santonian age for the English Chalk and Italian Scaglia strata indicating widespread organic carbon burial during this time (Jenkyns et al. 1994).

GEOLOGIC SETTING AND UPPER CRETACEOUS STRATIGRAPHY

The study area is located in the northeastern Gulf of Mexico including the eastern Gulf Coastal Plain of southwestern Alabama and offshore Alabama areas (text-fig. 4). Major structures in the study area include the easternmost extension of the Mississippi Interior Salt Basin and peripheral fault systems. Salt tectonics was active during the Late Cretaceous (Current 1948; Copeland et al. 1976; Pashin et al. 2000); salt movement had a significant impact on the sediment distribution patterns on the Late Cretaceous continental shelf. Upper Cretaceous (mid-Cenomanian to Maastrichtian) strata in the northeastern Gulf of Mexico comprise a thick section of siliciclastic and carbonate sediments of about 3000 feet in total thickness. These strata were deposited on a broad shelf that was frequently flooded by a shallow-water sea (Salvador 1991; Sohl et al. 1991; Puckett 1991). Although sea level in the Late Cretaceous was generally high, with this period being a first-order transgression in Earth history (Vail et al. 1977b; Haq et al. 1987), large scale fluctuations in sea level occurred during this period (Salvador 1991; Miller et al. 2003). Sea-level changes shifted sedimentary facies on the shelf; Upper Cretaceous strata in the study area were strongly overprinted by sea-level changes.

Upper Cretaceous strata in this area are exposed in a broad belt extending from Tennessee through northeastern Mississippi and western and central Alabama into central Georgia and occur throughout the subsurface of the coastal plain provinces in these states. These strata are divided into several groups and formations (text-fig. 5). The Tuscaloosa Group unconformably overlies strata of Paleozoic to Early Cretaceous age. In the subsurface, the contact between the Tuscaloosa Group and the Washita Group is marked by a prominent unconformity referred to as the mid-Cretaceous unconformity/sequence boundary. The Tuscaloosa Group is divided into three formations in the subsurface, the Lower Tuscaloosa Formation, the Marine



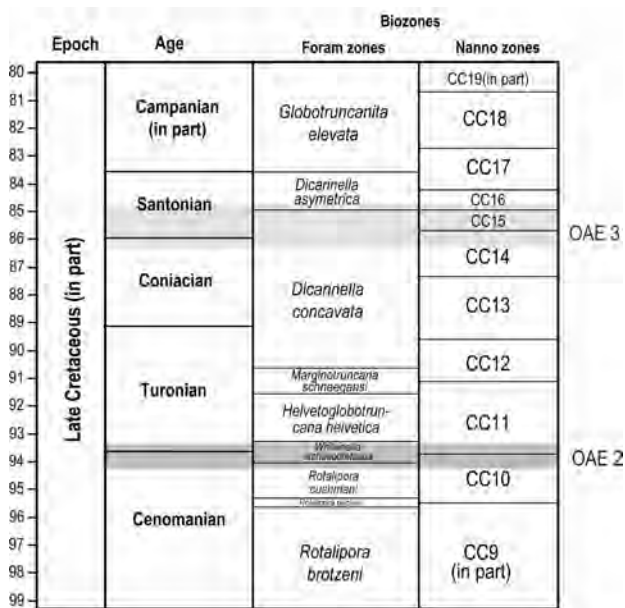
TEXT-FIGURE 2

Cretaceous Oceanic Anoxic Events and global coastal onlap curve of Haq et al. (1987), from Erbacher et al. (1996). Four individual OAE events were identified during the Aptian and Albian. Erbacher et al. (1996) reported that OAEs 1a, 1b, 1d, and 2 occurred during transgressions and OAE 1c occurred during a regression.

Tuscaloosa Formation and the Upper Tuscaloosa Formation based on well log responses (Winter 1954; Mancini et al. 1987). The Eutaw Formation overlies the Tuscaloosa Group with the contact representing another major unconformity. The Selma Group conformably overlies the Eutaw Formation. In the outcrop area in western Alabama, the Selma Group consists of about 900 feet of mixed siliciclastic and carbonate chalk/marl sediments. The Selma Group is divided into several formations from bottom to top: the Mooreville Chalk (including the Arcola Limestone Member), the Demopolis Chalk (including the Bluffport Marl Member), the Ripley Formation, and the Prairie Bluff Chalk (text-fig. 5).

The Marine Tuscaloosa Formation

The Marine Tuscaloosa Formation consists of dark gray to black, organic-rich, laminated shale deposited during the late Cenomanian to early Turonian in the northeastern Gulf of Mexico and coincident with the global OAE 2. The Marine Tuscaloosa Formation has been studied in the South Carlton field, Clarke and Baldwin counties, and in the Pollard field, Escambia County, Alabama (Mancini et al. 1980; Mancini and Payton 1981; Mancini et al. 1987; Claypool and Mancini 1989). The Marine Tuscaloosa Formation in the Wall et al. # 3-9 well (well 2182 in Figure 4) in the South Carlton field, Clarke



TEXT-FIGURE 3

Late Cretaceous biostratigraphic framework modified from Hardenbol et al. (1998). Cretaceous nannoplankton zonation follows Sissingh (1977) zonal scheme, as modified by Perch-Nielsen (1985). Cretaceous foraminiferal zonation follows that of Caron (1985). The time scale of Gradstein et al. (1995) is used for Cretaceous polarity boundaries.

County, Alabama is about 220 feet in thickness (Figure 6a). The lower 10.5 feet of the Marine Tuscaloosa Formation was cored. This interval consists of laminated, dark gray, silty, micaceous, fossiliferous claystone (Mancini et al. 1980; Mancini and Payton 1981; Mancini et al. 1987). Macroinvertebrates found in this core include ammonites, inoceramids and other bivalves that indicate an open marine, middle shelf environment. The organic carbon content of the black shale is about 1.2%-2.8%, and the dominant kerogen type is typically amorphous (algal) (Table 1). The lower part of the Marine Tuscaloosa was assigned to the upper Cenomanian foraminiferal *R. cushmani* zone by Mancini et al. (1980) (text-figures 3 and 6a).

The Eutaw Formation

The Eutaw Formation and its downdip shale facies were deposited in the northeastern Gulf of Mexico during the late Coniacian to early Santonian and coincident with OAE 3 (text-figure 5). The Eutaw Formation crops out from northeastern Mississippi through central Alabama to western Georgia. In outcrop, the Eutaw Formation is divided into two members: the upper part is a massive, glauconitic, fossiliferous sand unit called the Tombigbee Sand Member; the lower part is referred to as the unnamed member of the Eutaw Formation and consists of light-greenish-gray, fine- to medium-grained, well-sorted, micaceous, cross-bedded sand that is fossiliferous and glauconitic in part and contains beds of greenish-gray, micaceous, silty clay and medium-dark-gray carbonaceous clay (Raymond et al. 1988). The Eutaw Formation has been interpreted as having been deposited in a nearshore environment that consisted of isolated, widely dispersed barrier bars and shoals with associated back-barrier and tidal inlet facies (Frazier and Taylor 1980; Cook 1993). And there is a general agreement that Eutaw sediments accumulated during a marine transgression (Conant 1967; Pashin et al. 2000; Mancini et al. 1996; Liu

2004, 2005). The age of the Tombigbee Sand Member has been dated as late Santonian to early Campanian (Mancini et al. 1996). The unnamed member of the Eutaw Formation contains few foraminifera or nannoplankton. Most age dating for the basal Eutaw Formation (sometimes called the McShan Formation) is based on palynomorph studies. Smith and Mancini (1983) and Christopher et al. (1999) assigned the McShan Formation to the *Complexiopollis exigua-Santalacites minor* Assemblage Zone (Pollen zone VA; middle and late Coniacian to early Santonian); and Christopher et al. (1999) correlated this zone with CC14 (*Micula decussata* Zone; late Coniacian) and the lower part of CC15 (*Reinhardtites anthophorus* Zone; early Santonian) of the calcareous nannofossil zonation of Sissingh (1977) as modified by Perch-Nielsen (1985).

In the subsurface, the facies of the Eutaw Formation changes significantly in a basinward direction. The thickness of the glauconitic sandstone beds, typical of the Eutaw Formation in the outcrop, decreases in a basinward direction. The upper beds of the Eutaw Formation grade into chalk and marl beds assigned to the Selma Group; the lower beds of the Eutaw Formation grade into carbonaceous shale beds in the Mississippi Interior Salt Basin and south of the basin (Liu 2005). These shale beds are referred to as the “downdip Eutaw shale”.

DATA SET

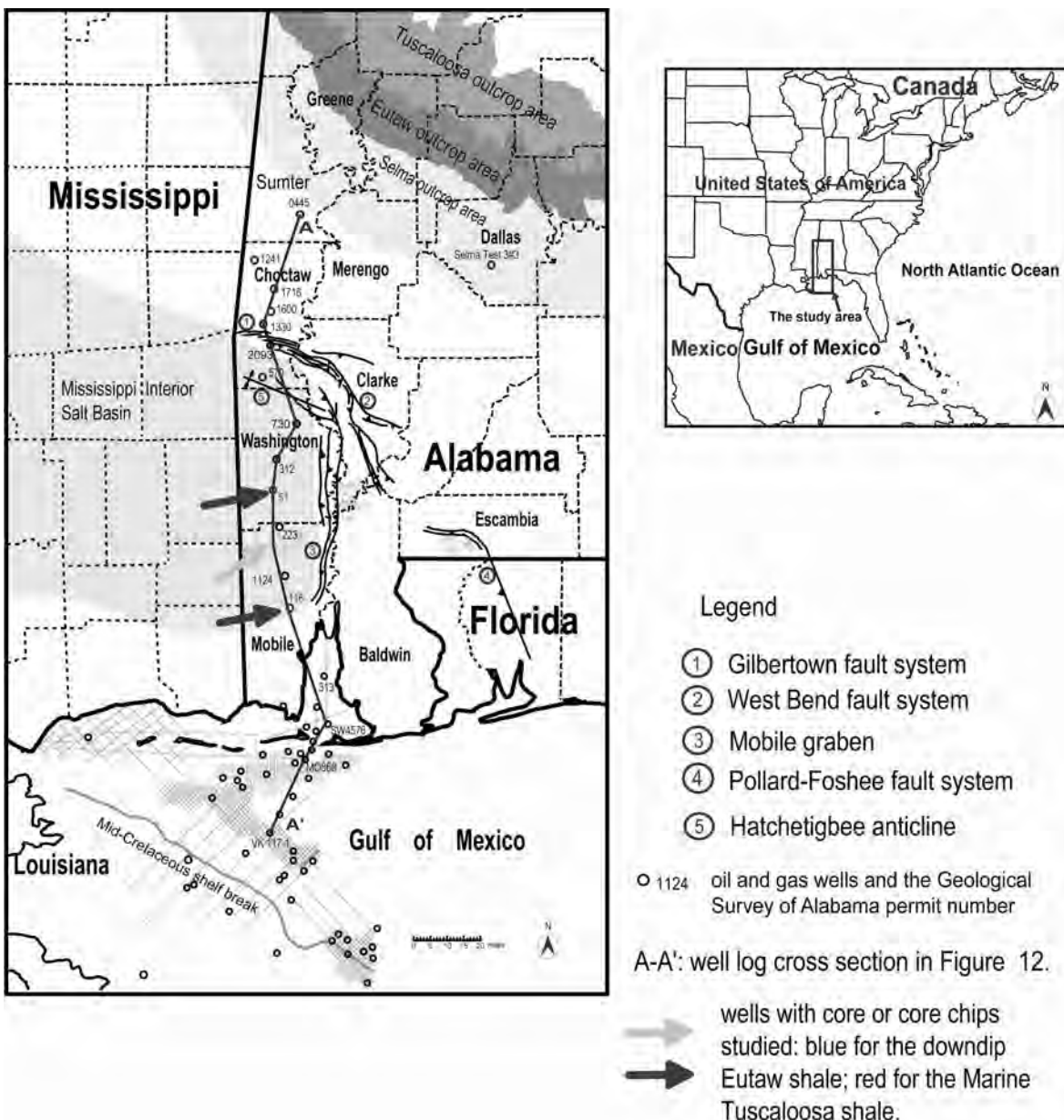
- Core and core chips: Core and core chips from three wells (well 51, well 116, and well 163) from Washington and Mobile counties, Alabama were studied.
- Well logs: Wireline log data from oil and gas wells are available across the study area. In most cases, spontaneous potential (SP) logs were used for the purpose of regional correlation and defining lithostratigraphic units in the subsurface. Where sonic logs were available, they were used to construct synthetic seismograms to calibrate well-log data with seismic data.
- Seismic data: 202 high quality, two dimensional, multi-channel seismic sections were used in this study (approximately 3,500 kilometers in total length). All data were acquired by Western Geophysical Company during the period from 1981 to 1992. These data cover mainly five areas offshore in the north-eastern Gulf of Mexico including (text-fig. 7): Mobile Bay area (3 lines, 1985), federal waters offshore Mobile (Mobile area, 49 lines, 1981), Mississippi Sound (33 lines, 1984), Viosca Knoll area (84 lines, 1992), and the east addition of the Main Pass area (33 lines, 1992). Surveys in the Mobile area were acquired using an Aquapulse® source with 6 guns and the LRS-888 recording system. Acquisition parameters of surveys in other areas are not available to the author because of their proprietary nature.

METHODOLOGY

The sequence stratigraphic model of Vail and Mitchum (1977), Vail et al. (1977a, 1977b), Posamentier et al. (1988), Posamentier and Vail (1988) was used in this study. An integrated approach that incorporates seismic and well-log data, and core chips and cores, was used to perform sequence stratigraphic analysis for the recognition of depositional sequences to interpret sea-level fluctuations and their relationship to OAEs.

Core and core chip studies:

Cores and core chips from intervals that were possibly deposited during OAE 2 and 3 were examined and described; depositional environments of these strata were interpreted. Samples were also taken for nannoplankton biostratigraphic analyses to



TEXT-FIGURE 4

The study area and geologic setting. Seismic lines are shown as gray lines in the offshore Alabama and Mississippi area.

determine their relative ages. A total of ten samples from wells 51, 116, 163 were analyzed by Charles C. Smith at the Geological Survey of Alabama. Total organic carbon analysis and visual kerogen isolation and assessment for thirteen samples from cored intervals from wells 51, 116 and 163 were conducted by Geochemical Laboratories Inc. in Houston.

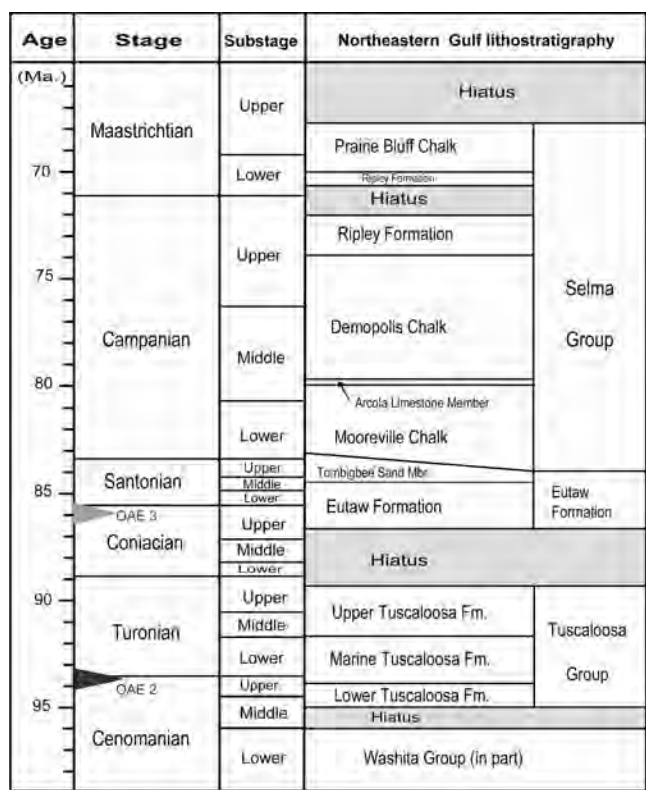
Seismic interpretation and well log-seismic calibration:

Depositional sequences were identified from seismic sections following the methodology and procedure established by Mitchum et al. (1977), Mitchum and Vail (1977), and Vail (1987). Important seismic reflectors with chronostratigraphic significance, such as maximum flooding surfaces and sequence boundaries, were identified and traced throughout the seismic coverage area. Sequence boundaries and maximum flooding surfaces were recognized by identifying seismic reflector termina-

nation patterns: sequence boundary as an onlap surface, and maximum flooding surface as a downlap surface (text-fig. 8). Seismic data can provide a sequence stratigraphic framework in which facies changes, depositional environments, and sea-level fluctuations can be interpreted. However, OAEs could not be identified on seismic data because there is no apparent relationship between OAEs and seismic reflection configurations. Check-shot surveys and synthetic seismograms were used to calibrate well-log data with seismic data so that sequence boundaries and maximum flooding surfaces recognized from seismic data could be projected onto well logs.

Well-log cross section construction:

A cross section for the Upper Cretaceous strata based on SP log data was constructed from the area near the mid-Cretaceous shelf break northward to the southern limit of the outcrop belt in



TEXT-FIGURE 5

Upper Cretaceous stratigraphy in the northeastern Gulf of Mexico area, after Mancini and Puckett (2002). Four unconformities were recognized by previous outcrop and subsurface studies. The Marine Tuscaloosa Formation and the Eutaw Formation were deposited during the periods when OAEs 2 and 3 were reported to occur.

west central Alabama (text-fig. 4). Sequence boundaries and maximum flooding surfaces interpreted from seismic data in the offshore Alabama area were traced across the Late Cretaceous continental shelf. OAE carbonaceous shales, including the Marine Tuscaloosa shale and the downdip Eutaw shale, identified from cores and core chips were also correlated using this well-log cross section.

Integrated analysis:

The sequence stratigraphic positions of OAE sediments were determined using the established sequence stratigraphic framework. Relative changes in sea level were determined from sedimentation patterns and facies stacking patterns of these sediments as observed from seismic data and well-log data. The relationship between sea-level fluctuations and the deposition of OAE 2 and 3 black shales was then interpreted.

OBSERVATIONS AND INTERPRETATIONS

Core and core chip studies

The Marine Tuscaloosa shale

The Marine Tuscaloosa Formation in the Board of School Commissioners #1 well (well 163 in text-fig. 4) in northern Mobile County is about 150 feet in thickness; the lower 20 feet (7081-7101 feet) was cored (text-fig. 6b). The Marine Tuscaloosa Formation consists of dark gray to black, laminated,

fossiliferous shale. Organic carbon content of this black shale was measured to be about 6.0%-6.24%; and the dominant kerogen type is herbaceous (spore/pollen) (Table 1). Nannoplankton analysis indicates that this shale can be assigned to the upper Cenomanian calcareous nannofossil zone CC10 (*Micro-rhabdulus decoratus* Zone). The presence of nannoplankton indicates that this shale was deposited in an open marine environment. The Marine Tuscaloosa shale, a black, organic-rich, laminated shale unit, is, therefore, identified as being the sediment associated with the global OAE 2 in the northeastern Gulf of Mexico area.

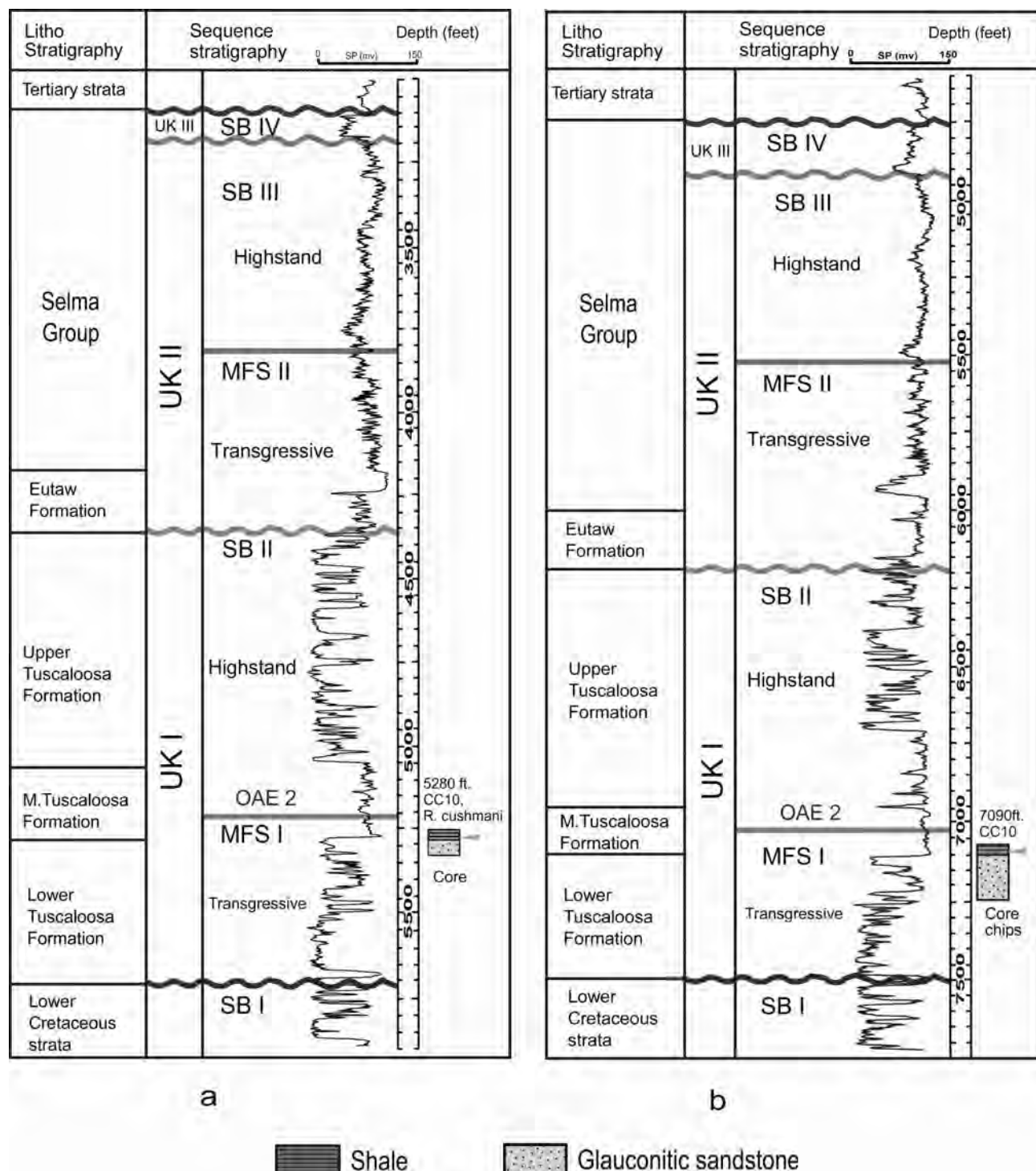
The downdip Eutaw shale

In the Mississippi Interior Salt Basin, the downdip Eutaw Formation is composed of three units: an upper glauconitic sand unit, a middle black carbonaceous shale unit, and a lower glauconitic sand unit (text-fig. 9a). The middle shale unit is about 150 feet in thickness in well 51 near the center of the easternmost part of the Mississippi Interior Salt Basin (text-fig. 9a). In the southern part of the Mississippi Interior Salt Basin, the upper and lower glauconitic sandstone units pinch out and the entire Eutaw Formation consists of a shale unit generally less than 90 feet in thickness (text-fig. 9b). These two downdip Eutaw shale units are OAE 3 sediments in the northeastern Gulf of Mexico area. Two wells (wells 51 and 116 in text-fig. 4) have core chips recovered from these two shale units.

The W.E. Odum #1 well (well 51 in text-fig. 4), Washington County, is located in the center of the easternmost extension of the Mississippi Interior Salt Basin. Core samples were recovered from this well at a depth from 6238 to 6524 feet. This core includes the lower 192 feet of the Selma Group and 94 feet of the upper part of the Eutaw Formation (text-fig. 9a). The lower Selma Group consists of light gray, indurated marly chalk. Nannoplankton analyses assigned this chalk to the CC16 Zone (*Lucianorhabdus cayeuxii* Zone) of mid-Santonian age (text-figs. 3 and 9a). The upper 50 feet of the Eutaw Formation is a glauconitic sand unit also dated as Santonian (CC16). The upper 44 feet of the middle shale unit was cored, and consists of black and dark gray laminated shale with abundant plant debris. Most of the recovered shale beds are noncalcareous, which, in combination with the abundance of plant debris, suggests a restricted marine (lagoonal) environment. Certain layers of the shale contain calcareous nannoplankton; a sample at the depth of 6502 feet was assigned to the CC15 zone (*Reinhardtites anthophorus* Zone). Although the lower part of this middle shale was not cored, it is most likely late Coniacian to early Santonian in age. The organic carbon content of this interval of the downdip Eutaw shale from core chips from well 51 is about 1.03-1.58%, and the dominant kerogen type is herbaceous and woody structured (Table 1).

Based on these data, the Eutaw Formation in the Mississippi Interior Salt Basin is interpreted to have been deposited in a transgressive barrier-lagoonal system (text-fig. 9a). The lower sandstone is interpreted to represent shoreface deposits; the middle shale bed to represent lagoonal sediments; and the upper sandstone to be reworked barrier island and inner neritic sediments. These strata are further overlain by the deeper water, middle to outer neritic chalk sediment of the Selma Group.

The Eutaw Formation consists of a shale unit of less than 90 feet in the southern part of the Mississippi Interior Salt Basin. Further southward toward the mid-Cretaceous shelf break, this shale unit pinches out in the outer shelf area. Core chips from

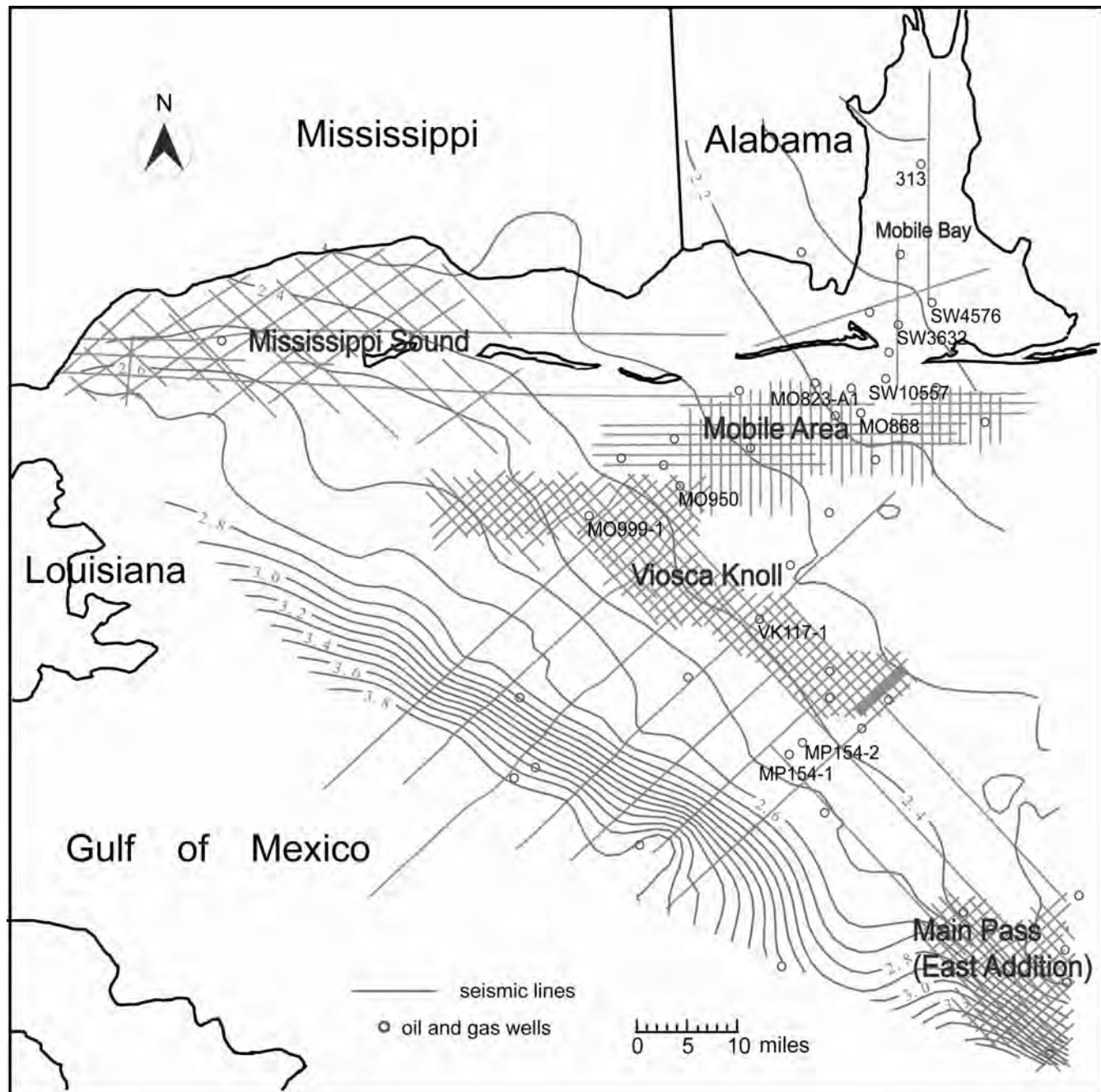


TEXT-FIGURE 6

Well log patterns from (a) well 2182, Clarke County, and (b) well 163, Washington County, Alabama, showing sequence stratigraphic interpretations of the Upper Cretaceous strata from seismic data. OAE 2 is associated with the maximum flooding surface of the UK I sequence. MFS = maximum flooding surface, SB = sequence boundary.

Mike Vergos #1 well (well 116 in text-fig. 4) in Mobile County, Alabama, indicate that this shale unit consists of dark gray and black, laminated, indurated calcareous shale (text-fig. 9b). Fish scales are abundant and exceptionally well preserved in this shale, which suggests that it most likely accumulated under ox-

ygen-deficient bottom water conditions. Calcareous nannofossil analyses indicate a mid-Santonian age (CC16 zone, *Lucianorhabdus cayeuxii* Zone) for this unit. This shale unit is interpreted as having been deposited in an inner to middle neritic, open marine environment probably after the barrier island-la-



TEXT-FIGURE 7

Seismic grid and well locations in the offshore area. The contour lines show the structure contour of the mid-Cretaceous Sequence Boundary, expressed in two-way travel time (seconds). Seismic lines are shown as gray lines cutting across contours. Circle symbols indicate oil and gas wells.

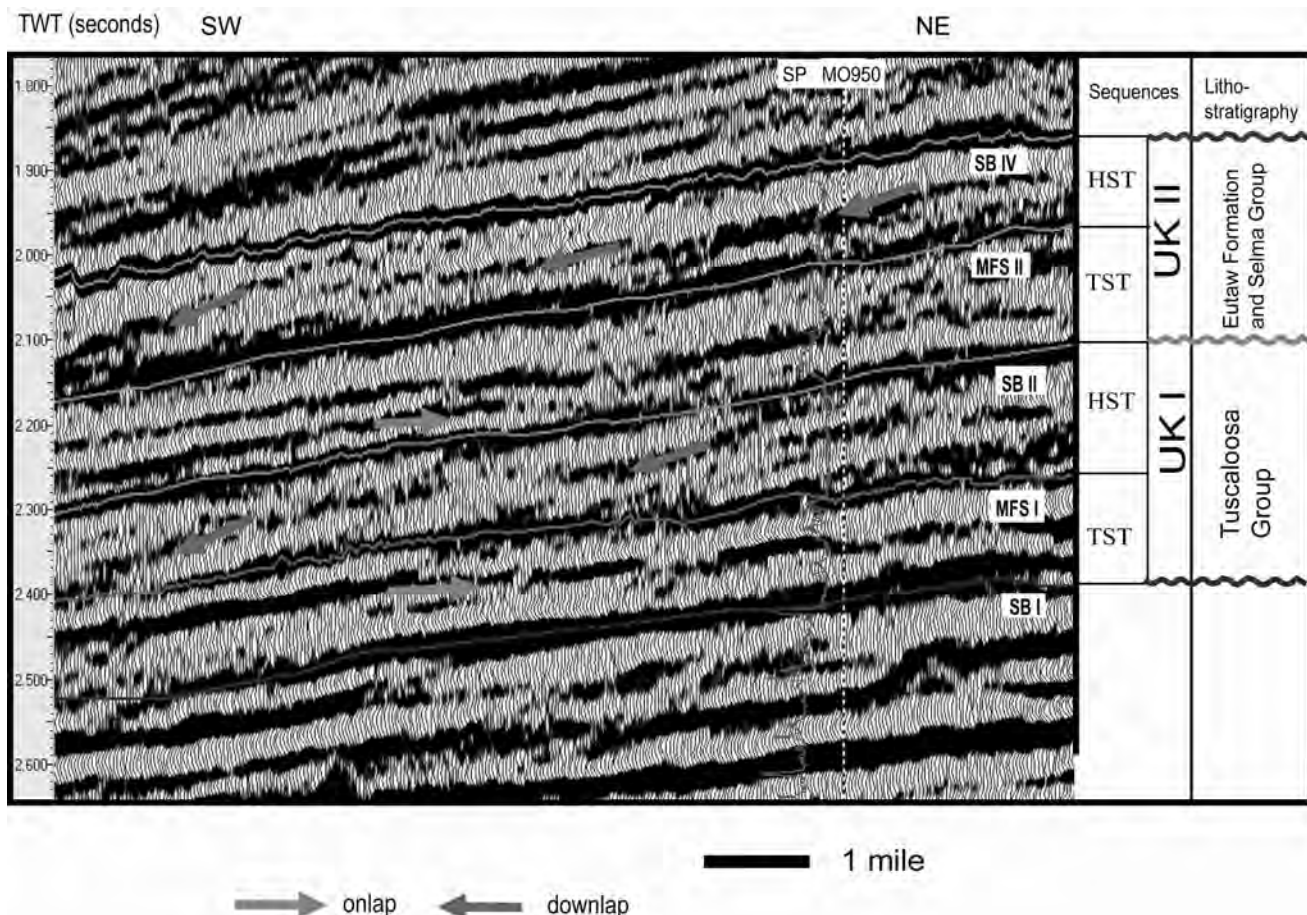
goonal system migrated to a more landward position (text-fig. 9b). Organic carbon analyses indicate that this downdip interval of open marine Eutaw shale has a total organic carbon content of about 0.93-0.96% with a dominant kerogen type of relic amorphous-sapropel (Table 1). Its relatively low organic content suggests that this shale unit was probably deposited during the final stage of OAE 3.

Two black shales, the Marine Tuscaloosa shale and the downdip Eutaw shale in the northeastern Gulf of Mexico area, therefore, are interpreted as OAE 2 and 3 sediments, respec-

tively. In order to investigate the relationship between OAEs and sea-level fluctuations, these two black shales are placed into a sequence stratigraphic framework based on seismic interpretations and well log correlations.

Seismic stratigraphic analysis

Six prominent seismic reflectors (four sequence boundaries and two maximum flooding surfaces) were identified from seismic sections in the study area. They were numbered from bottom to top (text-fig. 10). These reflectors are strong, continuous, and traceable on most of the seismic sections in the offshore Ala-



TEXT-FIGURE 8

Seismic dip section in the Viosca Knoll area, after Liu (2004). Sequence boundaries and maximum flooding surfaces are recognized by identifying seismic reflector termination patterns: sequence boundary as onlap surface and maximum flooding surface as downlap surface. SB III is not recognized in this section because the UK III sequence is very thin here. SB = sequence boundary, MFS = maximum flooding surface, TST = transgressive systems tract, HST = highstand systems tract, TWT = two-way travel time.

bama and Mississippi area. Three third-order sequences (UK I, UK II and UK III) are, therefore, delineated by these four sequence boundaries. The uppermost sequence, UK III, is thin in the Mobile Bay area but becomes thicker toward the shelf break where it could be resolved on seismic sections. Maximum flooding surfaces were recognized in the UK I and UK II sequences, and they separate the transgressive systems tract from the highstand systems tract (Liu 2004).

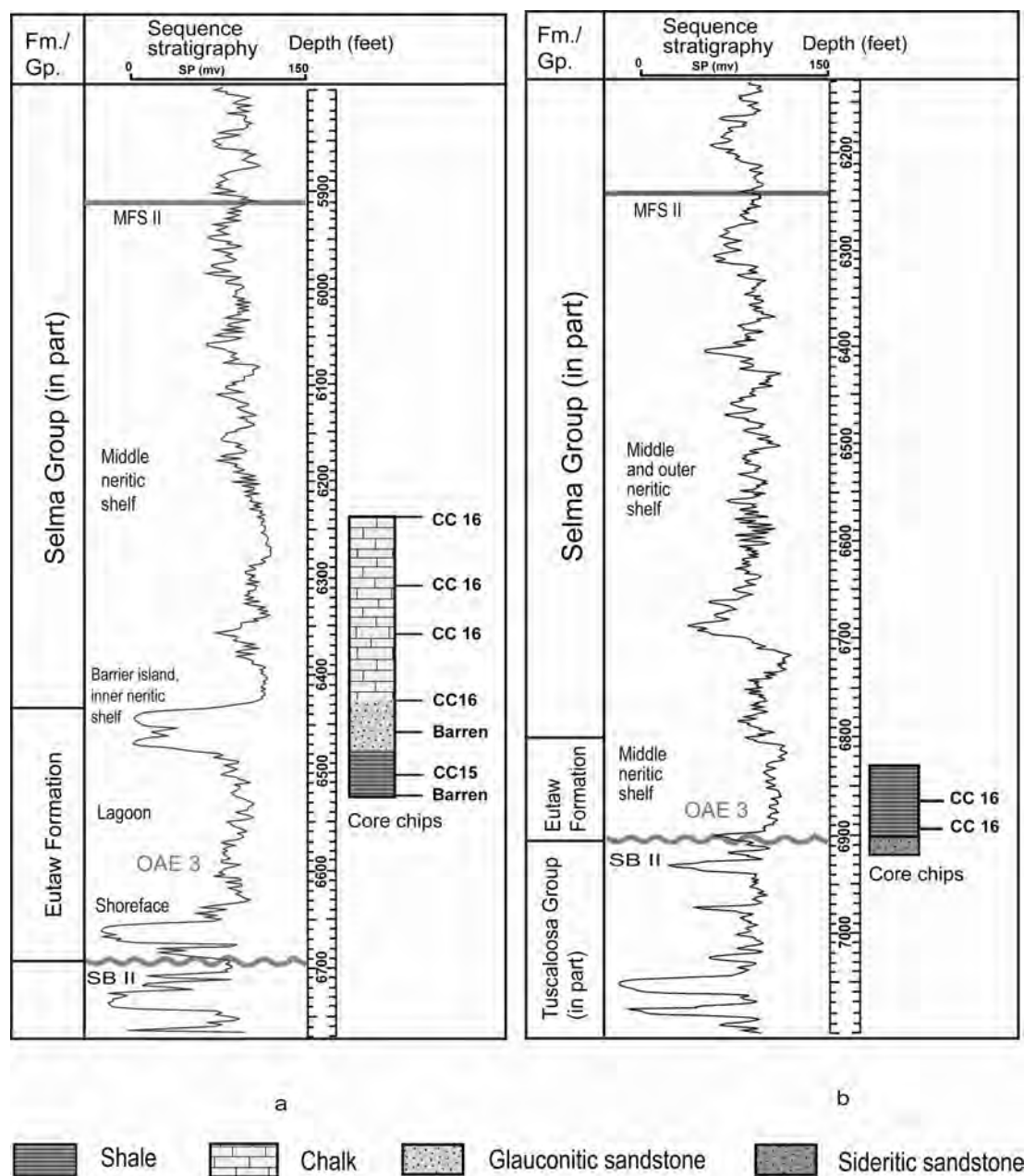
After calibrating well-log data with seismic data using synthetic seismograms (text-fig. 11), sequence boundaries and maximum flooding surfaces that were identified on seismic sections were projected onto well logs and then correlated across the Late Cretaceous continental shelf area (text-figs. 6, 9 and 12). These four sequence boundaries were found to correspond to the four major unconformities identified by previous outcrop and subsurface studies (text-fig. 11). Sequence Boundary I corresponds to the widespread mid-Cretaceous unconformity/sequence boundary. Sequence Boundary II corresponds to the unconformity between the Tuscaloosa Group and the Eutaw Formation. Sequence Boundary III corresponds to the intraformational unconformity within the Ripley Formation in western Alabama and to the unconformity between the Ripley Formation and the Owl Creek Formation in northern Mississippi. Sequence Boundary IV corresponds to the unconformity between the Selma Group and the Midway Group (Tertiary).

Well-log cross section construction

A cross section was constructed using SP log signatures. This cross section (text-fig. 12) includes wells from the outer shelf area of offshore Alabama northward to wells in west central Alabama near the southern limit of the outcrop belt (see text-fig. 4 for well locations). The top of the Selma Group is used as the mapping datum. The prominent depression, or low, encountered in well 51 represents the Mississippi Interior Salt Basin area.

The four sequence boundaries and two maximum flooding surfaces recognized from seismic sections were located on this cross section and correlated into the updip area. The Upper Cretaceous strata are divided into three depositional sequences, UK I, UK II, and UK III by these four sequence boundaries. The uppermost sequence, UK III, is very thin but becomes thicker in the outer shelf area. Two maximum flooding surfaces, MFS I and MFS II, divide the UK I and UK II sequences into a transgressive systems tract and a highstand systems tract, respectively.

Five major shale beds can be recognized on this cross section (text-fig. 12). In southwestern Alabama, the Marine Tuscaloosa Formation is a thick shale unit (Shale unit 1) lying between the predominantly sand units of the Upper Tuscaloosa and Lower Tuscaloosa formations. The Upper Tuscaloosa Formation



TEXT-FIGURE 9

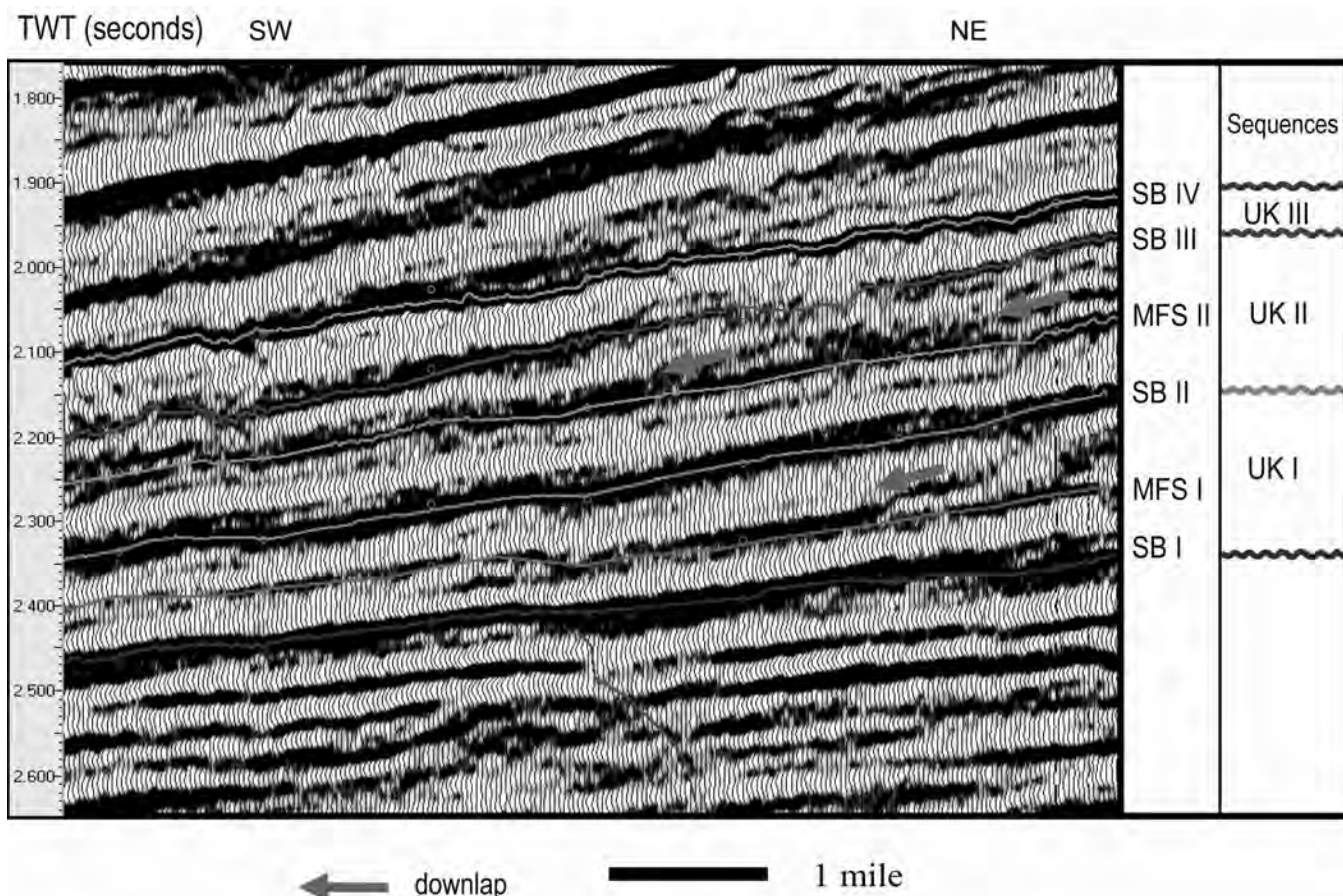
Well log patterns from (a) well 51, Washington County and (b) well 116, Mobile County, Alabama, showing sequence stratigraphic interpretations from seismic data. OAE 3 is associated with the early transgressive systems tract of the UK II sequence. MFS = maximum flooding surface, SB = sequence boundary.

grades into the second thick shale unit (Shale unit 2) in a basinward direction. The Marine Tuscaloosa Formation, which was deposited during the late Cenomanian to early Turonian and correlative with other OAE 2 strata, is associated with the maximum flooding surface/condensed section of the UK I sequence (text-figs. 6 and 12).

In the Mississippi Interior Salt Basin, the downdip Eutaw shale is composed of two shale units, Shale units 3 and 4. These two shale units grade into the glauconitic sandstone beds of the lower Eutaw Formation in the updip area (text-fig. 12). The downdip Eutaw shale, which was deposited during the late

Coniacian to early Santonian and correlative with other OAE 3 strata, is part of an early transgressive systems tract (text-figs. 9 and 12). During the early transgression, large land areas were inundated. In addition, subsidence in the salt basin during the transgression provided additional accommodation space for the deposition of the downdip Eutaw shale and accumulation of organic carbon.

The fifth shale bed (Shale unit 5) corresponds to the maximum flooding surface/condensed section of the UK II sequence (text-fig. 12). This shale unit is about 300 feet thick in the outer shelf area (well VK 117-1, text-fig. 12), but it pinches out in the



TEXT-FIGURE 10

Seismic dip section in the Viosca Knoll area, after Liu (2004). Four sequence boundaries and two maximum flooding surfaces were identified in the Upper Cretaceous strata in the northeastern Gulf of Mexico area. Three sequences are delineated by these four sequence boundaries; the lower two sequences are further divided by maximum flooding surfaces into a transgressive systems tract and a highstand systems tract. SB = sequence boundary, MFS = maximum flooding surface, TWT = two-way travel time.

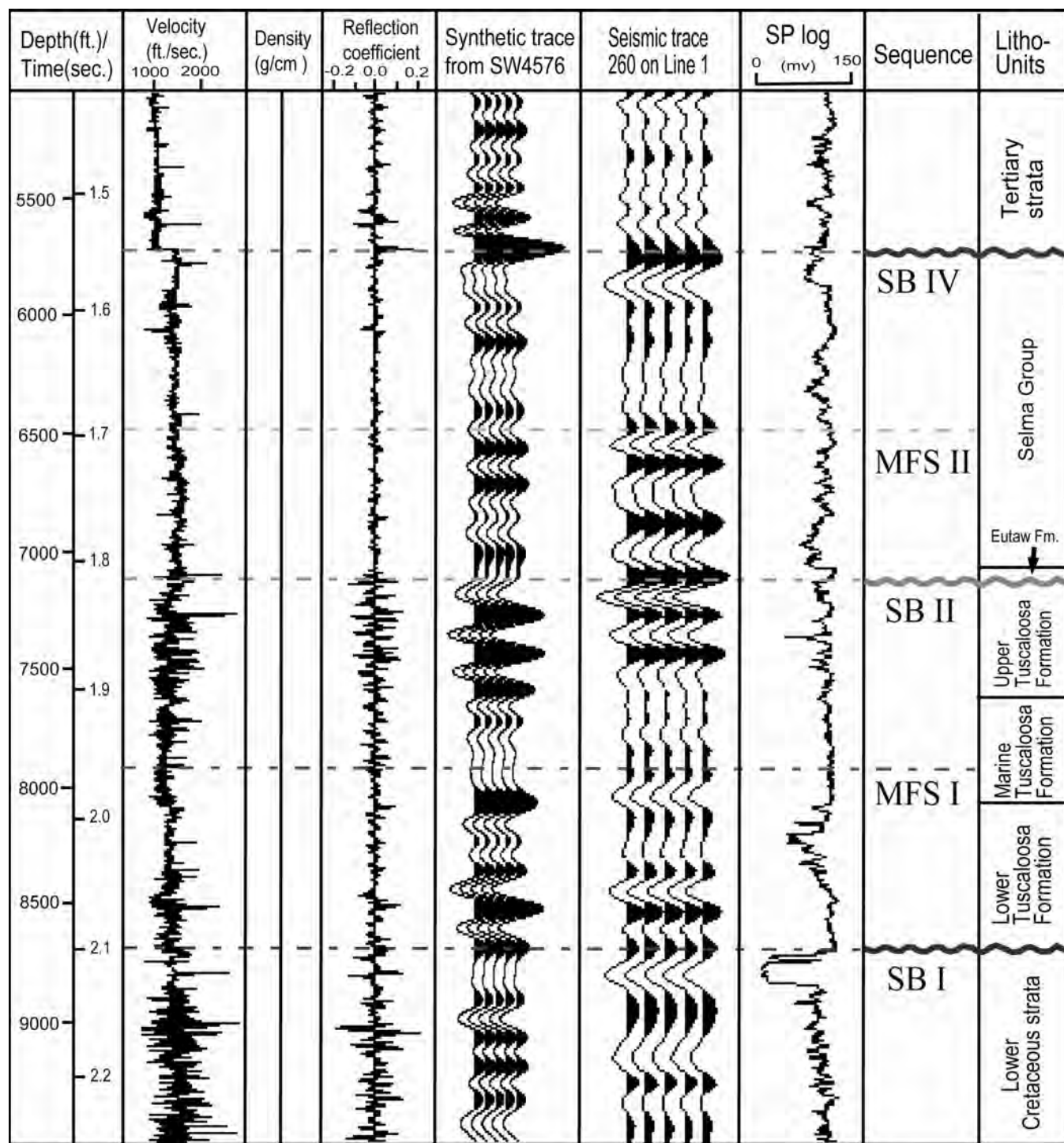
Mobile Bay area (well SW4576, text-fig. 12). Liu (2004) identified this shale bed from seismic data and well-log data; however, no core or core chips were available for further study. Although this shale bed pinches out, the log signature associated with the maximum flooding surface can be traced on the well-log cross section across the Late Cretaceous continental shelf to areas near the southern limit of the outcrop belt. It is located in the Mooreville Chalk, approximately 260 feet below the Arcola Limestone Member in well 445 in Sumter County in west central Alabama (text-fig. 12). The age of the maximum flooding surface associated with this shale unit has been reported to be the latest Santonian to earliest Campanian (Liu, 2005). This shale unit is the counterpart of the Marine Tuscaloosa Formation in the UK II sequence. However, no OAE occurred at this time, perhaps due to low sediment and nutrient supply during maximum flooding.

Late Cretaceous sea level and OAE 2 and 3

Based on this study, fluctuations in sea level during the Late Cretaceous and the depositional history of Upper Cretaceous strata in the northeastern Gulf of Mexico can be interpreted. This sea-level history interpretation is in general agreement with the interpretations made from biostratigraphic and

sedimentological studies of the outcrop by Mancini et al. (1996), Puckett and Mancini (2000), and Mancini and Puckett (2002).

Late Cretaceous sedimentation in the northeastern Gulf of Mexico area began as sea level rose after the mid-Cenomanian sea-level fall that formed the prominent mid-Cretaceous unconformity/sequence boundary. Sediments of the transgressive systems tract of the Lower Tuscaloosa Formation were deposited on the shelf in deltaic and other marginal marine environments (text-fig. 13a). When the shoreline migrated updip to its maximum extent during the late Cenomanian to early Turonian, an extensive open epicontinental sea formed in the northeastern Gulf of Mexico. Black shale of the Marine Tuscaloosa Formation (Shale unit 1) was deposited across the continental shelf area, corresponding to the occurrence of the global OAE 2 (text-fig. 13b). When sea-level rise slowed or even ceased in the middle Turonian, the Upper Tuscaloosa sand advanced seaward as prograding delta and shoreline sand deposits. The Upper Tuscaloosa sand facies grade into shale (Shale unit 2) in the downdip area away from the paleo-shoreline (text-fig. 12 and 13c). A prominent sea-level drop in the late Turonian or early Coniacian ended the Tuscaloosa transgressive-regressive cycle (UK I sequence).

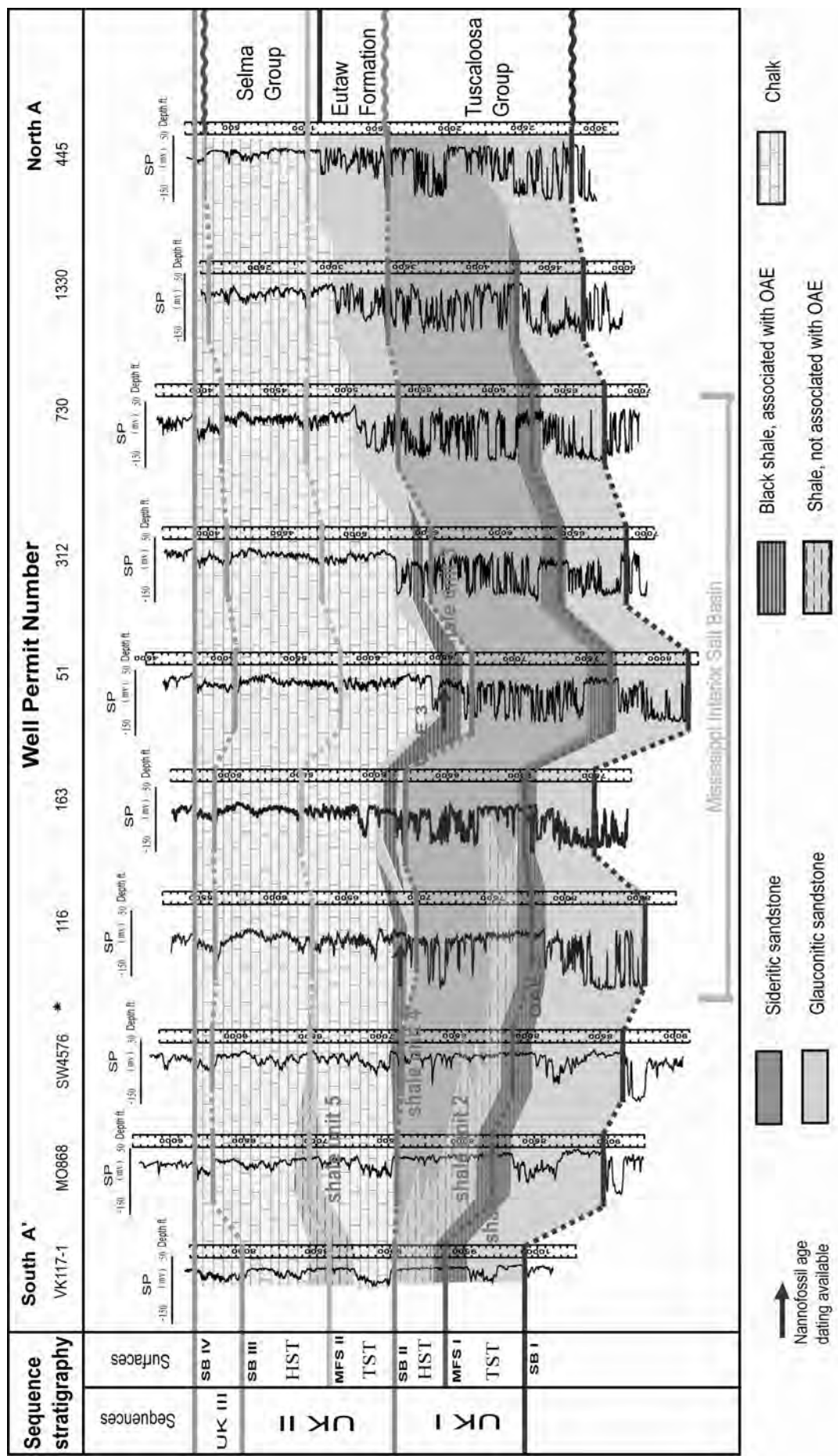


TEXT-FIGURE 11

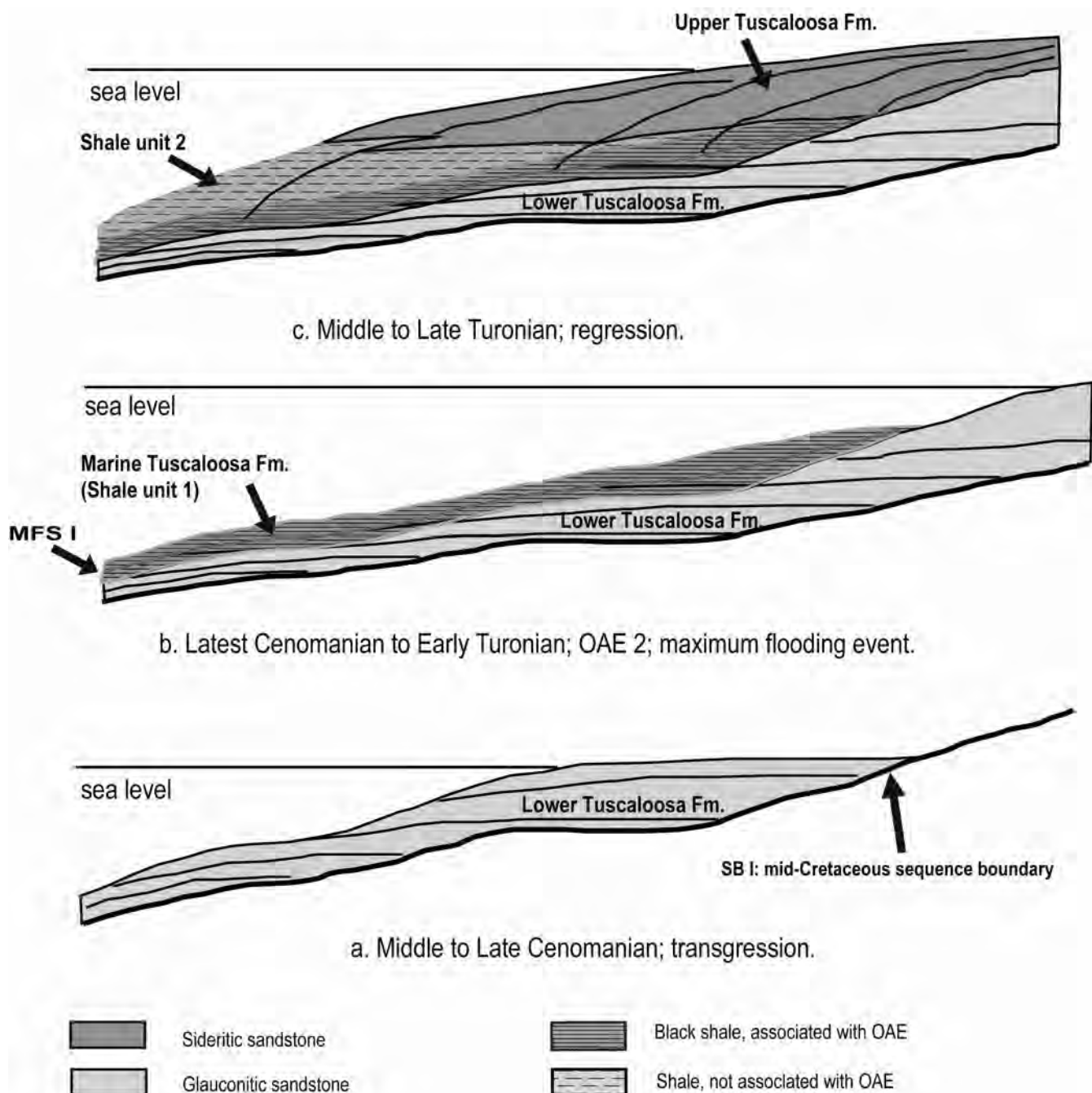
Synthetic seismogram constructed for well SW4576, after Liu (2004). Maximum flooding surfaces and sequence boundaries identified on seismic data were projected onto well logs. Four sequence boundaries were found to correspond to four prominent unconformities identified in previous outcrop and subsurface studies. SB III was not recognized, because the UK III sequence is too thin in this area. SB = sequence boundary, MFS = maximum flooding surface.

The UK II sequence began as sea level rose in the late Coniacian. When the sea advanced landward and flooded the Mississippi Interior Salt Basin, a barrier island-lagoonal system was established (text-fig. 14a). The Mississippi Interior Salt Basin became a large lagoon or bay, with a barrier-island or is-

land chain enclosing its southern rim. This lagoon acted as a sediment trap with accommodation space provided by both sea-level rise and basin subsidence. Most of the sandy sediment was trapped on the northern side of the lagoon, while mud and clay (Shale unit 3) were deposited in the center. Large quantities



TEXT-FIGURE 12
Well-log cross section A-A' from the outcrop area to the offshore area showing facies changes of Upper Cretaceous strata on the continental shelf. See text-figure 4 for well locations and position of the cross section. Sequence boundaries and maximum flooding surfaces were recognized from seismic data (see text-figures 7 and 10) and projected onto well logs using synthetic seismograms and check-shot surveys (See text-figure 11). *Synthetic seismogram was constructed for well SW4576 (see text-figure 11). SB = sequence boundary, MFS = sequence boundary, MFS = maximum flooding surface, TST = transgressive systems tract, HST = highstand systems tract.

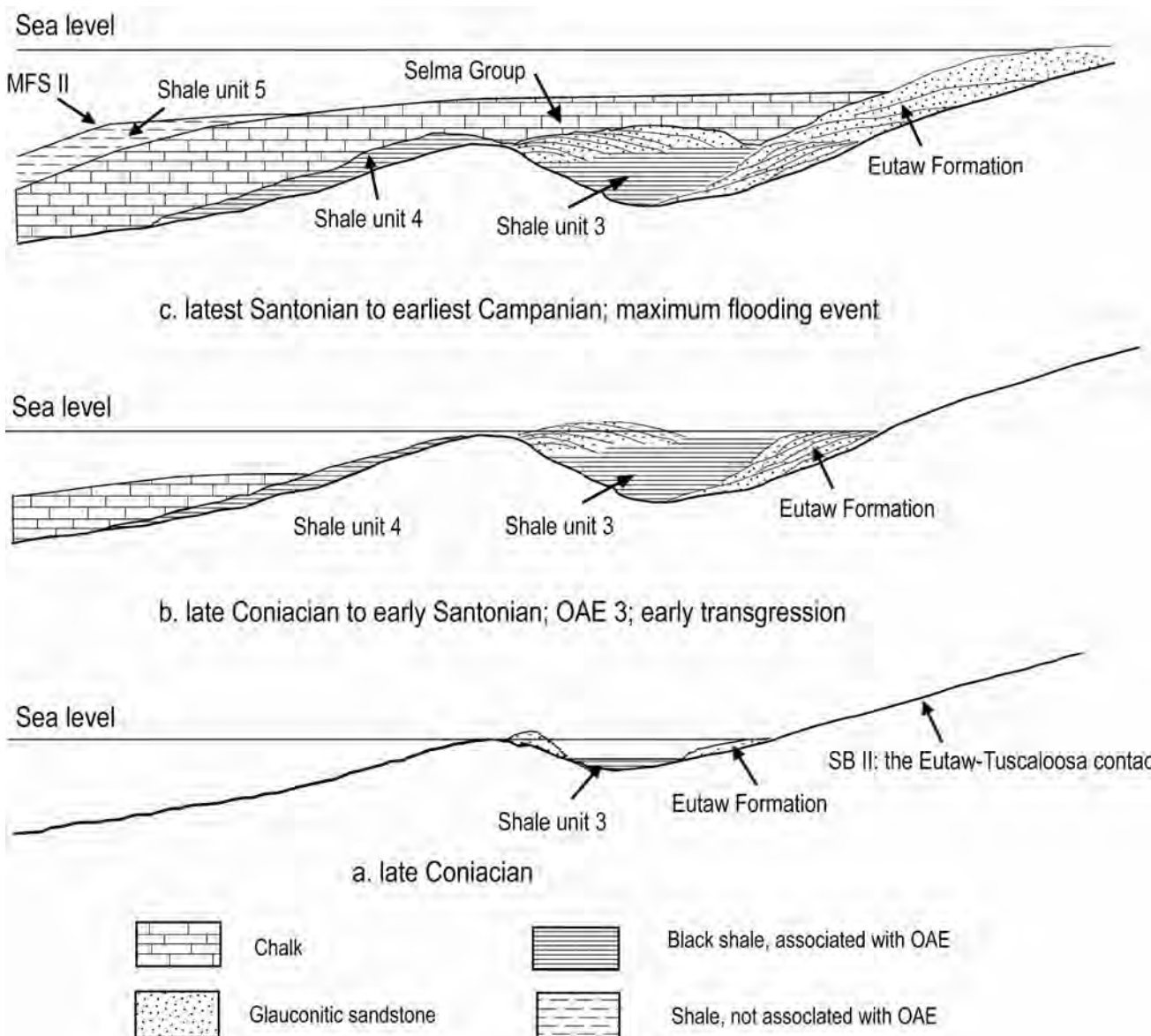


TEXT-FIGURE 13

Depositional history of the UK I sequence and its relationship with OAE 2 (Type I OAE). The Lower Tuscaloosa Formation was deposited in a backstepping manner as the transgressive systems tract. OAE 2 occurred when the Marine Tuscaloosa Formation (Shale unit 1) was being deposited during the maximum flooding event of the UK I sequence. The Upper Tuscaloosa Formation was deposited in a prograding manner as the highstand systems tract. Sandstone beds of the Upper Tuscaloosa Formation in the updip area grade downdip into shale (Shale unit 2).

of plant debris were brought into the lagoon by rivers draining the continent and subsequently buried. With continued rise of sea level during the early and middle Santonian, the barrier islands migrated landward and covered the lagoonal mud (text-fig. 14b). At the same time, seaward of the barrier island, shale (Shale unit 4) and carbonate sediments (the Selma Group) began to be deposited because of diminished siliciclastic sediment supply (text-fig. 14b). Sediment of the Eutaw Formation continued to be deposited in a backstepping pattern along with

the landward migration of the shoreline during the late Santonian. The maximum flooding event occurred during the latest Santonian to earliest Campanian, chalk and marl sediment of the Selma Group was deposited across most of the shelf area, with shale (Shale unit 5) being deposited in the outer shelf area (text-fig. 14c). Relatively pure chalk was deposited as highstand systems tract on the shelf areas after the maximum flooding event, probably due to low siliciclastic sediment supplies during the Campanian in the northeastern Gulf of Mexico area.



TEXT-FIGURE 14

Depositional history of the UK II sequence and its relationship with OAE 3 (Type II OAE). The Eutaw strata and the lower beds of the Selma Group were deposited in a backstepping manner as the transgressive systems tract. The downdip Eutaw shale (Shale units 3 and 4) were deposited when OAE 3 occurred. OAE 3 was associated with the early transgressive stage of the UK II sequence, during which rapid sea-level rise inundated vast land area of the coastal plain. Shale unit 5 was deposited during the maximum flooding event of the UK II sequence.

It is clear that OAE 2 and 3 occurred at different stages of a marine transgression. Two types of OAEs, therefore, can be differentiated based on their relationship with sea-level fluctuations. Type I OAE (for example, OAE 2) occurred when the sea transgressed to its maximum extent (text-fig. 13), while Type II OAE (for example, OAE 3) occurred during the early transgressive stage when large land areas were inundated and barrier island-lagoonal systems were established (text-fig. 14).

Although the mechanism responsible for the genesis of an OAE is still not clear, a comparison between OAE 2 and 3 as observed in the northeastern Gulf of Mexico has the potential to assist with determining the controlling factors of OAEs. That is, sediment/nutrient supply during a sea-level cycle could be critical for the genesis of OAEs. Sediment supply was abundant

during the UK I cycle, so abundant that the Lower Tuscaloosa sands can be found in the outer shelf areas. During the maximum flooding event, black shale of the Marine Tuscaloosa Formation was deposited across the continental shelf. Furthermore, in the highstand systems tract or infilling stage, the siliciclastic Upper Tuscaloosa Formation prograded into middle and outer shelf areas. On the contrary, during the UK II cycle, sediment supply was apparently limited. The transgressive sand of the Eutaw Formation was mainly confined to the area north of the Mississippi Interior Salt Basin. During the maximum flooding stage, the shale associated with the maximum flooding event was only deposited in the outer shelf area (text-figs. 12 and 14). In addition, the highstand systems tract of the UK II sequence is primarily composed of chalk and marl beds. Low nutrient supply associated with insufficient terrestrial input during the depo-

TABLE 1

Organic geochemical analyses of core and core chip samples from southwestern Alabama for the Marine Tuscaloosa Shale. See Figure 4 for well locations. Data source: (1) Claypool and Mancini (1989); (2) Mancini and Payton (1981); (3) this study. Analyses by Geochem Laboratories, Houston, Texas.

Rock unit	County	Well premit number	Depth (feet)	Organic carbon %	Kerogen type	Data source
Marine Tuscaloosa Shale	Escambia	355	5814	1.18	Am (Al)	1
		427	6080	2.63	Am (Al)	1
	Clark		5270	1.63	Am	2
		2182	5271	2.75	Am (Al)	1
			5273	1.33	Am (Al)	2
			5250	0.88	H	2
		245	5255	1.85	Am (Al)	2
			5265	2.91	Am (Al)	2
		199	5275	2.90	Am (Al)	2
		243	5256	1.79	Am (Al)	2
	Mobile	163	7083	6.00-6.24	H*	3

sition of the UK II sequence might have limited the primary productivity in the water column, therefore, restricted the development of bottom water anoxia.

CONCLUSIONS

Two Upper Cretaceous black shales, the Marine Tuscaloosa shale and the downdip Eutaw shale, were identified as OAE 2 and 3 sediments in the northeastern Gulf of Mexico shelf area. The Marine Tuscaloosa Formation (upper Cenomanian-lower Turonian) is the black shale related to the global OAE 2. This shale unit was deposited in open marine, middle and outer neritic settings. The downdip Eutaw shale facies is associated with OAE 3. The downdip Eutaw shale facies (upper Coniacian-lower Santonian) was mainly deposited in a marginal marine setting consisting of barrier islands and back barrier lagoons.

With respect to the relationship with sea-level changes, two types of Oceanic Anoxic Events can be identified according to their positions in the sequence stratigraphic framework. Type I OAE occurred when the seashore transgressed furthest landward. Sediments of this type of OAE are associated with the maximum flooding surface/condensed section, which can be recognized as the turning point between the backstepping deposits of the transgressive systems tract and the infilling and prograding deposits of the highstand systems tract (regressive). On the contrary, Type II OAE is associated with the early transgressive systems tract. Black shales associated with this type of OAE were deposited in restricted marine environments, such as back barrier lagoons. Rapid transgression inundated vast land areas and transformed lowlands into lagoons or ponds in which large quantities of fine-grained sediment and terrestrial organic carbon were trapped and buried. This classification of OAEs and the methodology used in this study have the potential to be applied to other regions and to other OAEs. An integrated approach, which utilizes all available information including seismic data, well logs, well cores, and outcrop studies, is required to understand the sequence stratigraphic and depositional setting of OAEs.

TABLE 2

Organic geochemical analyses of core and core chip samples from southwestern Alabama for the downdip Eutaw shale. See Figure 4 for well locations. Data source (3) this study. Analyses by Geochem Laboratories, Houston, Texas.

Rock unit	County	Well premit number	Depth range (feet)	Organic carbon %	Kerogen type	Data source
Downdip Eutaw Shale	Washington	6490-6494	1.03	W, H*, I(Am**)	3	
		6497-6500	1.58	H, W	3	
		6504-6507	0.53		3	
		6510-6514	1.13	H, W	3	
		6514-6517	1.05		3	
		6517-6520	1.13	H, W, I	3	
		6520-6524	1.04		3	
		6870-6875	0.93	Am**	3	
Mobile	116	6875-6880	0.96	Am**, H-W, I	3	

Al: Algal

Am: Amorphous-Sapropel

Am**: Relic Amorphous-Sapropel

H: Herbaceous-Spore/Pollen

H*: Degraded Herbaceous

W: Woody-Structured

I: Inertinite

ACKNOWLEDGMENTS

The author expresses his sincere appreciations to Dr. Ernest A. Mancini, Dr. Charles C. Smith, and Dr. Antonio B. Rodriguez, who critically reviewed this paper before it was submitted. In addition, Dr. Charles C. Smith conducted the nannofossil analyses incorporated in this study. Thorough reviews by Dr. Karen Bice and Dr. R. Mark Leckie significantly improved the quality of the final manuscript.

REFERENCES

- ARTHUR, M.A. and SCHLANGER, S.O., 1979. Cretaceous "Oceanic Anoxic Event" as causal factors in development of reef-reservoir giant oil fields. *American Association of Petroleum Geologists Bulletin*, 63:870-885.
- ARTHUR, M.A. and PREMOLI SILVA, I., 1982. Development of widespread organic carbon-rich strata in the Mediterranean Tethys. In: Schlanger, S.O. and Cita, M.B., Eds., *Nature and origin of Cretaceous carbon-rich facies*, 7-54. New York: Academic Press.
- ARTHUR, M.A., SCHLANGER, S.O. and JENKYNS, H.C., 1987. The Cenomanian-Turonian oceanic anoxic event, II. palaeoceanographic controls on organic-matter production and preservation. In: Brooks, J. and Fleet, A.J., Eds. *Marine petroleum source rocks*. Geological Society Special Publication, No. 26, 401-420. London, the Geological Society of London.
- ARTHUR, M.A., DEAN, W.E. and PRATT, L.M., 1988. Geochemical and climatic effects of increased marine organic carbon burial at the Cenomanian/Turonian boundary. *Nature*, 335: 714-717.
- ARTHUR, M.A., JENKYNS, H.C., BRUMSACK, H.J. and SCHLANGER, S.O., 1990. Stratigraphy, geochemistry, and paleoceanography of organic carbon-rich Cretaceous sequences. In: Ginsburg, R.N. and Beaudoin, B., Eds. *Cretaceous resources, events and rhythms: background and plans for research*, 75-199. Amsterdam: Kluwer Academic Publishers.
- BERGER, W.H. and VON RAD, U., 1972. Cretaceous and Cenozoic sediments from the Atlantic Ocean. In: Hayes, D.E. and Pimm, A.C. et al., Eds., *Initial Reports of the Deep Sea Drilling Project*, volume 14: 787-954. Washington, DC: US Government Printing Office.

- BRALOWER, T.J., 1988. Calcareous nannofossil biostratigraphy and assemblages of the Cenomanian-Turonian boundary interval: implications for the origin and timing of oceanic anoxia. *Paleoceanography*, 3: 275-316.
- BRALOWER, T.J., SLITER, W.V., ARTHUR, M.A., LECKIE, R.M., ALLARD, D. and SCHLANGER, S.O., 1993. Dysoxic/anoxic episodes in the Aptian-Albian (Early Cretaceous). In: Pringle, M.S., Sager, W.W., Sliter, W.V. and Stein, S., Eds., *The Mesozoic Pacific: geology, tectonics, and volcanism*, Geophysical Monograph, 77: 5-37. Washington, DC: American Geophysical Union
- BRALOWER, T.J., ARTHUR, M.A., LECKIE, R.M., SLITER, W.V., ALLARD, D.J. and SCHLANGER, S.O., 1994. Timing and paleoceanography of oceanic dysoxia/anoxia in the late Barremian to early Aptian (Early Cretaceous). *Palaios*, 9: 335-369.
- CARON, M., 1985. Cretaceous planktic foraminifera. In: Bolli, H.M., Saunders, J.B. and Perch-Nielsen, K., Eds., *Plankton stratigraphy*, 17-86. London: Cambridge University Press.
- CHRISTOPHER, R.A., SELF-TRAIL, J.M., PROWELL, D.C. and GOHN, G.S., 1999. The stratigraphic importance of the Late Cretaceous pollen genus *Sohlipollis* gen.nov. in the coastal plain province. *South Carolina Geology*, 41: 27-44.
- CLAYPOOL, G.E. and MANCINI, E.A., 1989. Geochemical relationships of petroleum in Mesozoic reservoirs to carbonate source rocks of Jurassic Smackover Formation, southwestern Alabama. *American Association of Petroleum Geologists Bulletin*, 73: 904-924.
- COCCIONI, R. and GALEOTTI, S., 2003. The mid-Cenomanian event: prelude to OAE 2. *Palaeogeography, Palaeoclimatology, Palaeoecology*, 190: 427-440.
- CONANT, L.C., 1967. The pre-Selma Cretaceous strata. In: Jones, D.E., Ed. *Geology of the Coastal Plain of Alabama: A guide book for the 80th annual meeting of the Geological Society of America*, 4-11. Alabama Geological Society.
- COOK, M.R., 1993. The Eutaw aquifer in Alabama. *Geological Survey of Alabama Bulletin*, 156: 1-105.
- COPELAND, C.W., Jr., NEWTON, J.G. and SELF, D.M., 1976. Cretaceous and Tertiary faults in southwestern Alabama. *Alabama geological society fourteenth annual field trip guidebook*, 1-114.
- CURRENT, A.M., 1948. *Gilbertown field, Choctaw County, Alabama. Structure of typical american oil fields*, v. 3, 1-4. Tulsa: American Association of Petroleum Geologists.
- ERBACHER, J., THUROW, J. and LITTKE, R., 1996. Evolution patterns of radiolaria and organic matter variations: a new approach to identify sea-level changes in mid-Cretaceous pelagic environments. *Geology*, 24: 499-502.
- ERBACHER, J. and THUROW, J., 1997. Influence of oceanic anoxic events on the evolution of mid-Cretaceous radiolaria in the North Atlantic and western Tethys. *Marine Micropaleontology*, 30: 139-158.
- ERBACHER, J., HUBER, B.T., NORRIS, R.D. and MARKEY, M., 2001. Increased thermohaline stratification as a possible cause for an ocean anoxic event in the Cretaceous period. *Nature*, 409: 325-327.
- ERLICH, R.N., PALMER-KOLEMAN, S.E. and LORENTE, M.A., 1999. Geochemical characterization of oceanographic and climatic changes recorded in upper Albian to lower Maastrichtian strata, western Venezuela. *Cretaceous Research*, 20: 547-581.
- FRAZIER, W.J. and TAYLOR, R.S., 1980. Facies changes and paleogeographic interpretations of the Eutaw Formation (Upper Cretaceous) from western Georgia to central Alabama. In: Tull, J.F., Ed. *Field trips for the Southeastern Section of Geological Society of America*, 1-27. Birmingham, Alabama.
- GRADSTEIN, F.M., AGTERBERG, F.P., OGG, J.G., HARDENBOL, J., VEEN, P.V., THIERRY, J. and HUANG, Z., 1995. A Triassic, Jurassic and Cretaceous time scale. In: Bergren, W.A., Kent, D.V., Aubry, M-P. and Hardenbol, J., Eds. *Geochronology, time scales, and global stratigraphic correlation*. Society of Economic Paleontologists and Mineralogists Special Publication, No. 54: 95-126.
- HALLAM, A., 1977. Secular changes in marine inundation of USSR and North America through the Phanerozoic. *Nature*, 269: 769-772.
- _____, 1987. Mesozoic marine organic-rich shales. In: Brooks, J. and Fleet, A.J., Eds. *Marine petroleum source rocks*. London, the Geological Society of London Special Publication, No. 26: 251-261.
- HANCOCK, J.M. and KAUFFMAN, E.G., 1979. The great transgressions of the Late Cretaceous. *Journal of the Geological Society, London*, 136: 175-186.
- HAQ, B.U., HARDENBOL, J. and VAIL, P.R., 1987. Chronology of fluctuating sea levels since the Triassic. *Science*, 235: 1156-1167.
- HARDENBOL, J., THIERRY, J., FARLEY, M.B., JACQUIN, T., DE GRACIANSKY, P.-C. and VAIL, P.R., 1998. Mesozoic and Cenozoic sequence chronostratigraphic framework of European Basins. In: De Graciansky, P.-C., Hardenbol, J., Jacquin, T. and Vail, P.R., Eds. *Mesozoic and Cenozoic Sequence Stratigraphy of European Basins*. SEPM Special Publication, No. 60: 3-13.
- HART, M.B., 1993. Cretaceous foraminiferal events. In: Hailwood, E.A. and Kidd, R.B., Eds., *High resolution stratigraphy*. The Geological Society of London Special Publication, No. 70: 227-240.
- HAYS, J.D. and PITMAN, W.C., III, 1973. Lithospheric plate motion, sea level changes and climatic and ecological consequences. *Nature*, 246: 18-22.
- HOCHULI, P.A., MENEGATTI, A.P., WEISSERT, H., RIVA, A., ERBA, E. and PREMOLI SILVA, I., 1999. Episodes of high productivity and cooling in the early Aptian Alpine Tethys. *Geology*, 27: 657-660.
- HOFMANN, P., WAGNER, T. and BECKMANN, B., 2003. Millennial- to centennial-scale record of African climate variability and organic carbon accumulation in the Coniacian-Santonian eastern tropical Atlantic (Ocean Drilling Program Site 959, off Ivory Coast and Ghana). *Geology*, 31: 135-138.
- HOLBOURN, A.E.L. and KUHNT, W., 1998. Turonian-Santonian benthic foraminifer assemblages from site 959D (Côte d'Ivoire-Ghana Transform Margin, equatorial Atlantic): indication of a late Cretaceous oxygen minimum zone. In: Mascle, J., Lohmann, G.P. and Moullade, M., Eds. *Proceedings of the Ocean Drilling Program, Scientific Results*, volume 159: 375-387. Washington, DC: US Government Printing Office.
- HUBER, B.T., LECKIE, R.M., NORRIS, R.D., BRALOWER, T.J. and COBABE, E., 1999. Foraminiferal assemblage and stable isotopic changes across the Cenomanian-Turonian boundary in the subtropical North Atlantic. *Journal of Foraminiferal Research*, 29: 392-417.
- JACKSON, E.D. and SCHLANGER, S.O., 1976. Regional synthesis, Line Islands Chain, and Manihiki Plateau, Central Pacific Ocean, DSDP Leg 33. In: Schlanger, S.O. and Jackson, E.D. et al., Eds. *Initial Reports of the Deep Sea Drilling Project*, volume 33: 915-927. Washington, DC: US Government Printing Office.
- JENKYN, H.C., 1980. Cretaceous anoxic events: from continents to oceans. *Journal of the Geological Society, London*, 137: 171-188.

- JENKYNS, H.C., GALE, A.S. and CORFIELD, R.M., 1994. Carbon- and oxygen-isotope stratigraphy of the English Chalk and Italian Scaglia and its palaeoclimatic significance. *Geological Magazine*, 131: 1-34.
- JONES, C.E. and JENKYNS, H.C., 2001. Seawater strontium isotopes, oceanic anoxic events, and seafloor hydrothermal activity in the Jurassic and Cretaceous. *American Journal of Science*, 301: 112-149.
- KAUFFMAN, E.G. and CALDWELL, W.G.E., 1993. The Western Interior Basin in space and time. In: Caldwell, W.G.E. and Kauffman, E.G., Eds., *Evolution of the Western Interior Basin*. Geological Association of Canada Special Paper, 39: 1-30.
- KELLER, G. and PARDO, A., 2004. Age and paleoenvironment of the Cenomanian-Turonian global stratotype section and point at Pueblo, Colorado. *Marine Micropaleontology*, 51: 95-128.
- LECKIE, R.M., 1985. Foraminifera of the Cenomanian-Turonian boundary interval, Greenhorn Formation, Rock Canyon Anticline, Pueblo, Colorado. In: Pratt, L.M., Kauffman, E.G. and Zelt, F.B., Eds., *Fine-grained deposits and biofacies of the cretaceous western interior seaway: evidence of cyclic sedimentary process*. SEPM Field Trip Guidebook, No. 4: 139-149. Tulsa, Oklahoma, Society of Economist, Paleontologist, Mineralogists.
- LECKIE, R.M., BRALOWER, T.J. and CASHMAN, R., 2002. Oceanic anoxic events and plankton evolution: biotic response to tectonic forcing during the mid-Cretaceous. *Paleoceanography*, 17(3): 10.1029/2001PA000623.
- LIU, K., 2004. Seismic and sequence stratigraphy of Upper Cretaceous strata, offshore Alabama and Mississippi area. *Gulf Coast Association of Geological Societies Transactions*, 54: 347-360.
- _____, 2005 (in press). Updip-downdip facies changes of the Eutaw Formation (Coniacian-Santonian), northeastern Gulf of Mexico area. *Gulf Coast Association of Geological Societies Transactions*, 55.
- LÜNING, S., KOLONIC, S., BELHADJ, E.M., BELHADJ, Z., COTA, L., BARIË, G. and WAGNER, T., 2004. Integrated depositional model for the Cenomanian-Turonian organic-rich strata in North Africa. *Earth-Science Reviews*, 64: 51-117.
- MANCINI, E.A., SMITH, C.C. and PAYTON, J.W., 1980. Geological age and depositional environment of the "Pilot Sand" and "Marine Shale" Tuscaloosa Group, South Carlton field, South Alabama. In: *Geology of the Woodbine and Tuscaloosa Formations*. Gulf Coast Section of the Society of Economic Paleontologists and Mineralogists First Annual Research Conference, 24-25.
- MANCINI, E.A. and PAYTON, J.W., 1981. Petroleum geology of South Carlton field, Lower Tuscaloosa "Pilot Sand", Clarke and Baldwin counties, Alabama. *Gulf Coast Association of Geological Societies Transactions*, 31: 139-147.
- MANCINI, E.A., MINK, R.M., PAYTON, J.W. and BEARDEN, B.L., 1987. Environments of deposition and petroleum geology of Tuscaloosa Group (Upper Cretaceous), South Carlton and Pollard fields, southwestern Alabama. *American Association of Petroleum Geologists Bulletin*, 71: 1128-1142.
- MANCINI, E.A., PUCKETT, T.M. and TEW, B.H., 1996. Integrated biostratigraphic and sequence stratigraphic framework for Upper Cretaceous strata of the eastern Gulf Coastal Plain, USA. *Cretaceous Research*, 17: 645-669.
- MANCINI, E.A. and PUCKETT, T.M., 2002. Transgressive-regressive cycles: application to petroleum exploration for hydrocarbons associated with Cretaceous shelf carbonates and coastal and fluvial-deltaic siliciclastics, northeastern Gulf of Mexico. In: Armentrout, J.A., Ed. *Proceedings of the 22nd Annual Bob F. Perkins Research Conference, Sequence Stratigraphic Models for Exploration and Production: Evolving Methodology, Emerging Models and Application Case Histories*, 173-199. Gulf Coast Section, SEPM Foundation.
- MELLO, M.R., KOUTSOUKOS, E.A.M., HART, M.B., BRASSELL, S.C. and MAXWELL, J.R., 1989. Late Cretaceous anoxic events in the Brazilian continental margin. *Organic Geochemistry*, 14: 529-542.
- MILLER, K.G., SUGARMAN, P.J., BROWNING, J.V., KOMINZ, M.A., HERNÁNDEZ, J.C., OLSSON, R.K., WRIGHT, J.D., FEIGENSON, M.D. and VAN SICKEL, W., 2003. Late Cretaceous chronology of large, rapid sea-level changes: glacioeustasy during the greenhouse world. *Geology*, 31: 585-588.
- MITCHUM, R.M., Jr., VAIL, P.R. and SANGREE, J.B., 1977. Seismic stratigraphy and global changes of sea level, part 6: stratigraphic interpretation of seismic reflection patterns in depositional sequences. In: Payton, C.E., Ed., *Seismic Stratigraphy—applications to hydrocarbon exploration*, AAPG Memoir 26:117-133. Tulsa, Oklahoma: American Association of Petroleum Geologists.
- MITCHUM, R.M. and VAIL, P.R., 1977. Seismic stratigraphy and global changes of sea level, part 7: seismic stratigraphic interpretation procedure. In: Payton, C.E., Ed., *Seismic stratigraphy—applications to hydrocarbon exploration*, AAPG Memoir 26:135-143. Tulsa, Oklahoma: American Association of Petroleum Geologists.
- MOBERLY, R. and LARSON, R.L., 1975. Mesozoic magnetic anomalies, oceanic plateaus, and seamount chains in the northwestern Pacific Ocean. In: Larson, R.L., Moberly, R. et al., Eds. *Initial Reports of the Deep Sea Drilling Project*, volume 32: 945-957. Washington, U.S. Government Printing Office.
- NORRIS, R.D., BICE, K.L., MAGNO, E.A. and WILSON, P.A., 2002. Jiggling the tropical thermostat in the Cretaceous hothouse. *Geology*, 30: 299-302.
- NZOUESSI-MBASSANI, P., DISNAR, J.-R. and LAGGOUN-DÉFARGE, F., 2003. Organic matter characteristics of Cenomanian-Turonian source rocks: implications for petroleum and gas exploration onshore Senegal. *Marine and Petroleum Geology*, 20: 411-427.
- PASHIN, J.C., RAYMOND, D.E., ALABI, G.G., GROSHONG, R.H., JR, and JIN, G., 2000. Revitalizing Gilbertown oil field: characterization of fractured chalk and glauconitic sandstone reservoirs in an extensional fault system. *Geological Survey of Alabama Bulletin*, 168: 1-81.
- PEDERSEN, T.F. and CALVERT, S.E., 1990. Anoxia vs. productivity: what controls the formation of organic-carbon-rich sediments and sedimentary rocks. *American Association of Petroleum Geologists Bulletin*, 74: 454-466.
- PERCH-NIELSEN, K., 1985. Mesozoic calcareous nannofossils. In: Bolli, H.M., Saunders, J.B. and Perch-Nielsen, K., Eds. *Plankton stratigraphy*, 329-426.. London: Cambridge University Press.
- POSAMENTIER, H.W., JERVEY, M.T. and VAIL, P.R., 1988. Eustatic controls on clastic deposition I—conceptual framework. In: Wilgus, C.K., Hastings, B.S., Kendall, C.G.St.C., Posamentier, H.W., Ross, C.A., and Van Wagoner, J.C., Eds., *Sea-level changes: an integrated approach*. SEPM Special Publication No. 42: 109-124.
- POSAMENTIER, H.W. and VAIL, P.R., 1988. Eustatic controls on clastic deposition II — sequence and systems tract models. In: Wilgus, C.K., Hastings, B.S., Kendall, C.G.St.C. Posamentier, H.W., Ross, C.A. and Van Wagoner, J.C., Eds. *Sea-level Changes: An Integrated Approach*. SEPM Special Publication No. 42: 125-154.

- PRATT, L.M., 1984. Influence of paleoenvironmental factors on preservation of organic matter in middle Cretaceous Greenhorn Formation, Pueblo, Colorado. *American Association of Petroleum Geologists Bulletin*, 68: 1146-1159.
- PRATT, L.M., ARTHUR, M.A., DEAN, W.E., SCHOLLE, P.A., 1993. Paleo-oceanographic cycles and events during the Late Cretaceous in the Western Interior Seaway of North America. In: Caldwell, W.G.E. and Kauffman, E.G., Eds. *Evolution of the Western Interior Basin*. Geological Association of Canada Special Paper, 39: 333-353.
- PREMOLI SILVA, I., ERBA, E., SALVINI, G., LOCATELLI, C. and VERGA, D., 1999. Biotic changes in Cretaceous oceanic anoxic events of the Tethys. *Journal of Foraminiferal Research*, 29: 352-370.
- PUCKETT, T.M., 1991. Absolute paleobathymetry of Upper Cretaceous chalks based on ostracodes-evidence from the Demopolis Chalk (Campanian and Maastrichtian) of the northern Gulf Coastal Plain. *Geology*, 19: 449-452.
- PUCKETT, T.M. and MANCINI, E.A., 2000. Microfossil characteristics of deposits of systems tracts in the Upper Cretaceous strata of Mississippi and Alabama. *Gulf Coast Association of Geological Societies Transactions*, 50: 389-398.
- RAYMOND, D.E., OSBORNE, W.E., COPELAND, C.W. and NEATHERY, T.L., 1988. *Alabama stratigraphy*. Geological Survey of Alabama Circular, 140: 1-97.
- REY, O., SIMO (TONI), J.A. and LORENTE, M.A., 2004. A record of long- and short-term environmental and climatic change during OAE3: La Luna Formation, Late Cretaceous (Santonian—early Campanian), Venezuela. *Sedimentary Geology*, 170: 85-105.
- SALVADOR, A., 1991. Origin and development of the Gulf of Mexico Basin. In: Salvador, A., Ed. *The Gulf of Mexico Basin: The geology of North America*. v. J: 389-444. Boulder, Colorado, Geological Society of America,.
- SCHLANGER, S.O. and JENKYNS, H.C., 1976. Cretaceous oceanic anoxic events: causes and consequences. *Geologie en Mijnbouw*, 55: 179-184.
- SCHLANGER, S.O., ARTHUR, M.A., JENKYNS, H.C. and SCHOLLE, P.A., 1987. The Cenomanian-Turonian oceanic anoxic event, I. Stratigraphy and distribution of organic carbon-rich beds and the marine $\delta^{13}\text{C}$ excursion. In: Brooks, J. and Fleet, A.J., Eds. *Marine petroleum source rocks*. The Geological Society of London, Special Publication, No. 26: 371-399.
- SCHOLLE, P. A. and ARTHUR, M.A., 1980. Carbon isotope fluctuations in Cretaceous pelagic limestones: potential stratigraphic and petroleum exploration tool. *American Association of Petroleum Geologists Bulletin*, 64: 67-87.
- SCHRÖDER-ADAMS, C.J., CUMBAA, S.L., BLOCH, J., LECKIE, D.A., CRAIG, J., SEIF EL-DEIN, S.A., SIMONS, D. H.A.E. and KENIG, F., 2001. Late Cretaceous (Cenomanian to Campanian) paleoenvironmental history of the Eastern Canadian margin of the Western Interior Seaway: bonebeds and anoxic events. *Palaeogeography, Palaeoclimatology, Palaeoecology*, 170: 261-289.
- SCOPELLITI, G., BELLANCA, A., COCCIONI, R., LUCIANI, V., NERI, R., BAUDIN, F., CHIARI, M. and MARCUCCI, M., 2004. High-resolution geochemical and biotic records of the Tethyan ‘Bonarelli Level’ (OAE2, Latest Cenomanian) from the Calabianca-Guidaloca composite section, northwestern Sicily, Italy. *Palaeogeography, Palaeoclimatology, Palaeoecology*, 208: 293-317.
- SINNINGHE DAMSTÉ, J.S. and KÖSTER, J., 1998. A euxinic southern North Atlantic Ocean during the Cenomanian/Turonian oceanic anoxic event. *Earth and Planetary Science Letters*, 158: 165-173.
- SISSINGH, W., 1977. Biostratigraphy of Cretaceous calcareous nannoplankton. *Geologie en Mijnbouw*, 56: 37-65.
- SLITER, W.V., 1976. Cretaceous foraminifers from the southern Atlantic Ocean, Leg 36, Deep Sea Drilling Project. In: Barker, P.F. and I.W.D. Dalziel, et al., Eds. *Initial Reports of the Deep Sea Drilling Project*, v. 36. Washington, DC: US Government Printing Office, 519-537.
- SMITH, C.C. and MANCINI, E.A., 1983. Calcareous nannofossil and planktonic foraminiferal biostratigraphy. In: Russell, E.E., Keady, D.M., Mancini, E.A. and Smith, C.C., Eds., *Upper Cretaceous lithostratigraphy and biostratigraphy in northeast Mississippi, southwest Tennessee and northwest Alabama, shelf chalks and coastal clastics*, 15-28 Spring Field Trip, the Geological Survey of Alabama.
- SOHL, N.F., MARTINEZ, R.E., SALMERON-URENA, P. and SOTO-JARAMILLO, F., 1991. Upper Cretaceous. In: Salvador, A., Ed., *The Gulf of Mexico Basin: The geology of North America*. v. J: 205-244. Boulder, Colorado, Geological Society of America.
- STERZINAR, E. and LECKIE, R.M., 2004. Foraminiferal assemblages and paleoceanography of the Upper Cretaceous (Coniacian) of Western Kansas during Ocean Anoxic Event 3. *Geological Society of American, Abstracts with Programs*, 36(5): 292.
- SUMMERHAYS, C.P., 1981. Organic facies of middle Cretaceous black shales in deep North Atlantic. *American Association of Petroleum Geologists Bulletin*, 65: 2364-2380.
- THIERSTEIN, H.R. and BERGER, W.H., 1978. Injection events in ocean history. *Nature*, 276: 461-466.
- TSIKOS, H., JENKYNS, H.C., WALSWORTH-BELL, B., PETRIZZO, M.R., FORSTER, A., KOLONIC, S., ERBA, E., PREMOLI SILVA, I., BAAS, M., WAGNER, T. and SINNINGHE DAMSTÉ, J.S., 2004. Carbon-isotope stratigraphy recorded by the Cenomanian-Turonian oceanic anoxic event: correlation and implications based on three key localities. *Journal of the Geological Society of London*, 161: 711-719.
- VAIL, P.R. and MITCHUM, R.M., Jr., 1977. Seismic stratigraphy and global changes of sea level, part 1: overview. In: Payton, C.E., Ed. *Seismic stratigraphy — applications to hydrocarbon exploration*, Tulsa, Oklahoma: American Association of Petroleum Geologists Memoir 26 : 51-52. .
- VAIL, P.R., MITCHUM, R.M., Jr., and THOMPSON, S., III, 1977a. Seismic stratigraphy and global changes of sea level, part 3: relative changes of sea level from coastal onlap. In: Payton, C.E., Ed. *Seismic Stratigraphy — applications to hydrocarbon exploration*. AAPG Memoir 26: 63-81. Tulsa, Oklahoma: American Association of Petroleum Geologists.
- , 1977b. Seismic stratigraphy and global changes of sea level, part 4: global cycles of relative changes of sea level. In: Payton, C.E., Ed., *Seismic Stratigraphy — applications to hydrocarbon exploration*. AAPG Memoir 26: 83-97. Tulsa, Oklahoma: American Association of Petroleum Geologists.
- VAIL, P.R., 1987. Seismic stratigraphy interpretation procedure. In: Bally, A.W., Ed., *Atlas of seismic stratigraphy*. Tulsa, Oklahoma: American Association of Petroleum Geologists, Studies in geology, No. 27, v. 1: 1-10.
- VALLIER, T., THIEDE, J., ADELSECK, C., BOERSMA, A., et al., 1979. Leg 62 probes the paleoenvironments. *Geotimes*, 24(2): 24-26.

- VALLIER, T., THIEDE, J., ADELSECK, C., BOERSMA, A., et al., 1979. Leg 62 probes the paleoenvironments. *Geotimes*, 24(2): 24-26.
- VOIGT, S., 2000. Cenomanian-Turonian composite $\delta^{13}\text{C}$ curve for western and central Europe: the role of organic and inorganic carbon fluxes. *Palaeogeography, Palaeoclimatology, Palaeoecology*, 160: 91-104.
- WAGNER, T., 2002. Late Cretaceous to early Quaternary organic sedimentation in the eastern Equatorial Atlantic. *Palaeogeography, Palaeoclimatology, Palaeoecology*, 179: 113-147.
- WAN, X., WIGNALL, P.B. and ZHAO, W., 2003. The Cenomanian-Turonian extinction and oceanic anoxic event: evidence from southern Tibet. *Palaeogeography, Palaeoclimatology, Palaeoecology*, 199: 283-298.
- WANG, C.S., HU, X.M., JANSA, L., WAN, X.Q. and TAO, R., 2001. The Cenomanian -Turonian anoxic event in southern Tibet. *Cretaceous Research*, 22: 481-490.
- WHATLEY, R.C., PYNE, R.S. and WILKINSON, I.P., 2003. Ostracoda and palaeo-oxygen levels, with particular reference to the Upper Cretaceous of East Anglia. *Palaeogeography, Palaeoclimatology, Palaeoecology*, 194: 355-386.
- WILSON, P.A. and NORRIS, R.D., 2001. Warm tropical ocean surface and global anoxia during the mid-Cretaceous period. *Nature*, 412: 425-429.
- WINTER, C.V., Jr., 1954. Pollard field, Escambia County, Alabama. *Gulf Coast Association of Geological Societies Transactions*, 4: 121-142.

Manuscript received March 8, 2005

Manuscript accepted September 21, 2005

The coral fauna of the Holkerian/Asbian boundary stratotype section (Carboniferous) at Little Asby Scar (Cumbria, England) and implications for the boundary

Markus Aretz¹ and John Nudds²

¹Institut für Geologie und Mineralogie, Universität Köln, Zülpicher Str. 49a, 50674 Köln, Germany

markus.arez@uni-koeln.de

²School of Earth, Atmospheric and Environmental Sciences, The University of Manchester, Manchester M13 9PL, UK,

john.nudds@manchester.ac.uk

ABSTRACT: Five coral assemblages from the Holkerian-Asbian succession at the stratotype section at Little Asby Scar, Cumbria (England) have been studied. The stratotype section is located near a fault zone, and contact of the Potts Beck Limestone (earlier Asbian) and the Knipe Scar Limestones (later Asbian) is tectonically controlled.

The coral fauna of the limestone bed which defines the base of the Asbian consists of a coral assemblage which does not contain any coral taxa appearing in the Asbian. The first *Dibunophyllum*, the traditional coral genus for the Asbian-Brigantian, is not known until the overlying Knipe Scar Limestone. However, other coral taxa from the Knipe Scar Limestone are typical of the later Asbian. No coral assemblages can be doubtless assigned to the earlier Asbian. The coral assemblages of Little Asby Scar proved that the first appearance of *Siphonodendron junceum* is in the upper Asbian.

The distribution of other important biostratigraphic groups, the foraminifera and brachiopods, supports a relocation of the originally defined Holkerian-Asbian boundary. However, the bases of the biozones of the two most abundant groups, corals and foraminifera, do not coincide; Asbian foraminifera appear earlier than Asbian corals.

The attempt to correlate the Little Asby Scar succession to the Belgian Namur-Dinant basin and its standardized sedimentary sequences based on a simple presence-absence comparison of corals and foraminifera does not result in a definite correlation.

It is evident that the Holkerian-Asbian boundary as originally defined is lithostratigraphic, and that the absence of any biostratigraphic support prevents the use of that level in a chronostratigraphic context. Therefore, after a consensus on the criterion for the base of the Asbian, the stratotype section should be relocated to a better exposed section.

INTRODUCTION

Stratotype sections form the basis for regional and/or global correlation and thus are important spikes in the stratigraphical column. They are often linked to significant changes within the geological record (e.g. fauna or lithofacies) and the concept of stratotype sections is widely accepted.

The first modern biostratigraphic framework for the Lower Carboniferous succession of southern England was introduced by Vaughan (1905) who used a combination of lithology and “biozones” of brachiopods and corals (text-fig. 1). Since this pioneer work in the Bristol area, various attempts have been made to establish a general correlation for the whole of the British Isles. Facies shifts and biogeographical provincialism hampered this approach for many years. Important correlations were proposed by Garwood (1913) and Bisat (1928), but were limited to a particular region or facies. Hill (1938-41) described the distribution of rugose corals within the British Lower Carboniferous succession, and added some remarks on the existing stratigraphical framework.

It is important in the context of this study that two of Vaughan’s “zones” of the upper Viséan were named after the rugose coral genus *Dibunophyllum* (text-fig. 1) and that this genus has been used as the marker for the interval now referred to the Asbian and Brigantian substages.

Based on what was then a new stratotype concept George et al. (1976) established a chronostratigraphical framework for the Lower Carboniferous succession of the British Isles, dividing it into six regional stages: Courceyan, Chadian, Arundian, Holkerian, Asbian and Brigantian (text-fig. 1). To be consistent with the internationally recognized stratigraphic chart (Gradstein et al. 2004) these regional stages now become substages.

This subdivision was a combination of the older systems with two new approaches, first, the eustatically-controlled sea-level fluctuations (Ramsbottom 1973, 1979), and secondly, a biostratigraphy based on microfossils (Hallet 1970, Butler 1973, Conil et al. 1980). A stratotype section was established for the lower boundary of each substage. Thanks to this attempt many major problems of British Lower Carboniferous stratigraphy have been solved. As a consequence of its modern chronostratigraphical approach with defined boundaries, it was used for international correlation and was adapted in many other countries (e.g. Portugal: Herbig et al. 1999, Germany: Herbig 1998, Weyer 2001, France: Poty et al. 2002, Brazil: Melo and Lobosziak 2000, Eastern Canada: Giles and Boutilier 2003).

Notwithstanding its international recognition, further work on successions of different ages and different parts of Britain have highlighted problems in precise recognition of substage boundaries, e.g. in indicating the transitional character of the fauna considered to be significant for a stage (e.g. Somerville and

Stage	Sub-Stage	Forami-niferans	Vaughan 1905	Garwood 1913	Mitchell 1989	Meso-thems	Stainmore Trough	
VISÉAN (part)	Asbian	Brigantian						
			<i>Neoarchaediscus</i> Cf6	Horizon E	D _δ	K	limestones and shales	
Holkerian			$\alpha-\beta$	D ₂	D _δ	J	D6b	
			γ	D ₁	D ₂	I	D6a	Robinson Lst
			δ			H		
						G	D5b	Knipe Scar Limestone
				D ₁		F	D5a	Potts Beck Limestone
						E	D4	Ashfell Limestone
			S ₂	S ₂				
		<i>Kosinkotextularia</i> <i>Pojarkovella nibilis</i> Cf5						

TEXT-FIGURE 1

FIGURE 1
Overview of different British stratigraphical zonations for the Holkerian – Brigantian time interval (after Riley 1993). Foraminiferans (after White 1992, Riley 1993), mesothems (Ramsbottom 1979), lithostratigraphy of Stainmore Trough (George et al. 1976).

Strank 1984, Cozar and Somerville 2004). Riley (1993) reviewed the Lower Carboniferous biostratigraphy and chronostratigraphy, and evaluated the stratotype sections and the problems linked to them.

The use of rugose corals in Lower Carboniferous biostratigraphy is still valuable, especially in shallow-water or reefal facies. Poty (1985, and in Conil et al. 1991) proposed a biozonation based on Belgian coral assemblages applicable for regional as well as long-distance correlation. Its application is consistent in Spain, France (Boulonnais, Montagne Noire), western Germany, and most likely in Britain. Mitchell (1989) proposed a coral biostratigraphy for Britain and Jones and Somerville (1996) highlighted that rugose corals are a useful tool in Irish biostratigraphy.

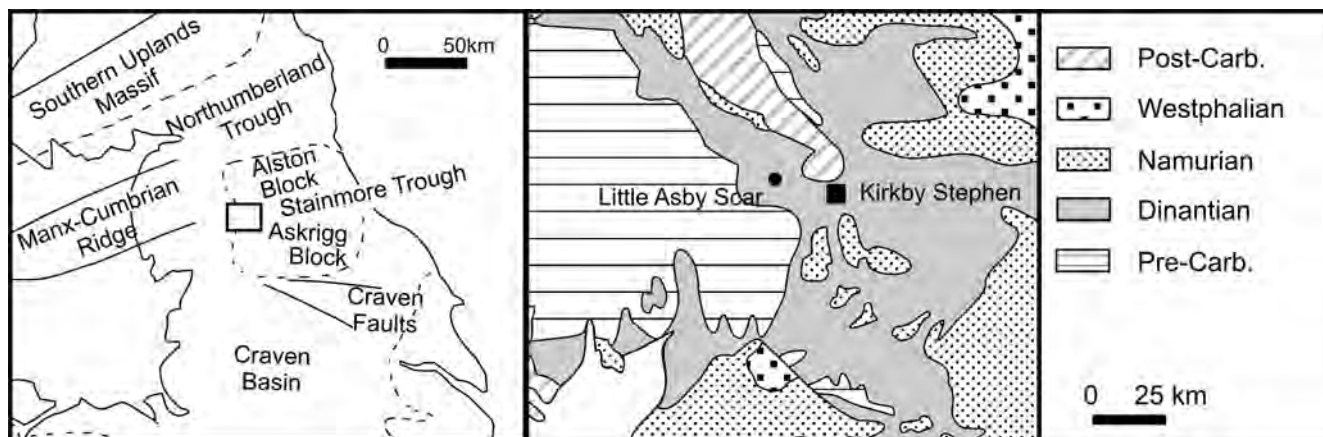
It is the aim of this study (1) to describe the diverse coral fauna of the section at Little Asby Scar, (2) to place the taxa into their

biostratigraphic context, and (3) to discuss the position of the Holkerian/Ashian boundary.

SETTING AND SUCCESSION

The Holkerian/Asbian boundary was defined at Little Asby Scar, near Ravenstonedale (Cumbria, northern England) by George et al. (1976). Little Asby Scar is situated in the Stainmore Trough, a small intraplatform "basin" between the Alston and Askrigg Blocks (text-fig. 2).

The exact location of the stratotype section is in a hillside north of Potts Beck and east of Mazon Waths farm (NY 6988 0827). The boundary interval crops out discontinuously for at least one hundred metres. The precise boundary is a thin mudstone/shale bed (bed e of George et al. 1976) between the Ashfell Limestone (Holkerian) and the Potts Beck Limestone (Asbian), which could not be traced horizontally for the entire exposed boundary interval by the authors, and which shows significant



TEXT-FIGURE 2
Location of the stratotype section at Little Asby Scar (after Ramsbottom 1981).

variations in thickness throughout its exposures (0-15cm) (text-fig. 3).

The original published log of the section comprised only the boundary interval of the succession (George et al. 1976). More complete and detailed logs can be found in Ramsbottom (1981), Strank (1981) and White (1992). The boundary interval is well exposed and well documented, but in the younger part the logs show some inconsistencies due to poor outcrop. One problem is the continuity between the lower and upper benches of the scarp (so-called in Ramsbottom 1981), which are equivalent to the Potts Beck Limestone and overlying Knipe Scar Limestone, respectively (White 1992; See also text-fig. 3 herein.) The contact is not exposed; Ramsbottom estimated a 1.4 m thick black mudstone, whereas White (1992) found no evidence for this and speculated on a fault-bounded contact (for a discussion of this problem see below).

The succession of the stratotype area is characterized by fast changing shallow-marine facies conditions. According to earlier workers crinoidal limestones of various composition and texture dominate the succession. Various lithotypes (e.g. bioclastic limestone, shales, dolomites) are intercalated into this dominant lithotype. Each lithotype does not represent a distinctive unit; the units of George et al. (1976) and Ramsbottom (1981) are often composite. The macrofauna is mostly fragmented, and cross-bedding is seen on various surfaces throughout the succession.

At the top of the Ashfell Limestone, the succession is dominated by medium bedded, fine-grained limestone. Some shaly, grey-coloured intercalations occur in varying thickness, and are of discontinuous horizontal extension.

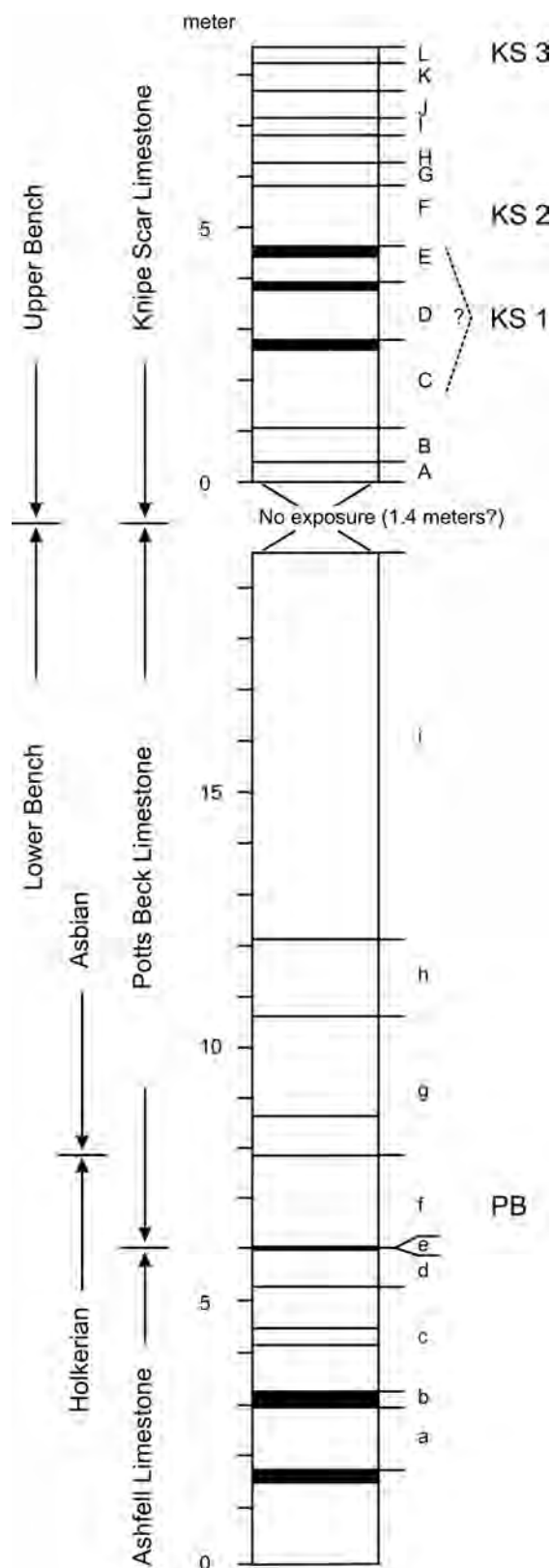
The lowest bed of the Potts Beck Limestone (bed f of George et al. 1976; text-fig 3 herein) is rich in chert and corals, and is referred to herein as the 'biostrome'. Aretz and Nudds (in press) provide detailed analyses of the biotic composition and facies, and an interpretation of its formation. This bed is the best exposed of the entire succession. From the stratotype section, it can easily be traced along strike for about 900 m towards the west, but only 50 m towards the east, where it bends downwards, follows a ridge and disappears under huge blocks of scree. Further east it is not exposed.

The biostrome is 1.4 m thick in the stratotype area and consists mainly of fragments of *Siphonodendron* and chaetetid sponges. The bed is highly silicified, seen in numerous chert-nodules, but also in the silicified macrofauna and some layered chert-concentrations. The grain-sizes vary throughout the bed, but are generally coarse. Cross-stratification, upside-down orientations, and numerous fragmented bioclasts are seen on various surfaces of the exposure and indicate shallow water environments at the boundary interval.

Above the biostrome the Potts Beck Limestone consists of bedded limestone of various grain-sizes, mostly rich in crinoids. Most parts of the succession might be bioclastic, often grainstones. Micrite-dominated textures, weathered to a brownish colour, are rare, but some of them are very rich in vertebrate remains (pers. com. Dr. H. M. Weber, Bergisch-Gladbach). Vertical and horizontal variations of the grain sizes occur over short distances and the different textures given by White (1992) are common. Small-scale cycles might be indicated by the variation of grain-sizes and textures (see also White 1992, text-fig. 8.29). A diverse macrofauna (brachiopods, corals, gastropods, and pelmatozoans) is observed and seems to be more common in coarser textures.

Aretz and Nudds (in press) showed the dominance of three facies types at the boundary interval: (1) fine-grained foram-iniferan-*Koninckopora* grainstone, (2) coarse-grained bioclastic grainstone, and (3) coral-chaetetid rudstones. Facies type 3 is restricted to the biostrome, while facies types 1 and 2 are found below and above it. Occasionally facies type 2 is also found within the biostrome. Facies type 1 dominates the units well below the biostrome, but directly below it facies type 2 is dominant. Above the biostrome, the distribution is less obvious. A clear vertical zonation of facies types is not seen, but within the first metre, facies type 2 again is dominant.

The biostrome indicates a general phenomenon of the geological structure observed in this area. The view from the opposite hillside, on the southern bank of Potts Beck, reveals that west of the stratotype the beds are sub-horizontal, whereas immediately east of the stratotype the beds turn steeply down (30-40°). Further east, the exposure is again sub-horizontal. This arrangement is also seen in the morphology of the hillside (text-fig. 4).



TEXT-FIGURE 3

Stratigraphic log of the stratotype section at Little Asby Scar Scar (re-drawn from Ramsbottom 1981). Bed numbers of Ramsbottom (1981), The positions of the coral associations PB and KS 1-3 are indicated. The log shows the proposed position of the Holkerian/Asbian boundary based on the coral fauna

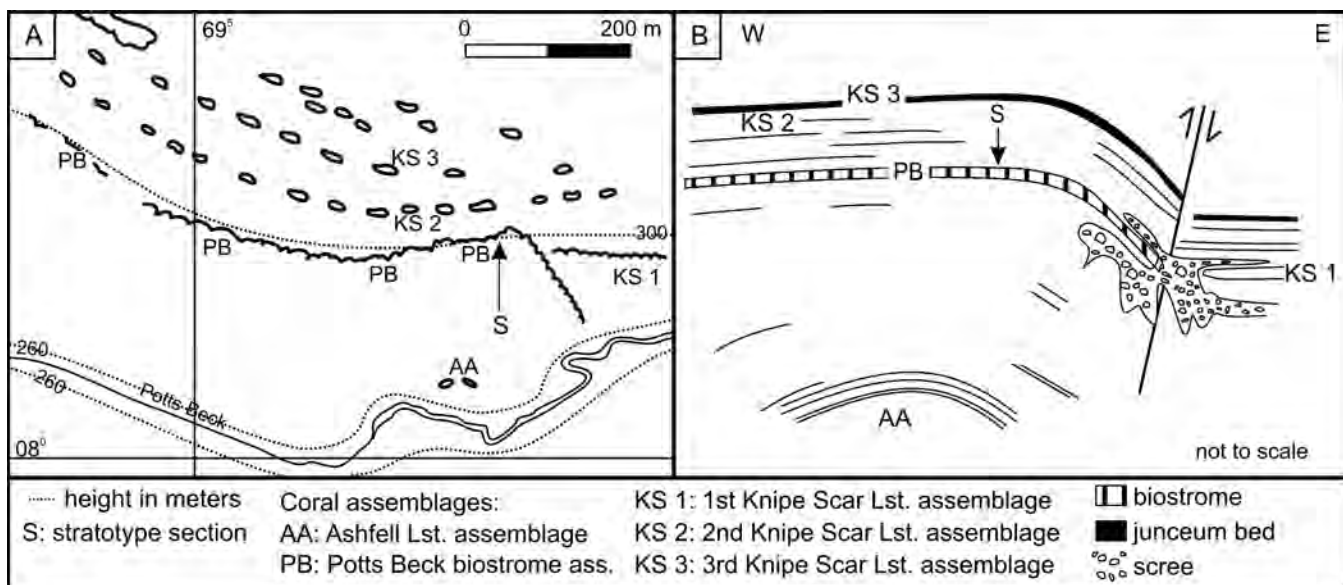
At the bottom of the hillside (50m below the stratotype), an exposure of limestones beds, containing highly silicified rugose corals and gastropods, reveals an explanation of the structure observed higher up. These beds (AA, text-fig. 4) show an anticline, with a smooth western flank and a somewhat steeper eastern flank.

Higher up the hill this anticline is seen in its wider extent. The eastern flank is disturbed by a fault which downthrows to the east and separates the lower and upper benches of Ramsbottom (1981). Therefore, at least on the eastern flank up to the area of the stratotype section the contact of the Potts Beck Limestone and Knipe Scar Limestone is due to tectonic movements. The exact orientation and position of the fault could not be deduced from the outcrop due to the poor exposures, but it is important since the completeness of the succession and the contact of Potts Beck and Knipe Scar limestones depend on its geometry. The biostrome (PB in text-fig. 4) follows the anticlinal structure perfectly, but it could not be traced to the east of the fault zone where it is possibly hidden by scree and grass. However, the fault zone does not disturb the succession in the immediate stratotype section, and therefore it does not affect the defined Holkerian/Asbian boundary.

CORAL FAUNA

Rugose coral assemblages (more than 150 specimens) have been collected at five localities on Little Asby Scar (text-fig. 4). A few samples came from the bottom of the hillside (AA), from the small exposure of the Ashfell Limestone referred to above. Numerous corallites have been collected from the biostrome (PB), and also in a slightly higher coral bed which outcrops east of the fault (KS 1). Two further assemblages were found approximately 21m and 24m above the biostrome in the vertical prolongation of the stratotype section, in the ridge which forms the crest of Little Asby Scar (KS 2 and KS 3).

The composition of these five coral assemblages differs significantly (text-fig. 5). Besides a few undeterminable fragments of solitary corals, only highly silicified colonies of *Lithostrotion vorticale* (Parkinson 1808) have been recovered from assemblage AA. The coral fauna of the biostrome (PB) is relatively diverse. It comprises *Siphonodendron* sp., *Siphonodendron martini* (Milne-Edwards and Haime 1851), *Siphonophyllia sibylli* Semenoff-Tian-Chansky 1974, *Axophyllum vaughani* (Salée 1913), *Caninophyllum archiaci* (Milne-Edwards and Haime 1852), numerous heterocorals, and syringoporoid tabulate corals. Assemblage KS 1, east of the fault zone, comprises *Siphonodendron martini*, *Caninophyllum archiaci* (Milne-Edwards and Haime 1852), *Dibunophyllum bipartitum* (McCoy 1849), *Koninckophyllum* sp., *Haplolasma* sp., undeterminable axophyllids, and syringoporid corals. Assemblage KS 2, high on the western scarp, contains *Lithostrotion maccoyanum* Milne-Edwards and Haime 1851, *Siphonodendron junceum* (Fleming 1828), *Siphonodendron pauciradiata* (McCoy 1844), *Siphonodendron martini* (Milne-Edwards and Haime 1851), *Siphonodendron cf. scaleberense* Nudds and Somerville 1987, *Palaeosmilia murchisoni* Milne-Edwards and Haime 1848, and rare heterocorals. Finally at the top of both the western and eastern scarps is a bed packed with *Siphonodendron junceum* (KS 3), which is an excellent marker horizon and which allows interpretation of the folding and faulting in this area (text-fig. 4). This bed probably equates with bed L of Ramsbottom (1981), the uppermost bed of the Knipe Scar Limestone in his measured section (see text-fig. 3).



TEXT-FIGURE 4

The stratotype section at Little Asby Scar. A, topographic map (modified from Ramsbottom 1981); B, sketch of the structure of the hillside from the southern bank of the Potts Beck (not to scale).

Heterocorals occur in greater abundance in assemblage PB, especially in the upper part of the biostrome, but occur scattered throughout the entire succession. Tabulate corals are common in parts of the biostrome (see Aretz and Nudds, in press), but only single corallite fragments have been recovered elsewhere.

TAXONOMY

The detailed descriptions of the Little Asby Scar specimens allow some precisions on the variability of the taxa, especially for some rare taxa as *Siphonophyllia sibilyi*.

Class ANTHOZOA Ehrenberg 1834

Subclass RUGOSA Milne-Edwards and Haime 1850

Order STAURIIDA Verrill 1865

Suborder CANINIINA Wang 1950

Family CYATHOPSIDAE Dybowski 1873

Genus *Siphonophyllia* Scouler in McCoy 1844

Siphonophyllia sibilyi Semenoff-Tian-Chansky 1974

Plate 1, figures 1-3

"A Campophyllid" Sibily 1906, p.369, pl. 31, fig. 3.

**Siphonophyllia sibilyi* SEMENOFF-TIAN-CHANSKY 1974, p. 184, fig. 68, pl. 47, fig. 1-3, pl. 50, fig. 1. — KHOA 1977, p. 371, pl. 19, fig. 1a-e. — POTY 1981 p. 53, pl. 26, fig. 5. — RODRIGUEZ and FALCES 1992, p. 191, pl. 16, fig. 3. — SOMERVILLE 1997, pl. 2, fig. 6.

Diagnosis. Emended from Semenoff-Tian-Chansky (1974) and Poty (1981). Medium-sized *Siphonophyllia* of up to 4cm in diameter. Thin and sinuous major septa often slightly thickened at the base of the tabularium. Length of the major septa 2/3 of the corallite-radius. Short minor septa eventually developed in the tabularium, mostly reduced to spines in the inner dissepimentarium. Dissepimentarium consists of an inner zone of simple and lonsdaleoid dissepiments, and an outer zone of large lonsdaleoid dissepiments. Marked cardinal fossula, alar fossulae may be developed. Wall and septa mostly laminar.

Material. Fragments of four corallites from the biostrome (PB). LAS 104, 110, 148, 150.

Description. (i) external characters. The abraded corallites are up to 2.8cm in diameter; original maximum diameter are of about 3.5cm. The corallites are ceratoid to sub-cylindrical. The outer surface shows transversal growth rings and longitudinal furrows and ribs. Furrows and ribs are not connected to the insertion of the septa. Rejuvenescence might occur.

(ii) internal characters. 40-50 septa in two orders. The major septa are thin and sinuous, but might be slightly thickened at the base of the tabularium. Lonsdaleoid dissepiments interrupt the major septa in the outer dissepimentarium, where they might persist as septal crests. The major septa extend up to 2/3 of the corallite-radius. The cardinal septum is shortened and a distinctive fossula developed. Alar fossulae might be developed. The minor septa are short and mostly reduced to spines within the inner dissepimentarium and the base of the tabularium.

The dissepimentarium is narrow (4–6mm) and consists of an outer, often slightly thicker zone of lonsdaleoid dissepiments and an inner zone of simple and lonsdaleoid dissepiments. The tabularium comprises 2/3 of the corallite diameter.

The dissepiments are elongated and subvertical declined. The tabulae are complete, flat, and slope down at the margins. There are 8-10 tabulae per centimetre.

Discussion. The larger size of the Little Asby Scar specimens is the only differences to those described from Algeria (Semenoff-Tian-Chansky 1974) and Belgium (Poty 1981). This confirms the observation by Semenoff-Tian-Chansky when comparing his Algerian specimens to a "campophyllid" described by Sibily (1906) from the Mendips. The Polish specimen described by Khoa (1977) is very close to some Little Asby Scar specimens, especially in the development of alar fossulae. However, because the descriptions are based on very few specimens,

there is not much known about the variability of this rare species. The development of an alar fossulae may be a significant difference, but Khoa (1977) reported it not from all sections of his single specimen, thus indicating some important intra-specific variability. The Belgian and Algerian specimens do not show the phenomenon at all.

Age and occurrence. The Algerian type material is probably Brigantian in age. The British specimen of Sibly is D1 (=Asbian) in age. Poty (1981) reported *S. siblyi* from the Calcaire de Seilles (now Seilles Member of the Grands Malades Formation, Poty et al. 2002). This correlates to the Holkerian substage in Britain. The Spanish material (Rodriguez and Falces 1992) is from the Asbian, the Irish from the Brigantian (Somerville 1997).

Genus *Caninophyllum* Lewis 1929

Caninophyllum archiaci (Milne-Edwards and Haime 1852)
Plate 1, figures 4, 6

**Cyathophyllum archiaci* MILNE-EDWARDS and HAIME 1852, p. 183, pl. 34, fig. 7. — POTY 1981, p. 50, figs., 46, 47, pl. 23, fig. 6, pl. 24, fig. 1. [cum syn.]

Material. Three large fragments: two from KS 1 (LAS 71, 182), one from PB (LAS 135).

Description. (i) external characters. The fragments lack their outer walls and parts of their dissepimentarium. They are up to 10.4cm long and up to 4.5-6.4cm in width assuming a cylindrical corallite.

(ii) internal characters. There are two series of up to 60 septa. The long major septa (up to 30mm) are sinuous in the dissepimentarium and become straight to slightly sinuous in the tabularium. They do not reach the centre and leave an open central area of 1-1.5cm in diameter. Major septa are thin (0.1mm) within the dissepimentarium, become thick at the base of the tabularium (0.8mm) and thin towards the centre. The dilation is weaker in the counter than in the cardinal quadrants of the tabularium. The cardinal septum shortens (at least 4.3mm) in a prominent fossula. The length of the minor septa varies. In specimen LAS 71 they are continuous throughout the dissepimentarium and end after a few millimeters in the tabularium. Near the fossula minor septa are dilated at the proximal end and might be connected to the neighbouring major septum. The minor septa are thickened when entering the tabularium. This thickening is more prominent in the cardinal areas. In specimen LAS 182, they are shorter and do not persist within the tabularium.

The dissepiments are mostly simple, but they become very irregular when minor septa are short, are sometimes arranged in a herringbone pattern, sometimes discontinuous. The structure of the dissepimentarium is highly variable.

In longitudinal section, the dissepimentarium consists of numerous rows of steeply declined globose to elongated dissepiments (0.7-1.5mm long, 0.7-0.9mm high). The wide tabularium comprises up to 2/3 of the corallite. The complete tabulae with slightly downturned edges are wide and horizontally arranged. There are about 8 tabulae per centimetre.

Discussion. These specimens fit well into the description of Lewis (1929) who observed modifications in the thickness of the septa, the arrangement of the dissepimentarium and the length of the cardinal septum throughout the stratigraphic re-

cord of this species (from S1-D3= Upper Arundian – Brigantian). Lewis distinguished three distinctive types for the S1, S2-D1 and D2-D3 intervals. The specimens recovered at Little Asby Scar probably belong to the “*halkynense*” type (=S2-D1).

Age and occurrence. Reported in the British Isles from the late Arundian to Brigantian (Lewis 1929), in Belgium from the Lives-Formation, Livian, Middle Visean. (Poty 1981).

Suborder AULOPHYLLINA Hill 1981

Family PALAEOSMILIIDAE Hill 1940

Genus *Palaeosmilia* Milne-Edwards and Haime 1848

Palaeosmilia murchisoni Milne-Edwards and Haime 1848
Plate 1, figure 5

**Palaeosmilia murchisoni* MILNE-EDWARDS AND HAIME 1848, p. 261. SEMENOFF-TIAN-CHANSKY 1974, p. 160, fig. 60-62, 64, pl. 39, fig. 1-5, pl. 40, fig. 1, 2, pl. 41, fig. 1-5, pl. 42, fig. 1-3, pl. 71, fig. 4. [cum syn.]. — POTY in KIMPE et al. 1978, pl. 5, fig. 6, 7. — POTY 1981, p. 46, fig. 43, pl. 20, fig. 7, 8, pl. 21, fig. 2. — POTY and HANNAY 1994, p. 60, pl. 3, fig. 1.

Material. Three fragments recovered from assemblage KS 2 (LAS 50-52)

Description. The recovered fragments fit well into the variability of this species (Semenoff-Tian-Chansky 1974). The LAS specimens are up to 5.9cm in diameter. There are two series of 50-81 septa. The major septa always reach to the axis. The minor septa are up to 2/3 as long as the major septa. Septa are thin and for the most part slightly sinuous. The dissepimentarium consists of numerous rows of often elongated, regular dissepiments. The dissepiments are often arranged sub-horizontally in the outer part of the dissepimentarium; towards the axis they become inclined. Sometimes lonsdaleoid dissepiments might be developed at the outer edge of the corallite. The tabularium consists of domed tabulae, sagging in its central part.

Age and occurrence. This species is common throughout the entire Viséan (entry in Cf4a2 biozone) and early Namurian (Serpukhovian) successions of Europe and Northern Africa (see Mitchell 1989, Perret and Semenoff-Tian-Chansky 1971, Semenoff-Tian-Chansky 1974).

Family AULOPHYLLIDAE Dybowski 1873

Genus *Dibunophyllum* Thomson and Nicholson 1876

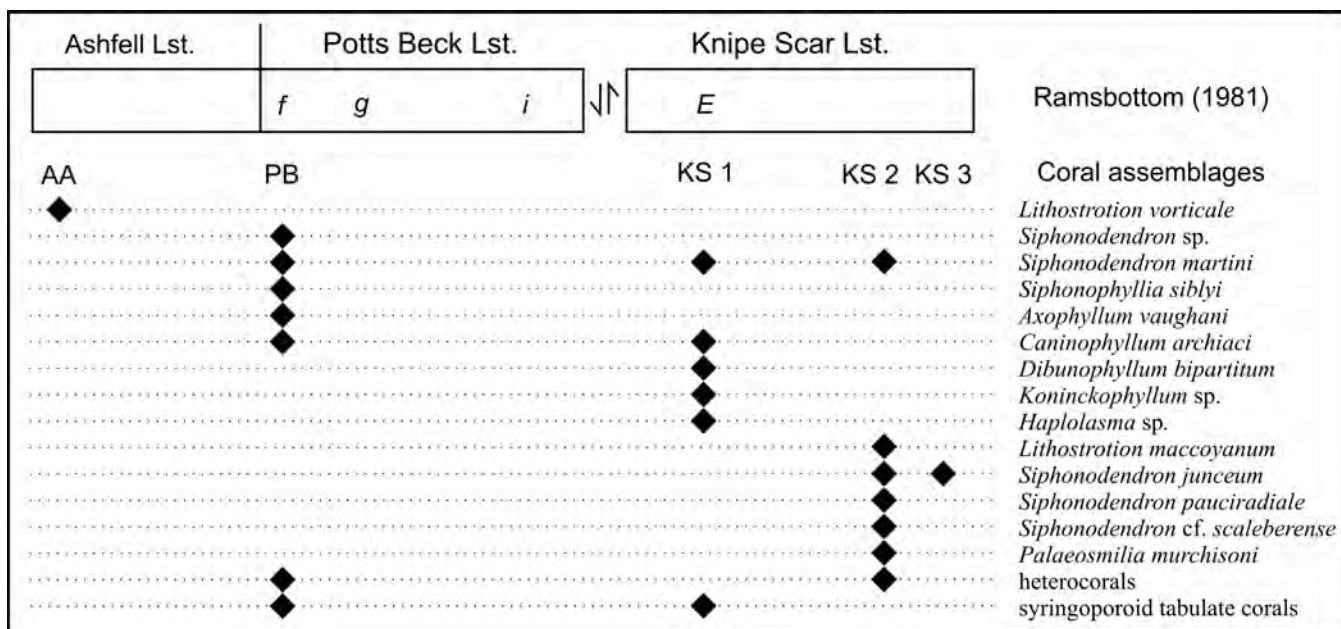
Remarks. Following the definition of Hill (1938-1941), later amended by Semenoff-Tian-Chansky (1974), the main characteristics of this genus are highly variable. The genus was derived from many rapidly evolving phylogenetic branches and its separation from related genera, such as *Clisiophyllum*, *Koninkophyllum* and *Arachnolasma*, maybe sometimes highly questionable (Fedorowski 1971). Therefore, many species in different genera are synonymous (see Hill 1938-41).

Dibunophyllum bipartitum (McCoy 1849)

Plate 2, figures 1-6

**Clisiophyllum bipartitum* MCCOY 1849, p. 2. — FEDOROWSKI 1971, p. 57, text-fig. 18, 19, 20, 21, pl. 3, fig. 6-9, pl. 4, fig. 1-8, pl. 5, fig. 1-8, pl. 15, fig. 1-8.

Dibunophyllum bipartitum (McCoy). — POTY 1981, p. 41, text-fig. 40, pl. 18, fig. 1-3. [cum syn.]. — HERBIG 1986, p. 195, Fig. 3, fig. 6. — POTY and HANNAY 1994, p. 60, pl. 3, fig. 1. — SOMERVILLE 1997, pl. 1, fig. 3.



TEXT-FIGURE 5

Distribution of the corals in the Little Asby Scar section showing the bed numbers of Ramsbottom (1981) and the coral assemblages (this paper).

?*Dibunophyllum burhennei* (Brüning 1923). — Weyer 2001, pl. 4, fig. 2. — Rodriguez 2002 et al. p. 67, pl. 3, 1-9.

Material. Ten corallites, mostly fragments, from assemblage KS 1, LAS 70, 72, 73, 170, 173, 174, 176, 178, 179, 185.

Description. (i) external characters. The corallites are trochoid to cylindrical. The maximum diameter is 2.8cm and the maximum height 4.5cm. The outer surface shows horizontal growth lines. The calice is not preserved.

(ii) internal characters. Septa are arranged in two series, each series comprises up to 53 septa. The major septa are straight near the wall, sometimes curved. Thickenings are observed at the base of the tabularium. The cardinal septum is shorter than the other major septa. The counter septum is often linked to the prominent axial structure. The minor septa are short (< 2.5mm) or sometimes developed just spines and are restricted to the outer dissepimentarium.

The axial structure is large and comprises about 1/3 of the corallite diameter. It consists of a thicker medial plate (up to 0.4mm thick) and is surrounded by some septal laminae (4-8 on each side) and numerous axial tabellae. The organization of the axial structure is variable, the prominence of the medial plate might be reduced, the number of axial lamellae and axial tabellae (highly variable) changes.

The dissepimentarium is wide (1/3 of the corallite) and consists of regular dissepiments; herringbone dissepiments are partly observed. The dissepiments are often elongated (up to 3.2mm long and 1.0mm high; mean 0.6mm high and 1.6mm wide), rarely globose. There are 3 to 6 rows of dissepiments, steeply declined (45-75°). Tabulae are incomplete, generally inclined (20°) and convex. The axial tabellae are numerous, either convex, and domed or steeply inclined (70°).

Discussion. The Little Asby Scar material is typical for this well-known species. Differentiation into subspecies according to Hill (1938-41) is not made, since Semenoff-Tian-Chansky (1974) showed the existence of form groups within this species.

Age and occurrence. *D. bipartitum* is widely distributed in late Viséan and early Namurian European successions. Mitchell (1989) concluded that *D. bipartitum* appears in the Asbian, but did not record it from the lower part of the Asbian. This observation is confirmed by the Belgian and French datasets (Poty 1981, Poty and Hannay 1994) where this species appears in foraminiferan biozone Cf6β = middle part of RC7α.

Genus *Koninckophyllum* Thomson and Nicholson 1876

Koninckophyllum sp.

Plate 2, figure 7

Material. One transverse section in a fragment from assemblage KS 1. LAS 181

Description. (i) external characters. The fragment is 2.3cm in diameter and several mm long. The calice and outer surface are not preserved.

(ii) internal characters. There are two series of 54 septa. The major septa are thin, mostly straight and become somewhat sinuous towards their end. They end free in the tabularium and are not longer than 1.0cm. Only the counter septum (?) reaches the axis and is connected to the columella. Minor septa are short and mostly restricted to the dissepimentarium, sometimes entering the tabularium as short spines.

The columella is distinct (3.7mm long) and thickened in its centre (0.5mm).

The dissepimentarium is narrow (2–4mm) and consists of some irregular rows of regular dissepiments. Herringbone structures might develop where minor septa are very short.

Discussion. The genus *Koninckophyllum* is fairly common in the British Carboniferous. Numerous species have been described, but they might be partly synonymous (see Hill 1938). The characteristic variability in this genus could not be deduced from only one transverse section. Therefore, a specific assignment of the single specimen found at Little Asby Scar is not possible.

Sudorder LITHOSTROTIONINA Spasskiy and Kachanov 1971

Family LITHOSTROTIONIDAE D'Orbigny 1852

Subfamily LITHOSTROTIONINAE D'Orbigny 1852

Genus *Lithostrotion* Fleming 1828

Lithostrotion maccowanum Milne-Edwards and Haime 1851

**Lithostrotion maccowanum* MILNE-EDWARDS and HAIME 1851, p. 444.—NUDDS 1980, p. 388, fig. 3a.—POTY 1981, p. 24, fig. 14–16, pl. 7, fig. 3. [cum syn.].—ARETZ 2001, fig. 3/5.—ARETZ 2002, p. 109, pl. 9, fig. 4, 5.

Material. Fragment from assemblages KS 2, LL.12667.

Description. (i) external characters. The corallum is massive and cerioid with polygonal corallites, sometimes slightly cylindrical. Their diameter varies from 2–4mm. The calices are shallow with a prominent columella. Increase has not been observed.

(ii) internal characters. Corallites are polygonal, sometimes pentagonal, hexagonal or heptagonal. The septa are in two orders, major and minor which are usually easily distinguishable. The number of septa varies between 12–14 of both orders and the major septa usually extend to the columella or abut onto neighbouring septa. Minor septa are variable in length; they just extend into the tabularium so that their length is proportional to the width of the dissepimentarium which itself is very variable. Both orders of septa are dilated in the dissepimentarium and thinner at their axial ends. All septa normally extend to the epitheca and there is usually a prominent columella. The narrow tabularium of this species is characteristic; it has an overall mean of 1.5mm. The width of the dissepimentarium is less characteristic showing considerable variation. In some corallites there is only one row of dissepiments; in others there may

be three or four rows. The inner row of dissepiments is dilated and regular, whereas outer dissepiments are thinner and more irregular. All sections of dissepiments are concave towards the axis. The overall tabularium-diameter is very variable due to variation in the width of the dissepimentarium. It ranges from 2.0mm to 4.0mm. Tabulae are usually complete and tent-shaped. Occasionally they are incomplete when a periaxial series is developed at the periphery of the tabularium.

Discussion. This is the smallest known cerioid species of *Lithostrotion*. The specimen recovered at Little Asby Scar fits well into the descriptions of Semenoff-Tian-Chansky and Nudds (1979).

Age and occurrence. *L. maccowanum* is fairly common in Europe (Mitchell 1989, Poty 1981, Rodriguez et al. 2002, Jones and Somerville 1996). Its short stratigraphic range (late Asbian – early Brigantian) is important for stratigraphic correlations.

Lithostrotion vortcale (Parkinson 1808)

Plate 2, figure 8

**Madrepora vorticalis* Parkinson 1808, p. 45, pl. 5, fig. 3, 6.

Lithostrotion vortcale (Parkinson).—NUDDS 1980, p. 388, fig. 3c.—POTY 1981, pl. 22, fig. 12, 13, 15, 16, pl. 6 fig. 1–3, pl. 7, fig. 1, 2. [cum syn.].—RODRIGUEZ and FALCES 1992, p. 200, pl. 18, fig. 4.—POTY and HANNAY 1994, p. 63, pl. 4, fig. 3.—RODRIGUEZ et al. 2002, p. 20, fig. 6a–i.—ARETZ 2002, p. 111, pl. 10, fig. 3.

Material. Two strongly silicified fragments from assemblage AA, LAS 54, 55.

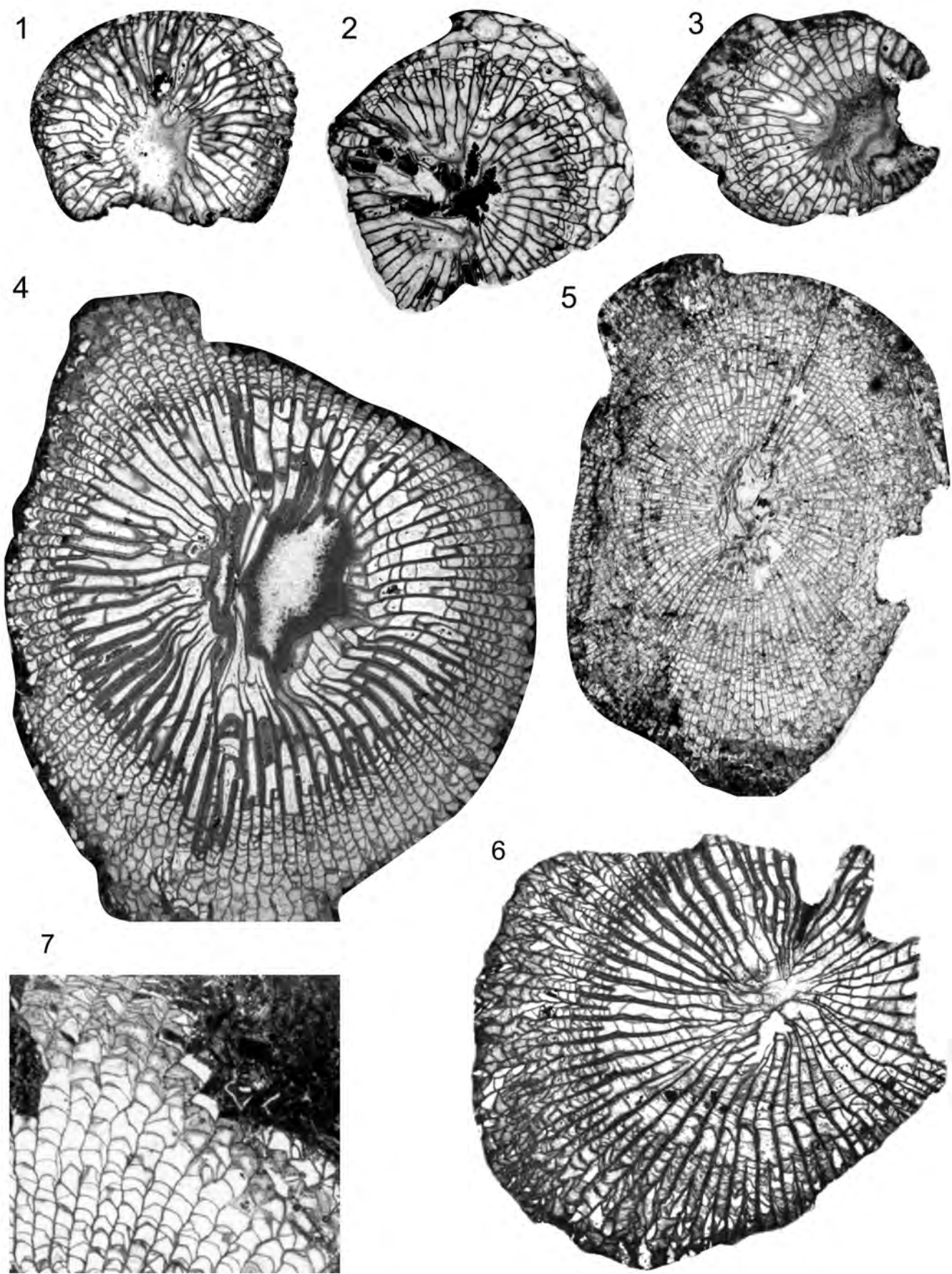
Description. (i) external characters. Hemispherical, massive corallum with a maximum height of 15cm and a diameter of 25cm. Corallites are polygonal, often pentagonal or hexagonal. Their width varies from 5 to 12mm. Increase is by non-parricidal lateral budding. The calice has not been observed.

(ii) internal characters. The corallite wall is often only 0.1mm thick. The septa are straight to slightly sinuous. They are in two series, 20–23 of each. The length of the major septa is variable (2.2–3.2mm). Septa are often connected to the styliform columella, blind-ending septa occur. Cardinal and counter septum are recognized by the orientation of the columella and are connected to it, otherwise they are not differentiable from the other major septa. The columella itself, consists of a single lenticular plate of varying thickness within one corallite. The minor septa cross the dissepimentarium and end after about 0.2–

PLATE 1

All specimens $\times 2$, except number 7, $\times 5$.

- 1–3 transverse sections of *Siphonophyllum sibblyi* Semenoff-Tian-Chansky 1974, LAS 148 (2), LAS 150 (1, 3), Potts Beck Biostrome assemblage, Holkerian?
- 4, 6, 7 *Caninophyllum archiaci* (Milne-Edwards and Haime 1852), transverse sections; 4, from the biostrome, LAS 135, Holkerian; 6, Knipe Scar assemblage 2, later Asbian, LAS 71; 7, detail of the irregular organized dissepimentarium of LAS 71.
- 5 *Palaeosmilia murchisoni* Milne-Edwards and Haime 1848, transverse section LAS 50, Knipe Scar assemblage 2, later Asbian.



0.4mm within the tabularium. The diameter of the tabularium is 3.0–4.5mm in width (mean 3.6mm). Dissepiments are globose to elongated (0.17–0.7mm long). The structure of the dissepimentarium in a single corallite is very variable: the inclination of the dissepiments varies from 0 to 60° and the number of dissepimental rows from 1 to 4. Some lonsdaleoid dissepiments might be developed often connected to future offsets. The tabulae are incomplete and increasingly convex towards the axis.

Discussion. The two specimens recovered at Little Asby Scar fit well into the species-descriptions of Hill (1940) and Poty (1981).

Age and occurrence. In Britain, *L. vorticale* appears in the Holkerian and continues to the Late Brigantian (Mitchell 1989). Similar observations are made from western Europe by Poty and Hannay (1994) and Rodriguez et al. (2002).

Genus *Siphonodendron* McCoy 1849

Siphonodendron junceum (Fleming 1828)

Plate 2, figures 9-10

**Caryophyllia juncea* FLEMING 1828, p. 508.

Lithostrotion junceum (Fleming). — CALDWELL and CHARLES-WORTH, 1962 p. 374, pl. 14, fig. 1. — NUDDS 1980, p. 387, fig. 1a.

Siphonodendron junceum (Fleming). — POTY 1981, p. 32, fig. 26, pl. 13, fig. 1. [cun syn.]. — FONTAINE et al. 1991, p.46. — POTY and HANNAY 1994, p. 65, pl. 5, fig. 4. — SOMERVILLE 1997, pl. 1, fig. 6.— ARETZ 2001, fig. 3/7. — RODRIGUEZ et al. 2002, p. 24, fig. 10a-f. — ARETZ 2002, p. 111, pl. 3, fig. 1, 2; pl. 10, fig. 4-6.

Material: 3 specimens from assemblages KS 2 and KS 3, LAS 51, GIK 1771, LL. 12668.

Description. (i) external characters. Phaceloid, sometimes dendroid colonies with a spreading corallum ranging up to a metre in diameter and 35cm in height. The cylindrical corallites are 2.4 to 3.2mm in diameter. The increase is lateral. The surface and calice have not been observed.

(ii) internal characters. There are 14-18 septa in mature stages. The major septa are thin and slightly sinuous. Their length is variable, sometimes they are connected to the columella, sometimes they leave a central space. The columella is often a thin axial plate (lanceolate), but thickenings in its middle part are also common and a simple spider-web structure might be developed by connection to the major septa. Less commonly it is absent; such a diphymorphic state is usually restricted to single corallites, but sometimes affects large parts of the corallum. Minor septa are mostly developed as short spines. A disse-

pimentarium is not observed. The morphology of the tabularium depends on the organization of the columella. The incomplete tabulae (6-8 per 0.5cm length) generally rise convex (20-50°) towards the columella. A depression of the tabulae might be developed near the wall. The tabulae are complete in diphymorphic corallites and arranged horizontally in the centre of the corallite.

Age and occurrence. This species is common in Asbian and Brigantian successions of northwestern Europe and Spain. Its biostratigraphical occurrence is somewhat unclear. Mitchell (1989) reported *S. junceum* from the beginning of the Asbian (Fauna F) to the Late Brigantian (Fauna K) based on British coral assemblages. Mainly based on coral associations of Belgium, the Boulonnais and southern Britain, Poty (1981, 1985, 1991 in Conil et al.) considered the entry of this species to be somewhat later in the foraminiferan biozone (Cf6γ), equivalent to the Late Asbian. In his coral biozonation, the appearance of *S. junceum*, *L. maccoyanum* and *Aulophyllum fungites* marks the biozone RC7β. In north-western Ireland, *S. junceum* first appears in the foraminiferan biozone (Cf6γ) as in Belgium (Cozar et al., in press). In Spain, *S. junceum* occurs in the Asbian and continues through the Brigantian (Rodriguez et al. 2002, fig. 2).

Siphonodendron pauciradiata (McCoy 1844)

**Lithodendron pauciradialis* MCCOY 1844, p. 189, pl. 27, fig. 7.

Lithostrotion pauciradiata (McCoy). — CALDWELL and CHARLESWORTH 1962 , p. 376, pl. 14, fig. 2.

Siphonodendron pauciradiata (McCoy). — NUDDS 1980, p. 387, fig. 1e. — POTY 1981, p. 31, fig. 25, pl. 12, fig. 5, 6. [cun syn.]. — FONTAINE et al. 1991, p.47. — SOMERVILLE 1997 p.45, pl. 1, fig. 1.— RODRIGUEZ et al. 2002 p. 26, tab. 4, fig. 12 a-d. — ARETZ 2002, p. 11, fig. 1-3.

Material. A single fragment from assemblage KS 2. LL.12669.

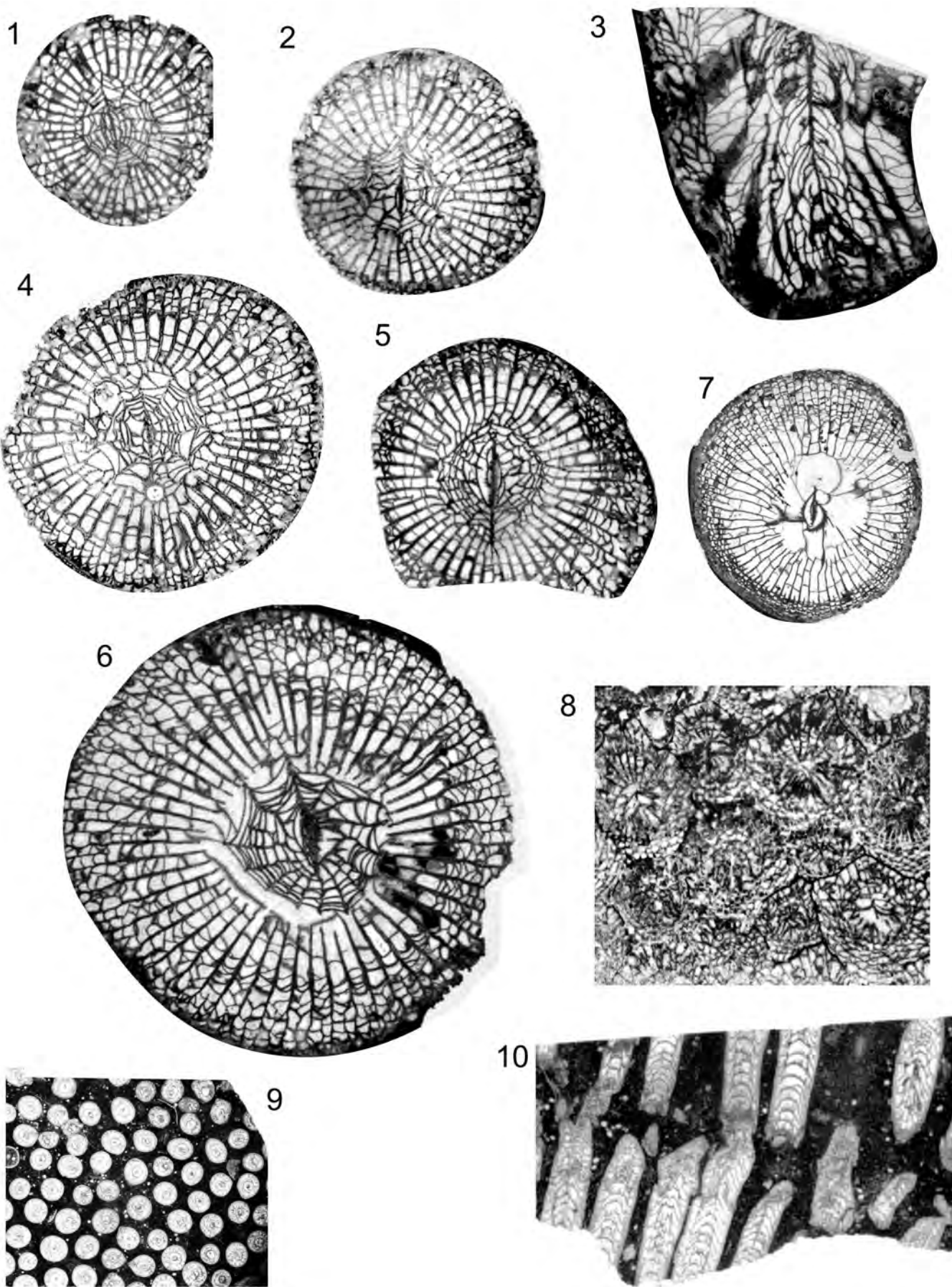
Description. (i) external characters. The corallum is fasciculate and phaceloid with sub-parallel cylindrical corallites which often temporarily coalesce in a partly cerioid habit. Calices and epithecal surfaces have not been observed.

(ii) internal characters. The number of major septa ranges from 18-22. Some of the major septa are long, extending to the columella; this is usually the case with the cardinal and counter cardinal septa and some of the other primary septa. Other major septa extend only halfway to the axis or abut onto the adjacent major septa. Minor septa are short, only just penetrating the tabularium. Both orders of septa may be slightly dilated in the dissepimentarium although this is not marked. A columella is usually present which may also be dilated.

PLATE 2

- 1-6 *Dibunophyllum bipartitum* (McCoy 1849), transverse sections and longitudinal section [LAS 174a(1), LAS 73 (2,4), LAS 176 (3), LAS 185 (5), LAS 72 (6)], Knipe Scar assemblage 1, later Asbian, all ×3.
7 *Koninckophyllum* sp., transverse section LAS 181, Knipe Scar assemblage 1, later Asbian, ×2.

- 8 *Lithostrotion vorticale* (Parkinson 1808), transverse section LAS 55, Ashfell assemblage, Holkerian, ×3.
9,10 *Siphonodendron junceum* (Fleming 1828), transverse and longitudinal section, Knipe Scar assemblage 3, late Asbian. LAS 58, ×3.



There is never more than one complete row of dissepiments, although 2-3 dissepiments may be developed in those parts of a corallite which coalesce with adjacent corallites. The single row of dissepiments is usually dilated and forms a regular inner circle. Because the dissepimentarium is so constant, the overall diameter of this species is less variable than in most fasciculate species. Moreover, as the dissepimentarium is so narrow, tabularium diameter is only slightly smaller than the overall diameter. Tabulae are tent-shaped and usually complete.

Discussion. This species is easily recognisable by its single row of dissepiments.

Age and occurrence. *S. pauciradiale* appears in the early Asbian (Fauna F, Mitchell 1989) and persists into the Brigantian.

***Siphonodendron* sp.**

Plate 3, figure 1

Lithostrotion sp.n. A, NUDDS 1980, p. 387, fig. 1d.
Siphonodendron irregularare (Phillips). — ARETZ 2002, p. 112, pl. 5, fig. 4, pl. 11, fig. 4.

Material. Very abundant in the biostrome (PB) on the western scarp, mostly fragments. LAS 5, 7a, 9, 112, 114, 143.

Description. (i) external characters. Large, fasciculate, sometimes dendroid corallum. The corallites, 4.5 to 6.2mm in diameter (mean about 5.3mm), are cylindrical and sometimes in contact with each other, forming a pseudo-ceriod habit. Increase is non-parricidal and lateral. Calices and surface are not observed; the latter due to silification.

(ii) internal characters. The number of major septa ranges from 19-23. The major septa are thin and either straight or sinuous in the tabularium. They end in an open central area. In most corallites a simple axial plate forms an axial structure (lanceolate); rarely this structure is missing and the corallites become diphymorphic. The orientation of this axial structure distinguishes the cardinal and counter septum, which otherwise cannot be differentiated. The minor septa cross the dissepimentarium

and end as septal spines in the tabularium, reaching a length of up to 1/3 of the major septa.

The dissepimentarium consists of two or three rows of globose to elongated dissepiments. The tabulae are incomplete. They rise convex towards the axial structure and are curved peripherally downwards. There are approximately 24 tabulae and 28 dissepiments per centimetre.

Discussion. The correct specific assignment of *Siphonodendron* specimens between the two well-defined species *S. pauciradiale* (McCoy 1844) and *S. martini* (Milne-Edwards and Haime 1851) has been the cause of much confusion. The main problems are firstly the validity of *S. irregularare* (Phillips 1836), which was based on an inadequate description and the type specimens of which are now lost, and secondly the intra-colonial variability of the taxa, which have been described in recent studies under *S. irregularare* and *S. intermedium* (Poty 1981).

One of us (M.A.) favours an assignment to *S. irregularare*, the other (J.N.) to *S. intermedium*.

The Little Asby Scar specimens differ from *S. irregularare* (sensu Nudds 1980;) in the constant development of a second row of dissepiments, and its slightly larger dimensions. Compared to *S. intermedium* Poty 1981, the major septa of the Little Asby Scar specimens are longer and the number of septa smaller.

Age and occurrence. Due to the confusion concerning the correct specific assignments, the occurrence of these species in Britain is somewhat uncertain.

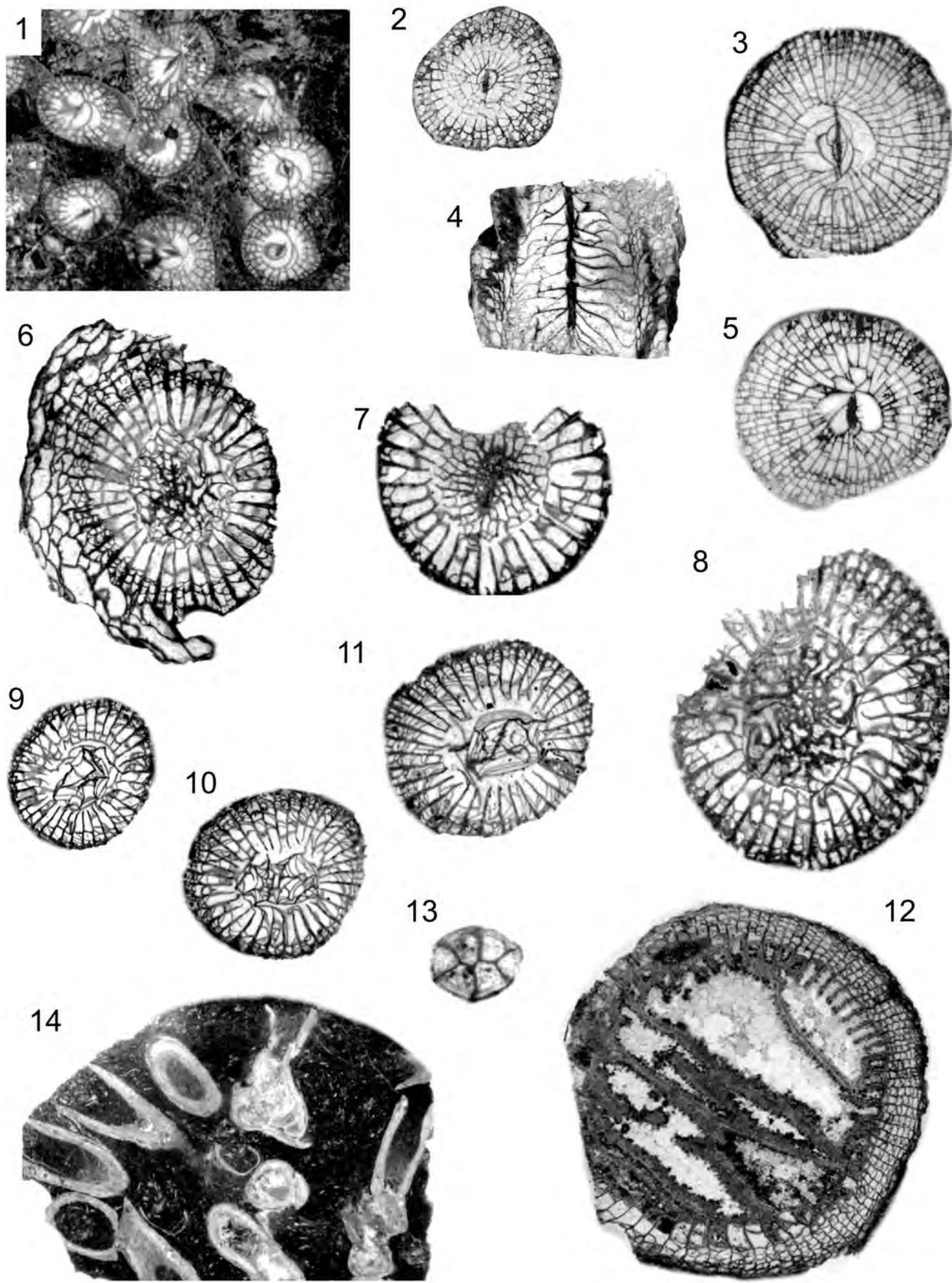
***Siphonodendron martini* (Milne-Edwards and Haime 1851)**

Plate 3, figure 2

**Lithostrotion martini* MILNE-EDWARDS and HAIME, 1851, p. 436.
— CALDWELL and CHARLESWORTH 1962, p. 377, pl. 14, fig. 5, 5a.— SEMENOFF-TIAN-CHANSKY and NUDDS 1979, p. 258, fig. 3, pl. 5, fig. 1-4, pl. 6, fig. 6, 7. [cun syn.]. — NUDDS 1980, p. 387, fig. 1e.
Siphonodendron martini (Milne-Edwards and Haime). — POTY 1981, p. 24, fig. 14-16, pl. 7, fig. 3. — RODRIGUEZ and FALCES 1992, p. 205, pl. 19, fig. 4, 5, 6. — POTY and HANNAY 1994 p. 64, pl. 4, fig.

PLATE 3

- 1 *Siphonodendron* sp., transverse section, biostrome, Holkerian, LAS 9, ×3.
- 2 *Siphonodendron martini* (Milne-Edwards and Haime 1851), transverse section, biostrome, Holkerian, LAS 155, ×3.
- 3-5 *Siphonodendron* cf. *scalaberense* (Nudds and Somerville 1987), transverse and longitudinal sections LAS 53 (3) and LAS 172 (4-5), KS 2, later Asbian, ×3.
- 6-11 *Axophyllum vaughani* (Salée 1913), transverse sections showing the high variability of the axial struc-
- ture, all from the biostrome, Holkerian, LAS 101 (6), LAS 139 (7), LAS 102 (8), all ×3, LAS 146 (9-11) ×2.
- 12-14 *Haplolasma*, transverse section, KS 1, later Asbian, LAS 171; 13, transverse section of heterocoral LAS 103, biostrome, Holkerian, *Hexaphyllia mirabilis* (Duncan 1867) or *Hexaphyllia marginata* (Fleming 1828) depending on the species concept, discussion in the text.
- 14 Syringoporid coral, LAS 57, biostrome, Holkerian. Due to incomplete silification tabulae were preserved only in few corallites.



2.—ARETZ 2001, fig. 3/7.—RODRIGUEZ et al. 2002, p. 30, fig. 14a-f, 15.—ARETZ 2002, p. 113, pl. 12, fig. 1-3.

Material. Numerous specimens from the biostrome (PB) on the western scarp, mostly fragments. LAS 59, 142, 155, LL. 10793, 10794, 10810.

Description. (i) external characters. The corallum is fasciculate and phaceloid, with cylindrical corallites, but many coralla are partly cerioid and have adjacent corallites growing in periodic coalescence. The corallites are bound by a thickened outer wall showing longitudinal inter-septal ridges. The calice is conical and deep with a prominent columella.

(ii) internal characters. The number of septa varies from 24-28 of both orders. Major septa are of variable length, but cardinal and counter septa extend to the columella in most colonies. Sometimes the other major septa continue to the axis, but more often they reach only half way to the axis. Minor septa are about half the length of the major septa, just entering the tabularium. Both major and minor septa are more dilated in the dissepimentarium than in the tabularium. A columella is usually present elongated in the cardinal plane. It may be strongly dilated or just a thin plate. Dissepiments vary from 2-4 rows and are generally regular and concentric. The innermost row is often strongly dilated and the dilation fuses with the dilation of the septa in the dissepimentarium. All dissepiments are quite steeply inclined. The width of the dissepimentarium is variable depending on the number of dissepiments present and accordingly the diameter of the corallite is variable in a similar way. The mean diameter is 7.8mm, with a total range from 6-10mm. Tabularium diameter is a more constant feature and reaching a mean diameter of 5.8mm. Tabulae are tent-shaped, incomplete and in two series.

Discussion. This is perhaps the most common species of *Siphonodendron*. All specimens recovered at Little Asby Scar fit well in the description of Semenoff-Tian-Chansky and Nudds (1979).

Siphonodendron cf. S. scaleberense Nudds and Somerville 1987
Plate 3, figures 3-5

cf. *Lithostrotion* sp. B NUDDS 1980 , p. 387, fig. 1g.
cf. *Siphonodendron scaleberense* NUDDS and SOMERVILLE 1987, p. 295, fig. 2 A-E, fig. 5 A, B.

Material. Two fragments from assemblage KS 2. LAS 53, 172.

Description. The corallites are 11.5-14mm in diameter. There are two series of 35-38 septa. The major septa are thin and straight to slightly sinuous, reaching a length of 3.5 to 5.2mm. The minor septa are 1/3-1/2 as long as the major septa. The counter septum is elongated and connected to the lanceolate columella. The cardinal septum is shortened and a fossula is developed.

The dissepimentarium consists of up to 2-5 rows of dissepiments, which are globular to elongated. There are 14-16 incomplete tabulae per centimetre. The tabulae rise convex towards the columella. Towards the periphery, tabulae are depressed, but rise towards the wall. The wall is simple and relatively thin (0.1mm).

Discussion. A full description of *S. scaleberense* was given by Nudds and Somerville (1987), but definite placement in this species is not possible due to the paucity of material.

Age and occurrence. *S. scaleberense* is known from Holkerian and Asbian succession of the British Isles (Nudds and Somerville 1987; Cozar et al., in press) and from the Asbian of Spain (Rodriguez et al. 2002).

Suborder LONSDALEIINA Spassky 1974

Family AXOPHYLLIDAE Milne-Edwards and Haime 1851

Genus *Axophyllum* Milne-Edwards and Haime 1850

Axophyllum vaughani (Salée 1913)

Plate 3, figures 6-11

*“*Clisiophyllum*” (*Carcinophyllum*) σ VAUGHAN 1905, p. 285, pl. 24, fig. 3-3b.

Axophyllum vaughani (Salée). — POTY 1981, p. 59, text-fig. 52, pl. 28, fig. 3, 4. [cun syn.]. — FONTAINE et al. 1991 , p. 54, pl. 26, fig. 1-3. — POTY and HANNAY 1994, p. 66, pl. 2, fig. 11. — SOMERVILLE 1997, p. 41, pl. 2, fig. 3.

?*Axophyllum cf. vaughani* (Salée). — RODRIGUEZ and FALCES 1992, p. 210, pl. 21, fig. 2.

Diagnosis. A ceratoid to sub-cylindrical *Axophyllum* of up to 2.5cm in diameter. Relatively deep calyx. Prominent axial structure rising significantly from calice floor. Transversal rugae and longitudinal furrows and ribs on outer surface. Up to 39 septa for each cycle. Major septa straight to sinuous, interrupted in marginal dissepimentarium, thickened at base. Minor septa short to absent. Axial structure comprises 1/3 of the tabularium, highly variable, sometimes gangamophyllid. Dissepimentarium of large lonsdaleoid dissepiments, comprises 1/3 of the corallite. Tabulae flat or concave.

Material. Numerous corallite fragments from the biostrome (PB). The dissepimentarium is rarely preserved. 50 specimens sampled and cut; thin sections of the better preserved specimens: LAS 74, 100, 101, 102, 103, 105, 106, 107, 108, 112, 113, 136, 137, 138, 139, 140, 141, 144, 145, 146, 147, 149, 151, 152, 153, 156, 157, 175, 177, 180, 183, 184.

Description. (i) external characters. One corallite, almost completely preserved, allows a detailed description of the external characters. The corallite is ceratoid to sub-cylindrical. Its diameter is 0.4cm at its apex and 2.3cm at the calice. The calice is relatively deep (0.9cm). The axial structure consists of numerous curving axial lamellae (?) revolved on a thicker median plate and rises at least 0.6cm from the calice floor. The outer surface shows rugae and longitudinal furrows and ribs.

(ii) internal characters. The number of major septa ranges from 30-39. They are straight to sinuous and at least 6.3mm long. Major septa are interrupted at the marginal part of the dissepimentarium by lonsdaleoid dissepiments, but sometimes they persist as septal crests. Their thickness decreases from a maximum of 0.4mm at their thickened base to 0.05-0.1 at their proximal end within the tabularium. Sometimes they are connected to the axial structure.

Minor septa are short or absent.

The axial structure comprises 1/5 to 1/4 of the corallite and about 1/3 of the tabularium. In general, the axial structure consists of a straight to sinuous, thick medial plate, surrounded by curved axial lamellae and irregular axial tabellae. In some corallites, the axial structure becomes gangamophyllid (medial plate not differentiated from the axial lamellae). The variability within one corallite is high especially regarding thickness and arrangements of median plate and axial lamellae.

The disseipmentarium comprises up to 1/3 of the corallite and is often dominated by large lonsdaleoid disseipments. The disseipments are elongated and declined. The tabulae are flat or concave. The axial tabellae are slightly convex or concave and inclined at 30-65°.

Discussion. The Little Asby Scar specimens are very similar to the Belgian material described by Poty (1981) although the latter are of smaller dimensions. There is more variability in the axial structure in the Asby specimens, but Poty's description was based on much less material.

Age and occurrence. The stratigraphical record of *A. vaughani* ranges in Britain from the Holkerian to the early Brigantian (Fauna E-H, Mitchell 1989). In Belgium and northern France, this species is limited to the Livian (=Holkerian). Rodriguez and Falces (1992) reported this species from the lowest unit of the succession in the Los Santos de Maimona Basin, which, according to the coral fauna, is Asbian in age.

In addition to the rugose corals described above, a transverse section of specimen LAS 171 is figured (pl. 3, fig. 12). This section is made in a thin fragment (2-3mm) and with some doubt it could be assigned to *Haplolasma*.

?Order HETEROCORALLIA Schindewolf 1941

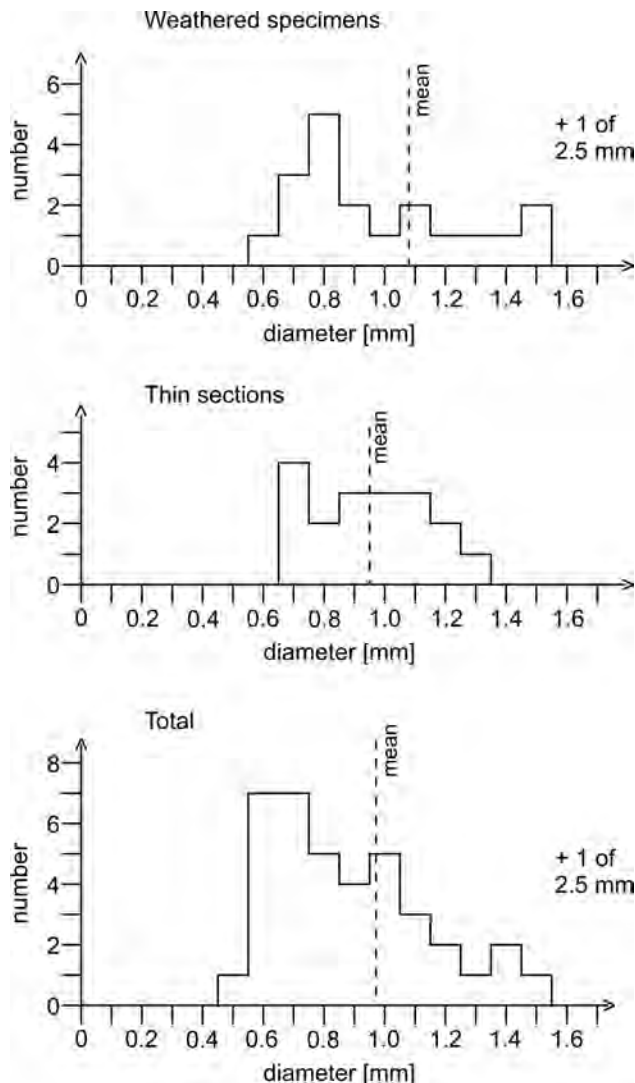
Family HETEROPHYLLIDAE Dybowski 1873
Plate 3, figure 13

Material. Numerous fragments from the biostrome (PB) of the western scarp. 41 measured specimens; 20 in thin sections, mostly transverse and 21 measured from weathered material. LAS 103, 111, 112.

Description. Up to 9mm long fragments of elongated, prismatic (hexagonal) heterocorals. There is a clear yellowish colour to the skeleton, a characteristic observed in different outcrops throughout the Lower Carboniferous of the British Isles. The outer surface is "ornamented" by concentric structures, 0.1mm high and 0.05-0.2mm in diameter, interpreted as the base of longer spines which have been destroyed during transportation of the specimens (see Cossey 1997). Most sections of weathered material and thin sections, show 6 septa meeting at or near the axis. In two small corallites (0.5mm) only 5 septa are observed. The peripheral edges of the septa are thickened, cross the wall and form costae. The cardinal and counter cardinal septa are easily distinguished, since only the two alar septa are separated.

The tabulae are domed. The diameter of the heterocorals ranges from 0.5mm (for stages with 5 septa) to 1.5mm; a diameter of 2.5 is observed only once. Following the previous work of Poty (1978, 1981), Rodriguez and Comas-Rengifo (1989) and Cossey (1997) the frequency of the measured diameters are shown in histograms (text-fig. 6).

Generic discussion. Heterocorals with six septa of Lower Carboniferous age have mostly been assigned to *Hexaphyllia* Stuckenbergh 1904. However, Poty (1978) demonstrated that a six septa stage occurs equally in *Heterophyllia* McCoy 1849, being somewhat smaller in diameter than in *Hexaphyllia*. Cossey (1997) found significant variations in the number of septa (3-6) in *Hexaphyllia*, which is very high in early ontogenetic stages. Rodriguez and Comas-Rengifo (1989) showed that 44% of their 700 adult *Hexaphyllia* specimens had



TEXT-FIGURE 6

Histograms of the number/diameter of the heterocorals recovered from the base of the Potts Beck Limestone (bed f). A: weathered out specimens, B: specimen in thin sections, C: total.

7-9 septa. Although the histogram (their fig. 3) does not show the gap of Poty (1978), the first peak in the small diameters may represent the young stages of *Heterophyllia*, subsequently older and larger stages are hidden in the *Hexaphyllia* range, but may be detected by the abundance of 7-9 septa stages. Separation of two morphologically similar genera using only a biometric character is highly questionable. Up to now, it is not clear if *Hexaphyllia* is a younger synonym of *Heterophyllia*.

Cossey (1997) demonstrated the synonymy of a number of species. According to his measured corallite diameter (traditionally used to differentiate species in *Hexaphyllia*) *Hexaphyllia marginata* (Fleming 1828) has a wide variability and most traditional species are ontogenetic stages of this species.

A significant number of the Asby Scar heterocorals (text-fig. 6) have diameters ranging from 0.7-0.8mm. The mean for the entire measured specimens is 0.964mm. 75% of the corals range from 0.6-1.1mm in diameter. Larger specimens are rare. There is a major gap between 1.5 and 2.5mm (text-fig. 6).

According to Poty (1978, 1981) it would appear that young stages of *Heterophyllia* as well as *Hexaphyllia* occur in the Asby Scar heterocoral assemblage. However, since no specimens with more than six septa have been found in the assemblage, it is very unlikely that *Heterophyllia* is only present in its immature (6 septa) stage, and it is more likely that all of the Asby Scar material is actually *Hexaphyllia*. It then becomes difficult to separate the two genera based on diameter since the Asby Scar material closes the gap in Poty's histograms (1978, 1981). Thus *Hexaphyllia* cannot be differentiated from *Heterophyllia* based on this character alone and would become its younger synonym.

In contrast to Cossey (1997), we do not see any evidence for a continuous range of corallite diameters up to 2.6mm. In fact, we observe a concentration of thinner corallites (0.6-1.1mm). The observation that larger heterocorals are very rare is in agreement with Poty (1981) and Rodriguez and Comas-Rengifo (1989).

Possible explanations of this pattern are, first, a selective removal of thicker corallites (Cossey 1997), or secondly, the existence of more than one species (Poty 1981). A number of points have to be taken into account.

The Asby Scar material was transported. The effect of this transport on the heterocorals must have been destructive as seen in broken spines and broken corallites. Otherwise the heterocorals are incorporated into a sediment of very different grain sizes having single grains much thicker and larger than the largest heterocorals. Thus removal during transport should not change the original distribution. Single corallites in the growth range 1.6-2.4mm should occur. Otherwise the single heterocoral with a corallite diameter of 2.5mm might be an unusual "giant" specimen of the same species since its size is the only obvious difference.

The number of corallites recovered at Little Asby Scar is not significantly high to decide whether we accept selective removal or whether we accept that there are two species. Accepting the selective transport theory of Cossey (1997), all specimens belong to *Hexaphyllia marginata*. Following Poty (1981), the smaller specimens belong to *Hexaphyllia mirabilis* (Duncan 1867) and the larger one to *Hexaphyllia marginata* (Fleming 1828).

Subclass **Tabulata** Milne-Edwards and Haime 1850
Plate 3, figure 14

Tabulate corals occur relatively frequent within the biostrome (PB). Ramsbottom (1981) reported *Syringopora geniculata* Phillips (1836) and *Michelinia* sp.

The specimens recovered during this study are mostly small fragments of one to several corallites, but also include some larger fragments of almost complete colonies. The tabulate corals are silicified and often incomplete. The outer form of the corallite is generally better preserved, but the inner part is rarely well preserved. Thus important diagnostic internal characters of the corallites are often missing making identification difficult.

Syringopora sp. ?

Material. 4 larger silicified fragments of corallum and numerous small fragments. Thin sections: LAS 57

Description. The corallum is fasciculate. The corallites are cylindrical and connected by horizontal tubuli and platforms. Two morphotypes could be differentiated by the size of the corallites, the wall-thickness, and the intercolonial distances.

Morphotype 1: The corallites are 2.5-3mm in diameter, the wall is 0.4-0.5mm thick and the intercolonial corallite-distances are 3-4.5mm.

Morphotype 2: The corallite-diameter is 1.5-1.9, the wall-thickness 0.1-0.3mm thick and the intercolonial corallite-distances are only 0.5-2.3mm.

Tabulae are rare in both morphotypes.

A genetic or specific designation of both morphotypes is not possible. Tourneur et al. (1989) suggest that silification commonly makes diagnostic descriptions of Lower Carboniferous tabulate corals difficult. A designation to *Syringopora* Goldfuss seems likely, but further investigations are needed and at present we refer the material to "syringoporoid corals".

BIOSTRATIGRAPHY

Biostratigraphic implications of the coral assemblages

Assemblage AA

The oldest coral assemblage (AA) consists only of *Lithostrotion vorticale* (text-fig. 5) and its biostratigraphic relevance is low. *Lithostrotion vorticale* appears from the Holkerian to the Brigantian.

Assemblage PB

The early Asbian is characterized by coral fauna F of Mitchell (1989). This comprises *Dibunophyllum bourtonense*, *Koninckophyllum vaughani*, "Caninia" juddi, *Siphonodendron pauciradiate*, *Siphonodendron junceum*, *Aulophyllum redendale*, *Clisiophyllum keyserlingi*, and *Siphonophyllum benburensis*. [The appearance of some of these species in the early Asbian is questionable; e.g. *Siphonodendron junceum* does not appear until the later Asbian in Belgium (Poty 1985, Aretz 2001), or Ireland (Cozar et al. 2005)].

The assemblage PB, recovered from the lowermost bed of the Potts Beck Limestone (bed f of George et al. 1976), is relatively diverse and contains different colonial and solitary taxa. However, all of the taxa of this assemblage (text-fig. 5) are known to appear before the Asbian. Our intense search at the boundary level for any of the diagnostic Asbian rugose coral taxa of Mitchell's fauna F has not been successful. All solitary corals with a complex axial structure recovered from the biostrome were sectioned and examined carefully in the hope that we might identify *Dibunophyllum*, but were all found to belong to the Axophyllidae. The prominence of the medium plate of the axial structure might be reduced or become inconspicuous (= gangamophyllid), but there is no doubt that these specimens belong to this family (see taxonomy section). Although abundant, *Axophyllum vaughani* is not an indicative Asbian taxa, since it appears in the Holkerian and it is known in the stratotype section of that substage (Ramsbottom 1981; Mitchell 1989).

Assemblage KS 1

Asbian rugose coral taxa have been found higher up in the succession (text-fig. 5). Numerous *Dibunophyllum bipartitum* have been found in the coral assemblage KS 1 east of the fault zone. *Siphonodendron martini*, and *Caninophyllum archiaci* (also re-

corded from this assemblage) are already known from older strata (e.g. Mitchell 1989).

Assemblage KS 2

Assemblage KS2 contains a typical late Asbian coral fauna including several members of the Lithostrotionidae which are useful biostratigraphic markers (text-fig. 5). *Siphonodendron junceum* and *Lithostrotion maccoyanum* occur in the late Asbian (see discussion above). *Siphonodendron pauciradiale* appears in the early Asbian. The other taxa of the assemblage KS 2 do not have much stratigraphic value, but are often accessory taxa in the upper Viséan.

D. bipartitum and *L. maccoyanum* are considered to represent fauna G of Mitchell (1989) (=later Asbian). *L. maccoyanum* is an excellent stratigraphic marker, since its range is relatively small (late Asbian – early Brigantian). However, *D. bipartitum* occurs already in the biozone Cf6 α (Poty and Hannay 1994), which indicates an early Asbian age. No coral that marks the Brigantian, e.g. *Actinocyathus* or *Orionastraea*, has been found in the studied section.

Summary

Taking into account only the stratigraphical distribution of corals (text-figs. 7, 8A), assemblage AA is mostly likely Holkerian in age. The age of the coral fauna of the boundary bed (PB) is uncertain, but is most probably Holkerian, due to the absence of any Asbian taxon; however, an Asbian age cannot be ruled out. KS 1 is early Asbian in age, since it contains Asbian corals and the first later Asbian taxa do not occur until assemblage KS 2.

From the coral dataset presented here and the uncertainty about the previous record of *Dibunophyllum* (Riley 1993), the Holkerian/Asbian boundary might be best placed somewhere between assemblages PB and KS 1. This coral-based boundary does not correspond to the originally defined boundary at the base of the bioherm (PB). During this study, only corals which appear already in the Holkerian have been recovered from the Potts Beck Limestone.

Discussion

The problems in the recognition of the base of the Asbian are not restricted to the Little Asby Scar section. Riley (1990) in his work on the Wiston Shale Group of the Craven Basin shifted the base of the Asbian into the Pendleside Limestone Formation.

The original definition of the Holkerian/Asbian boundary (George et al. 1976:11) does not contain a biostratigraphic marker. It was originally established as the boundary between the Ashfell Limestone and the Potts Beck Limestone (text-fig. 3). Therefore, it is purely a lithostratigraphic boundary, which eventually coincides with a mesothem boundary of Ramsbottom (1973).

The first appearance dates (FAD) of the coral taxa mentioned by George et al. (1976) do not correspond to the then defined Holkerian/Asbian boundary. Additionally, Dunham and Wilson (1985) questioned the Asbian FAD of the brachiopod *Daviesiella llangollensis* based on the appearance of Holkerian foraminiferan assemblages in the *Daviesiella* beds of the Wye Valley section, North Derbyshire.

Ramsbottom (1981) give a detailed distribution of the macrofauna in the boundary beds (a-i) at Little Asby Scar

(text-fig. 3). It is notable that *Dibunophyllum bourtonense* was the only Asbian marker which he recorded from bed f, the basal Asbian bed following the original definition of George et al. (1976). Riley (1993) noted that the record of *Dibunophyllum bourtonense* has never been repeated and that Ramsbottom's original specimen has been lost (pers. com. Riley). Despite our extensive searching we have found no record of *Dibunophyllum*, or even of the family Aulophyllidae, within the biostrome (text-figs. 5, 7A).

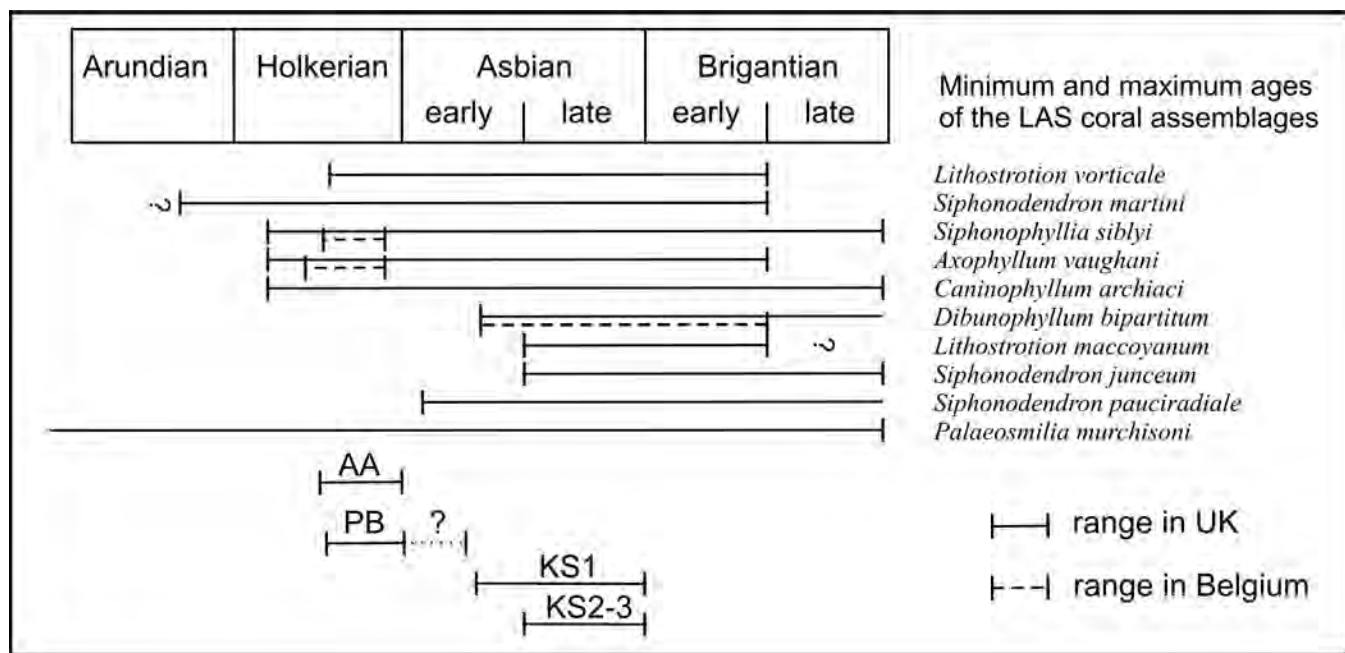
The distribution of other macrofauna in Ramsbottom (1981) indicates *Gigantoprotodus ex. gr. maximus* in bed a (= top of the Ashfell Limestone). Pattison (1981) reported *Gigantoprotodus maximus* only from the Potts Beck Limestone, and Legrand-Blain (1990) indicated that *Gigantoprotodus* appeared in the Asbian. Therefore an Asbian brachiopod below the boundary is somewhat surprising; in addition none of the typical Asbian brachiopods of George et al. (1976) have been listed in Ramsbottom (1981).

Probably a good hint in George et al. (1976) for the biostratigraphic base of the Asbian substage is the statement, "R. Conil (pers. com.) confirms that on evidence of the foraminifera, the base of the stage coincides with the Belgian biozonal change between the V3a and V3b" (George et al. 1976:11). This faunal change is defined at the base of the foraminiferan biozone Cf6 (see also Conil et al. 1977), which is marked by the entry of *Neoarchaeodiscus*, *Vissariotaxis*, and double walled Palaeotextulariidae (Conil et al. 1991). According to Poty (pers. com.) the first upper Viséan corals (*Dibunophyllum*, *Diphyphyllum*) occur at the base of the Thon Samson Member, which coincides with boundary of Cf6.

The foraminiferan datasets of the stratotype reveal some discrepancies. Strank (in Ramsbottom 1981) observed that Asbian foraminiferans first appeared 19.6m above the Holkerian/Asbian boundary. However, White (1992) recorded the first Asbian taxa (*Vissariotaxis* sp.) in bed g (only 3 m above the boundary) and the first late Asbian taxa in Ramsbottom's bed E (text-fig. 3). Somerville (pers. com.) questioned the correct identification of *Vissariotaxis* by White. Some thin sections made for the identification of corals and microfacies analysis (Aretz and Nudds, in press) are relatively rich in foraminiferans and have been analysed by Dr. L. Hance (Louvain-la-Neuve). The first double-walled Palaeotextulariidae has been found 1 m below the boundary, while the first indicators of the biozone Cf6 γ appear with coral assemblage KS1 (text-fig. 8A). However, an earlier FAD of double-walled Palaeotextulariidae can not be ruled out, since our sampling of the Ashfell Limestone was very limited.

Only preliminary conodont data (Ramsbottom 1981) are available so far, and again the characteristic taxon (*Gnathodus bileneatus*) of George et al. (1976) is not listed at Little Asby Scar.

Summing up the datasets of the different fossil groups, it becomes clear that none of them supports a biostratigraphic boundary at the present position of the Holkerian/Asbian boundary (i.e. below bed f). Due to the discrepancies between the first appearance of so-called Asbian taxa and the defined boundary, Riley (1993) proposed to relocate the boundary 19.6m up section in the stratotype where the first Asbian foraminiferans (sensu Strank) appear and *Dibunophyllum* also occurs (Riley 1993). However, the datasets of White (1992) and the present study report Asbian foraminiferans well below this



TEXT-FIGURE 7

Stratigraphic range of selected coral taxa. Indicating minimum and maximum ages of the coral assemblages.

level. Our datasets suggest that at Little Asby Scar the bases of the first Asbian biozones are not synchronous; “Asbian” foraminiferans and possibly brachiopods seem to appear earlier than “Asbian” corals.

Correlation with Belgium

It is interesting to correlate the Little Asby succession to the succession of the Dinant-Namur Basin (Belgium) based on the coral fauna (text-fig. 11B), since both successions belong to the same geotectonic unit (Southern shelf of Laurussia) and occurred in comparable shallow-water facies. The coral assemblage recovered from the biostrome (PB)(=bed f) at Little Asby Scar is very similar to the coral fauna of the Seilles Member (lower Grands Malades Formation) in Belgium. *Dibunophyllum* first appears at the base of the Thon Samson Member, but the species *D. bipartitum* (present in KS 1 and 2) does not appear until the Poilvache Member of the River Bonne Formation. *Siphonodendron junceum* and *Lithostrotion maccoyanum* (both in KS 2) appear at the base of the Anhée Formation.

An attempted correlation with Belgian sedimentary sequences (Hance et al. 2001) indicates the boundary of sequence 7/8 above the beds of the Potts Beck Limestone, which contain assemblage PB. The coral assemblage KS 1 and 2 indicate sequence 9 for the Knipe Scar Limestone. Therefore, sequence 8 would be represented by most of the Potts Beck Limestone.

This simplistic approach is not fully backed by the foraminiferan datasets (text-fig. 8B). The appearance of double-walled Palaeotextularidae in the top of the Ashfell Limestone already indicates a correlation of these beds to the base of the River Bonne Formation. This discrepancy may be partly due to the absence of corals in the Bay Bonnet Member in Belgium (mainly stromatolithic limestones), which may be result in a miscorrelation of bed f to the Seilles Member, but the

correlation to the Bonne River Formation should be confirmed by the coral fauna.

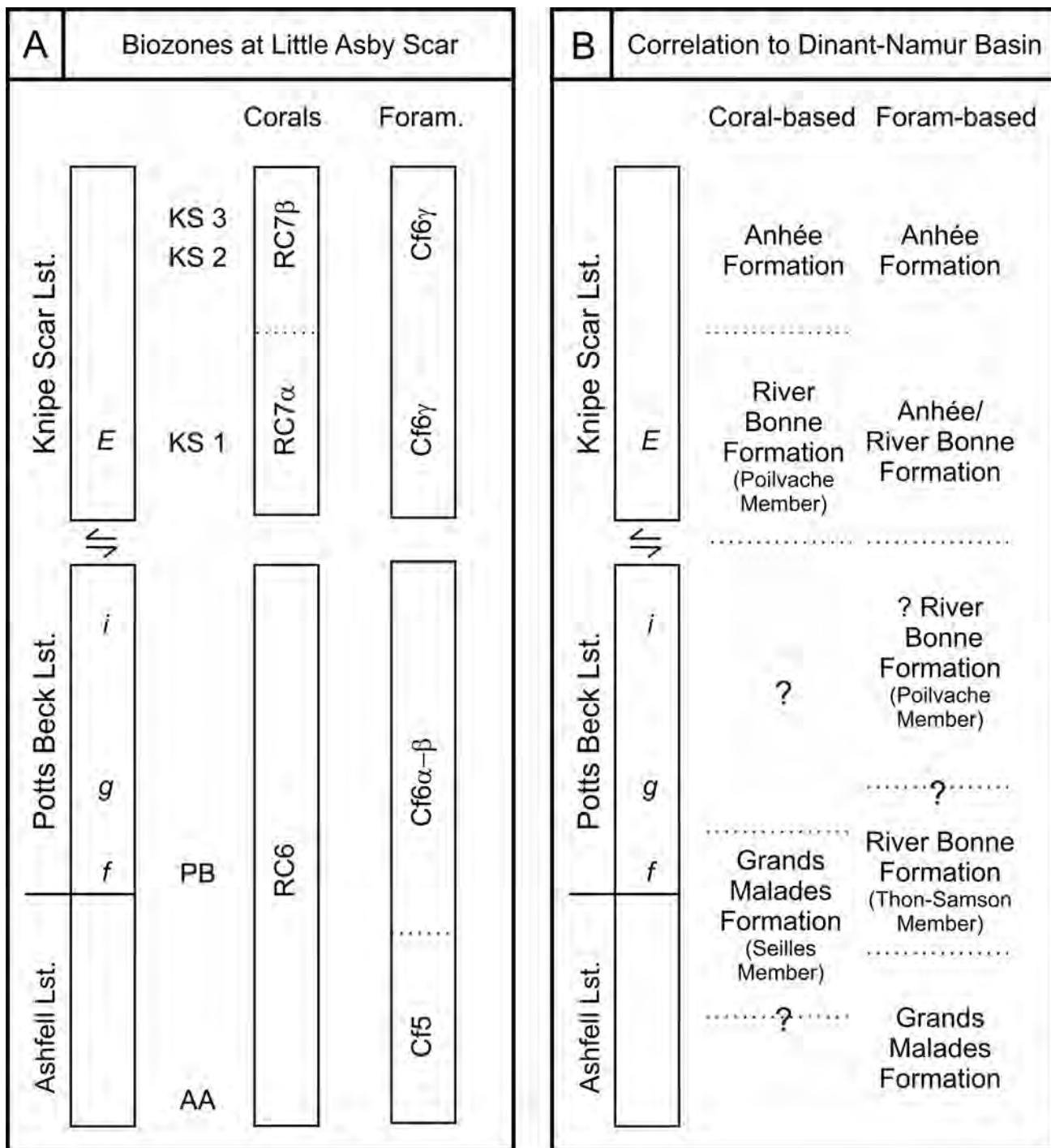
The simultaneous appearance of index taxa of corals and foraminiferans at the base of the Bonne River Formation in Belgium is possibly the effect of the disappearance of the unsuitable facies of the Bay Bonnet Member, which may have obscured the FAD of possible markers. Regions with more open marine facies during Bay-Bonnet time should record an evolution and distribution different from Belgium.

However, in the upper part coral- and foraminiferan-based correlations agree much better. The first markers for Cf6γ co-occur with KS1. Since Cf6γ slightly predates RC7β, this level may be correlated to the top of the Poilvache Member (River Bonne Formation). However, the foraminifer dataset confirms that *Siphonodendron junceum* does not appear at Little Asby Scar until the later Asbian. Therefore, the application of the boundary of biozones RC7α and RC7β should be possible in Britain as also confirmed by Cozar et al. (2005).

The use of the presence/absence criteria of corals and/or foraminifera does not take into account the facies dependency of these groups (e.g. Gallagher 1998). However, biostratigraphic correlation is consistent in the Belgian Dinant-Namur basin, but inter-regional correlations may be somewhat difficult. Thus, the same has to be tested in Britain, and may be more important due to the higher differentiation of the British shelf system.

Implications

The original definition of the Asbian stratotype is purely lithostratigraphic. The mudstone bed e (text-fig. 3), which is variable in thickness, disappears for at least some hundred meters in the sections west of the stratotype section, and therefore is already in itself an unsuitable marker bed. Lithostratigraphic



TEXT-FIGURE 8

A. Biozonal Scheme for corals and foraminiferans for the Little Asby Scar section (using the Belgian terminology); B. The correlation of the Little Asby Scar section to the formations of the Belgian Dinant-Namur Basin reveals major differences when using different biozones.

boundaries are mostly diachronous, and therefore are not suitable for the definition of substages in the Mississippian of Britain.

The base of the Asbian substage should be defined by biostratigraphic means, although the potential markers are benthic organisms with facies dependencies. Two groups seem to be the best options: corals or foraminiferans.

Foraminiferans as microfossils might be considered more suitable markers, due to their abundance. However, Gallagher (1998) showed that many Asbian foraminiferan taxa, including some index fossils, are facies dependent. Ramsbottom (1981:1.2) pointed out that, "The base was originally defined on the basis of the entry of corals of the D1 Zone, including *Dibunophyllum* in the basal beds of the Asbian", and highlighted the differences of the base of the D1 zone in northern

England and its somewhat younger position in the Avon Gorge section. This statement clearly indicates the importance of the appearance of *Dibunophyllum* for the original definition of the Asbian substage. Following the intention of all previous authors and in accordance with the appearance of *Dibunophyllum* at the base of Warnantian in Belgium, the base of the Asbian should therefore approximate to the first appearance of *Dibunophyllum*. Hence Riley (1993) proposed to relocate the boundary 19.6m up section to the first appearance of *Dibunophyllum*, which he considered also approximated to the appearance of Asbian foraminiferans (*sensu* Strank). However, because more recent foraminiferan datasets (White, and this study) now suggest that Asbian taxa appear lower in the succession, Riley's proposal should be reconsidered. In addition *Dibunophyllum bipartitum*, the first dibunophyllid coral in the Little Asby Scar section, may be not the oldest species of the genus.

This study clearly shows that, at least in the Little Asby Scar section, the bases of coral and foraminiferan biozones do not correspond, and, moreover, that the original boundary of George et al. (1976) does not correspond to any boundary of the biozones. To ensure the chronostratigraphic status of an Asbian substage, a formal decision on a new definition based on a suitable marker must be made. Candidates may be found among foraminiferans and rugose corals, but further detailed work on their distribution is needed.

According to the results of this study, this will lead to a relocation of the boundary in the Little Asby section. Taking into account the poor quality of the natural exposures at Little Asby Scar and the associated problems with faulting, a relocation of the stratotype section to a continuous section (e.g. cliff or quarry) is necessary, and a consensus on the criterion to define this boundary is therefore needed. All regions of the British Isles should be included in the search for a new section, but key locations might be found in Derbyshire and North Wales.

CONCLUSIONS

A rich and diverse coral fauna has been found in various parts of the stratotype section. The rugose corals belong to 7 genera with 12 species. Among many common taxa, some taxa are relatively rare. The diameters of heterocorals have been measured and histograms show the difficulties of separating genera and species based on this character. The taxonomic description of the tabulate corals is hampered by silification of the material.

The rugose corals recovered from the biostrome (assemblage PB) at the Holkerian/Asbian boundary stratotype at Little Asby Scar, and previously defined as being lowest Asbian, do not include any Asbian taxa, and may in fact be of Holkerian age. Some of the taxa do persist into the Asbian, but this assemblage does not confirm previous results (George et al. 1976, Ramsbottom 1981). The first typical Asbian corals appear in the higher coral assemblages, KS 1 - 3, all of which belong to the Knipe Scar Limestone. No coral taxa which appear in the Asbian have been recovered from the Potts Beck Limestone.

The Holkerian/Asbian boundary as defined by George et al. (1976) is a lithostratigraphic boundary, which is not supported by any biostratigraphy. There are no potential index taxa in either corals, brachiopods, foraminiferans or conodonts at this level. The first coral, which definitely appears in the Asbian is *Dibunophyllum bipartitum* and this does not occur until the lower Knipe Scar Limestone east of the fault zone. None of the existing foraminiferan datasets (Strank, White, Hance) support a

Holkerian/Asbian boundary in its present position, but they are not in agreement in their definition of the base of the Asbian.

After agreement on a biostratigraphic marker for the base of the Asbian, the stratotype should be relocated into a section of better outcrop quality, possibly in Derbyshire or North Wales. It is desirable, that the base of the Asbian will be defined near to the FAD of *Dibunophyllum* (after the evolution of the genus is better constrained).

However, without any formal decision the base of the Asbian substage has to be retained at its present position at the base of the Potts Beck Limestone.

ACKNOWLEDGMENTS

The present study includes results of the project He 1610/11 generously financed by the Deutsche Forschungsgemeinschaft (DFG). E. Poty (Liège), S. Schröder (Cologne) and an anonymous reviewer provided many helpful comments on the manuscript. We are obliged to all students and staff at Cologne, Liège and Manchester who carefully prepared the numerous thin sections. Specimens are lodged in the collections of the University of Cologne (LAS, GIK) and Manchester University Museum (LL).

REFERENCES

- ARETZ M., 2001. The upper Viséan coral-horizons of Royseux – The development of an unusual facies in Belgian Early Carboniferous. *Bulletin of the Tohoku University Museum* 1: 86-95.
- , 2002. Habitatanalyse und Riffbildungspotential kolonialer rugosier Korallen im Unterkarbon (Mississippium) von Westeuropa. *Kölner Forum für Geologie und Paläontologie* 10: 1-155.
- ARETZ, M. AND NUDDS, J., in press. Palaeoecology of the Late Viséan (Dinantian) coral-chaetid biostrome at Little Asby Scar (Cumbria, Great Britain). *Erdwissenschaftliche Kommission der Österreichischen Akademie der Wissenschaften*.
- BISAT, W.S., 1928. The Carboniferous goniatite zones of England and their continental equivalents. In: *Compte Rendue du premier congrès international de stratigraphie et de géologie du Carbonifère*, Heerlen 1927 Volume 1: 117-133.
- BUTLER, M., 1973. Lower Carboniferous conodont faunas from the Eastern Mendips. *Paleontology* 16: 477-517.
- CALDWELL, W.G.E. and CHARLESWORTH, H.A.K., 1962. Viséan coral reefs in the Bricklieve Mountains of Ireland. *Proceedings of the Geological Association* 73: 359-381.
- CONIL, R., GROESSENS, and E. PIRLET, H., 1977. Nouvelle charte stratigraphique du Dinantien type de la Belgique. *Annales de la Société Géologique du Nord* 96: 363-371.
- CONIL, R., GROESSENS, E., LALOUX, M., POTY, E. and TOURNEUR, F., 1991. Carboniferous guide foraminifera, corals and conodonts in the Franco-Belgian and Campine basins: their potential for widespread correlation. *Courier Forschungsinstitut Senckenberg* 130: 15-30.
- CONIL, R., LONGERSTAEG, P. and RAMSBOTTOM, W., 1980. Matériaux pour l'étude micropaléontologique du Dinantien de Grande-Bretagne. *Mémoire de l'Institut Géologique de l'Université de Louvain* 30: 1-186.
- COSSEY, P.J., 1997. *Hexaphyllia*: A spiny heterocoral form Lower Carboniferous Reef Limestone in Derbyshire, England. *Paleontology* 40: 1031-1059.

- COZAR, P. and SOMERVILLE, I.D., 2004. New algal and foraminaliferal assemblages and evidence for recognition of the Asbian-Brigantian boundary in northern England. *Proceedings of the Yorkshire Geological Society* 55: 43-65.
- COZAR, P., SOMERVILLE, I.D., ARETZ, M. and HERBIG, H.-G., in press. Biostratigraphic dating of the Bricklieve Limestone Formation (NW-Ireland) using foraminifers, calcareous algae and rugose corals. *Irish Journal of Earth Sciences*.
- DUNCAN, P.M., 1867. On the Genera *Heterophyllia*, *Battersbyia*, *Palaeocyclus*, and *Asterosmilia*; the Anatomy of their Species, and their Position in the classification of the Sclerodermic Zoantharia. *Philosophical Transactions of the Royal Society London*, 157: 643-656.
- DUNHAM, K.C., 1990. Geology of the Northern Pennine Orefield, Volume 1, Tyne to Stainmore (2nd ed.). *Geological Memoir British Geological Survey*, 1-299.
- DYBOWSKI, W.N., 1873. Monographie der Zoantharia Sclerodermata Rugosa aus der Silurformation Estlands, Nordlivlands und der Insel Gotland. *Archiv für Naturkunde Liv-, Ehst- und Kurlands* 5: 257-414.
- EHRENBERG, C.G., 1834. Beiträge zur physiologischen Kenntniss der Corallenthiere im allgemeinen, und besonders des rothen Meeres, nebst einem Versuche zur physiologischen Systematik derselben. *Abhandlungen der Königlichen Akademie der Wissenschaften zu Berlin* 1832: 225-380.
- FEDOROWSKI, J., 1971. Aulophyllidae (Tetracoralla) from the upper Viséan of Sudetes and Holy Cross Mountains. *Palaeontologica Polonica* 24: 1-137.
- FLEMING, J., 1828. *A history of British animals*. Bell and Bradfute Edinburgh and London.
- FONTAINE H., SUTEETHORN, V. and JONGKANJANASOON-TORN, Y., 1991. Carboniferous corals of Thailand. *CCOP Technical Bulletin* 22: 1-82.
- GALLAGHER, S.J. 1998. Controls on the distribution of calcareous Foraminifera in the Lower Carboniferous of Ireland. *Marine Micropaleontology* 34: 187-211.
- GARWOOD, E.J., 1913. The Lower Carboniferous succession in the North-West of England. *Quarterly Journal of the Geological Society of London* 68: 449-582.
- GARWOOD, E.J. and GOODYEAR, E., 1924. The Lower Carboniferous succession on the Settle district and along the line of the Craven faults. *Quarterly Journal of the Geological Society of London* 80: 184-273.
- GEORGE, T.N., JOHNSON, G.A.L., MITCHELL, M., PRENTICE, J.E., RAMSBOTTOM, W.H.C., SEVASTOPULO, G.D. and WILSON, R.B., 1976. *A correlation of the Dinantian rocks in the British Isles*. Special reports of the Geological Society 7: 1-87.
- GILES, P.S. and BOUTILIER, R., 2003. Spectral analysis of degraded synthetic time series-modelling spectra of the orbital periods from the late Visean Windsor Group of Atlantic Canada. *Abstracts with Programs - Geological Society of America* 35:11.
- GRADSTEIN, F.M., OGG, J.G., SMITH, A.G., BLEEKER, W. and LOURENS, L.J., 2004. A New Geologic Time Scale, with special reference to Precambrian and Neogene. *Episodes* 27: 83-100.
- HALLET, D., 1970. Foraminifera and algae from the Yoredale "series" (Viséan – Namurian) of northern England. In: *Compte Rendu 6ème Congrès International du Stratigraphie et Géologie du Carbonifère, Sheffield 1967*, Volume 3: 873-900.
- HANCE L., POTY, E. AND DEVUYST, F.X., 2001. Stratigraphie séquentielle du Dinantien type (Belgique) et corrélation avec le Nord de la France (Boulonnais, Avesnois). *Bulletin de la Société géologique de France* 172: 411-426.
- HERBIG, H.-G., 1986. Rugosa und Heterocorallia aus Obervisé-Gerölle der Marbella-Formation (Betische Kordillere, Südspanien). *Paläontologische Zeitschrift* 60: 189-225.
- , 1998. The late Asbian transgression in the central European Culm basins (Late Viséan, cd III α). *Zeitschrift der deutschen geologischen Gesellschaft* 149: 39-58.
- HERBIG, H.-G., KORN, D. AND MESTERMANN, B., 1999. Crenistria Event and Asbian-Brigantian transition in the South Portuguese Zone; sea level control on a hemipelagic late Dinantian platform. *Facies* 41: 183-196.
- HILL, D., 1938-1941. A monograph on the Carboniferous rugose corals of Scotland. *Palaeontographical Society of London* 1938, 1-78; 1939, 79-114; 1940, 115-204; 1941, 205-215.
- , 1981. Coelenterata: Anthozoa. Subclasses Rugosa, Tabulata. F1-F762 In: Teichert, C., Ed., *Treatise on Invertebrate Paleontology*, part F, Coelenterata. Boulder, Colorado and Lawrence, Kansas.
- JONES G.L. and SOMERVILLE, I., 1996. Irish Dinantian biostratigraphy: practical applications. In: Strogen P., Somerville, I. and Jones, G.L., Eds., *Recent advances in Lower Carboniferous geology*. Geological Society London, Special Publication 107: 371-385.
- KHOA, N.D., 1977. Carboniferous Rugosa and Heterocorallia form boreholes in the Lublin region (Poland). *Acta Palaeontologica Polonica* 22: 301-404.
- KIMPE, W. F. M., BLESS, M. J. M., BOUCKAERT, J., CONIL, R., GROESSENS, E., MEESEN, J. P. M. T., POTY, E., STREEL, M., THOREZ, J. and VANGUESTAINE, M. 1978. Paleozoic deposits east of the Brabant Massif in Belgium and the Netherlands. *Mededelingen Rijks Geologische Dienst. Nieuwe Serie* 30(2): 37-103.
- LEGRAND-BLAIN, M., 1990. Brachiopods as potential boundary-defining organisms in the Lower Carboniferous of Western Europe; recent data and productid distribution. *Courier Forschungsinstitut Senckenberg* 130: 157-171.
- LEWIS, H.P., 1929. On the Avonian coral *Caninophyllum*, gen. nov. and *C. archiaci* (Edwards and Haime). *Annals and Magazine of Natural History, series 10*, 3:456-468.
- MCCOY, F., 1844. *A synopsis of the characters of the Carboniferous Limestone Fossils of Ireland*. Dublin University Press, Dublin. 207 p.
- , 1849. On some new genera and species of Paleozoic corals and foraminifera. *Annals and Magazine of Natural History, series 2*, 3: 1-20, 119-136.
- MELO, J.H.G. and LOBOZIAK, S., 2000. Visean miospore biostratigraphy and correlation of the Poti Formation (Parnaiba Basin, northern Brazil). *Review of Palaeobotany and Palynology* 112: 147-165.
- MILNE-EDWARDS, H. and HAIME, J., 1850-1855. A monograph of the British fossil corals. *Palaeontographical Society Monographs* 1850, i-lxxxv, 1-71, 1851, 73-145, 1852, 147-210, 1853, 211-244, 1855, 245-299.
- , 1851. Monographie des polypiers fossiles des terrains paléozoïques. *Musée Histoire Naturelle de Paris, Archives* 5, 1-502.

- MITCHELL, M., 1989. Biostratigraphy of Viséan (Dinantian) rugose coral faunas of Britain. *Proceedings of the Yorkshire Geological Society* 47: 233-247.
- MONTY, C., 1964. Recherche paléoécologiques dans le V2a de la région "Huy-Moha". *Annales de la Société géologique de Belgique* 86: 407-431.
- NEAVERTON, E., 1929. Faunal horizons in the Carboniferous Limestone of the Vale of Clywd. *Proceedings Liverpool Geological Society* 15: 111-133.
- NUDDS, J., 1980. An illustrated key to the British lithostrotionid corals. *Acta Palaeontologica Polonica* 25: 385-394.
- NUDDS, J. and DAY, A., 1997. The effects of clastic sedimentation on a fasciculate rugose coral from the Lower Carboniferous of Northern England. *Boletín de la Real Sociedad Española de Historia Natural (Sección Geológica)* 91: 93-97.
- NUDDS, J. and SOMERVILLE, I.D., 1987. Two new species of *Siphonodendron* (Rugosa) from the Viséan of the British Isles. *Proceedings of the Yorkshire Geological Society* 46: 293-300.
- d'ORBIGNY, A. 1852. *Cours élémentaires de paléontologie et de géologie stratigraphique*. V. 2, 1, Victor Masson, Paris, 349 pp.
- PARKINSON, J., 1808. *Organic remains of a former world*. Volume 2 Zoophytes, London.
- PATTISON, J., 1981. The stratigraphical distribution of gigantoprotoceratid brachiopods in the Visean and Namurian rocks of some areas in northern England. *Report - Natural Environment Research Council, Institute of Geological Sciences* 81-9:1-30.
- PERRET M.-F. and SEMENOFF-TIAN-CHANSKY, P., 1971. Corallaires des calcaires carbonifères d'Ardengost (Hautes-Pyrénées). *Bulletin de la Société d'histoire naturelle de Toulouse* 107: 567-594.
- PHILLIPS, J., 1836. *Illustrations of the geology of Yorkshire, Part 2: The Mountain Limestone*. John Murray, London, 253 pp.
- POTY, E., 1978. Données nouvelles sur les héterocoralliaires du Dinantien belge. *Annales de la Société géologique de Belgique* 100: 233-243.
- , 1981. Recherches sur les tétracoralliaires et les héterocoralliaires du Viséen de la Belgique. *Mededelingen Rijks Geologische Dienst* 36: 1-161.
- , 1985. A rugose coral biozonation for the Dinantian of Belgium as a basis for a coral biozonation of the Dinantian of Eurasia. In: *Compte Rendu 10ème Congrès International du Stratigraphie et Géologie du Carbonifère*, Madrid 1983 4: 29-31.
- POTY, E., ARETZ, M. and BARCHY, L. 2002. Stratigraphie et sedimentologie des calcaires à Productus du Carbonifère inférieur de la Montagne noire (Massif central, France). *Comptes Rendus - Académie des sciences. Géoscience* 334: 843-848.
- POTY, E., HANCE, L., LEES, A. and HENNEBERT, M. 2002. Dinantian lithostratigraphic units (Belgium). *Geologica Belgica* 4: 69-94.
- POTY, E. and HANNAY, D. 1994. Stratigraphy of rugose corals in the Dinantian of the Boulonnais (France). *Mémoire de l'Institut Géologique de l'Université de Louvain* 35: 51-82.
- RAMSBOTTOM, W.H.C., 1973. Transgressions and regressions in the Dinantian: a new synthesis of British Dinantian stratigraphy. *Proceedings of the Yorkshire Geological Society* 39: 567-607.
- , 1979. Rates of transgression and regression in the Carboniferous of NW Europe. *Journal of the Geological Society London* 136: 147-153.
- , Editor, 1981. *Field guide to the boundary stratotypes of Carboniferous stages in Britain*. (Leeds, 25. August – 1 September 1981). Subcommission on Carboniferous stratigraphy.
- RILEY, N. 1990. Stratigraphy of the Worston Shale Group, Dinantian, Craven Basin, north-west England. *Proceedings of the Yorkshire Geological Society* 48: 163-187.
- , 1993. Dinantian (Lower Carboniferous) biostratigraphy and chronostratigraphy in the British Isles. *Journal of the Geological Society of London* 150: 427-446.
- RODRIGUEZ, S. and COMAS-RENGIFO, S. 1989. Los Heterocorales del Carbonífero de los Santos de Maimona (Badajoz, SE de España). *Coloquios de Paleontología* 42: 61-81.
- RODRIGUEZ, S. and FALCES, S. 1992. Corales rugosos. *Coloquios de Paleontología* 44: 159-218.
- RODRIGUEZ, S., HERNANDO, J.M. and RODRIGUEZ-CURT, L. 2002. Estudio de los corales lithostrotionidos del Viseense (Misisipense) de la Unidad de la Sierra del Castello (Córdoba, España). *Revista Española de Paleontología* 17: 13-36.
- SALÉE, A. 1913. Contribution à l'étude des polypiers du calcaire carbonifère de la Belgique. *Mémoire de l'Institut Géologique de l'Université de Louvain* 1: 177-293.
- SCHINDEWOLF, O.H. 1941. Zur Kenntnis der Heterophyllidean, einer eigentümlichen paläozoischen Korallengruppe. *Paläontologische Zeitschrift* 22: 213-306.
- SCOULER, J. in MCCOY, F. 1844. *A synopsis of the characters of the Carboniferous limestone fossils of Ireland*. Dublin University Press, Dublin. 207 p.
- SEmenoff-TIAN-CHANSKY, P. 1974. Recherches sur les tétracoralliaires du Carbonifère du Sahara occidental. *Centre de Recherches des Zones arides, série géologie* 21: 1-316.
- SEmenoff-TIAN-CHANSKY, P. and NUDDS, J. 1979. Révision de quelques espèces de Lithostrotion des îles Britanniques décrites par Milne-Edwards et Haime (tétracoralliaires carbonifères). *Bulletin Musée nationale d'Histoire naturelle*, 4 série 1: 245-283.
- SIBLY, T.F., 1906. On the Carboniferous Limestone (Upper Avonian) of the Mendip Area (Somerset), with special reference to the Palaeontological sequence. *Quarterly Journal of the Geological Society of London* 62: 324-380.
- SOMERVILLE, I.D., 1997. Rugose coral faunas form Upper Viséan (Asbian-Brigantian) buildups and adjacent platform limestones, Kingscourt, Ireland. *Boletín de la Real Sociedad Española de Historia Natural (Sección Geológica)* 92: 35-47.
- SOMERVILLE, I.D. and STRANK, A.R.E., 1984. The recognition of the Asbian/Brigantian boundary fauna and marker horizons in the Dinantian of North Wales. *Geological Journal* 19: 227-237.
- SPASSKIY, N.Y., 1974. Dialekticheskoe edinstvo prostranstvenno-vremenennykh zakonomernostey evolyutsii (na primere chetyrekh-luchevykh korallov). *Leningrad Gornyi Institut, Zapiski* 67:127-135.
- SPASSKIY, N.Y. and KACHANOV, E.I., 1971. Novye primitivnye rannekamennougolnye korally Altaya i Urala. *Leningrad Gornyi Institut, Zapiski* 59: 5-22.

- STRANK, A.R.E., 1981. "Foraminiferal biostratigraphy of the Holkerian, Asbian and Brigantian stages of the British Lower Carboniferous". Unpublished PhD thesis, University of Manchester, 423 pp.
- THOMSON J. and NICHOLSON H.A., 1876. Contribution to the study of the chief generic types of the Paleozoic corals. *Annals and Magazine of Natural History* 17: 60-70, 123-138, 290-305, 451-461.
- TOURNEUR, F., CONIL, R. and POTY, E., 1989. Données préliminaires sur les Tabules et les Chaetetides du Dinantian de la Belgique. *Bulletin de la Société belge de Géologie* 98: 401-442.
- VAUGHAN, A., 1905. The palaeontological sequence in the Carboniferous Limestone of the Bristol area. *Quarterly Journal of the Geological Society of London* 61: 181-307.
- VERILL, A.E., 1865. Classification of polyps (Extract condensed from a synopsis of the polypi of the North Pacific exploring Expedition, under captains Ringgold and Rodgers). *Essex Institution Proceedings* 4: 145-149.
- WANG, H.C., 1950. A revision of the zonantharie rugose in the light of their minute skeletal structures. *Philosophical Transactions Royal Society London series B*, no. 611(v. 234): 175-246.
- WEYER, D., 2001. Korallen im Unterkarbon Deutschlands. *Abhandlungen und Berichte für Naturkunde* 23: 58-91.
- WHITE, F. M., 1992. "Aspects of the palaeoecology and stratigraphic significance of Late Dinantian (Early Carboniferous) foraminifera of northern England." Unpublished PhD thesis, University of Manchester, 677 pp.

Manuscript received July 20, 2005

Manuscript accepted November 10, 2005

Definition and status of the Quaternary

I am pleased to announce that the voting membership of ICS, following intensive consultations and working group efforts, has approved recommendations to the IUGS for the establishment of the Quaternary as a formal chronostratigraphic unit within the Cenozoic Era. The recommendations, schematically diagrammed in text-figures 1 and 2, are as follows:

1. That the Quaternary spans the past 2.6 myr, with a formally designated base at the previously ratified Global Stratotype Section and Point (GSSP) at the base of the Gelasian stage of the Pliocene epoch.
2. That the Quaternary has the rank of a Sub-era (and Sub-erathem) in the Cenozoic Era (Erathem) in the standard geologic time scale.

The ICS has submitted these recommendations to the International Union of Quaternary Research (INQUA) for approval by its membership. The INQUA Executive has already stated that the Quaternary should encompass the past 2.6 myr, and has recommended its ranking as a Sub-era in the geologic time scale. Upon INQUA approval, the final step will be ratification by the International Union of Geological Sciences (IUGS) of the recommended terms for the inclusion of the Quaternary as a formal division of the international geologic time scale.

BACKGROUND TO ICS VOTING

In 1985, with the formal placement of the base-Pleistocene GSSP at Vrica, Calabria, “*The subject of defining the boundary between the Pliocene and Pleistocene was isolated from other more or less related problems, such as the pending definition of the Calabrian, and the status of the Quaternary within the chronostratigraphic scale.*” (quoting from E. Aguirre and G. Pasini, 1985, The Pliocene-Pleistocene Boundary. *Episodes* 8: 116-120, in the report of the official decision on the base-Pleistocene GSSP by a special joint INQUA-ICS working group to evaluate the final recommendation of a 20-year effort by IGCP 41, “N/Q Boundary”).

For various reasons, the “... *status of the Quaternary ...*” was never resolved, let alone submitted to ICS/IUGS for consideration or ratification. As a result, INQUA and self-identified Quaternary workers commonly use one definition, based on Earth’s major environmental changes, whereas recently published time scales have either omitted the Quaternary, or have adopted the unratified assumption that the base of the Quaternary was established at Vrica.

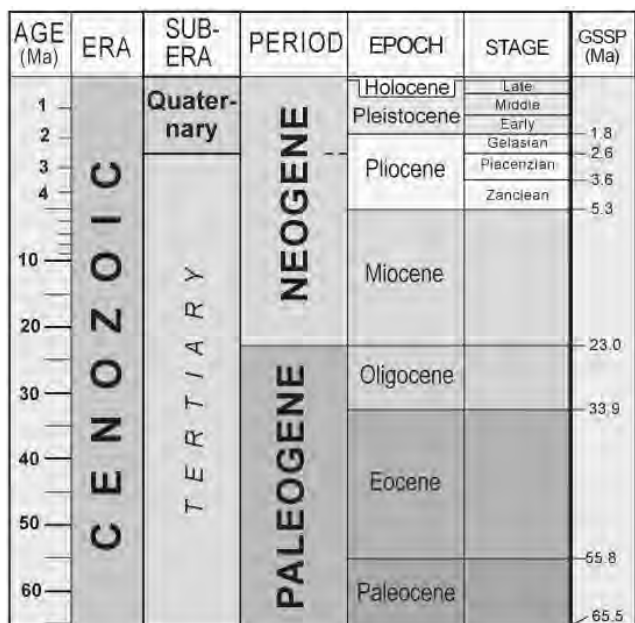
The Cenozoic has two formally ratified period-level subdivisions - Neogene and Paleogene. Most paleontologists, petroleum exploration groups and marine geologists consider the Neogene to extend to the present day, and an elaborate paleontological framework of Neogene biostratigraphic subdivisions using this definition has been in use for the past two decades. On the other hand, the climatic- and continental-based Quaternary has been commonly used for land-based geologic mapping and in discussions of Earth’s history during the latter of the Neogene.

The INQUA Executive, in consultation with the Quaternary community in 2004, found widespread support for defining the Quaternary as a formal chronostratigraphic unit with a base essentially dated to 2.6 Ma, which is approximately 0.8 myr older than the base of the Pleistocene epoch. As a consequence, ICS and INQUA considered it timely to make a final decision on the stratigraphic meaning of the Quaternary, so that it could be unequivocally placed in the standard global time scale. John Clague, President of INQUA and I, as Chair of ICS, with the assistance of outgoing IUGS President Ed de Mulder, agreed to establish a special working group for this purpose. This working group, which included members of the INQUA Chronology Commission and members of the Quaternary and Neogene Subcommissions of ICS, met in Cambridge, England, in March 2005, and voted to present the following recommendations to ICS (also posted at www.stratigraphy.org/news.htm):

- (1) That the Quaternary be recognized as a formal chronostratigraphic/geochronologic unit.
- (2) That the lower boundary of the Quaternary should coincide with the base of the Gelasian Stage (~2.6 Ma), and thus be defined by the Gelasian GSSP.
- (3) That the Quaternary should have the rank of *either* System/Period following the Neogene System/Period, with its lower boundary marking the top of a shortened Neogene, *or* Sub-erathem/Sub-era to be correlative with the upper part of the Neogene System/Period.

In early September 2005, the ICS held a meeting of the entire voting membership (all subcommission chairs, plus the ICS executive) with the chair of the INQUA Chronology Commission in Leuven, Belgium. The recommendations of the joint INQUA/ICS Quaternary Task Group were presented and debated, with proposals subjected to both open voting (show of hands) and written ballots. The recommendation that Quaternary should be a formal unit in the international geologic time scale met with unanimous approval. The ICS members were also in near-unanimous agreement with the Task Group that the Quaternary, as currently used by INQUA and Quaternary research specialists, should begin at about 2.6 Ma, where extensive evidence documents indicates a dramatic change in both continental and oceanic environments that can be considered as the earliest of the major “Ice Ages” and that the Gelasian GSSP was appropriate for the required stratigraphically defined boundary.

In considering the options offered by the Task Group as to the rank of Quaternary in the international time scale, the ICS members voted by a two-thirds super-majority to give the Quaternary the status of Sub-era and Sub-erathem. It was noted in discussions that this recommendation accommodates a Neogene period that extends to the present, as used by most paleontologists. At the same time, it allows for a revival of Tertiary to be a complementary Cenozoic division preceding Quaternary. While Tertiary is historically appropriate and logical to occupy the pre-Quaternary Sub-era, no such unit has been proposed, let alone ratified, and the use of “Tertiary” would be entirely informal at this time (see text-figure 2).



TEXT-FIGURE 1
Quaternary Sub-Era of Cenozoic (**not** to scale)

In conclusion, the definition, stratigraphically defined base, and formal rank of Quaternary have now been recommended by ICS for approval by INQUA and final ratification by IUGS. Pending this action, in December 2005 the ICS will place Quaternary on its public International Divisions of Geologic Time charts and tables, with a footnote that the final status of the Quaternary is under submission.

SUMMARY

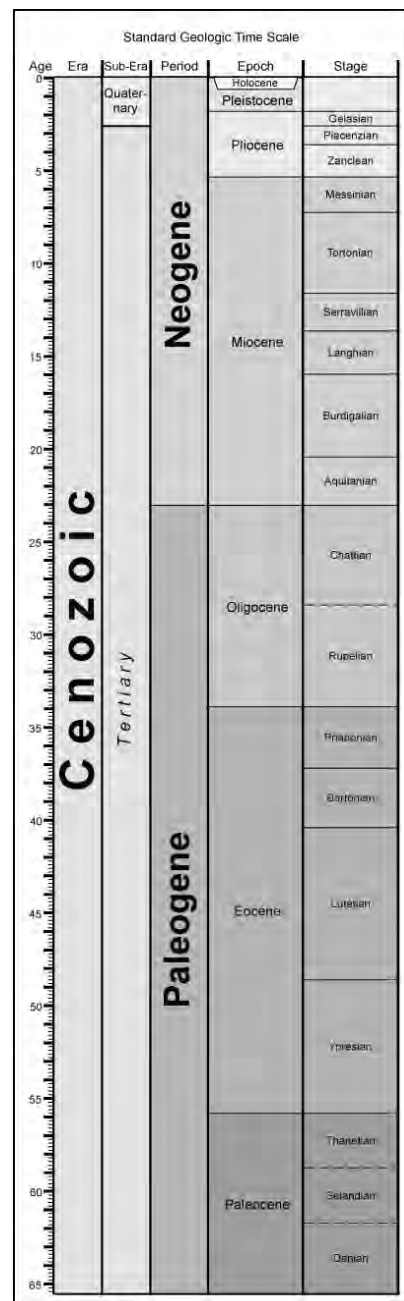
In September 2005 the ICS voting membership met in Leuven to consider, among other issues, the recommendations of the joint INQUA/ICS Quaternary Task Group, and voted as follows:

- Recommendation (1), to make the Quaternary a geochronologic-chronostratigraphic unit in the standard geological time scale, was unanimously approved by a show of hands.
- Recommendation (2) that the Quaternary should have a formal lower boundary coinciding with the base of the Gelasian Stage and defined by the Gelasian GSSP, at approximately 2.6 Ma, was approved (after extensive discussion) by a near unanimous show of hands.
- The two options in Recommendation (3) for the rank of the Quaternary, as well as other options, were discussed at length, and subjected to vote by a show of hands. The only option to receive a majority was that the Quaternary should have the rank of Sub-erathem/Sub-era.

The winning option was put to a written ballot with the following result::

Should the Quaternary be a formal Sub-Era / Sub-Erathem?

YES - 12 votes
NO - 5 votes
ABSTAIN - 1 vote



TEXT-FIGURE 2
Quaternary Sub-Era of Cenozoic (to scale)

With these votes, the International Commission on Stratigraphy is recommending to IUGS that the Quaternary should be recognized as a formal unit of the standard geological time scale with the rank of Sub-erathem/Sub-era, defined by a lower boundary coincident with the base of the Gelasian Stage. The Quaternary Sub-erathem/Sub-era is therefore coincident with the final ~2.6 myr of the Neogene System/Period.

Felix M. Gradstein, Chair
International Commission on Stratigraphy
Geology Museum, University of Oslo
PO Box 1172, Blindern
N-0318, Oslo, Norway
felix.gradstein@nhm.uio.no